TTI: 0-6913

Texas A&M Transportation Institute

CRASH TEST AND EVALUATION OF TL-2 SHORT RADIUS GUARDRAIL TREATMENT



ACCREDITED
ISO 17025 Laboratory
Testing Certificate # 2821.01

Crash testing performed at:
TTI Proving Ground
3100 SH 47, Building 7091
Bryan, TX 77807

Test Report 0-6913-R1

Cooperative Research Program

TEXAS A&M TRANSPORTATION INSTITUTE
COLLEGE STATION, TEXAS

TEXAS DEPARTMENT OF TRANSPORTATION

in cooperation with the
Federal Highway Administration and the
Texas Department of Transportation
http://tti.tamu.edu/documents/0-6913-R1.pdf

Technical Report Documentation Page

1. Report No.	2. Government Accession No.	3. Recipient's Catalog No.
FHWA/TX-18/0-6913-R1		

4. Title and Subtitle	5. Report Date
CRASH TEST AND EVALUATION OF TL-2 SHORT RADIUS GUARDRAIL TREATMENT	Published: April 2019
	6. Performing Organization Code

7. Author(s)	8. Performing Organization Report No.
Akram Y. Abu-Odeh, Nataly de la Fuente, Wanda L. Menges, and Darrell L. Kuhn	Report 0-6913-R1

9. Performing Organization Name and Address	10. Work Unit No. (TRAIS)
Texas A&M Transportation Institute College Station, Texas 77843-3135	11. Contract or Grant No. Project 0-6913

12. Sponsoring Agency Name and Address	13. Type of Report and Period Covered
Texas Department of Transportation Research and Technology Implementation Office 125 E. 11th Street Austin, Texas 78701-2483	Technical Report: September 2016–February 2018
	14. Sponsoring Agency Code

15. Supplementary Notes

Project performed in cooperation with the Texas Department of Transportation and the Federal Highway Administration.
Project Title: MASH Test Level 2 (TL-2) Short Radius Guardrail Treatment on Texas Roadways
URL: http://tti.tamu.edu/documents/0-6913-R1.pdf

16. Abstract

The purpose of the testing reported herein was to assess the performance of the *Manual for Assessing Safety Hardware* (*MASH)* TL-2 low-speed short radius guardrail treatment according to the safety-performance evaluation guidelines included in American Association of State Highway and Transportation Officials *MASH*. The crash tests performed were in accordance with *MASH* TL-2.

The Texas Department of Transportation low-speed short radius guardrail treatment performed acceptably for modified *MASH* Tests 2-33, 2-32, 2-31, 2-35, and 2-34.

17. Key Words	18. Distribution Statement
Guardrail, End Treatment, Terminal, Short Radius, Longitudinal Barriers, Crash Testing, Roadway Safety	No restrictions. This document is available to the public through NTIS: National Technical Information Service Alexandria, Virginia http://www.ntis.gov

19. Security Classif.(of this report)	20. Security Classif.(of this page)	21. No. of Pages	22. Price
Unclassified	Unclassified	290	

Form DOT F 1700.7 (8-72) Reproduction of completed page authorized

CRASH TESTING AND EVALUATION OF TL-2 SHORT RADIUS GUARDRAIL TREATMENT

by

Akram Y. Abu-Odeh, Ph.D.
Research Scientist
Texas A&M Transportation Institute

Nataly de la Fuente
Graduate Student
Texas A&M Transportation Institute

Wanda L. Menges
Research Specialist
Texas A&M Transportation Institute

and

Darrell L. Kuhn, P.E.
Research Specialist
Texas A&M Transportation Institute

Report 0-6913-R1
Project 0-6913
Project Title: MASH Test Level 2 (TL-2) Short Radius Guardrail Treatment on Texas Roadways

Performed in cooperation with the
Texas Department of Transportation
and the
Federal Highway Administration

Published: April 2019

TEXAS A&M TRANSPORTATION INSTITUTE
College Station, Texas 77843-3135

DISCLAIMER

This research was performed in cooperation with the Texas Department of Transportation (TxDOT) and the Federal Highway Administration (FHWA). The contents of this report reflect the views of the authors, who are responsible for the facts and the accuracy of the data presented herein. The contents do not necessarily reflect the official view or policies of the FHWA or TxDOT. This report does not constitute a standard, specification, or regulation.

This report is not intended for construction, bidding, or permit purposes. The researcher in charge of the project was Akram Y. Abu-Odeh.

The United States Government and the State of Texas do not endorse products or manufacturers. Trade or manufacturers' names appear herein solely because they are considered essential to the object of this report.

TTI PROVING GROUND QA/QC PROCESS

The results of the crash testing reported herein apply only to the article being tested.

ACCREDITED
ISO 17025 Laboratory
Testing Certificate # 2821.01

Crash testing performed at:
TTI Proving Ground
3100 SH 47, Building 7091
Bryan, TX 77807

Wanda L. Menges, Research Specialist
Deputy Quality Manager

Darrell L. Kuhn, Research Specialist
Quality Manager

Matthew N. Robinson, Senior Research Specialist
Technical Manager

ACKNOWLEDGMENTS

This research project was conducted under a cooperative program between the Texas A&M Transportation Institute, the Texas Department of Transportation, and the Federal Highway Administration. The TxDOT project manager for this research was Wade Odell, Research and Technology Implementation. Technical support and guidance were provided by Christopher Lindsey (Design Division). The authors acknowledge and appreciate their assistance. The authors acknowledge the computational support provided by the Texas A&M High Performance Research Computing (HPRC) (http://hprc.tamu.edu/). The authors appreciate the HPRC facility assistance.

TABLE OF CONTENTS

Page

List of Figures ..... **xiii**
List of Tables ..... **xxi**
Chapter 1: Introduction **1**
1.1 Problem 1
1.2 Scope of Research 1
1.2.1 Task 1. Establish Design Requirements and Site Constraints. 1
1.2.2 Task 2. Develop Finite Element Models for Candidate Designs 2
1.2.3 Task 3. Conduct Full-Scale Crash Testing 2
1.2.4 Task 4. Prepare Research Reports 3
1.3 Objective 3
Chapter 2: Development of Finite Element Models for candidate designs **5**
2.1. Background 5
2.2 Design Consideration 5
2.3 Simulation of Recommended Design Concepts 6
2.3.1 Case 1 – TL-3 System without Sand Drums 6
2.3.2 Case 2 – Large (16-ft) Radius System 10
2.3.3 Case 3 13
2.4 Simulation of Test 2-31 22
2.4.1 System Details 22
2.4.2 Simulation of Truck Impacting Short Radius with Strap and Cable from Front of Rail 24
2.5 Test 2-33 28
2.5.1 System Details 28
2.5.2 Simulation of Truck Impacting Short Radius with Strap and Cable at 25° 29
2.6 Test 2-33-2 30
2.6.1 System Details 30
2.6.2 Simulation of Truck Impacting Short Radius with Flare and 18-lb Sand Drums 30
2.7 Conclusions 34
Chapter 3: Simulations of Recommended Designs Concepts **37**
3.1. Background 37
3.2 Design Consideration 37
3.3 Simulation of Truck Impacting Short Radius with Tension Cable and Four 700-lb Sand Drums 39
3.4 Simulation of Truck Impacting Short Radius with Tension Cable and Four 700-lb Sand Drums 43
3.5 Simulation of Truck Impacting Short Radius with Tension Cable and Five 700-lb Sand Drums 46
3.6 Simulation of Truck Impacting Short Radius with Tension Cable and Six 700-lb Sand Drums 49
3.7 Simulation of Truck Impacting Short Radius with Two Tension Cables and Six 700-lb Sand Drums 52

TABLE OF CONTENTS (CONTINUED)

Page

3.8 Simulation of Truck Impacting Short Radius with Tension Cable and Six 700-lb Sand Drums 55
3.9 Simulation of Truck Impacting Short Radius with Two Tension Cables and Six 700-lb Sand Drums 57
3.10 Simulation of Truck Impacting Short Radius with Two Tension Cables and Six 700-lb Sand Drums 61
3.11 Simulation of Truck Impacting Short Radius with Two Tension Cables and Six 700-lb Sand Drums 64
3.12 Simulation of Truck Impacting Short Radius with Two Tension Cables and Six 700-lb Sand Drums 67
3.13 Simulation of Car Impacting Short Radius with Two Tension Cables and Six 700-lb Sand Drums 70
3.14 Simulation of Car Impacting Short Radius with Two Tension Cables and Six 700-lb Sand Drums 74
3.15 Simulation of Truck Impacting Short Radius with Two Tension Cables and Six 700-lb Sand Drums 77
3.16 Simulation of Car Impacting Short Radius with Two Tension Cables and Six 700-lb Sand Drums 80
3.17 Simulation of Car Impacting Short Radius with Two Tension Cables and Six 700-lb Sand Drums 85
3.18 Simulation of Car Impacting Short Radius with Two Tension Cables and Six 700-lb Sand Drums 90
3.19 Conclusions 94
Chapter 4: Test Article Design and Construction 95
4.1 Test Article and Installation Details 95
4.1.1 Guardrail 95
4.1.2 Parapet 96
4.1.3 Sand Drums 97
4.1.4 Ditch 97
4.2 Design Modifications during Testing 98
4.3 Soil Conditions 103
Chapter 5: Test Requirements and Evaluation Criteria 105
5.1 Crash Test Matrix 105
5.2 Evaluation Criteria 108
Chapter 6: Test Conditions 109
6.1 Test Facility 109
6.2 Vehicle Tow and Guidance system 109
6.3 Data Acquisition Systems 109
6.3.1 Vehicle Instrumentation and Data Processing 109
6.3.2 Anthropomorphic Dummy Instrumentation 110
6.3.3 Photographic Instrumentation and Data Processing 111

TABLE OF CONTENTS (CONTINUED)

Page

Chapter 7: *MASH* Test 2-33 (Crash Test No. 469137-3-1) 113
7.1 Test Designation and Actual Impact Conditions 113
7.2 Weather Conditions 113
7.3 Test Vehicle 113
7.4 Test Description 114
7.5 Damage to Test Installation 114
7.6 Damage to Test Vehicle 114
7.7 Occupant Risk Factors 115
7.8 Assessment of Test Results 120
Chapter 8: *MASH* Test 2-32 (Crash Test No. 469137-3-2) 123
8.1 Test Designation and Actual Impact Conditions 123
8.2 Weather Conditions 123
8.3 Test Vehicle 123
8.4 Test Description 124
8.5 Damage to Test Installation 125
8.6 Vehicle Damage 128
8.7 Occupant Risk Factors 129
8.8 Assessment of Test Results 130
Chapter 9: *MASH* Test 2-31 (Crash Test No. 469138-3-3) 133
9.1 Test Designation and Actual Impact Conditions 133
9.2 Weather Conditions 133
9.3 Test Vehicle 133
9.4 Test Description 134
9.5 Damage to Test Installation 135
9.6 Damage to Test Vehicle 137
9.7 Occupant Risk Factors 139
9.8 Assessment of Test Results 139
Chapter 10: *MASH* Test 2-35 (Crash Test No. 469138-3-4) 143
10.1 Test Designation and Actual Impact Conditions 143
10.2 Weather Conditions 143
10.3 Test Vehicle 143
10.4 Test Description 144
10.5 Damage to Test Installation 145
10.6 Damage to Test Vehicle 147
10.7 Occupant Risk Factors 147
10.8 Assessment of Test Results 149
Chapter 11: Modified *MASH* Test 2-34 (Crash Test No. 469138-3-5) 153
11.1 Test Designation and Actual Impact Conditions 153
11.2 Weather Conditions 153
11.3 Test Vehicle 153
11.4 Test Description 154
11.5 Damage to Test Installation 155
11.6 Vehicle Damage 156

TABLE OF CONTENTS (CONTINUED)

Page

11.7 Occupant Risk Factors 157
11.8 Assessment of Test Results 157
Chapter 12: Summary and Conclusions 161
12.1 Summary of Results 161
12.1.1 *MASH* Test 2-33 161
12.1.2 *MASH* Test 2-32 161
12.1.3 *MASH* Test 2-31 161
12.1.3 *MASH* Test 2-35 161
12.1.4 Modified *MASH* Test 2-34 162
12.2 Conclusions 162
Chapter 13: Implementation Statement 165
References 167
Appendix A. Details of the Guardrail Treatment for Test Nos. 469137-3-1 and 469137-3-2 169
Appendix B. Details of the Guardrail Treatment for Test Nos. 469138-3-3 through 469138-3-5 181
Appendix C. Soil Properties 195
Appendix D. *MASH* Test 2-33 (Crash Test No. 469137-3-1) 201
D.1 Vehicle Properties and Information 201
D.2 Sequential Photographs 205
D.3 Vehicle Angular Displacement 209
D.4 Vehicle Accelerations 210
Appendix E. *MASH* Test 2-32 (Crash Test No. 469137-3-2) 217
E.1 Vehicle Properties and Information 217
E.2 Sequential Photographs 220
E.3 Vehicle Angular Displacements 224
E.4 Vehicle Accelerations 225
Appendix F. *MASH* Test 2-31 (Crash Test No. 469138-3-3) 231
F.1 Vehicle Properties and Information 231
F.2 Sequential Photographs 235
F.3 Vehicle Angular Displacement 238
F.4 Vehicle Accelerations 239
Appendix G. *MASH* Test 2-35 (Crash Test No. 469138-3-4) 245
G.1 Vehicle Properties and Information 245
G.2 Sequential Photographs 249
G.3 Vehicle Angular Displacement 252
G.4 Vehicle Accelerations 253
Appendix H. Modified *MASH* Test 2-34 (Crash Test No. 469138-3-5) 259
H1 Vehicle Properties and Information 259
H2 Sequential Photographs 262
H3 Vehicle Angular Displacements 264
H4 Vehicle Accelerations 265

LIST OF FIGURES

		Page
Figure 2.1.	*MASH* TL-2 Transition before Test No. 420021-4.	6
Figure 2.2.	Entire System with Cable.	6
Figure 2.3.	Side View of Primary Roadway.	7
Figure 2.4.	Side View of Secondary Roadway.	7
Figure 2.5.	Sequential Images of Car Simulation with Cable.	7
Figure 2.6.	Initial State of the Simulation.	8
Figure 2.7.	Final State of the Simulation.	8
Figure 2.8.	Sequential Images of Truck Simulation with Flare.	9
Figure 2.9.	Initial State of Simulation.	10
Figure 2.10.	Final State of Simulation.	10
Figure 2.11.	Extended Short Radius System with No Flare.	11
Figure 2.12.	Primary Roadway Side View.	11
Figure 2.13.	Secondary Roadway Side View.	11
Figure 2.14.	Sequential Images of Simulation with No Cable.	12
Figure 2.15.	Initial State of Simulation.	12
Figure 2.16.	Final State of Simulation.	13
Figure 2.17.	Extended Short Radius with Strap.	13
Figure 2.18.	Back View of System Showing Strap.	14
Figure 2.19.	Primary Roadway Side View.	14
Figure 2.20.	Secondary Roadway Side View.	14
Figure 2.21.	Sequential Images of Car Simulation with Strap.	15
Figure 2.22.	Interaction of Car with System.	15
Figure 2.23.	Final State of Simulation.	16
Figure 2.24.	Longitudinal Accelerations for Car Simulation.	17
Figure 2.25.	Lateral Accelerations for Car Simulation.	17
Figure 2.26.	Roll, Pitch, and Yaw Angles for Car Simulation.	17
Figure 2.27.	Sequential Images of Truck Simulation with Strap.	18
Figure 2.28.	Interaction of Car with System.	19
Figure 2.29.	Final State of Simulation.	19
Figure 2.30.	Longitudinal Accelerations for Truck Simulation.	20
Figure 2.31.	Lateral Accelerations for Truck Simulation.	20
Figure 2.32.	Roll, Pitch, and Yaw Angles for Truck Simulation.	20
Figure 2.33.	Short Radius System with Back Plate.	21
Figure 2.34.	Amplified View of Guardrail System with Strap and Two Cables.	22
Figure 2.35.	Front View of Primary Cable.	22
Figure 2.36.	Back View of Primary Cable (Strap Hidden).	23
Figure 2.37.	Back View of Secondary Cable (Strap Hidden).	23
Figure 2.38.	Alignment of Truck with System.	24
Figure 2.39.	Sequential Images of Simulation of Truck from Front of Rail, with Strap and Cables.	25
Figure 2.40.	Sequential Images of Tire with System Interaction.	26
Figure 2.41.	Tire and Cable Interaction.	27
Figure 2.42.	Roll, Pitch, and Yaw Angles.	28

LIST OF FIGURES (CONTINUED)

		Page
Figure 2.43.	Alignment of Truck with System.	28
Figure 2.44.	Sequential Images of Simulation with Strap and Cables.	29
Figure 2.45.	Interaction of Truck with System.	30
Figure 2.46.	Flare and 18-lb Sand Drums behind Radius.	31
Figure 2.47.	Sequential Images of Truck Simulation, with Flare and 18-lb Sand Drums.	31
Figure 2.48.	Interaction of Truck with System.	32
Figure 2.49.	Longitudinal Accelerations for Truck Simulation.	33
Figure 2.50.	Lateral Accelerations for Truck Simulation.	33
Figure 2.51.	Vertical Accelerations for Truck Simulation.	34
Figure 2.52.	Roll, Pitch, and Yaw Angles for Truck Simulation.	34
Figure 3.1.	Guardrail System.	38
Figure 3.2.	Guardrail System-Back.	38
Figure 3.3.	Sand Drum Used in Simulations.	38
Figure 3.4.	Entire System with Tension Cable and Four 700-lb Sand Drums.	39
Figure 3.5.	Side View of Primary Roadway.	39
Figure 3.6.	Side View of Secondary Roadway.	40
Figure 3.7.	Alignment of Truck with System.	40
Figure 3.8.	Sequential Images of Truck Simulation with Tension Cable and Four 700-lb Sand Drums	41
Figure 3.9.	Interaction of Truck with System.	42
Figure 3.10.	Final State of Simulation.	42
Figure 3.11.	Alignment of Truck with System.	43
Figure 3.12.	Sequential Images of Truck Simulation with Tension Cable and Four 700-lb Sand Drums	44
Figure 3.13.	Sequential Images of Truck Simulation from Back of Rail (No Drums Visible).	45
Figure 3.14.	Interaction of Truck with System (No Drums Visible).	45
Figure 3.15.	Tension Cable and Five 700-lb Sand Drums.	46
Figure 3.16.	Sequential Images of Truck Simulation with Tension Cable and Five 700-lb Sand Drums	47
Figure 3.17.	Interaction of Truck with System (No Drums Visible).	48
Figure 3.18.	Final State of Truck (No Drums Visible).	48
Figure 3.19.	Alignment of Truck with System.	49
Figure 3.20.	Sequential Images of Truck Simulation with Tension Cable and Six 700-lb Sand Drums.	50
Figure 3.21.	Interaction of Truck with System.	51
Figure 3.22.	Final State of Truck.	51
Figure 3.23.	Alignment of Truck with System.	52
Figure 3.24.	Sequential Images of Truck Simulation with Two Tension Cables and Six 700-lb Sand Drums.	53
Figure 3.25.	Interaction of Truck with System (No Drums Visible).	54
Figure 3.26.	Final State of Truck Simulation (No Drums Visible).	54
Figure 3.27.	Alignment of Truck with System.	55

LIST OF FIGURES (CONTINUED)

		Page
Figure 3.28.	Sequential Images of Truck Simulation with Tension Cable and Six 700-lb Sand Drums.	56
Figure 3.29.	Interaction of Truck with System (No Drums Visible).	56
Figure 3.30.	Interaction of Truck with System (No Drums Visible).	57
Figure 3.31.	Alignment of Truck with System.	58
Figure 3.32.	Sequential Images of Truck Simulation with Two Tension Cables and Six 700-lb Sand Drums.	59
Figure 3.33.	Interaction of Truck with System (No Drums Visible).	60
Figure 3.34.	Sequential Images of Truck Simulation with Two Tension Cables and Six 700-lb Sand Drums.	62
Figure 3.35.	Interaction of Simulation with System (No Drums Visible).	63
Figure 3.36.	Final State of Truck (No Drums Visible).	63
Figure 3.37.	Two Tension Cables and 700-lb Sand Drums behind Radius.	64
Figure 3.38.	Sequential Images of Truck Simulation with Two Tension Cables and Six 700-lb Sand Drums.	65
Figure 3.39.	Interaction of Truck with System (No Drums Visible).	66
Figure 3.40.	Final State of Simulation (No Drums Visible).	66
Figure 3.41.	Alignment of Truck with System.	67
Figure 3.42.	Sequential Images of Truck Simulation with Two Tension Cables and Six 700-lb Sand Drums.	68
Figure 3.43.	Interaction of Truck with System (No Drums Visible).	69
Figure 3.44.	Final State of Simulation (No Drums Visible).	69
Figure 3.45.	Two Tension Cables and Six 700-lb Sand Drums behind Radius.	71
Figure 3.46.	Alignment of Car with System.	71
Figure 3.47.	Sequential Images of Car Simulation with Two Tension Cables and Six 700-lb Sand Drums.	72
Figure 3.48.	Interaction of Car with System (No Drums Visible).	73
Figure 3.49.	Final State of Simulation (No Drums Visible).	73
Figure 3.50.	Alignment of Car with System.	74
Figure 3.51.	Sequential Images of Car Simulation with Two Tension Cables and Six 700-lb Sand Drums.	75
Figure 3.52.	Interaction of Car with System (No Drums Visible).	76
Figure 3.53.	Final State of Simulation (No Drums Visible).	76
Figure 3.54.	Alignment of System with Truck.	77
Figure 3.55.	Sequential Images of Truck Simulation with Two Tension Cables and Six 700-lb Sand Drums.	78
Figure 3.56.	Sequential Images of Simulation from Front of Rail (No Drums Visible).	79
Figure 3.57.	Images of Simulation from Back of Rail (No Drums Visible).	79
Figure 3.58.	Alignment of Car with System (No Drums Visible).	81
Figure 3.59.	Sequential Images of Car Simulation with Two Tension Cables and Six 700-lb Sand Drums.	81
Figure 3.60.	Sequential Images of Simulation (Top View).	82
Figure 3.61.	Interaction of Car with System (No Drums Visible).	82

LIST OF FIGURES (CONTINUED)

		Page
Figure 3.62.	Interaction of Car with System (No Drums Visible).	83
Figure 3.63.	Longitudinal Acceleration of Car Impacting Short Radius with Two Tension Cables and Six 700-Lb Sand Drums.	84
Figure 3.64.	Longitudinal Acceleration of Car Impacting Short Radius with Two Tension Cables and Six 700-Lb Sand Drums.	84
Figure 3.65.	Longitudinal Acceleration of Car Impacting Short Radius with Two Tension Cables and Six 700-Lb Sand Drums.	84
Figure 3.66.	Roll, Pitch, and Yaw Angles for the Simulation of Car Impacting Short Radius with Two Tension Cables and Six 700-Lb Sand Drums.	85
Figure 3.67.	Alignment of Car with System.	85
Figure 3.68.	Sequential Images of Car Simulation with Two Tension Cables and Six 700-lb Sand Drums.	86
Figure 3.69.	Sequential Images of Simulation (Top View).	87
Figure 3.70.	Interaction of Car with System (No Drums Visible).	87
Figure 3.71.	Final State of Simulation (No Drums Visible).	88
Figure 3.72.	Longitudinal Acceleration of Car Impacting Short Radius with Two Tension Cables and Six 700-Lb Sand Drums.	89
Figure 3.73.	Longitudinal Acceleration of Car Impacting Short Radius with Two Tension Cables and Six 700-Lb Sand Drums.	89
Figure 3.74.	Longitudinal Acceleration of Car Impacting Short Radius with Two Tension Cables and Six 700-Lb Sand Drums.	89
Figure 3.75.	Roll, Pitch, and Yaw Angle of Car Impacting Short Radius with Two Tension Cables and Six 700-Lb Sand Drums.	90
Figure 3.76.	Alignment of Car with System.	90
Figure 3.77.	Sequential Images of Car Simulation with Two Tension Cables and Six 700-lb Sand Drums.	91
Figure 3.78.	Sequential Images of Simulation (Top View).	92
Figure 3.79.	Longitudinal Acceleration of Car Impacting Short Radius with Two Tension Cables and Six 700-Lb Sand Drums.	93
Figure 3.80.	Lateral Acceleration of Car Impacting Short Radius with Two Tension Cables and Six 700-Lb Sand Drums.	93
Figure 3.81.	Vertical Acceleration of Car Impacting Short Radius with Two Tension Cables and Six 700-Lb Sand Drums.	93
Figure 3.82.	Roll, Pitch, and Yaw Angles of Car Impacting Short Radius with Two Tension Cables and Six 700-Lb Sand Drums.	94
Figure 4.1.	Overall Details of the TxDOT Low-Speed Short Radius Guardrail Treatment.	99
Figure 4.2.	TxDOT Low-Speed Short Radius Guardrail Treatment prior to Test Nos. 469137-3-1 and 469138-3-4.	100
Figure 4.3.	Details of the Cable used for Test Nos. 469138-3-3 and 469138-3-4.	101
Figure 4.4.	Cable prior to Test Nos. 469138-3-3 and 469138-3-4.	103
Figure 5.1.	Target CIP for *MASH* Test 2-33 on the TxDOT Low-Speed Short Radius Guardrail Treatment.	105

LIST OF FIGURES (CONTINUED)

		Page
Figure 5.2.	Target CIP for *MASH* Test 2-32 on the TxDOT Low-Speed Short Radius Guardrail Treatment.	106
Figure 5.3.	Target CIP for *MASH* Test 2-31 on the TxDOT Low-Speed Short Radius Guardrail Treatment.	106
Figure 5.4.	Target CIP for *MASH* Test 2-35 on the TxDOT Low-Speed Short Radius Guardrail Treatment.	107
Figure 5.5.	Target CIP for Modified *MASH* Test 2-34 on the TxDOT Low-Speed Short Radius Guardrail Treatment.	107
Figure 7.1.	TxDOT Low-Speed Short Radius Guardrail Treatment/Test Vehicle Geometrics for Test No. 469137-3-1.	113
Figure 7.2.	Test Vehicle before Test No. 469137-3-1.	114
Figure 7.3.	TxDOT Low-Speed Short Radius Guardrail Treatment after Test No. 469137-3-1.	116
Figure 7.4.	Damage to Rail Section Perpendicular to Roadway after Test No. 469137-3-1.	117
Figure 7.5.	Damage to Nose after Test No. 469137-3-1.	118
Figure 7.6.	Damage to Rail Section Parallel to Roadway after Test No. 469137-3-1.	119
Figure 7.7.	Test Vehicle after Test No. 469137-3-1.	119
Figure 7.8.	Interior of Test Vehicle for Test No. 469137-3-1.	120
Figure 7.9.	Summary of Results for *MASH* Test 2-33 on the TxDOT Low-Speed Short Radius Guardrail Treatment.	121
Figure 8.1.	TxDOT Low-Speed Short Radius Guardrail Treatment/Test Vehicle Geometrics for Test No. 469137-3-2.	123
Figure 8.2.	Test Vehicle before Test No. 469137-3-2.	124
Figure 8.3.	TxDOT Low-Speed Short Radius Guardrail Treatment and Test Vehicle after Test No. 469137-3-2.	126
Figure 8.4.	Test Article after Test No. 469137-3-2.	126
Figure 8.5.	Field Side of Test Article after Test No. 469137-3-2.	127
Figure 8.6.	Damage to Cables after Test No. 469137-3-2.	127
Figure 8.7.	Test Vehicle after Test No. 469137-3-2.	128
Figure 8.8.	Interior of Test Vehicle for Test No. 469137-3-2.	129
Figure 8.9.	Summary of Results for *MASH* Test 2-32 on TxDOT Low-Speed Short Radius Guardrail Treatment.	131
Figure 9.1.	TxDOT Low-Speed Short Radius Guardrail Treatment/Test Vehicle Geometrics for Test No. 469138-3-3.	133
Figure 9.2.	Test Vehicle before Test No. 469138-3-3.	134
Figure 9.3.	TxDOT Low-Speed Short Radius Guardrail Treatment after Test No. 469138-3-3.	135
Figure 9.4.	Damage to Rail Section Perpendicular to Roadway after Test No. 469138-3-3.	136
Figure 9.5.	Damage to Rail Section Parallel to Roadway after Test No. 469138-3-3.	137
Figure 9.6.	Damage to Cable and Post 12 after Test No. 469138-3-3.	137
Figure 9.7.	Test Vehicle after Test No. 469138-3-3.	138

LIST OF FIGURES (CONTINUED)

		Page
Figure 9.8.	Interior of Test Vehicle for Test No. 469138-3-3.	138
Figure 9.9.	Summary of Results for *MASH* Test 2-31 on the TxDOT Low-Speed Short Radius Guardrail Treatment.	140
Figure 10.1.	TxDOT Low-Speed Short Radius Guardrail Treatment/Test Vehicle Geometrics for Test No. 469138-3-4.	143
Figure 10.2.	Test Vehicle before Test No. 469138-3-4.	144
Figure 10.3.	TxDOT Low-Speed Short Radius Guardrail Treatment after Test No. 469138-3-4.	145
Figure 10.4.	Damage to Rail Section Parallel to Roadway after Test No. 469138-3-4.	146
Figure 10.5.	Damage to Post 13 through 10 after Test No. 469138-3-4.	147
Figure 10.6.	Test Vehicle after Test No. 469138-3-4.	148
Figure 10.7.	Interior of Test Vehicle for Test No. 469138-3-4.	148
Figure 10.8.	Summary of Results for *MASH* Test 2-35 on the TxDOT Low-Speed Short Radius Guardrail Treatment.	150
Figure 11.1.	TxDOT Low-Speed Short Radius Guardrail /Test Vehicle Geometrics for Test No. 469138-3-5.	153
Figure 11.2.	Test Vehicle before Test No. 469138-3-5.	154
Figure 11.3.	TxDOT Low-Speed Short Radius Guardrail/Test Vehicle after Test No. 469138-3-5.	155
Figure 11.4.	TxDOT Low-Speed Short Radius Guardrail after Test No. 469138-3-5.	155
Figure 11.5.	Rear of Installation after Test No. 469138-3-5.	156
Figure 11.6.	Posts 11 through 14 after Test No. 469138-3-5.	156
Figure 11.7.	Test Vehicle after Test No. 469138-3-5.	157
Figure 11.8.	Interior of Test Vehicle for Test No. 469138-3-5.	157
Figure 11.9.	Summary of Results for *MASH* Test 2-34 on the TxDOT Low-Speed Short Radius Guardrail Treatment.	159
Figure D.1.	Sequential Photographs for Test No. 469137-3-1 (Overhead and Rear Views).	205
Figure D.2.	Sequential Photographs for Test No. 469137-3-1 (Perpendicular Views).	207
Figure D.3.	Vehicle Angular Displacements for Test No. 469137-3-1.	209
Figure D.4.	Vehicle Longitudinal Accelerometer Trace for Test No. 469137-3-1 (Accelerometer Located at Center of Gravity).	210
Figure D.5.	Vehicle Lateral Accelerometer Trace for Test No. 469137-3-1 (Accelerometer Located at Center of Gravity).	211
Figure D.6.	Vehicle Vertical Accelerometer Trace for Test No. 469137-3-1 (Accelerometer Located at Center of Gravity).	212
Figure D.7.	Vehicle Longitudinal Accelerometer Trace for Test No. 469137-3-1 (Accelerometer Located Rear of Center of Gravity).	213
Figure D.8.	Vehicle Lateral Accelerometer Trace for Test No. 469137-3-1 (Accelerometer Located Rear of Center of Gravity).	214
Figure D.9.	Vehicle Vertical Accelerometer Trace for Test No. 469137-3-1 (Accelerometer Located Rear of Center of Gravity).	215

LIST OF FIGURES (CONTINUED)

		Page
Figure E.1.	Sequential Photographs for Test No. 469137-3-2 (Overhead and Frontal Views).	220
Figure E.2.	Sequential Photographs for Test No. 469137-3-2 (Perpendicular Views).	222
Figure E.3.	Vehicle Angular Displacements for Test No. 469137-3-2.	224
Figure E.4.	Vehicle Longitudinal Accelerometer Trace for Test No. 469137-3-2 (Accelerometer Located at Center of Gravity).	225
Figure E.5.	Vehicle Lateral Accelerometer Trace for Test No. 469137-3-2 (Accelerometer Located at Center of Gravity).	226
Figure E.6.	Vehicle Vertical Accelerometer Trace for Test No. 469137-3-2 (Accelerometer Located at Center of Gravity).	227
Figure E.7.	Vehicle Longitudinal Accelerometer Trace for Test No. 469137-3-2 (Accelerometer Located Rear of Center of Gravity).	228
Figure E.8.	Vehicle Lateral Accelerometer Trace for Test No. 469137-3-2 (Accelerometer Located Rear of Center of Gravity).	229
Figure E.9.	Vehicle Vertical Accelerometer Trace for Test No. 469137-3-2 (Accelerometer Located Rear of Center of Gravity).	230
Figure F.1.	Sequential Photographs for Test No. 469138-3-3 (Overhead and Frontal Views).	235
Figure F.2.	Sequential Photographs for Test No. 469138-3-3 (Perpendicular View).	237
Figure F.3.	Vehicle Angular Displacements for Test No. 469138-3-3.	238
Figure F.4.	Vehicle Longitudinal Accelerometer Trace for Test No. 469138-3-3 (Accelerometer Located at Center of Gravity).	239
Figure F.5.	Vehicle Lateral Accelerometer Trace for Test No. 469138-3-3 (Accelerometer Located at Center of Gravity).	240
Figure F.6.	Vehicle Vertical Accelerometer Trace for Test No. 469138-3-3 (Accelerometer Located at Center of Gravity).	241
Figure F.7.	Vehicle Longitudinal Accelerometer Trace for Test No. 469138-3-3 (Accelerometer Located Rear of Center of Gravity).	242
Figure F.8.	Vehicle Lateral Accelerometer Trace for Test No. 469138-3-3 (Accelerometer Located Rear of Center of Gravity).	243
Figure F.9.	Vehicle Vertical Accelerometer Trace for Test No. 469138-3-3 (Accelerometer Located Rear of Center of Gravity).	244
Figure G.1.	Sequential Photographs for Test No. 469138-3-4 (Overhead and Frontal Views).	249
Figure G.2.	Sequential Photographs for Test No. 469138-3-4 (Rear View).	251
Figure G.3.	Vehicle Angular Displacements for Test No. 469138-3-4.	252
Figure G.4.	Vehicle Longitudinal Accelerometer Trace for Test No. 469138-3-4 (Accelerometer Located at Center of Gravity).	253
Figure G.5.	Vehicle Lateral Accelerometer Trace for Test No. 469138-3-4 (Accelerometer Located at Center of Gravity).	254
Figure G.6.	Vehicle Vertical Accelerometer Trace for Test No. 469138-3-4 (Accelerometer Located at Center of Gravity).	255

LIST OF FIGURES (CONTINUED)

		Page
Figure G.7.	Vehicle Longitudinal Accelerometer Trace for Test No. 469138-3-4 (Accelerometer Located Rear of Center of Gravity).	256
Figure G.8.	Vehicle Lateral Accelerometer Trace for Test No. 469138-3-4 (Accelerometer Located Rear of Center of Gravity).	257
Figure G.9.	Vehicle Vertical Accelerometer Trace for Test No. 469138-3-4 (Accelerometer Located Rear of Center of Gravity).	258
Figure H.1.	Sequential Photographs for Test No. 469138-3-5 (Overhead and Frontal Views).	262
Figure H.2.	Vehicle Angular Displacements for Test No. 469138-3-5.	264
Figure H.3.	Vehicle Longitudinal Accelerometer Trace for Test No. 469138-3-5 (Accelerometer Located at Center of Gravity).	265
Figure H.4.	Vehicle Lateral Accelerometer Trace for Test No. 469138-3-5 (Accelerometer Located at Center of Gravity).	266
Figure H.5.	Vehicle Vertical Accelerometer Trace for Test No. 469138-3-5 (Accelerometer Located at Center of Gravity).	267
Figure H.6.	Vehicle Longitudinal Accelerometer Trace for Test No. 469138-3-5 (Accelerometer Located Rear of Center of Gravity).	268
Figure H.7.	Vehicle Lateral Accelerometer Trace for Test No. 469138-3-5 (Accelerometer Located Rear of Center of Gravity).	269
Figure H.8.	Vehicle Vertical Accelerometer Trace for Test No. 469138-3-5 (Accelerometer Located Rear of Center of Gravity).	270

LIST OF TABLES

		Page
Table 2.1.	TRAP Summary Data for Simulation with Car and Strap.	16
Table 2.2.	TRAP Summary Data for Simulation with Truck and Strap.	19
Table 2.3.	TRAP Summary Data for Simulation of Truck with Flare and 18-lb Sand Drums.	32
Table 3.1.	TRAP Summary Data of Simulation with Tension Cable and Four 700-lb Sand Drums.	43
Table 3.2.	TRAP Summary Data of Simulation with Tension Cable and Four 700-lb Sand Drums.	46
Table 3.3.	TRAP Summary Data of Simulation with Tension Cable and Five 700-lb Sand Drums.	49
Table 3.4.	TRAP Summary Data of Simulation with Tension Cable and Six 700-lb Sand Drums.	52
Table 3.5.	TRAP Summary Data of Simulation with Two Tension Cables and 700-lb Sand Drums.	55
Table 3.6.	TRAP Summary Data of Simulation with Tension Cable and Six 700-lb Sand Drums.	57
Table 3.7.	TRAP Summary Data of Simulation with Two Tension Cables and Six 700-lb Sand Drums.	61
Table 3.8.	TRAP Summary Data of Simulation with Two Tension Cables and Six 700-lb Sand Drums.	64
Table 3.9.	TRAP Summary Data of Simulation with Two Tension Cables and Six 700-lb Sand Drums.	67
Table 3.10.	TRAP Summary Data of Simulation with Two Tension Cables and Six 700-lb Sand Drums.	70
Table 3.11.	TRAP Summary Data of Simulation with Two Tension Cables and Six 700-lb Sand Drums.	74
Table 3.12.	TRAP Summary Data of Simulation with Two Tension Cables and Six 700-lb Sand Drums.	77
Table 3.13.	TRAP Summary Data of Simulation with Two Tension Cables and Six 700-lb Sand Drums.	80
Table 3.14.	TRAP Summary Data of Simulation with Two Tension Cables and Six 700-lb Sand Drums.	83
Table 3.15.	TRAP Summary Data of Simulation with Two Tension Cables and Six 700-lb Sand Drums.	88
Table 5.1.	Test Conditions and Evaluation Criteria Specified for *MASH* TL-2 Non-Gating End Treatments.	105
Table 5.2.	Evaluation Criteria Required for *MASH* TL-2 Non-Gating End Treatments	108
Table 7.1.	Events during Test No. 469137-3-1.	115
Table 7.2.	Occupant Risk Factors for Test No. 469137-3-1.	120
Table 7.3.	Performance Evaluation Summary for *MASH* Test 2-33 on the TxDOT Low-Speed Short Radius Guardrail Treatment	122
Table 8.1.	Events during Test No. 469137-3-2.	124
Table 8.2.	Occupant Risk Factors for Test No. 469137-3-2.	130

LIST OF TABLES (CONTINUED)

		Page
Table 8.3.	Performance Evaluation Summary for *MASH* Test 2-32 on the TxDOT Low-Speed Short Radius Guardrail Treatment	132
Table 9.1.	Events during Test No. 469138-3-3.	134
Table 9.2.	Occupant Risk Factors for Test No. 469138-3-3.	139
Table 9.3.	Performance Evaluation Summary for *MASH* Test 2-31 on the TxDOT Low-Speed Short Radius Guardrail Treatment	141
Table 10.1.	Events during Test No. 469138-3-4.	144
Table 10.2.	Occupant Risk Factors for Test No. 469138-3-4.	149
Table 10.3.	Performance Evaluation Summary for *MASH* Test 2-35 on the TxDOT Low-Speed Short Radius Guardrail Treatment	151
Table 11.1.	Events during Test No. 469138-3-5.	154
Table 11.2.	Occupant Risk Factors for Test No. 469138-3-5.	158
Table 11.3.	Performance Evaluation Summary for Modified *MASH* Test 2-34 on the TxDOT Low-Speed Short Radius Guardrail Treatment.	160
Table 12.1.	Assessment Summary for *MASH* TL-2 Testing on the TxDOT Low-Speed Short Radius Guardrail Treatment.	163
Table C.1.	Summary of Strong Soil Test Results for Establishing Installation Procedure.	195
Table C.2.	Test Day Static Soil Strength Documentation for Test No. 469137-3-1.	196
Table C.3.	Test Day Static Soil Strength Documentation for Test No. 469137-3-2.	197
Table C.4.	Test Day Static Soil Strength Documentation for Test No. 469138-3-3.	198
Table C.5.	Test Day Static Soil Strength Documentation for Test No. 469138-3-4.	199
Table C.6.	Test Day Static Soil Strength Documentation for Test No. 469138-3-5.	200
Table D.1.	Vehicle Properties for Test No. 469137-3-1.	201
Table D.2.	Measurements of Vehicle Vertical CG for Test No. 469137-3-1.	202
Table D.3.	Exterior Crush Measurements of Vehicle for Test No. 469137-3-1.	203
Table D.4.	Occupant Compartment Measurements of Vehicle for Test No. 469137-3-1.	204
Table E.1.	Vehicle Properties for Test No. 469137-3-2.	217
Table E.2.	Exterior Crush Measurements for Test No. 469137-3-2.	218
Table E.3.	Occupant Compartment Measurements for Test No. 469137-3-2.	219
Table F.1.	Vehicle Properties for Test No. 469138-3-3.	231
Table F.2.	Measurements of Vehicle Vertical CG for Test No. 469137-3-1.	232
Table F.3.	Exterior Crush Measurements of Vehicle for Test No. 469138-3-3.	233
Table F.4.	Occupant Compartment Measurements of Vehicle for Test No. 469138-3-3	234
Table G.1.	Vehicle Properties for Test No. 469138-3-4.	245
Table G.2.	Measurements of Vehicle Vertical CG for Test No. 469138-3-4.	246
Table G.3.	Exterior Crush Measurements of Vehicle for Test No. 469138-3-4.	247
Table G.4.	Occupant Compartment Measurements of Vehicle for Test No. 469138-3-4	248
Table H.1.	Vehicle Properties for Test No. 469138-3-5.	259
Table H.2.	Exterior Crush Measurements for Test No. 469138-3-5.	260
Table H.3.	Occupant Compartment Measurements for Test No. 469138-3-5.	261

CHAPTER 1:
INTRODUCTION

1.1 PROBLEM

When a secondary road or driveway intersects a highway in close proximity to a bridge, it is difficult to fit the proper guardrail length along the primary roadway to properly protect motorists from hazards underlying the bridge. In such instances, the available right-of-way and constrained distance between the bridge and secondary roadway or driveway can severely limit the application of effective safety treatments. One solution is to apply a tight radius to the guardrail in order to turn it from the primary road to the secondary road. A crashworthy solution for a short radius guardrail treatment has eluded roadside safety researchers for two decades. Texas A&M Transportation Institute (TTI) researchers have developed an innovative short radius guardrail system for implementation on high-speed roadways; however, there are many roadways with restrictive roadside clearances that cannot accommodate the new short radius guardrail treatment. Many of these sites exist along low-speed roadways, which is classified as a roadway with a speed limit of 45 mph or less. A shorter, more economical short radius guardrail system, suitable for implementation on lower speed roadways, is needed. TTI researchers were tasked with developing a short radius guardrail system to meet American Association of State Highway and Transportation Officials (AASHTO) *Manual for Assessing Safety Hardware* (*MASH*) Test Level 2 (TL-2) performance criteria for use on low-speed roadways (*1*).

1.2 SCOPE OF RESEARCH

This project resulted in a *MASH* TL-2 crashworthy short radius guardrail system that is designed to be used by the Texas Department of Transportation (TxDOT) on applicable low-speed roadway intersections. TTI researchers incorporated the design details into the TxDOT standard specifications for use on applicable roadways statewide. Furthermore, this *MASH* TL-2 compliant short radius guardrail system was designed for national acceptance by AASHTO and possible implementation by other state departments of transportation.

In looking at the challenges facing the design of a successful low-speed short-radius guardrail system, TTI researchers addressed key features, such as energy absorption and tension of the guardrail system at the nose section. The remaining significant challenge was to design for more restrictive site conditions with a 45-mph impact speed. TTI researchers performed the tasks outlined below to address the research objectives.

1.2.1 Task 1. Establish Design Requirements and Site Constraints.

TTI researchers established design requirements and site constraints that influence the design of the *MASH* TL-2 short radius guardrail system. With due consideration given to the design requirements and constraints identified by TxDOT under the initial part of this task, TTI researchers conceptualized new designs for a *MASH* TL-2 short radius guardrail system. TTI researchers developed these initial design concepts using knowledge gleaned from engineering reviews of previous tests, crash test experiences gained from TxDOT Project 0-6711, Short Radius *MASH* TL-3 Guardrail Treatment, and the technical skills of TTI researchers (*3*, *4*). In addition to the key aspect of impact performance, TTI researchers considered factors including

hardware inventory, cost, maintenance and repair, compatibility with other existing systems, and others issues deemed appropriate by the TxDOT project team.

TTI researchers submitted drawings of the concepts to the TxDOT project team for review. Afterward, TTI researchers met with the TxDOT project team to discuss, select, and prioritize the design concepts for further engineering design and analysis under Task 2. TTI researchers incorporated the desired changes to the selected designs into the design concepts.

TTI researchers provided deliverables for Task 1 in a technical memorandum (TM-1), per the deliverables table, containing design concepts for further engineering design and analysis.

1.2.2 Task 2. Develop Finite Element Models for Candidate Designs

TTI researchers conducted finite element analyses of the recommended concepts developed in Task 1 to simulate the recommended *MASH* TL-2 test matrix for this system. TTI researchers explicitly modeled the recommended *MASH* TL-2 short radius designs to obtain high reliability in the simulation. Utilizing the already developed models for the *MASH* TL-3 short radius system developed in TxDOT project 0-6711, TTI researchers performed calibration given the available test data.

TTI researchers utilized simulations to provide performance evaluations for each short radius concept developed in Task 1:

a. Detailed modeling and enhanced simulation of promising concepts to identify candidate concept.

b. Detailed all key system components explicitly.

c. Simulated key crash tests conditions (3-31, 3-32, 3-33, and 3-35).

d. Reviewed designs with the TxDOT project team, identify the candidate design, and prioritize if there is more than one promising design.

e. Simulated other crash test conditions as needed.

f. Recommended candidates design for testing.

TTI researchers conveyed a recommendation of designs for full-scale crash testing to the TxDOT project team for approval and selection of the final candidate design.

The deliverable for Task 2 was a technical memorandum (TM-2), per the deliverables table, detailing the finite element models for candidate designs and their simulation performances under *MASH* TL-2 test conditions. The simulations are to be conducted using *LS-DYNA* nonlinear explicit finite element code (*2*).

1.2.3 Task 3. Conduct Full-Scale Crash Testing

TTI researchers constructed the recommended short radius guardrail system upon approval of the final design details by the TxDOT project team. TTI researchers conducted full-scale crash tests in compliance with *MASH* TL-2 test conditions following the test matrix established and agreed upon under Task 1. TTI researchers performed these tests using their facilities.

If the short radius system exhibits unsatisfactory performance in one of the four crash tests, TTI researchers were to address these deficiencies through design modifications and additional simulations. TTI researchers would then present any recommended design modifications to the TxDOT project team for review and approval.

TTI researchers would conduct further tests on a modified short radius system upon approval by the TxDOT project team. TTI researchers estimated two contingency crash tests for this purpose.

The deliverable for Task 3 shall be a technical memorandum (TM-3), per the deliverables table, containing details of the full-scale crash tests.

1.2.4 Task 4. Prepare Research Reports

TTI researchers documented the results in research report R1 and submited the report to TxDOT. This research report includes the developed design details of the successful *MASH* TL-2 short radius guardrail system that is to be used to develop a standard detail sheet.

1.3 OBJECTIVE

The purpose of the testing reported herein was to assess the performance of the *MASH* TL-2 low-speed short radius guardrail treatment according to the safety-performance evaluation guidelines included in AASHTO *MASH*. The crash tests performed were in accordance with *MASH* TL-2.

CHAPTER 2:
DEVELOPMENT OF FINITE ELEMENT MODELS FOR CANDIDATE DESIGNS

2.1. BACKGROUND

The research team conducted pendulum tests on several guardrail posts and reviewed promising design features for the guardrail system to obtain data. This in turn helped in developing a short radius guardrail system to meet *MASH* Test Level 2 (TL-2) performance criteria for use on low speed roadways.

Researchers sought to develop a short radius guardrail system design by reviewing the challenges encountered by previous designs, promising design features of previous designs and short radius concepts.

2.2 DESIGN CONSIDERATION

The short radius used for these tests consisted of a transition between a guardrail to concrete bridge rail. A TL-2 transition from a 31-inch tall strong-post W-beam approach guardrail to a rigid concrete bridge parapet was developed by researchers, R. Bligh and D. Arrington. The researchers performed analyses using a computer simulation technique to assess the ability of the selected design concepts to meet *MASH* impact performance criteria prior to conducting any full scale crash tests [3]. For each simulation, the approach guardrail was assumed to be a strong-post W-beam guardrail. The 12-gauge W-beam rail was mounted to 6-ft long, W6×9 steel posts at a height of 31 inches to the top of the rail. The posts were spaced on 6 ft-3 inch centers, and 8-inch deep offset blocks were incorporated between the rail and posts. The concrete bridge rail parapet was modeled as a rigid barrier to represent the worst-case condition. The details of the selected TL-2 transition design were finalized and subjected to full-scale crash tests in accordance with *MASH* guidelines.

The selected transition design from the parapet to the guardrail, includes a length of the bridge parapet and the approached guardrail. The concrete bridge parapet was an existing 36-inch tall single slope traffic rail (SSTR). A 37.5-inch long section of 12-gauge thrie beam rail was attached to the face of the parapet using a 10-gauge thrie beam terminal connector. For the test, the terminal connector and the parapet were attached by using five 0.825-inch diameter, A325 hex head through bolts.

Three different post types are permitted in a guardrail system by TxDOT: W6×9 steel posts, 7-inch diameter round wood posts, and 6-inch × 8-inch rectangular wood posts. Researchers concluded that a W6×9 steel post would be used, since it would constitute the most critical condition in regard to post snagging. By using the most critical post type, a successful result would also be applicable to the other post types.

The first W6×9 steel post is located 29 inches from the end of the parapet with a 6-inch × 8-inch × 22-inch routered wood blockout. The post included a 10-inch long button head bolt with recessed guardrail nut only on the top hole. The next two posts were spaced 37.5 inches on center. A 10-gauge thrie beam rail, 37.5 inches long, spanned the space between the parapet and post 11.

The new *MASH* TL-2 transition was developed and successfully crash tested. The results showed that the new *MASH* TL-2 transition met all the requirements of *MASH* for all crash tests. The vehicles remained stable and the occupant risk indices were below the preferred limits recommended in *MASH*. Figure 2.1 shows the described transition design tested. This transition system design was modeled as a point of reference for new design concepts that are incorporated in the TL-2 short radius system design.



Figure 2.1. *MASH* TL-2 Transition before Test No. 420021-4.

2.3 SIMULATION OF RECOMMENDED DESIGN CONCEPTS

2.3.1 Case 1 – TL-3 System without Sand Drums

2.3.1.1 System Details

A guardrail system design was evaluated in a simulation. Figure 2.2 depicts the whole guardrail system. This system includes a long tension cable behind the curved section of the rail. The vehicle impacted this system at the center of the radius at a 25° angle. The vehicle was approaching the system at a speed of 45 mph.



Figure 2.2. Entire System with Cable.

A single thrie beam system design was evaluated through simulations. The guardrail system consists of a 31-inch tall guardrail system with a 36-ft long primary-road from end of nose to end of parapet, and a 20-ft long secondary-road after the nose. The nose, curved section, has a radius of 8 ft-4 inches.

Figure 2.3 shows the side view of the primary roadway. The primary roadway consists of nine steel posts and three controlled release timber (CRT) posts. Figure 2.4 represents the side view of the secondary roadway. The secondary roadway has three CRT posts with only two CRT post with blockouts. A rigid post in the simulation anchored this end. The curved section has one CRT timber post, and the post includes a sheath. The simulated parapet section represents the stiffer portion of the installation.



Figure 2.3. Side View of Primary Roadway.

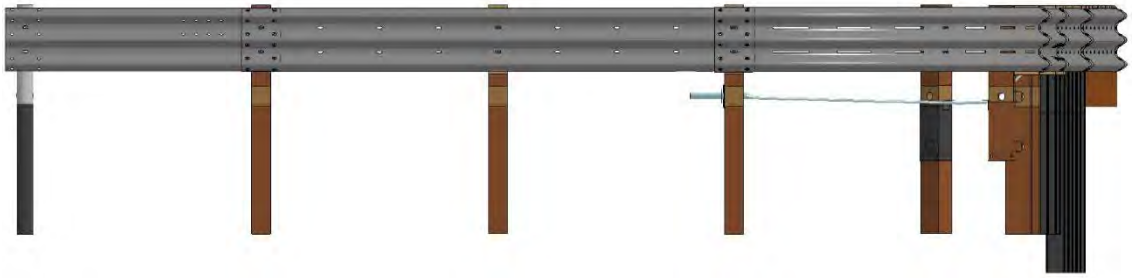


Figure 2.4. Side View of Secondary Roadway.

2.3.1.2 Simulation of Car Impacting TL-3 Short Radius System without Sand Barrels

Figure 2.5 presents the progression of the small car in this simulation. Upon impact, the rail and deformation of the front of the car progress into the windshield of the car, which is an undesirable behavior for the system.

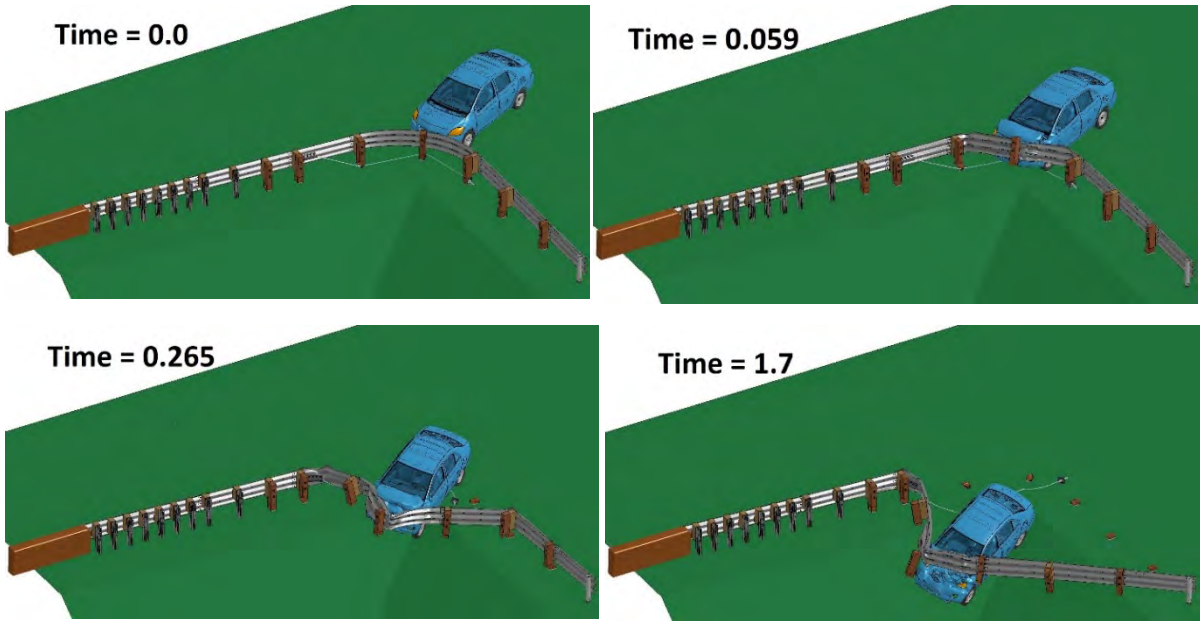


Figure 2.5. Sequential Images of Car Simulation with Cable.

Figures 2.6 and 2.7 show images of the initial and end state of the simulation, respectively. Figure 2.7 shows a close up image of the car going under the guardrail damaging the front of the car and windshield. It is also noticed that the tires rolled over the cable without much effect.

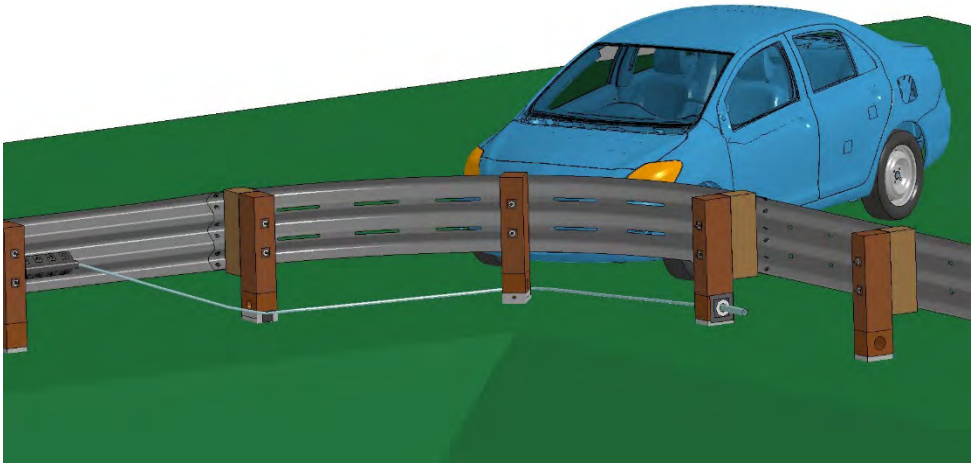


Figure 2.6. Initial State of the Simulation.

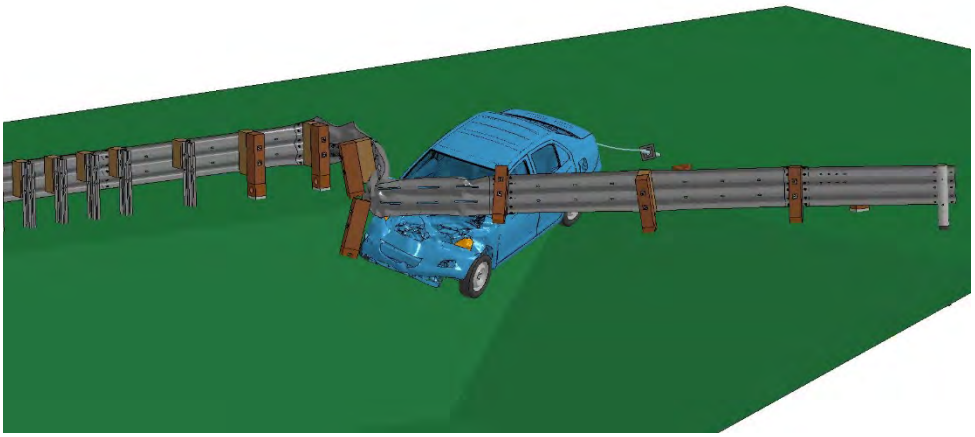


Figure 2.7. Final State of the Simulation.

2.3.1.3 Simulation of Truck Impacting Short Radius with Cable

Figure 2.8 shows sequential images of the simulation of the truck upon impact. The first image shows the initial position of the system and is followed by three images of the truck interacting with the rail. The guardrail system is already deforming by the time of 0.235 s. At time 0.415 s, the truck begins to override the guardrail system, and by 0.775 s, the truck has completely overridden the system. The truck was not contained by the guardrail system.

Figures 2.9 and 2.10 show the initial and final state images of the simulation of the truck with cable, respectively. Figure 2.10 shows the deformation of the guardrail system and the truck. Five posts from the system broke while the remaining posts stayed intact. The truck was bent from the front, and the right front tire was deformed as well.

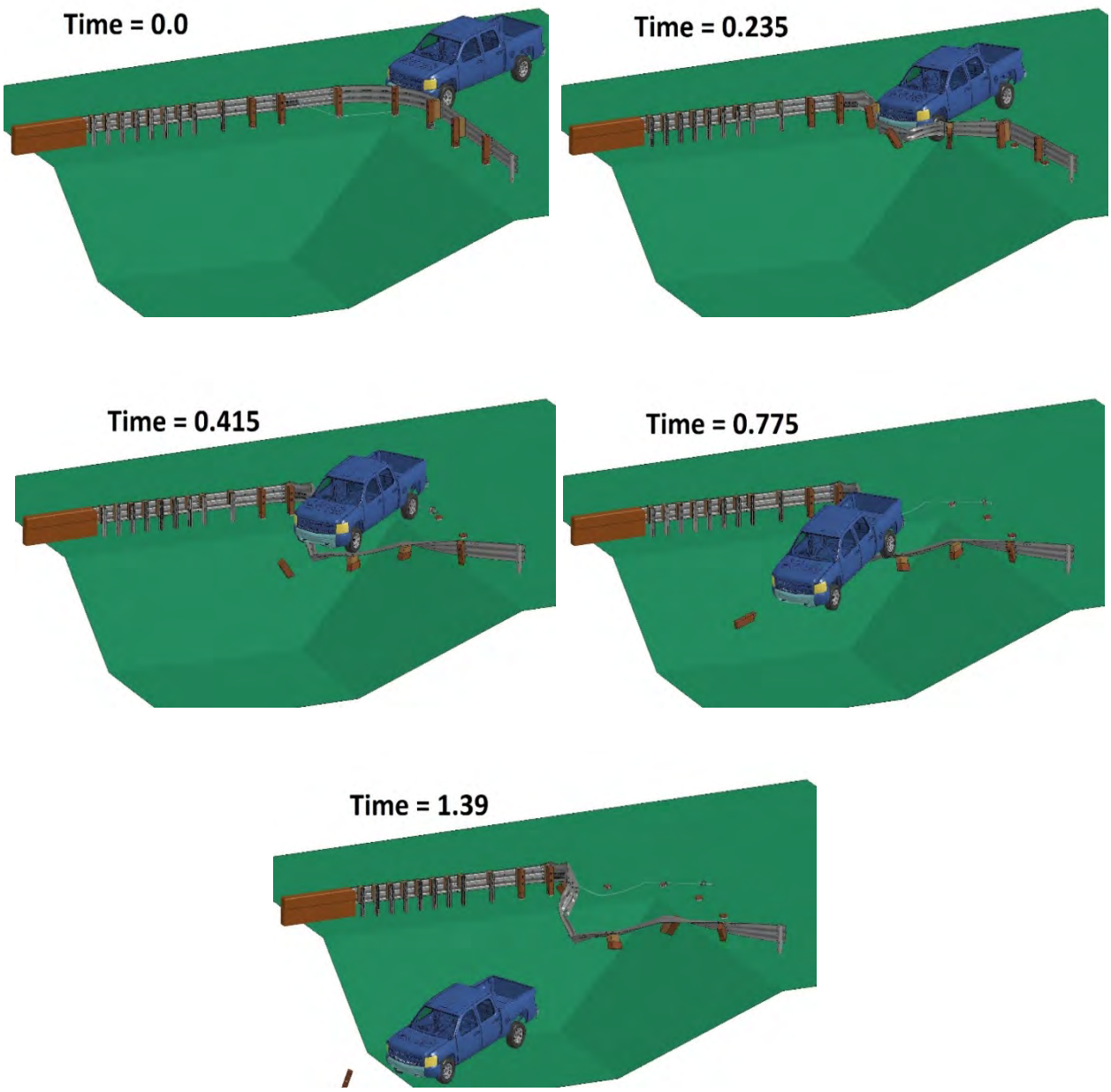


Figure 2.8. Sequential Images of Truck Simulation with Flare.

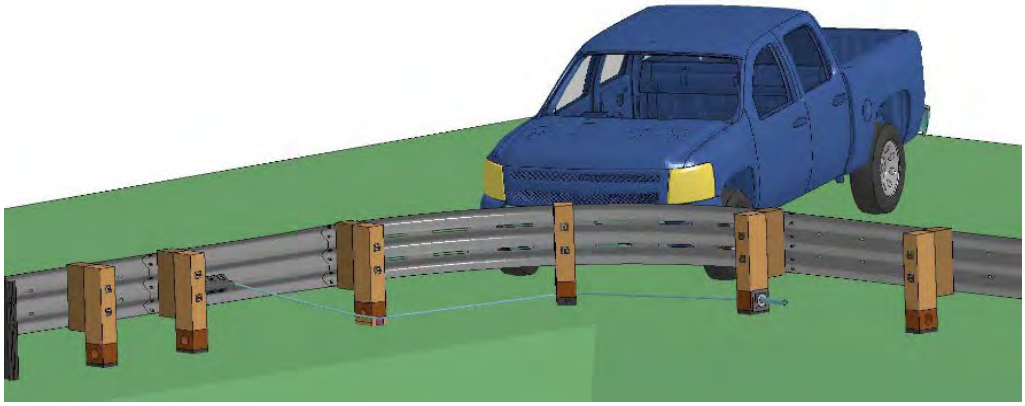


Figure 2.9. Initial State of Simulation.

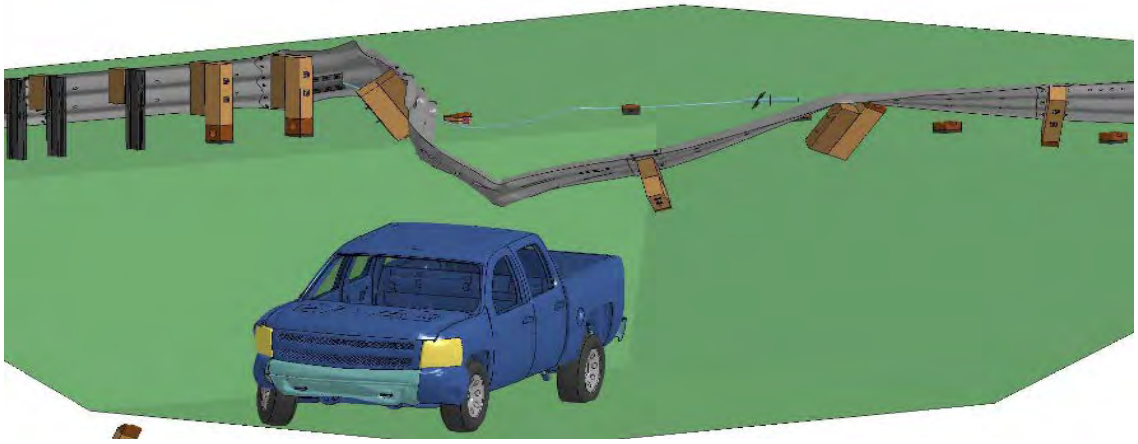


Figure 2.10. Final State of Simulation.

2.3.2 Case 2 – Large (16-ft) Radius System

2.3.2.1 System Details

The following simulation includes a different guardrail system design from the first simulation. Figure 2.11 depicts the whole guardrail system. It has no energy-absorbing systems behind the curved section of the rail. It is a longer guardrail system. The vehicle impact to the system has the same impact angle and speed from the first simulation, 45 mph at a 25° angle.

The guardrail system consists of a 31-inch tall, 104-ft long short radius guardrail system with a 17-ft long primary-road thrie-beam from end of nose to end of parapet, and a 90-ft long secondary-road after the nose, with a 7 ft-3 inch taper transition from a thrie-beam to W-beam. The nose, curved section, has a radius of 16 ft-8 inches.

Figure 2.12 shows the side view of the primary roadway. The primary roadway consists of three steel posts. Figure 2.13 represents the side view of the secondary roadway. The

secondary roadway has three CRT posts with a blockout and 11 steel posts. The curved section has three CRT posts. The simulated parapet section represents the stiffer portion of the rail.



Figure 2.11. Extended Short Radius System with No Flare.



Figure 2.12. Primary Roadway Side View.



Figure 2.13. Secondary Roadway Side View.

2.3.2.2 Simulation of Truck Impacting System

Figure 2.14 presents the sequential images of the motion of the truck as it impacts the nose section of the system. The truck remains stable during the simulation. The first image shows the initial position of the system and is followed by three images of the truck interacting with the rail. At time 0.375 s, the truck has overridden the system. The last image displays the end state of the simulation and shows that the truck has completely gone over the system. The simulation of the system shows that the system is not adequate to contain the truck.

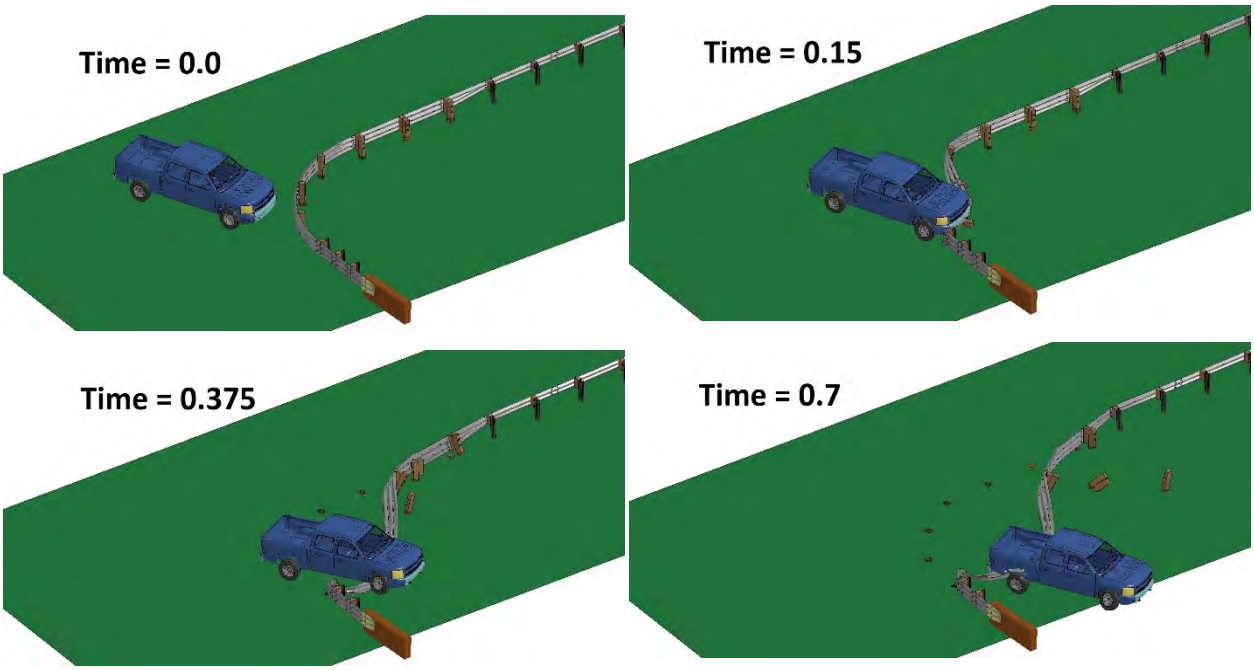


Figure 2.14. Sequential Images of Simulation with No Cable.

Figures 2.15 and 2.16 show the initial and final state of the simulation of the truck, respectively. In the final frame of the simulation, the guardrail system has deformed and seven of the posts broke while two steel posts to the right of the thrie beam end shoe appear to remain intact.

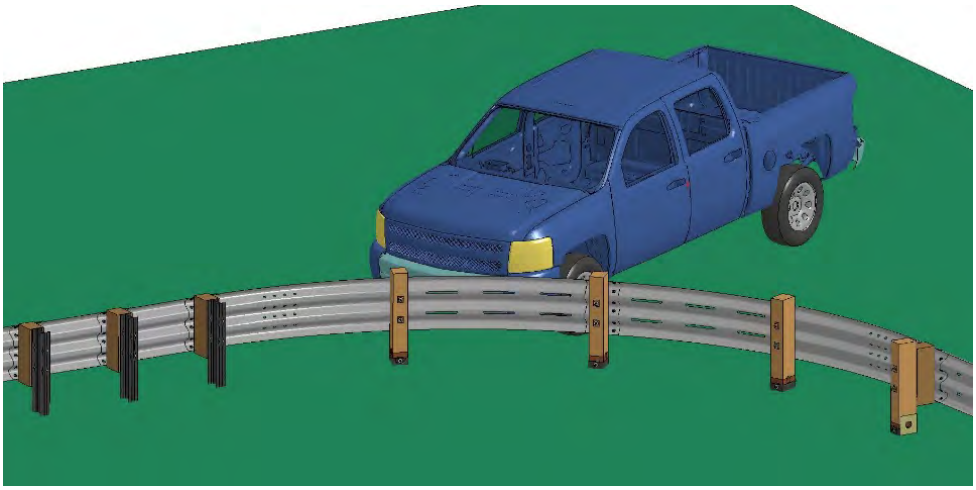


Figure 2.15. Initial State of Simulation.



Figure 2.16. Final State of Simulation.

2.3.3 Case 3

2.3.3.1 System Details

Figure 2.17 presents the system layout for this simulation. This system is surrounding a ditch. As previously concluded, since the system did not contain the truck, a strap was added to the back of the guardrail, as shown in Figure 2.18. To make the strap stand out, it has been colored red. The strap has a height of 12 inches and starts 7 ft from the end of the parapet. It goes along the guardrail to the secondary roadway and stops 9 ft-3 inches from the end of nose. Six new posts were included in the system that run along the strap.

Figure 2.19 shows the side view of the primary roadway. The primary roadway consists of two steel posts and two CRT posts with blockouts. It also includes one steel post that is attached to the beginning of the strap. Figure 2.20 represents the side view of the secondary roadway. The secondary roadway has three CRT posts with a blockout, one steel post attached to the end of the strap, and 11 steel posts. The curved section has three CRT posts and four CRT posts running along the strap. The simulated parapet section represents the stiffer portion of the rail.

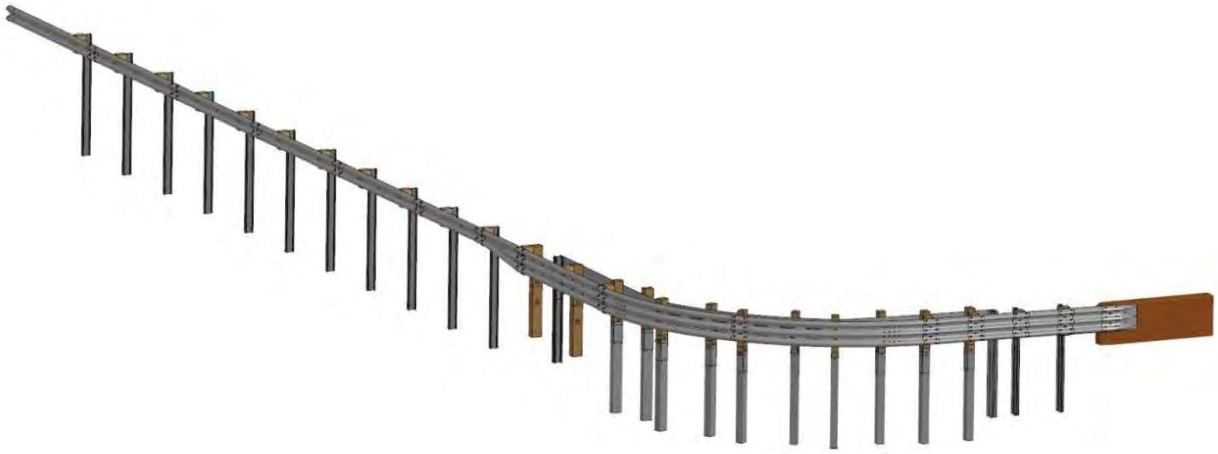


Figure 2.17. Extended Short Radius with Strap.

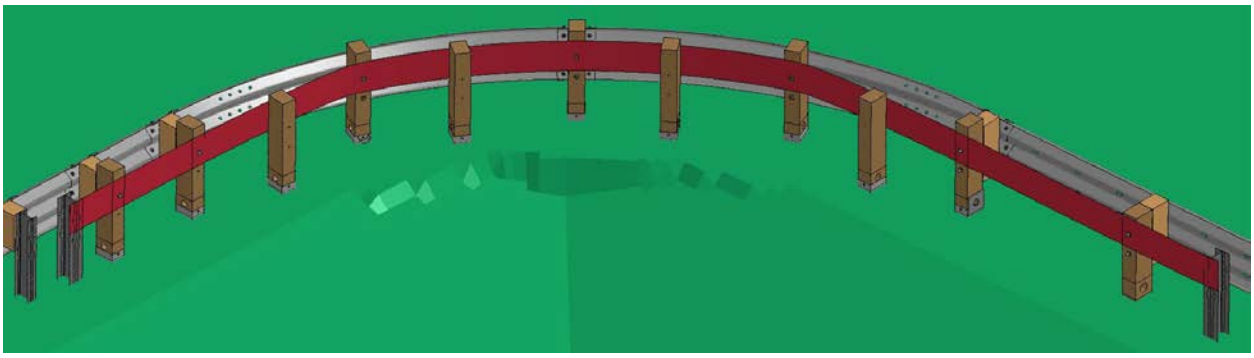


Figure 2.18. Back View of System Showing Strap.

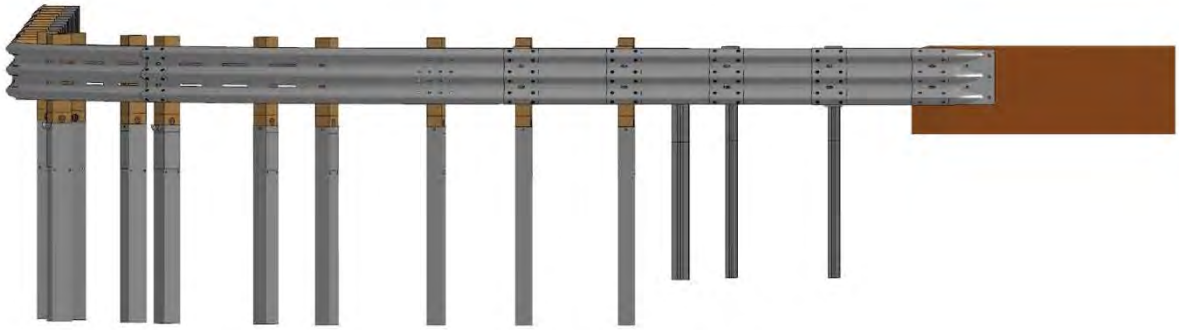


Figure 2.19. Primary Roadway Side View.



Figure 2.20. Secondary Roadway Side View.

The spacing for the guardrail supporting posts, 1 to 4 is 3-ft and for 4 to 8 are spaced at 6 ft-3 inches, as measured along the arc of the curved thrie beam. Posts 8 to 21 are equally spaced at 6 ft-3 inches. From post 1 to the end of the concrete parapet was approximately 10 ft-4 inches. The posts running along the strap are placed, post 1B is between posts 2 and 3, 2B is between 4 and 5, 3B is between 5 and 6, 4B between 6 and 7, 5B is between 7 and 8, and 6B is between 9 and 10.

2.3.3.2 Simulation of Car Impacting System

Figure 2.21 presents the sequential frames of the simulation of the car and the system. The first frame shows the initial state of the system and the car. It is followed by two images displaying the interaction of the car with the system. Just after the car interacts with the guardrail, the wood posts supporting both the guardrail and the strap break sequentially until the system goes to rest. During this process, the strap successfully contains the car from overriding

the guardrail and also plays a modest role in absorbing and releasing the impact energy of the system. The last frame depicts the end state of the simulation, showing car deformation at the front of car. The car remains stable throughout the simulation with the inclusion of the strap.

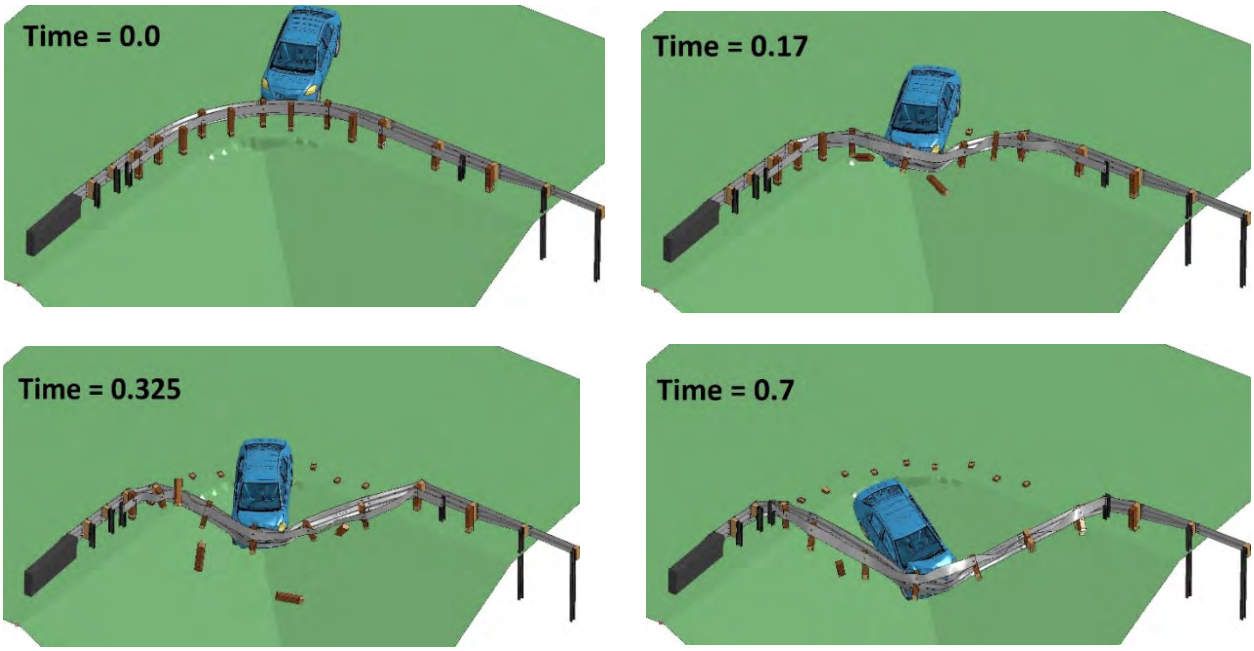


Figure 2.21. Sequential Images of Car Simulation with Strap.

Below are shown two significant frames of the simulation that give a closer look to the impact process. Figures 2.22 and 2.23 show the interaction in development and the end state of the simulation, respectively. In these figures, the containment ability of the strap is clearly seen. Also, the two steel posts attached to the strap ends appear to remain solid by the end of this simulation.

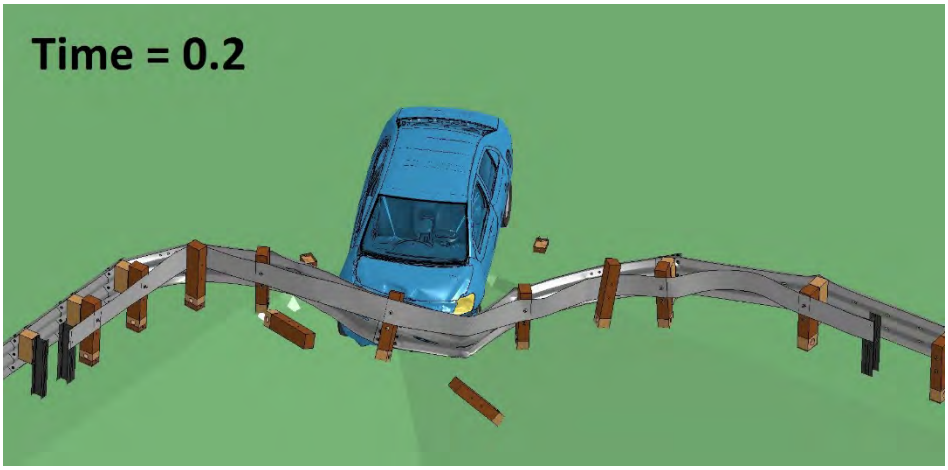


Figure 2.22. Interaction of Car with System.

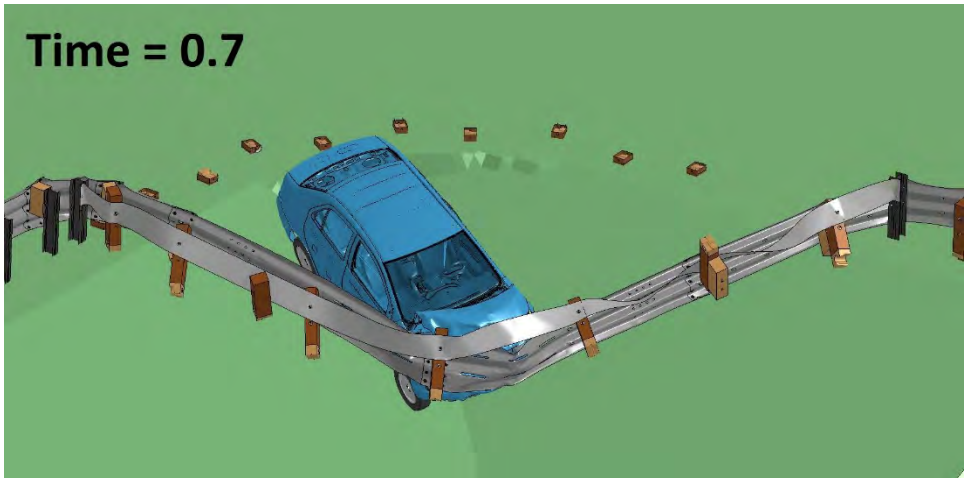


Figure 2.23. Final State of Simulation.

Table 2.1 displays the TRAP results for the occupant risk factors.

Table 2.1. TRAP Summary Data for Simulation with Car and Strap.

TRAP Results: Small Car Short Radius	
Impact Velocity, mph	43.5
Impact Angle (degrees)	25
Occupant Risk Factors	
Occupant Impact Velocity (OIV) (ft/s)	
x-direction	17.7
y-direction	4.6
Occupant Ridedown Accelerations (g's)	
x-direction	−10.5
y-direction	−2.6
Max Roll, Pitch, and Yaw Angles (degrees)	
Roll	12.8
Pitch	−13.4
Yaw	−40.2

Shown next are the graphic results of the truck simulation. Figure 2.24 shows the longitudinal accelerations, Figure 2.25 shows the lateral accelerations, and Figure 2.26 shows the roll, pitch, and yaw angles.

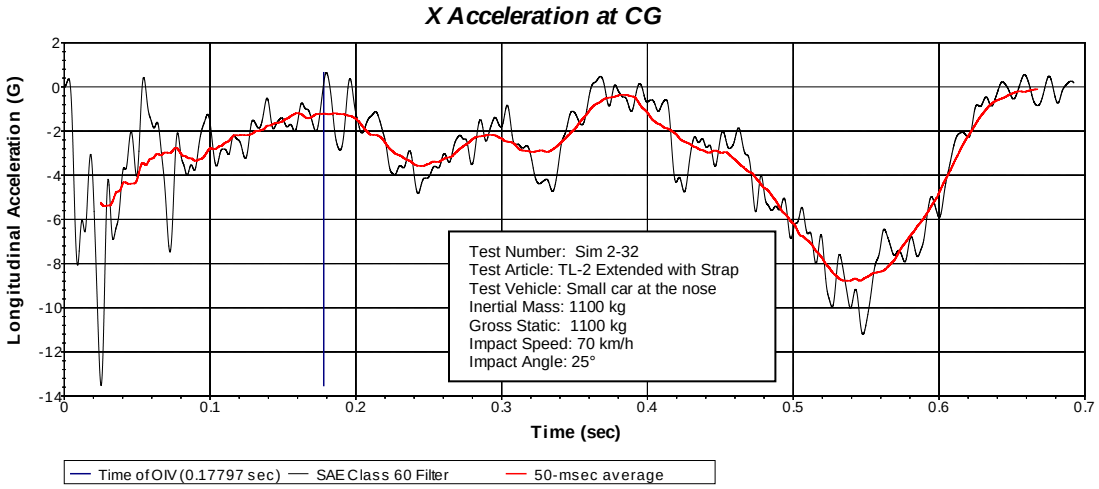


Figure 2.24. Longitudinal Accelerations for Car Simulation.

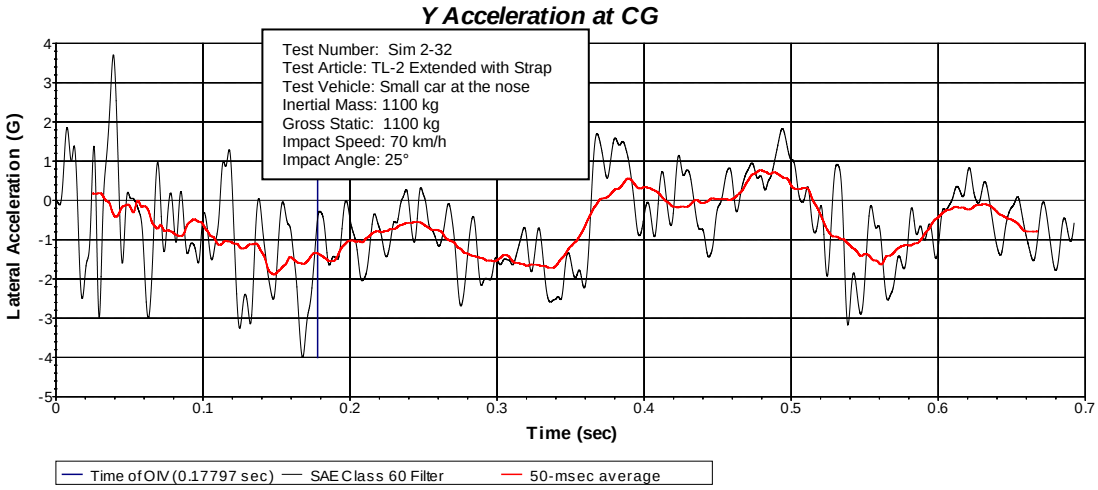


Figure 2.25. Lateral Accelerations for Car Simulation.

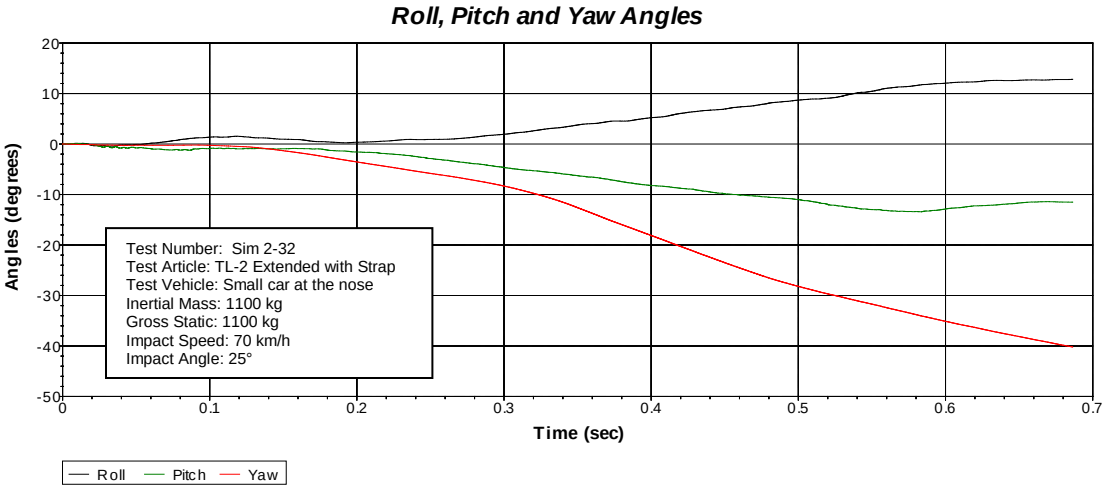


Figure 2.26. Roll, Pitch, and Yaw Angles for Car Simulation.

2.3.3.3 Simulation of Truck Impacting System

Figure 2.27 represents the chronological images of the movement of the truck in this simulation. The first image shows the initial position of the system and is followed by three images of the truck interacting with the guardrail. The simulation shows that the new system with the strap was able to contain the truck from overriding the guardrail.

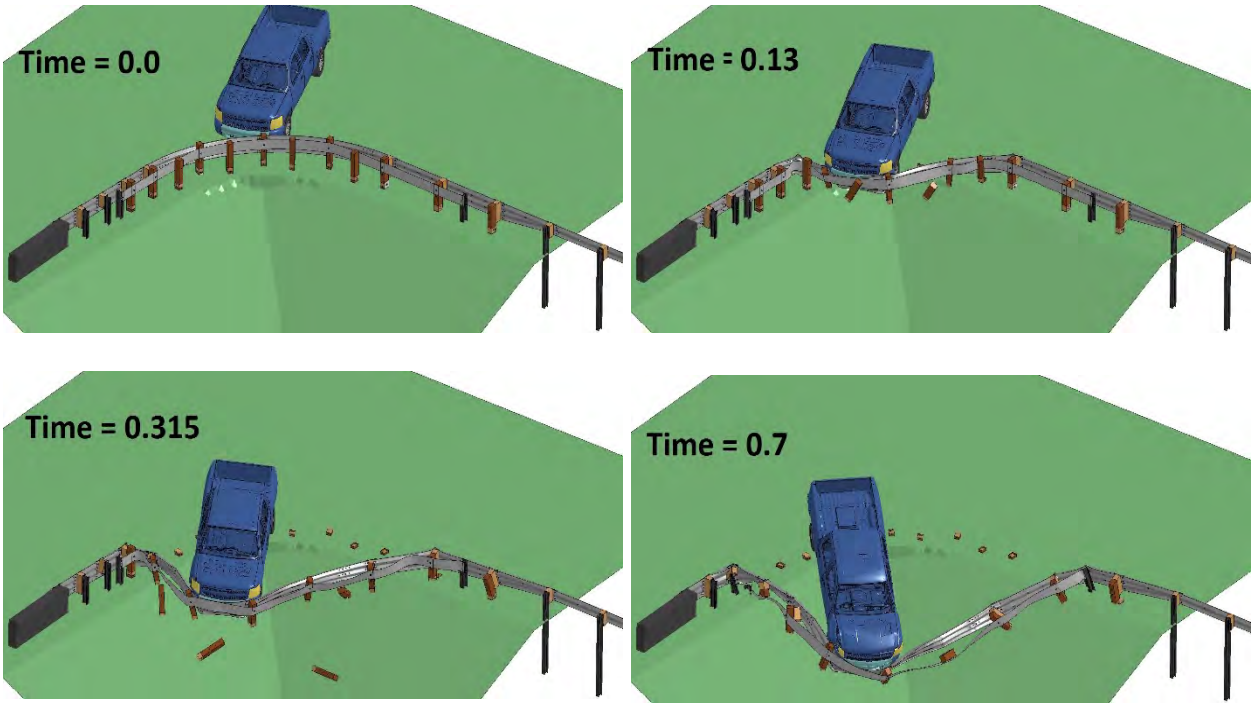


Figure 2.27. Sequential Images of Truck Simulation with Strap.

Figures 2.28 and 2.29 show the interaction in development and final state of the simulation of the truck, respectively. In both figures, it is seen that the strap supports and holds the guardrail in a position that prevents the truck from overriding it. Also, by the end of the simulation, the support steel post of the strap close to the thrie beam end shoe appears to break. Meanwhile, the support steel post on the other end of the strap, despite significant bending, it still remains solid.

Table 2.2 displays the TRAP results for the occupant risk factor.

Shown next are the graph results of the truck simulation. Figure 2.30 shows the longitudinal accelerations, Figure 2.31 shows the lateral accelerations, and Figure 2.32 shows the roll, pitch, and yaw angles.

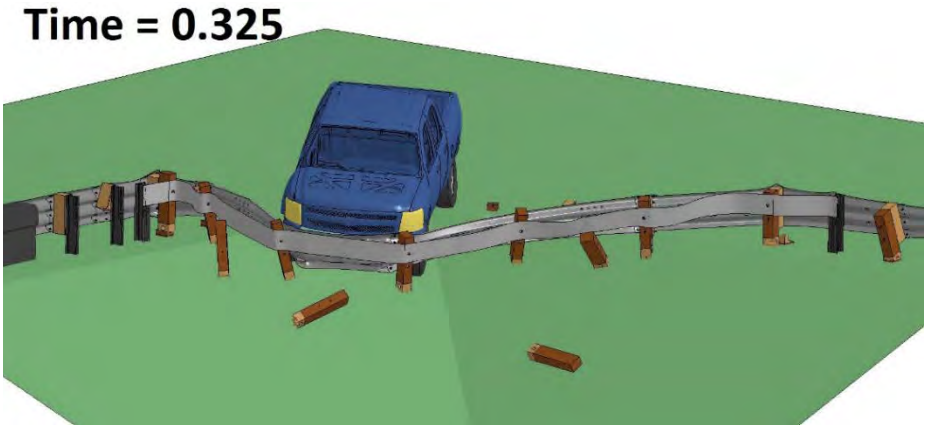


Figure 2.28. Interaction of Car with System.

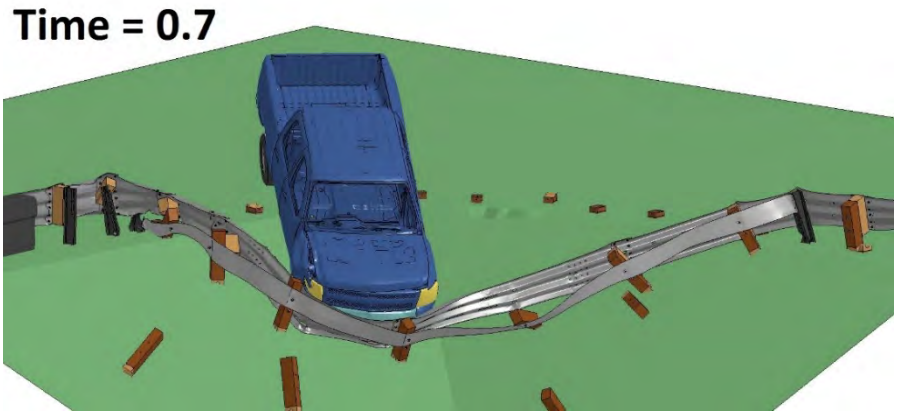


Figure 2.29. Final State of Simulation.

Table 2.2. TRAP Summary Data for Simulation with Truck and Strap.

TRAP Results: Truck Short Radius	
Impact Velocity, mph	43.5
Impact Angle (degrees)	25
Occupant Risk Factors	
OIV (ft/s)	
x-direction	14.8
y-direction	5.9
Occupant Ridedown Accelerations (g's)	
x-direction	−15
y-direction	−4.5
Max Roll, Pitch, and Yaw Angles (degrees)	
Roll	7.9
Pitch	−24
Yaw	−24.5

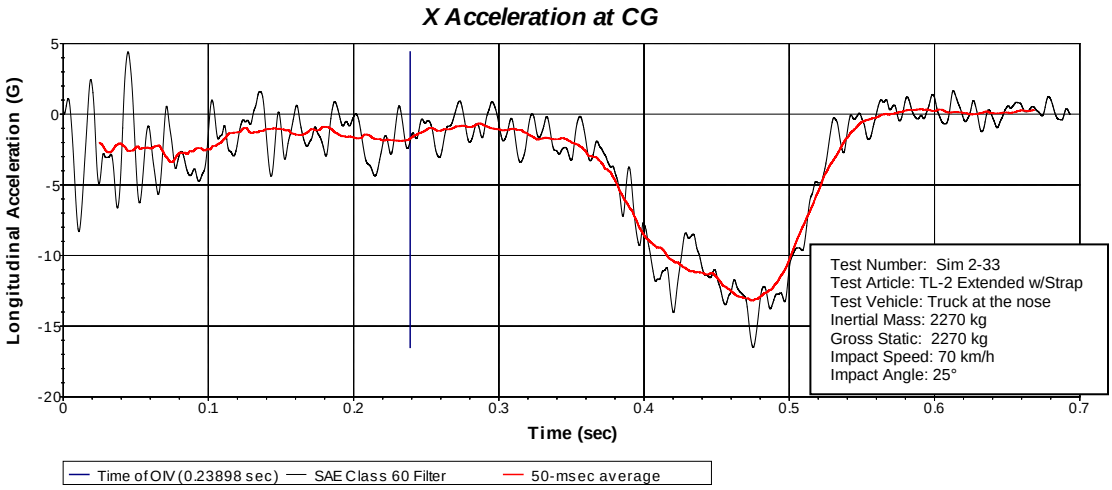


Figure 2.30. Longitudinal Accelerations for Truck Simulation.

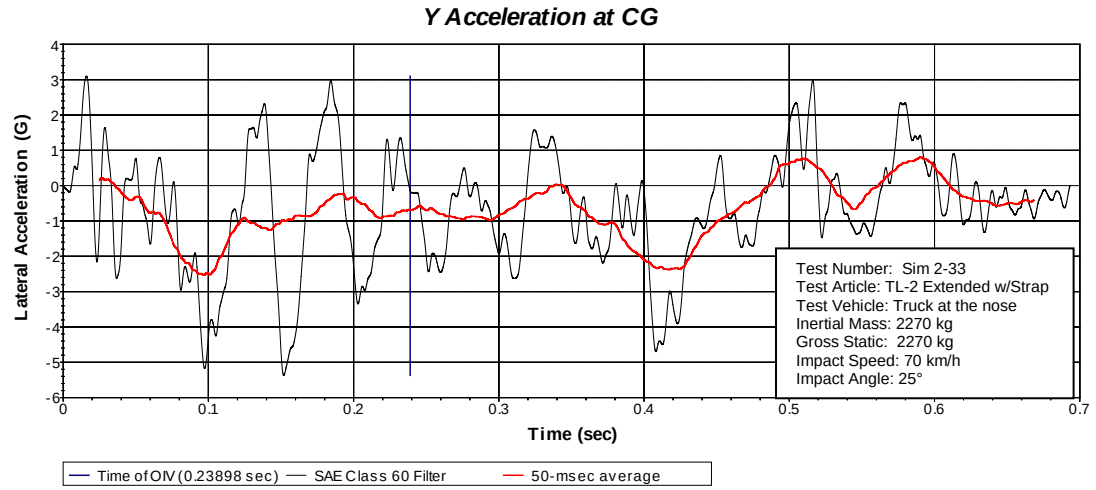


Figure 2.31. Lateral Accelerations for Truck Simulation.

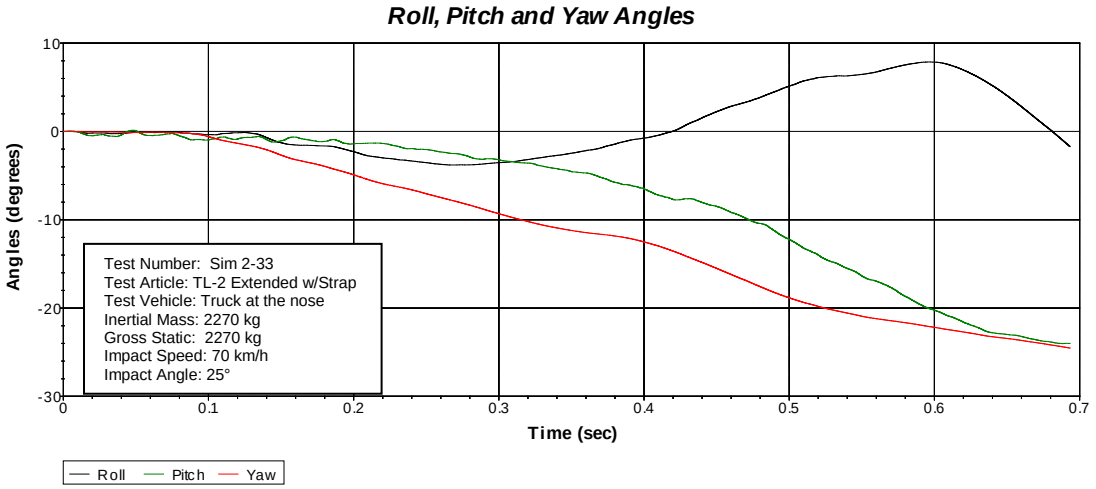


Figure 2.32. Roll, Pitch, and Yaw Angles for Truck Simulation.

A new design of the short radius guardrail system was created using Solidworks with the appropriate measurements. Figure 2.33 shows the system design surrounding a ditch. The design was based on the system simulation discussed above. As mentioned before, the system consists of a strap running behind the guardrail system with six CRT posts and two steel posts. The design includes two cables, a primary cable attached to the thrie beam running from the primary roadway to the secondary roadway and a secondary short cable on the secondary roadway.

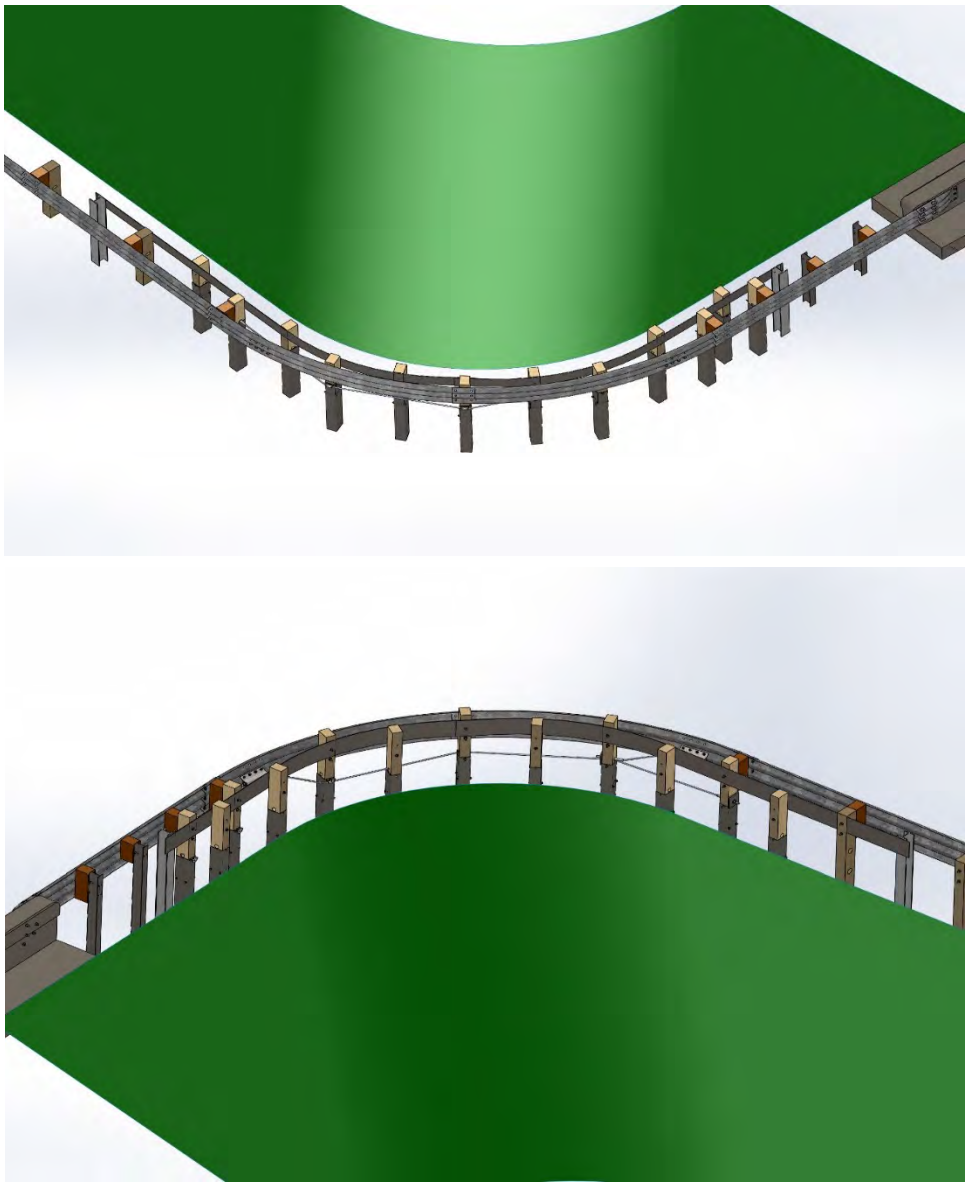


Figure 2.33. Short Radius System with Back Plate.

2.4 SIMULATION OF TEST 2-31

2.4.1 System Details

The following simulation includes the updated guardrail system. This new design includes two new cables, a primary cable and a secondary cable. The primary cable is attached to the thrie beam and is oriented to get to the ground by the third CRT post on the primary roadway. The cable runs under the cable shelf attached at ground level to the post on the primary roadway. The cable then runs along the ground and under the cable shelf attached to the two posts at the center of the radius. It passes along the ground and terminates at the post on the secondary roadway. The secondary cable is attached to the thrie beam and terminates at the post before the post on the secondary roadway.

Figure 2.34 depicts the new cable design that is described above. Figures 2.35 and 2.36 provide a front and back view, respectively, of the long tension cable from the simulation.

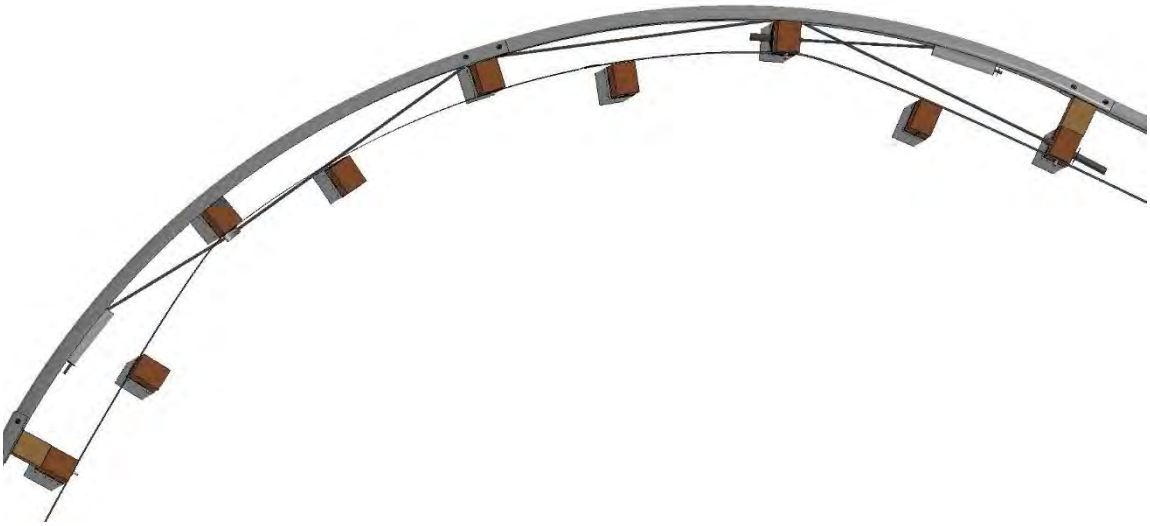


Figure 2.34. Amplified View of Guardrail System with Strap and Two Cables.

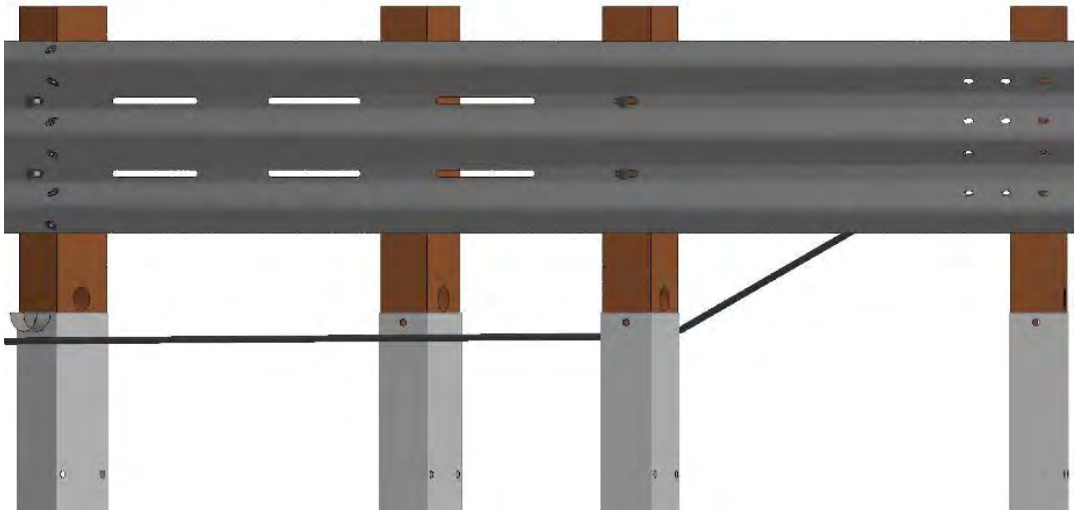


Figure 2.35. Front View of Primary Cable.

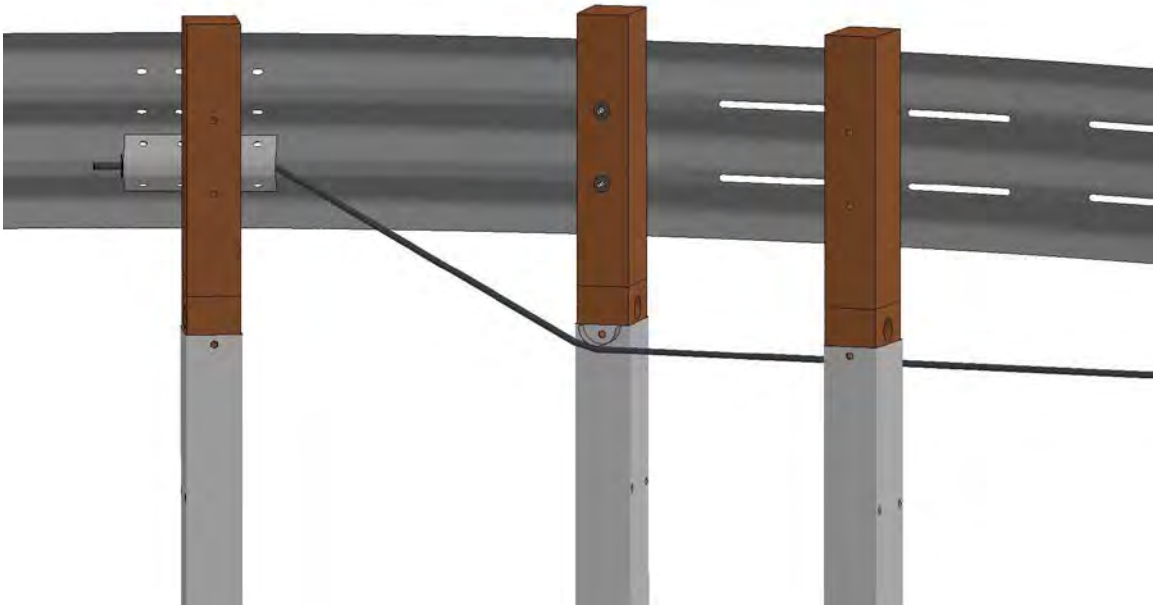


Figure 2.36. Back View of Primary Cable (Strap Hidden).

Figure 2.37 provides the back view of the short tension cable from the simulation. The back strap is hidden from the figures for clarity.

Figure 2.38 depicts the truck alignment with the system. The centerline of the truck is aligned with the traffic face of the concrete parapet located on the primary roadway.

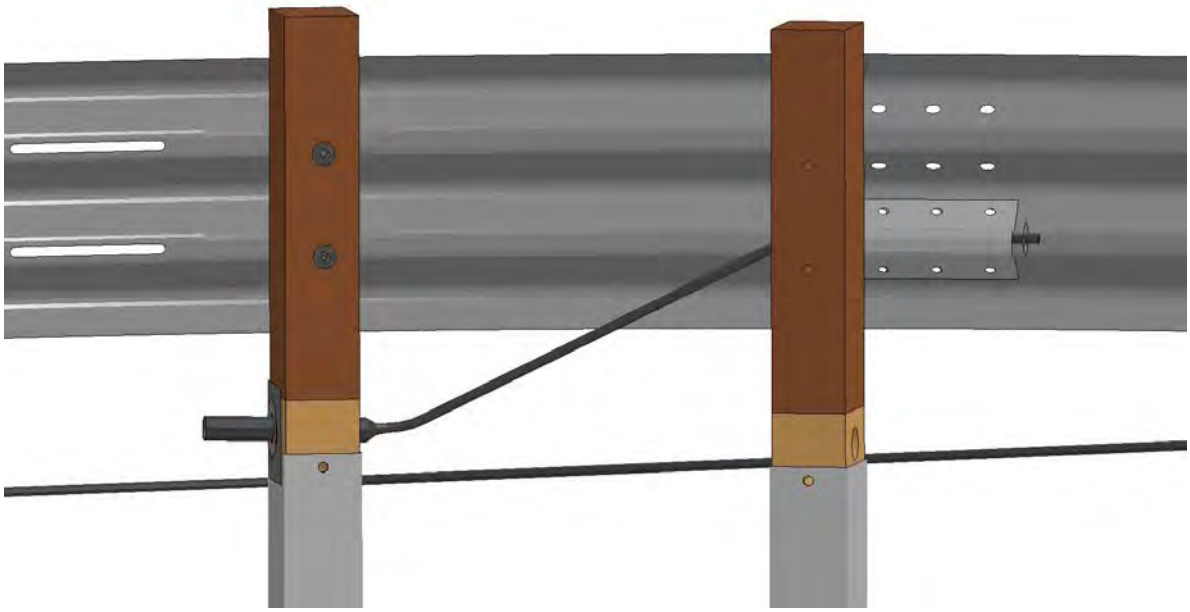


Figure 2.37. Back View of Secondary Cable (Strap Hidden).

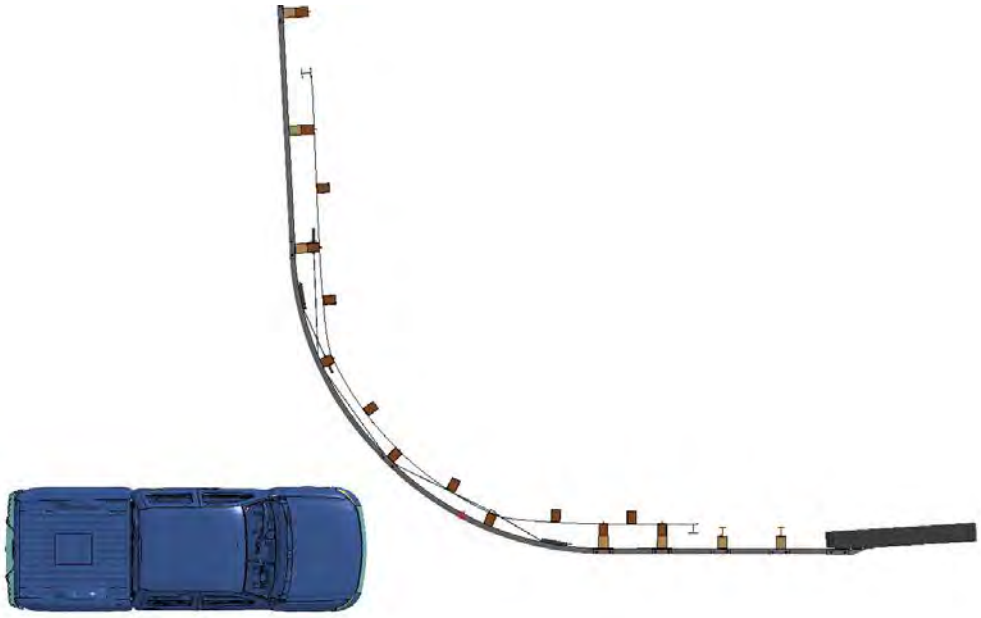


Figure 2.38. Alignment of Truck with System.

2.4.2 Simulation of Truck Impacting Short Radius with Strap and Cable from Front of Rail

Figure 2.39 shows sequential images depicting the performance of the system. The first contact with the guardrail happens at 0.065 s from the start of the simulation. The three wood posts surrounding the impact area seem to break simultaneously at 0.1 s. The primary cable maintains tension capacity and continues to be attached under the initial angle until the truck reaches the bracket, and consequently, the wood post behind it breaks. At 0.125 s, the front left tire begins to ride along the cable. By 0.215 s, the tire has passed from riding along the cable to riding up the rail. The front left truck tire appears to detach from the rail before 0.35 s, and the truck is unstable. By the end of the simulation, only six wood posts break, while the others remain intact, including the steel posts that hold the strap. The secondary cable maintains tension capacity and remains attached under the initial angle throughout the simulation.

The first frame shows the initial state of the system and the truck, followed by two frames depicting the initial and last state of the interaction progress. The conclusion that the system has an undesirable outcome is seen in these two images. The last frame of Figure 2.39 represents the last state of the simulation. To make them stand out, the cables have been colored red.

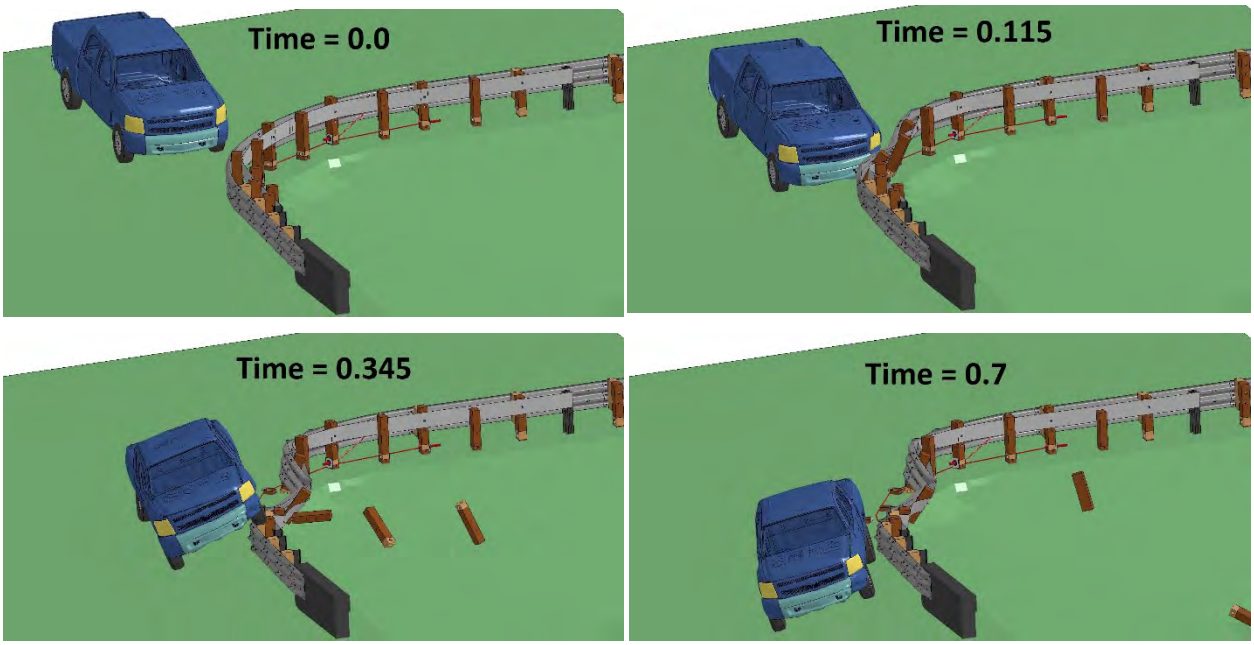


Figure 2.39. Sequential Images of Simulation of Truck from Front of Rail, with Strap and Cables.

Figure 2.40 shows how the truck tires interact with the cable initially and then with the rail. The front left truck tire rides up the cable onto the rail, followed by the back left tire riding up the rail, eventually causing the truck to be unstable. Figure 2.41 zooms in on the moment the left truck front tire rides along the cable, at 0.18 s, in two different angled views. Notice how the rail is pushed into the ditch of the system as the tire rides along the cable.

Figure 2.42 shows the graph results of the truck simulation for the roll, pitch, and yaw angles. The roll angle shown in the black solid line has a peak at 0.37 s, with an angle of 0.35°. The peak can be explained by analyzing the above simulating images, where it is observed that the moment that the truck rides up the rail matches with the time, the peak is represented in the graph.

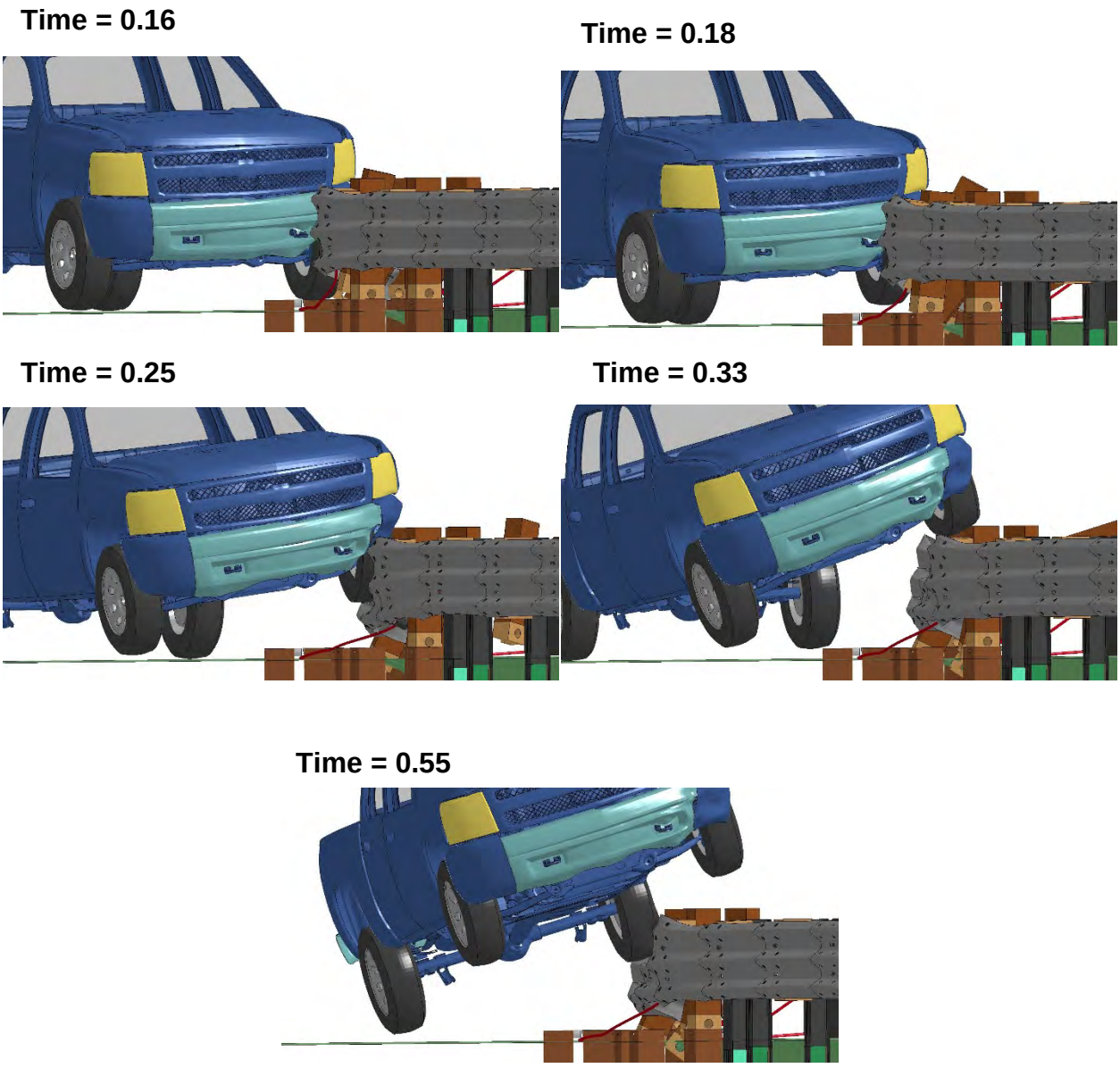


Figure 2.40. Sequential Images of Tire with System Interaction.

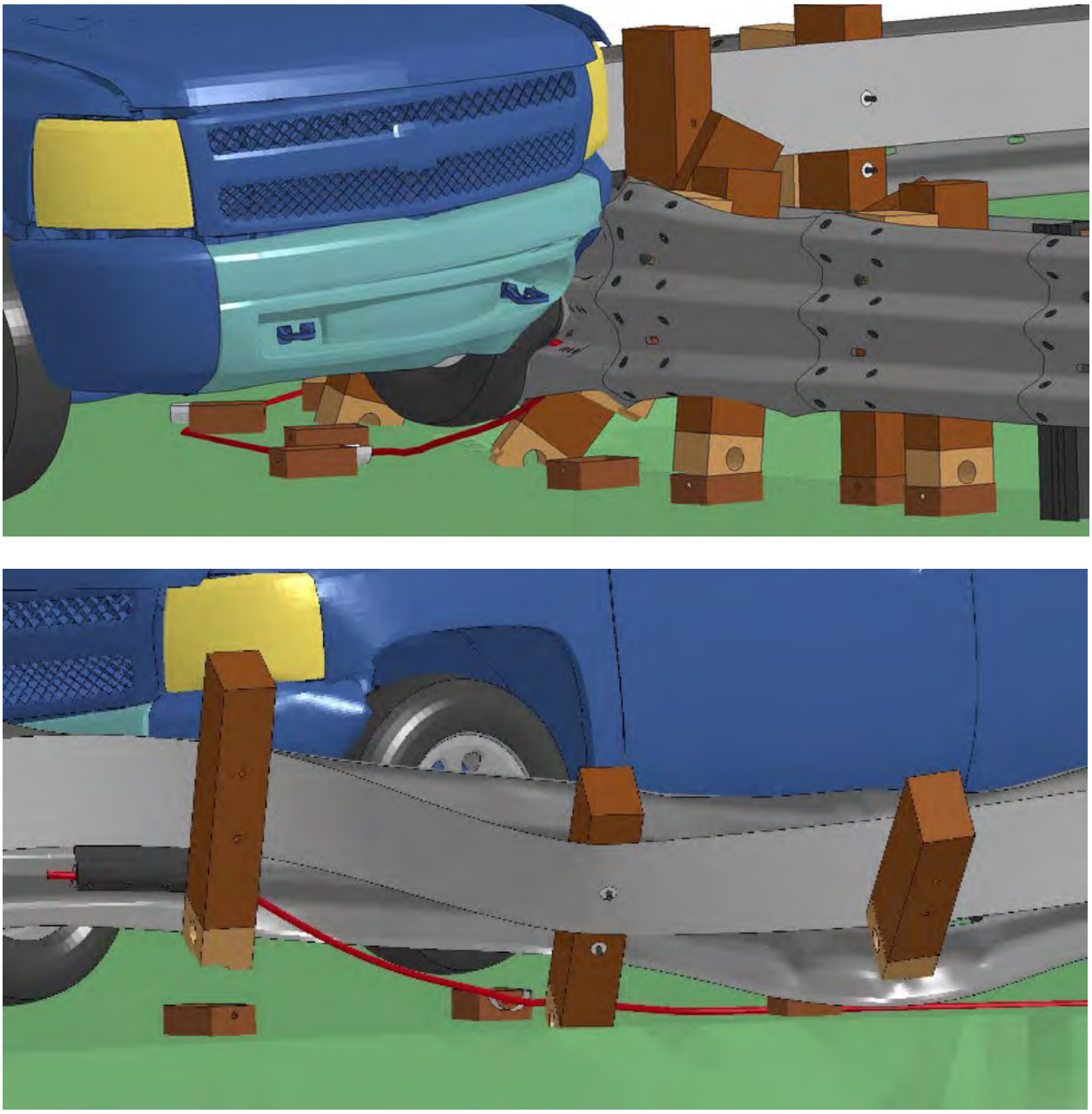


Figure 2.41. Tire and Cable Interaction.

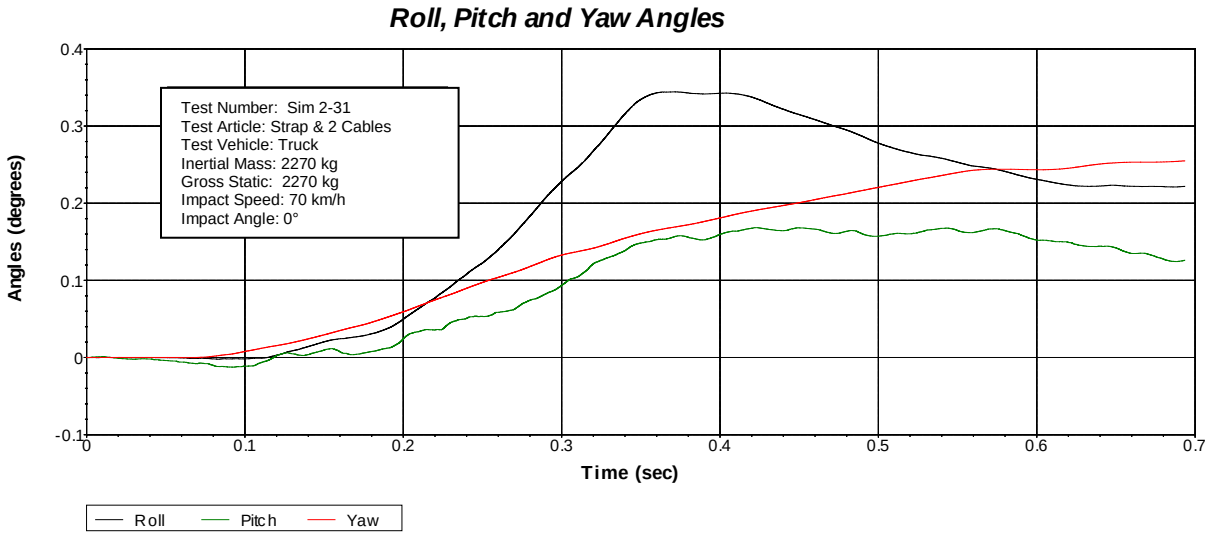


Figure 2.42. Roll, Pitch, and Yaw Angles.

2.5 TEST 2-33

2.5.1 System Details

Test 2-33 was simulated to determine the rail's capacity of containing or redirecting the truck. The same guardrail system design was used from test 2-31. The truck impacted the system at a 25° angle at the center of the radius. Figure 2.43 shows the alignment of the truck with the system.

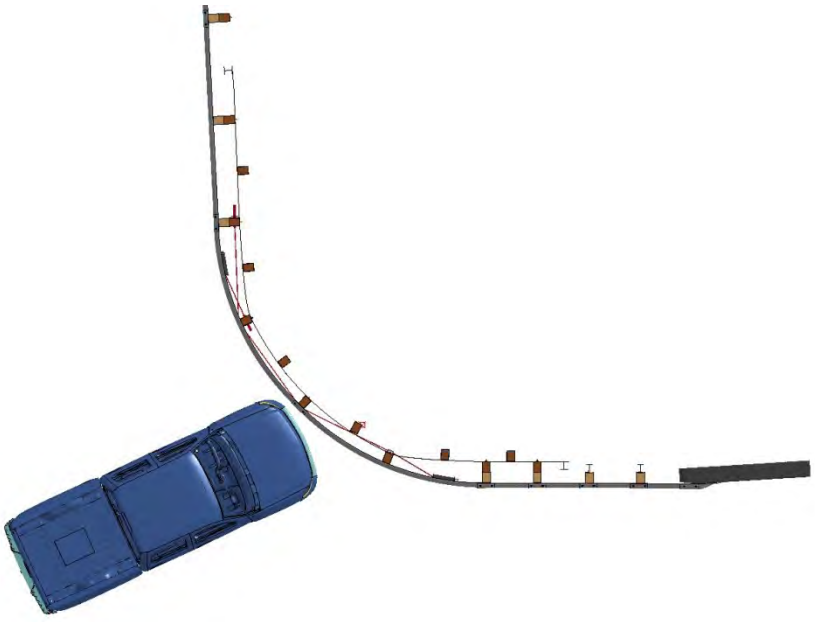


Figure 2.43. Alignment of Truck with System.

2.5.2 Simulation of Truck Impacting Short Radius with Strap and Cable at 25°

Figure 2.44 shows sequential images of the simulation of the truck interacting with the system. The initial contact with the rail happens at 0.015 s. The wood post in the middle of the radius breaks first at 0.035 s. Then, before 0.04 s the other two wood posts of the radius break. The next to break is the wood post holding the secondary cable before 0.05 s. The secondary cable maintained tension capacity and was attached under the initial angle until this point. From impact, the rail area holding the primary cable's bracket is pushed into the ditch side moving along with the cable. The cable first escapes from one the shelves at 0.105 s and consequently changes the angle of attachment. Before 0.14 s, the right truck front tire begins to run along the cable. Before 0.18 s, the tire has passed from riding along the cable to riding up the rail. By this point, also the left front tire is riding up the rail. The back truck tires follow and by 0.47 s they are up the rail. Before 0.5 s, the truck has completely detached from the system and is going down the ditch.

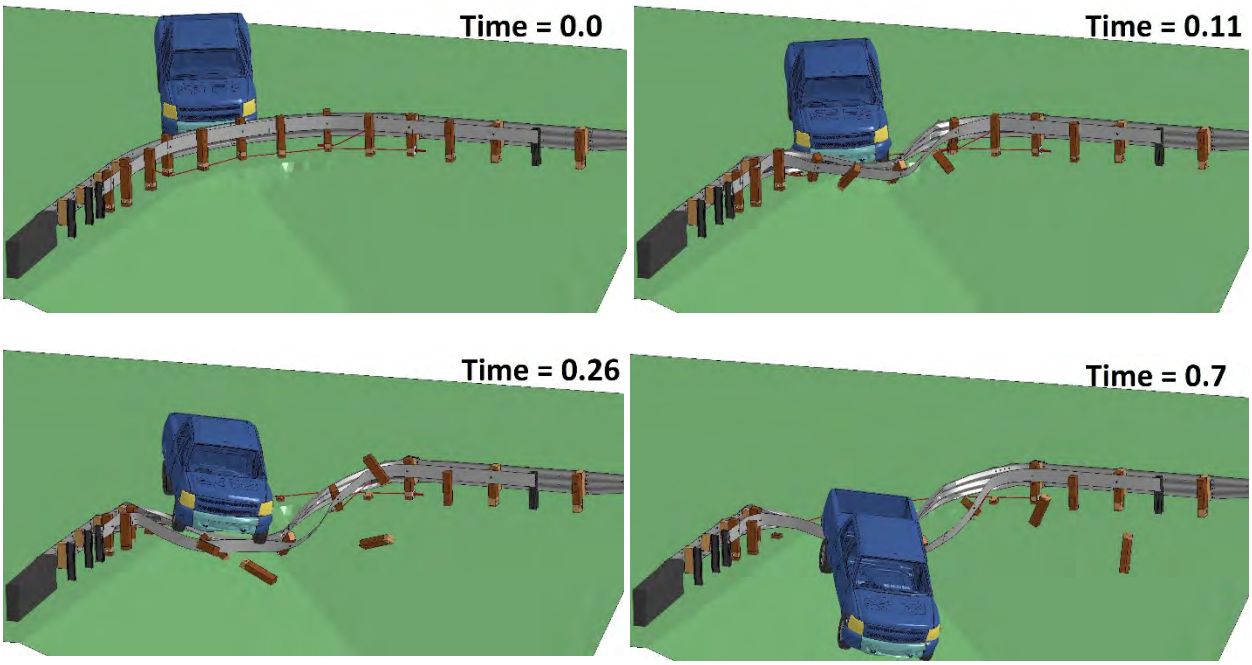


Figure 2.44. Sequential Images of Simulation with Strap and Cables.

The first frame shows the initial state of the simulation, followed by two frames representing the interaction between the truck and the system. The last frame is the last state of the simulation. This figure clearly draws the conclusion that the system is not adequate to contain the truck.

Figure 2.45 shows two amplified images on the moment the right front tire rides along the cable initially and then up the rail. Notice how the rail is pushed toward the ditch as the tire starts to ride along the cable. The tire rides along the cable from 0.14 s to 0.17 s. The cables have been colored red to make them stand out.

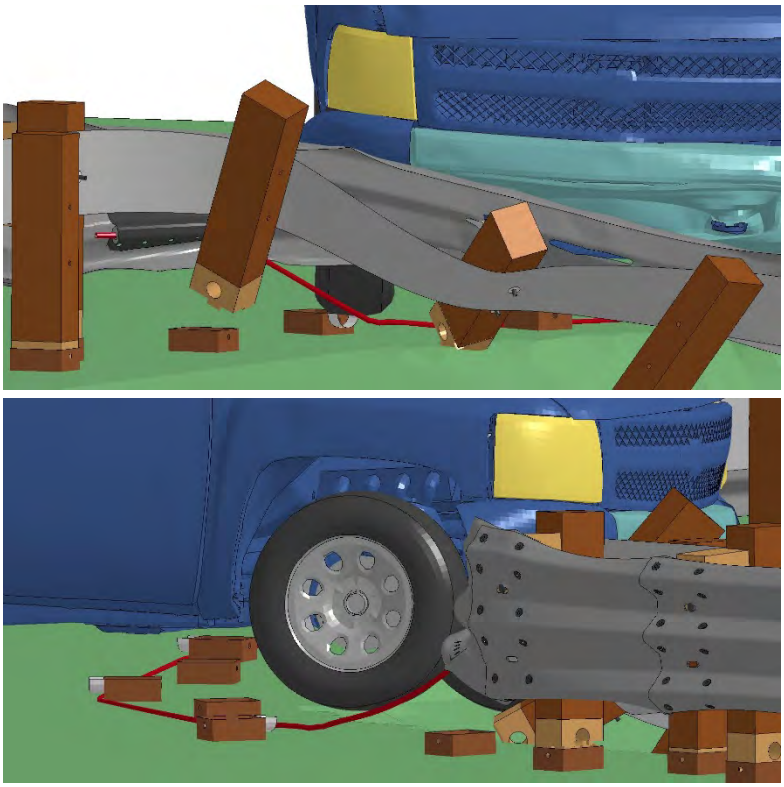


Figure 2.45. Interaction of Truck with System.

2.6 TEST 2-33-2

2.6.1 System Details

Since the previous system was overridden by the truck, the guardrail system was updated. The new system is shown in Figure 2.46. The system design includes drums filled with sand placed between posts. Each of the nine drums were raised by wood blockouts from the ground. From the primary roadway, the first drum is placed between posts 3 and 4, two drums are placed between posts 4 and 5, 5 and 6, and 6 and 7. One drum is placed between the ends of the secondary cable to post 8. The last drum is placed between 8 and 9. Since the ditch is really close to the system the drums were set as close as possible the guardrail. The strap and primary cable were removed from the system design.

2.6.2 Simulation of Truck Impacting Short Radius with Flare and 18-lb Sand Drums

Figure 2.47 shows the sequential images of the simulation of system with the truck. The truck remains stable during the simulation. The first image shows the initial position of the truck and the system, and is followed by two images that depict the interaction of the truck with the guardrail system and the drums. The last image is the last state of the simulation. The drums and the guardrail system engage to absorb the kinetic energy of the vehicle and successfully contain the truck.

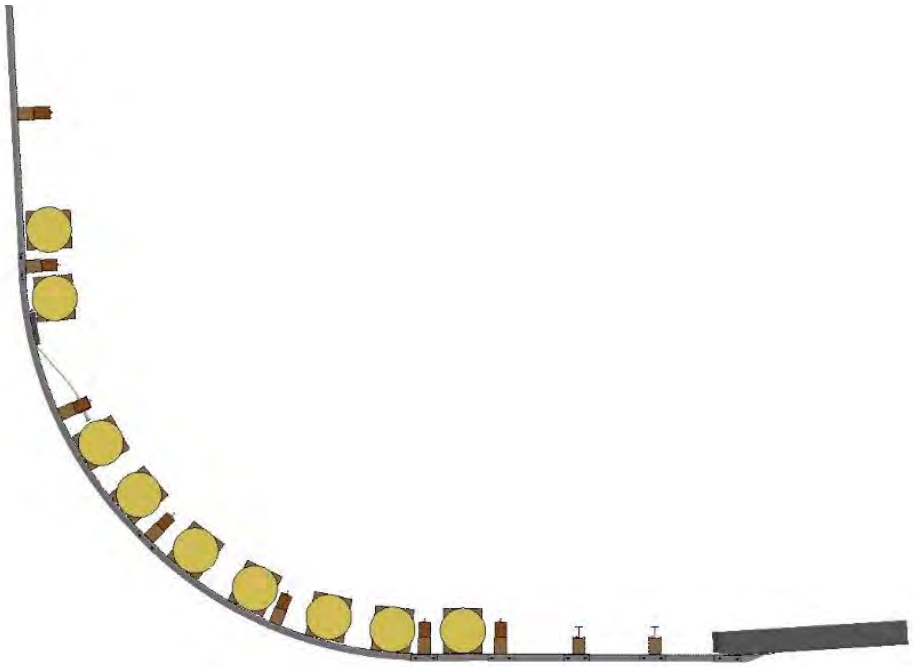


Figure 2.46. Flare and 18-lb Sand Drums behind Radius.

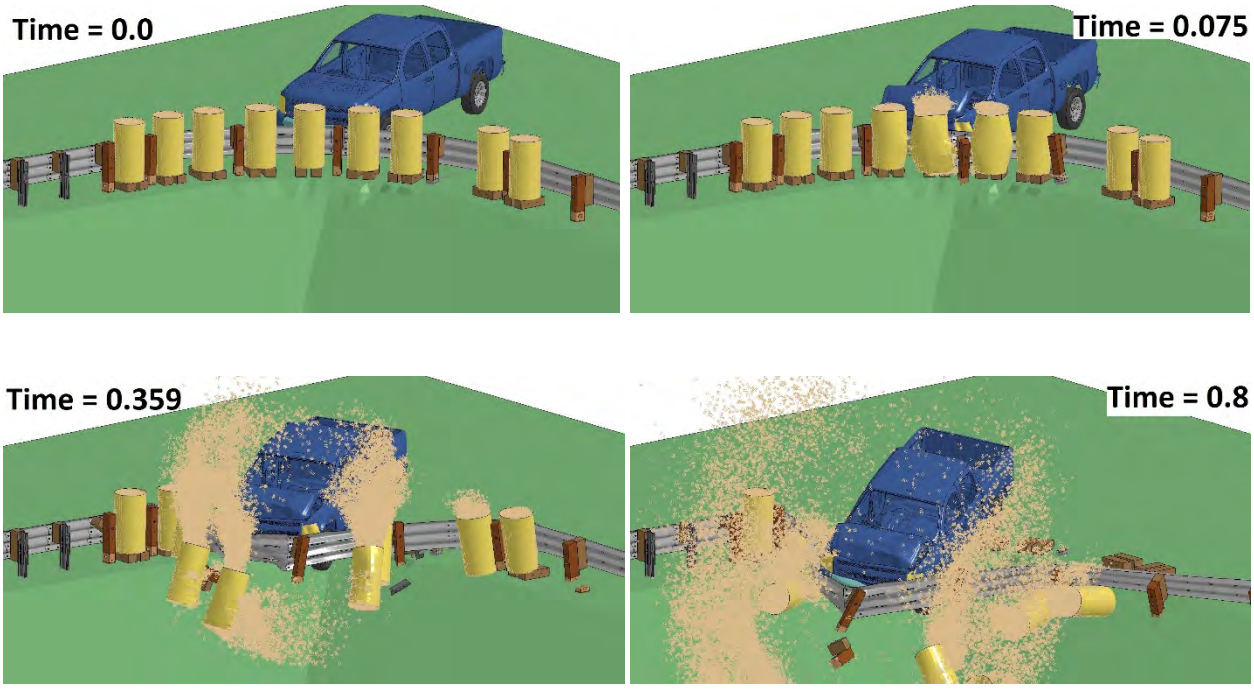


Figure 2.47. Sequential Images of Truck Simulation, with Flare and 18-lb Sand Drums.

Figure 2.48 offers alternate views of three key moments of the simulation. The first frame shows when the first impact occurs. The second one displays the moment after the drums have had their greatest impact. The third frame is the moment after the guardrail system has had its

impact and the truck reaches zero velocity. The third frame is also the last frame of the simulation.

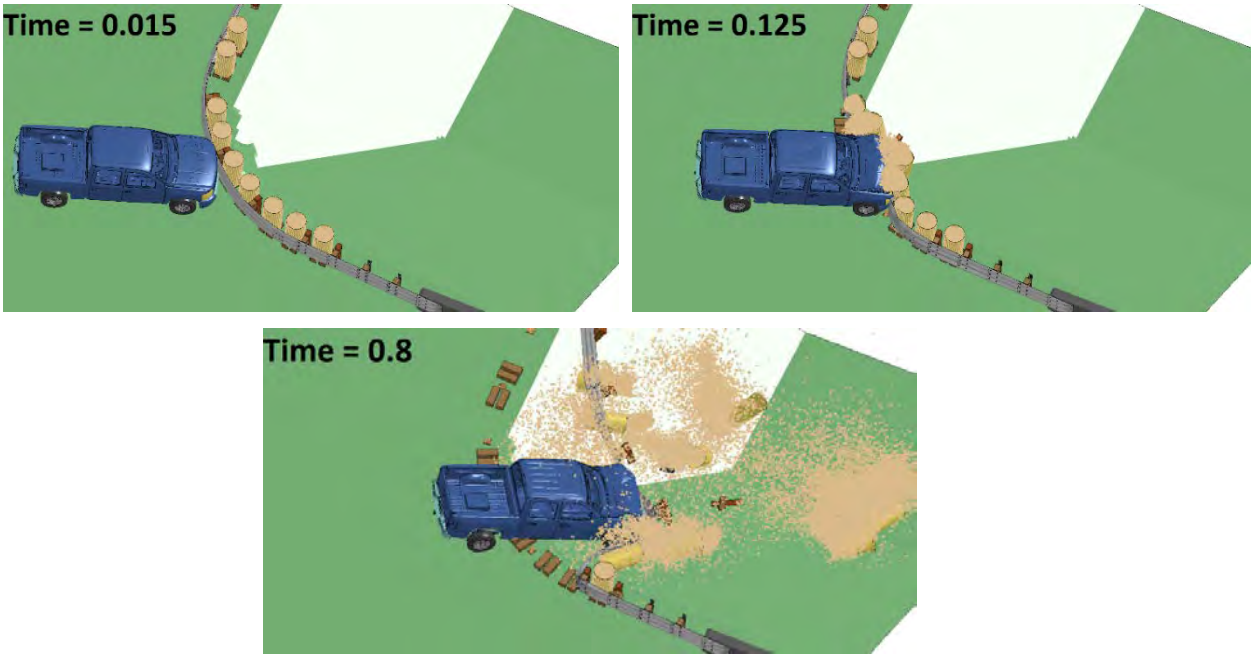


Figure 2.48. Interaction of Truck with System.

Table 2.3 shows the TRAP results for the occupant risk factors for the simulation system with flare and 18-lb sand drums.

Table 2.3. TRAP Summary Data for Simulation of Truck with Flare and 18-lb Sand Drums.

TRAP Results: Truck Short Radius	
Impact Velocity, mph	43.5
Impact Angle (degrees)	25
Occupant Risk Factors	
OIV (ft/s)	
x-direction	32.8
y-direction	1.0
Occupant Ridedown Accelerations (g's)	
x-direction	−4.9
y-direction	−3.8
Max Roll, Pitch, and Yaw Angles (degrees)	
Roll	−7.4
Pitch	−9.0
Yaw	−9.9

Figures 2.49, 2.50, and 2.51 are the results for the longitudinal accelerations, lateral accelerations, and vertical accelerations, respectively. Figure 2.52 shows the results of the roll, pitch, and yaw angles.

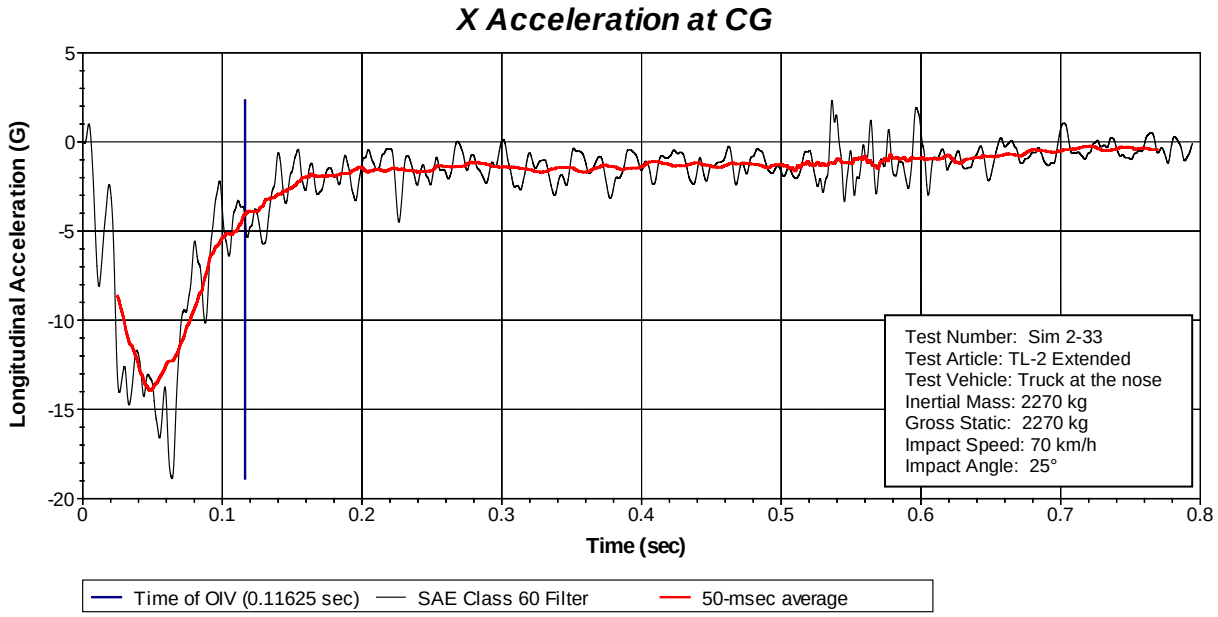


Figure 2.49. Longitudinal Accelerations for Truck Simulation.

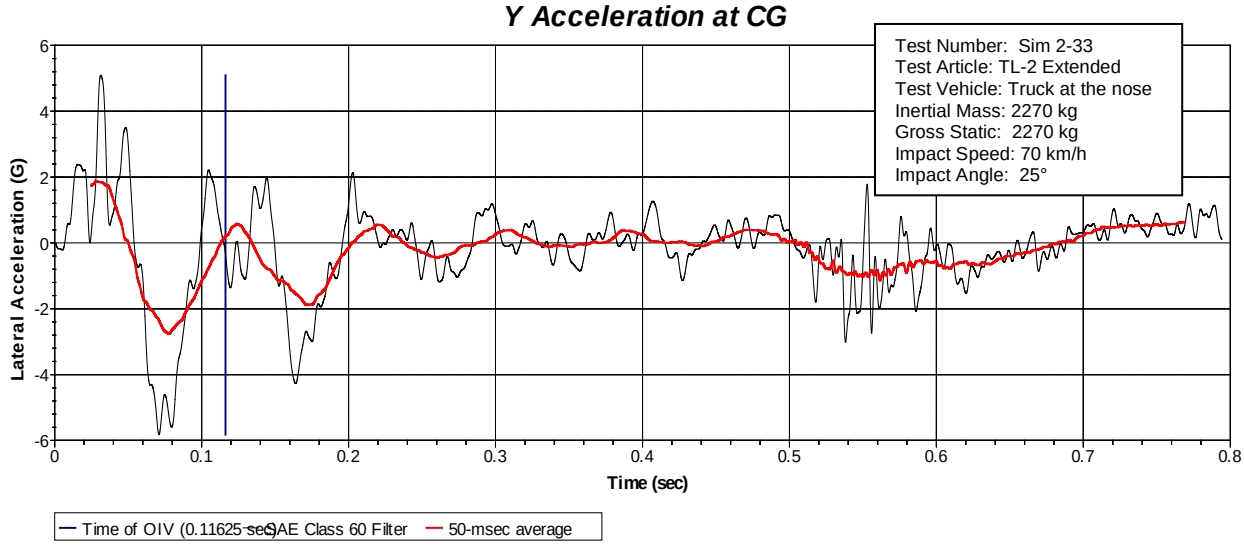


Figure 2.50. Lateral Accelerations for Truck Simulation.

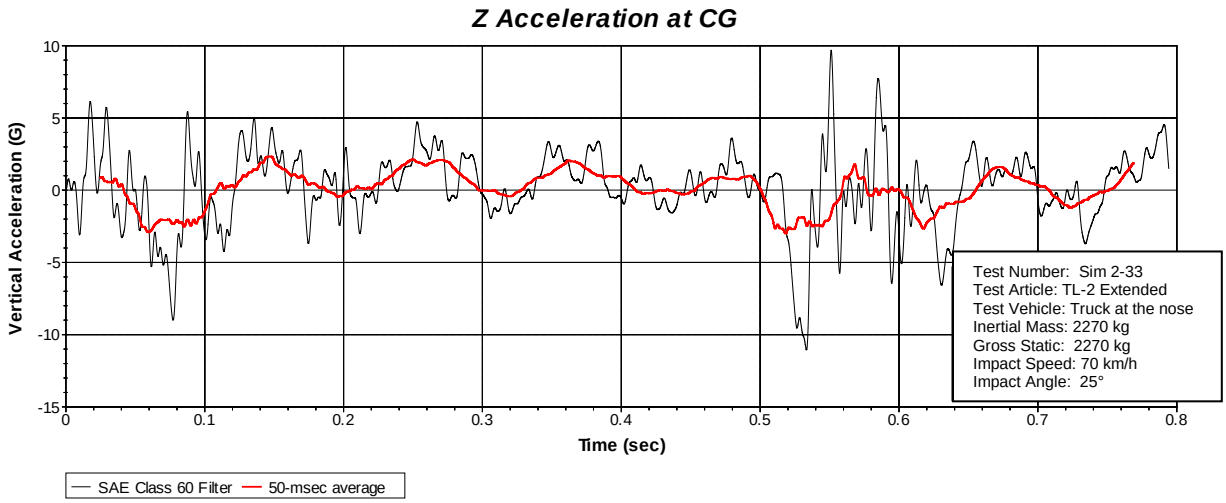


Figure 2.51. Vertical Accelerations for Truck Simulation.

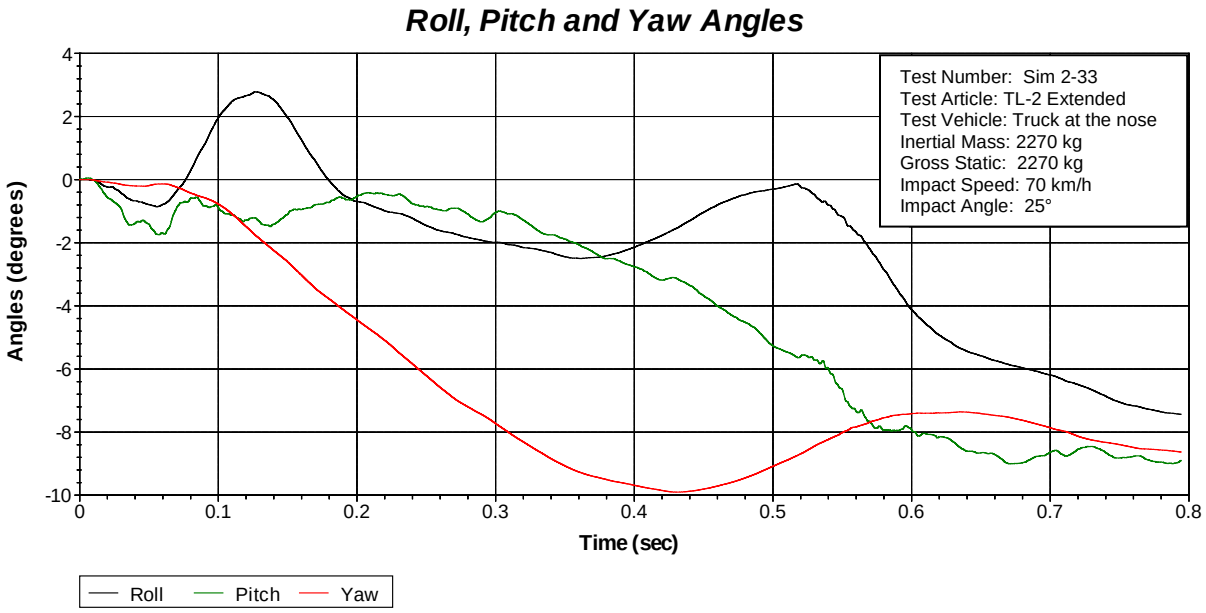


Figure 2.52. Roll, Pitch, and Yaw Angles for Truck Simulation.

2.7 CONCLUSIONS

The first simulation case was for the TL-3 short radius system but without the sand barrels. The simulation results show that the car was damaged up to the windshield and truck was overriding the system making it undesirable. The second simulation is an extended short radius system that did not include a cable, was extended from the secondary roadway, and had less post on the primary roadway. This simulation also resulted in the vehicle overriding the system.

In test 3, the introduction of the strap plays a positive role in the simulation results. The strap supports and prevents the guardrail from being overridden and plays a modest role in dissipating energy, using the tension capacity that is created between the holding wood posts.

Adding cables to the simulations did not result in improvement of the interaction between the vehicles and the system. In the first simulation, it appeared that the truck left front tire rides along the cable and then up the rail making the truck unstable. Even though, the simulation of test T2-31 did not produce a desirable behavior, positive recommendations can be drawn from it for future testing. Test T2-33 had a change of the interaction angle between the truck and system resulting in a significantly undesirable outcome of the simulation.

For test T2-33-2, the system was changed by removing the strap and primary cable and adding drums along the guardrail post. The drums seem to give favorable results because of the absorption of kinetic energy from the impact of the truck to the guardrail system.

CHAPTER 3:
SIMULATIONS OF RECOMMENDED DESIGNS CONCEPTS

3.1. BACKGROUND

A short radius guardrail system is to be developed for use on low speed roadways. There are two methods that can be used to analyze a guardrail system: full scale crash testing and finite element simulations. Finite element simulations and analysis has become a fundamental part of the design since it gives the researcher knowledge on the simulation results. Researchers performed various short radius guardrail system simulations to assess its ability to meet AASHTO *MASH* Test Level 2 performance criteria. These simulations included different guardrail system designs with no drums included. Every new design was developed and improved from the previous design to meet the requirements. Most of simulations overrode the system while other designs had some promising features that improved the guardrail system.

Following the guardrail system simulations that were previously designed, researchers reviewed the designs and the promising features to develop a short radius guardrail. The new guardrail system designs that are introduced in this report are promising designs that lead to the best guardrail simulation that accomplished the performance requirements. The simulations included drums that dissipate a large part of the kinetic energy imparted by the impacting vehicle. The goal of these simulations is to check that test vehicles are captured within an acceptable distance behind the rail. Other simulations are conducted to determine the critical impact point where the vehicle starts to redirect.

3.2 DESIGN CONSIDERATION

The short radius system used for these test simulations starts with a transition between a guardrail to a concrete bridge rail on the primary road. This transition included a 31-inch tall strong post thrie beam approach guardrail to a rigid concrete bridge parapet. The primary roadway consisted of two steel posts, two controlled release timber (CRT) posts, and a 12.5-ft thrie beam on the primary roadway. The first two posts are W6×9 steel post starting 29 inches form the end of the parapet with a 6-inch × 8-inch × 21-inch routed wood blockout. The next two posts were the CRT posts with a 6-inch × 8-inch × 14-inch. All posts included one bolt on the top hole shown on the thrie beam. The following thrie beam was the curved section with a radius of 16-ft; this section of the guardrail consisted of three CRT wood posts. Continuing to the secondary roadway, a 12.5-ft thrie beam connected with the curved section. The secondary roadway consisted of a 7 ft-3 inch taper transition from a thrie-beam to W-beam, three CRT wood posts, and two steel posts. Figures 3.1 and 3.2 show the described system from the front and back view. The guardrail system was set as a reference for the following simulations.

The idea of adding sand barrels for the short radius was not an option since they did not fit the between the distance of the guardrail to where the ditch begins. A new idea was developed in which included drums filled with sand. The difference between the sand barrel and sand drum was that the sand drum was shorter, more ductile, and a smaller diameter, which made it suitable to fit within the distance between the guardrail and beginning of the ditch.



Figure 3.1. Guardrail System.

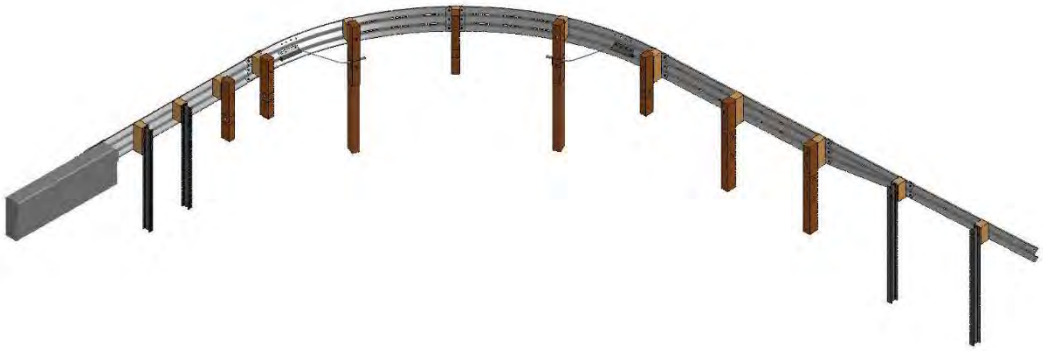


Figure 3.2. Guardrail System-Back.

The sand drums developed for the simulations were based on Eagle models, model number 1656, with a height of 36⅜-inches and 21-inch diameter. The drums were filled with sand and weighed approximately 700 lb. Figure 3.3 shows the drum used for the simulations.



Figure 3.3. Sand Drum Used in Simulations.

3.3 SIMULATION OF TRUCK IMPACTING SHORT RADIUS WITH TENSION CABLE AND FOUR 700-LB SAND DRUMS

A guardrail system design was evaluated in a simulation. This system includes only four drums and a tension cable. There are four 700-lb sand drums in the system used in this simulation, spread along the curved section of the rail. The drums are placed between posts, from posts 4 through 8. The goal of this simulation is to affirm that the truck is adequately captured within an acceptable distance behind the rail. The vehicle impacted the system at the center of the radius at a 25° angle. Figure 3.4 illustrates the whole guardrail system.

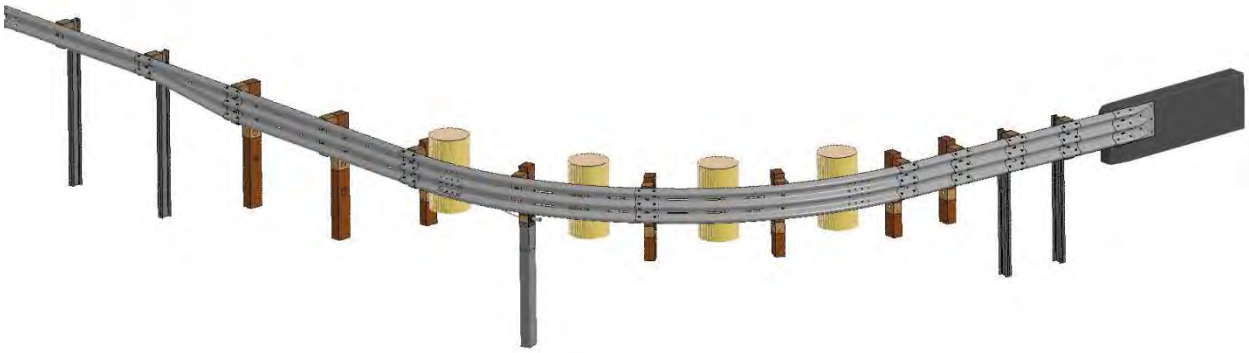


Figure 3.4. Entire System with Tension Cable and Four 700-lb Sand Drums.

Figure 3.5 shows the side view of the primary roadway. The primary roadway consists of two steel posts and two CRT posts. All four posts only contained one bolt. Figure 3.6 shows the side view of the secondary roadway. The secondary roadway consists of three CRT posts with blockouts and two steel posts. The curved section of the system consists of three CRT timber posts. The simulated parapet section represents the stiffer portion of the rail.

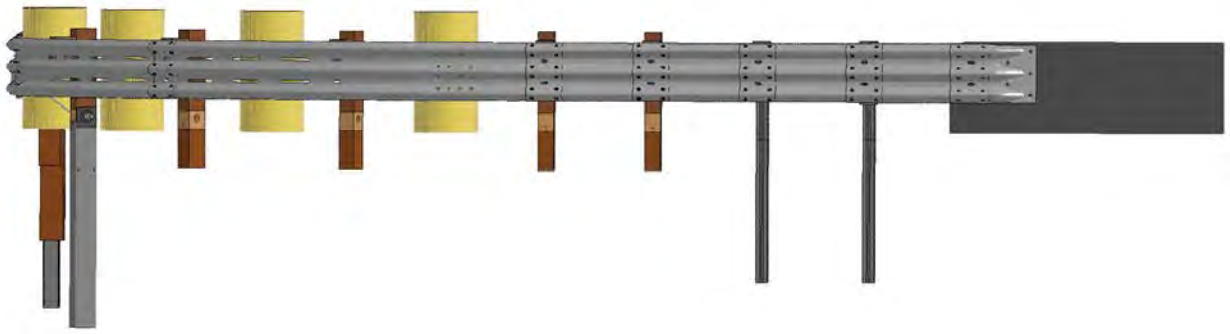


Figure 3.5. Side View of Primary Roadway.



Figure 3.6. Side View of Secondary Roadway.

The spacing for posts 1 to 4 is 3-ft and spacing for posts 4 to 12 is 6-ft 3-in. measured along the arc of the curved thrie beam. Figure 3.7 depicts the truck alignment with the system for this simulation.

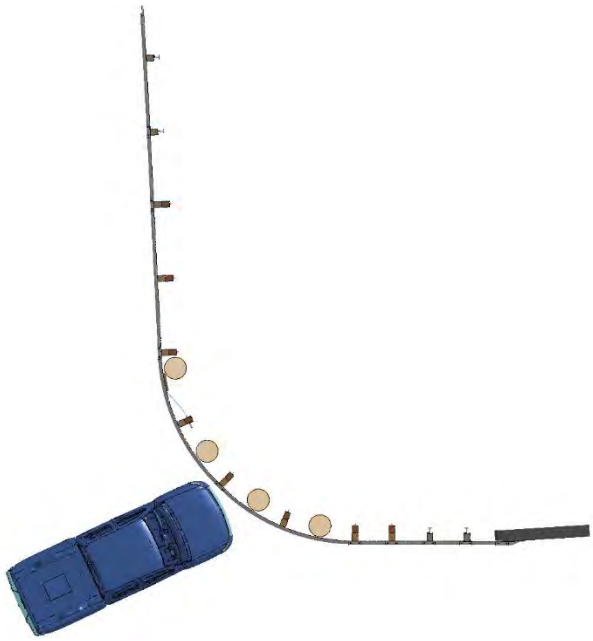


Figure 3.7. Alignment of Truck with System.

Figure 3.8 shows the sequential images of the simulation of the system with the truck. The first image shows the initial position of the truck and the system, and is followed by four images that depict the interaction of the truck with the guardrail system and the drums. By 0.075 s, the hood of the truck had deformed but had not passed into the windshield. At 0.26 s, three of the drums broke and the sand dispersed. The fourth drum was placed closer to the secondary roadway did not move from its place until 0.3 s. The last image displays the last state of the simulation. The drums and the guardrail system engaged to absorb the kinetic energy of the vehicle and successfully contain the truck.

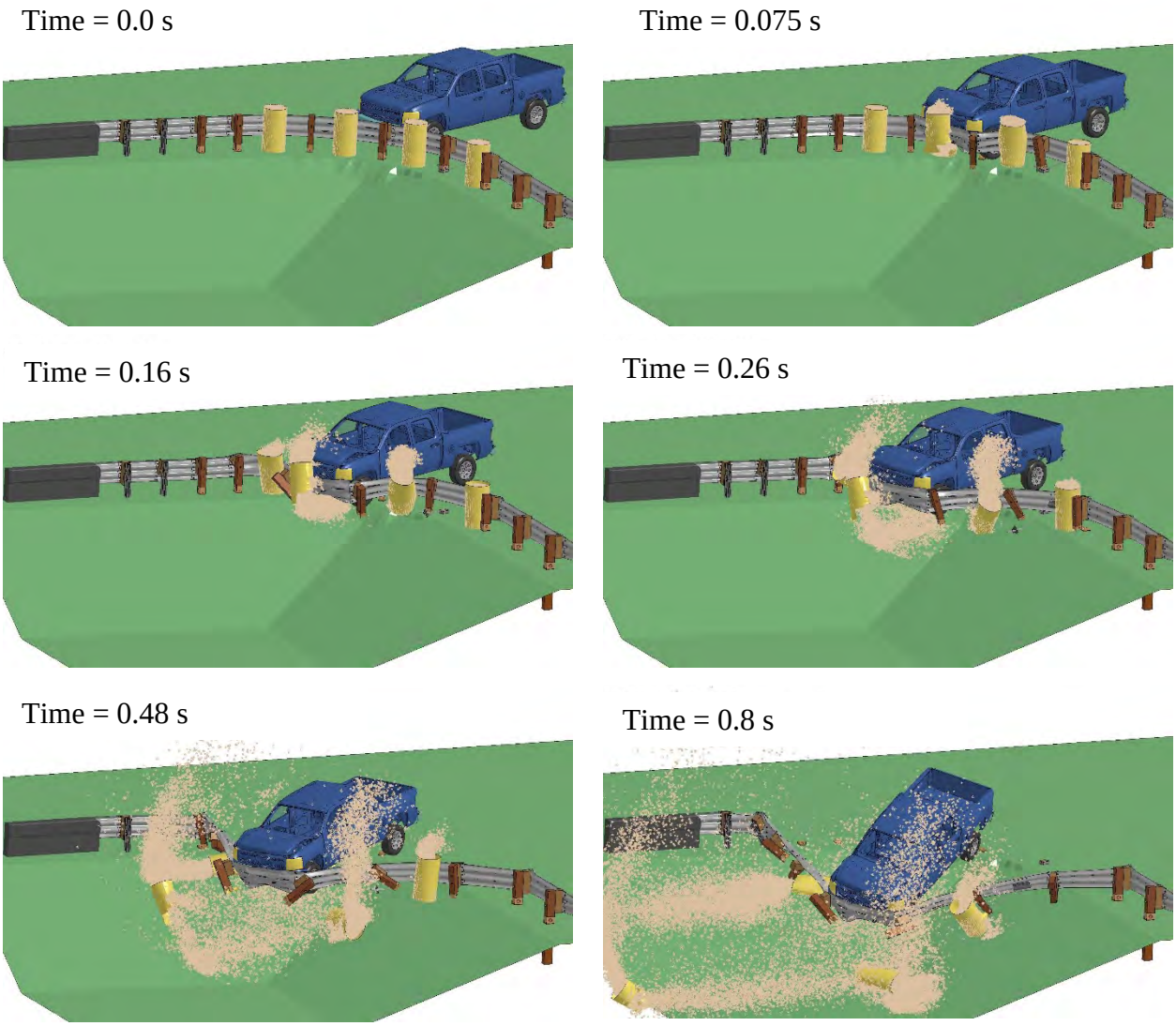


Figure 3.8. Sequential Images of Truck Simulation with Tension Cable and Four 700-lb Sand Drums.

Figures 3.9 and 3.10 show the interaction in the development and final state of the simulation of the truck, respectively. The drums have been hidden from the following images to better show the deformation happening between the vehicle and the system.

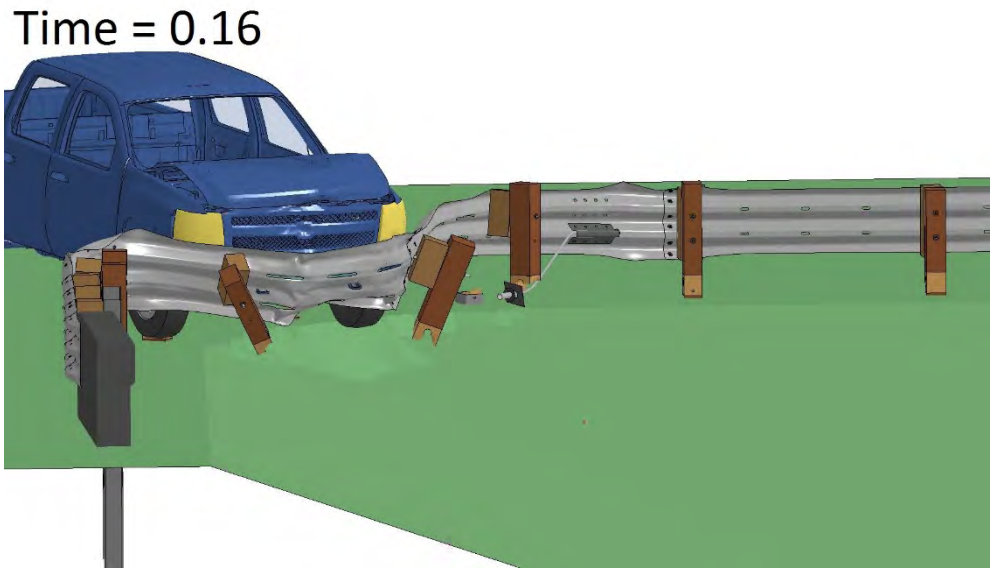


Figure 3.9. Interaction of Truck with System.

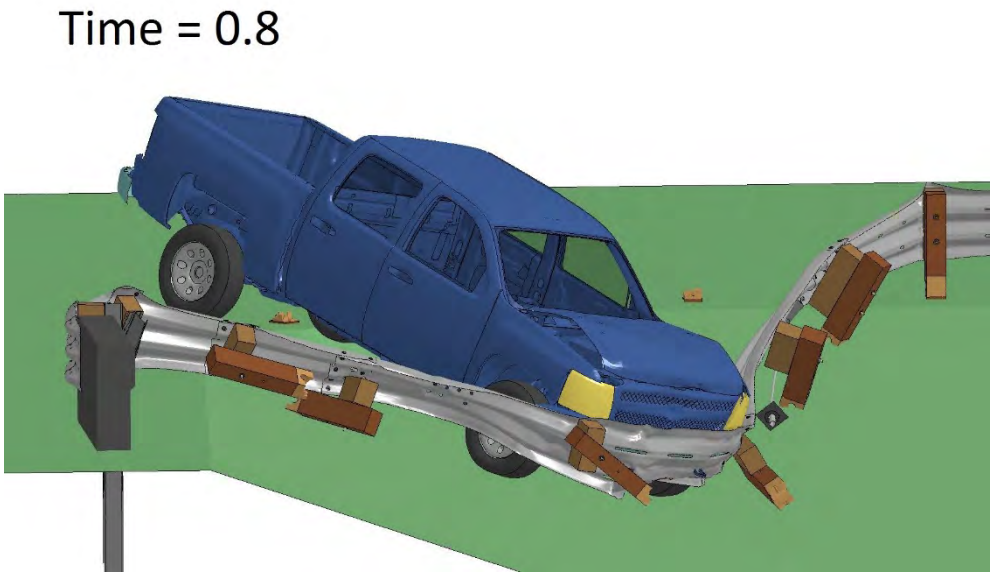


Figure 3.10. Final State of Simulation.

Table 3.1 shows the TRAP results of the occupant risk factor for the simulation with the Tension Cable and spread out 700-lb sand drums.

Table 3.1. TRAP Summary Data of Simulation with Tension Cable and Four 700-lb Sand Drums.

TRAP Results: Truck Short Radius	
Impact Velocity, mph	43.5
Impact Angle (degrees)	25
Occupant Risk Factors	
OIV (ft/s)	
x-direction	24.3
y-direction	0.67
Occupant Ridedown Accelerations (g's)	
x-direction	−4.4
y-direction	−2.3
Max Roll, Pitch, and Yaw Angles (degrees)	
Roll	−9.5
Pitch	−16.3
Yaw	−18

3.4 SIMULATION OF TRUCK IMPACTING SHORT RADIUS WITH TENSION CABLE AND FOUR 700-LB SAND DRUMS

This simulation case aligns the truck parallel with the primary roadway. Figure 3.11 shows the system used in this simulation and the alignment of the truck within the system. The system contains the four 700-lb sand drums spread along the curved section of the rail and the tension cable placed on the secondary roadway.

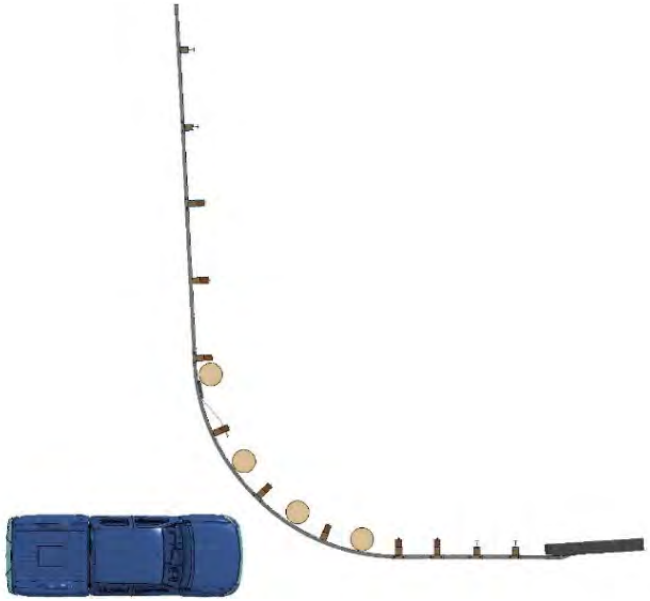


Figure 3.11. Alignment of Truck with System.

Figure 3.12 displays the truck in sequential images throughout the simulation. The truck remained stable throughout the impact. At 0.15 s, there is damage to the front left corner of truck and the rail has been pushed into the interior of the system. At 0.3 s, the truck begins to be redirected away from the guardrail system. By the end of the simulation, the truck has been redirected and its interaction with the system is complete. At this point in the simulation, two posts and two drums have broken, while the other remaining drums are still standing. The front corner and tire on the driver's side and the back corner on the same side were damaged.

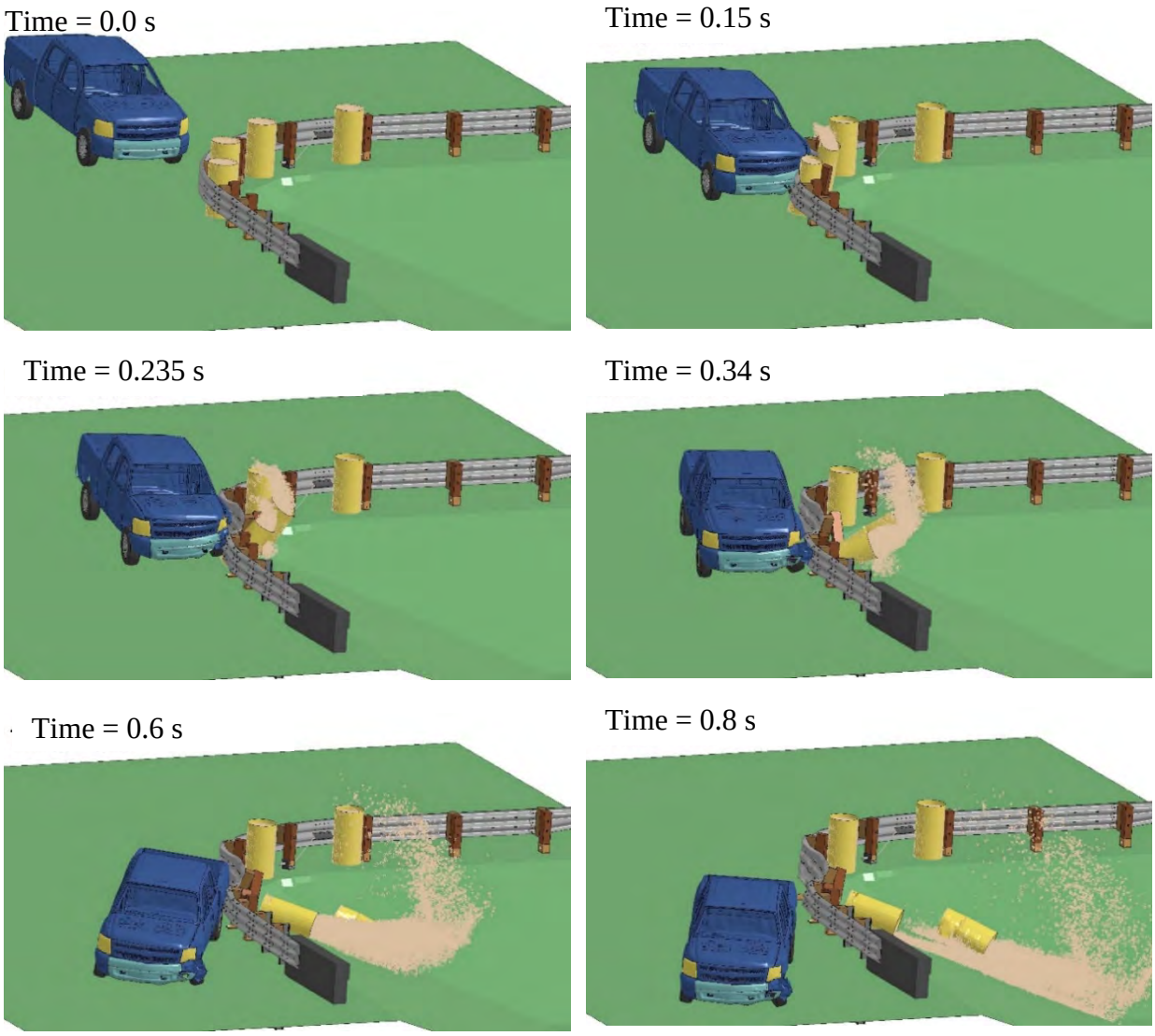


Figure 3.12. Sequential Images of Truck Simulation with Tension Cable and Four 700-lb Sand Drums.

The sequential images in Figure 3.13 show a closer view of the interaction between the guardrail and vehicle from the back of the system. The sand and the drums have been removed from these images to show the interaction of the rail and vehicle clearly. Figure 3.14 shows a closer view of the interaction.

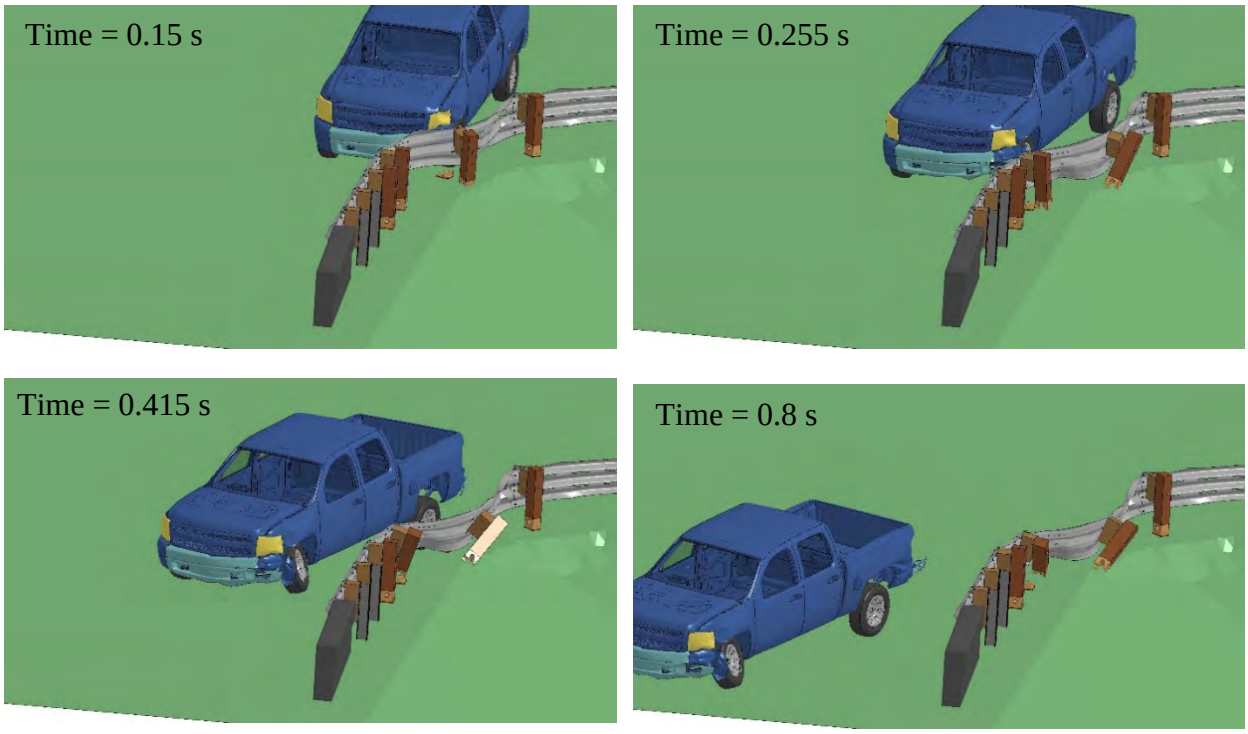


Figure 3.13. Sequential Images of Truck Simulation from Back of Rail (No Drums Visible).

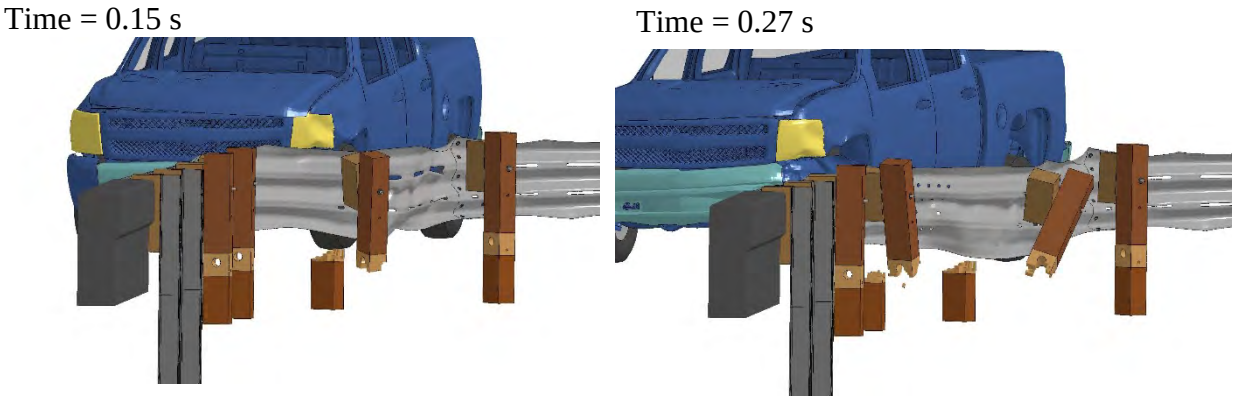


Figure 3.14. Interaction of Truck with System (No Drums Visible).

Table 3.2 shows the TRAP results of the occupant risk factor for the simulation with the Tension Cable and spread out 700-lb sand drums.

Table 3.2. TRAP Summary Data of Simulation with Tension Cable and Four 700-lb Sand Drums.

TRAP Results: Truck Short Radius	
Impact Velocity, mph	43.5
Impact Angle (degrees)	0
Occupant Risk Factors	
OIV (ft/s)	
x-direction	17.1
y-direction	−13.1
Occupant Ridedown Accelerations (g's)	
x-direction	−5.8
y-direction	3.8
Max Roll, Pitch, and Yaw Angles (degrees)	
Roll	−3.7
Pitch	−2.1
Yaw	27.7

3.5 SIMULATION OF TRUCK IMPACTING SHORT RADIUS WITH TENSION CABLE AND FIVE 700-LB SAND DRUMS

Figure 3.15 shows the system used for the simulation. The changes made to the system included an extra drum, placed between posts 11 and 12. A total of five drums are placed along the rail from posts 9 to 13. Two drums are placed between posts 11 and 12. The drum placed between posts 9 and 10 is placed 17 inches from center of drum to center of post 9. The same short cable placed on the secondary roadway between posts 9 and 10 is also included in the system. The cable is attached to the thrie beam and terminates at post 10 at an angle.



Figure 3.15. Tension Cable and Five 700-lb Sand Drums.

Figure 3.16 demonstrates the progression of the simulation to summarize the behavior of the vehicle. The rail and the deformation of the front of the truck did not pass as far into the windshield as on previous simulations. The back tires of the truck were in the air by 0.609 s. Six of the wood posts broke at the end of the simulation and all six drums broke and dispersed the sand.

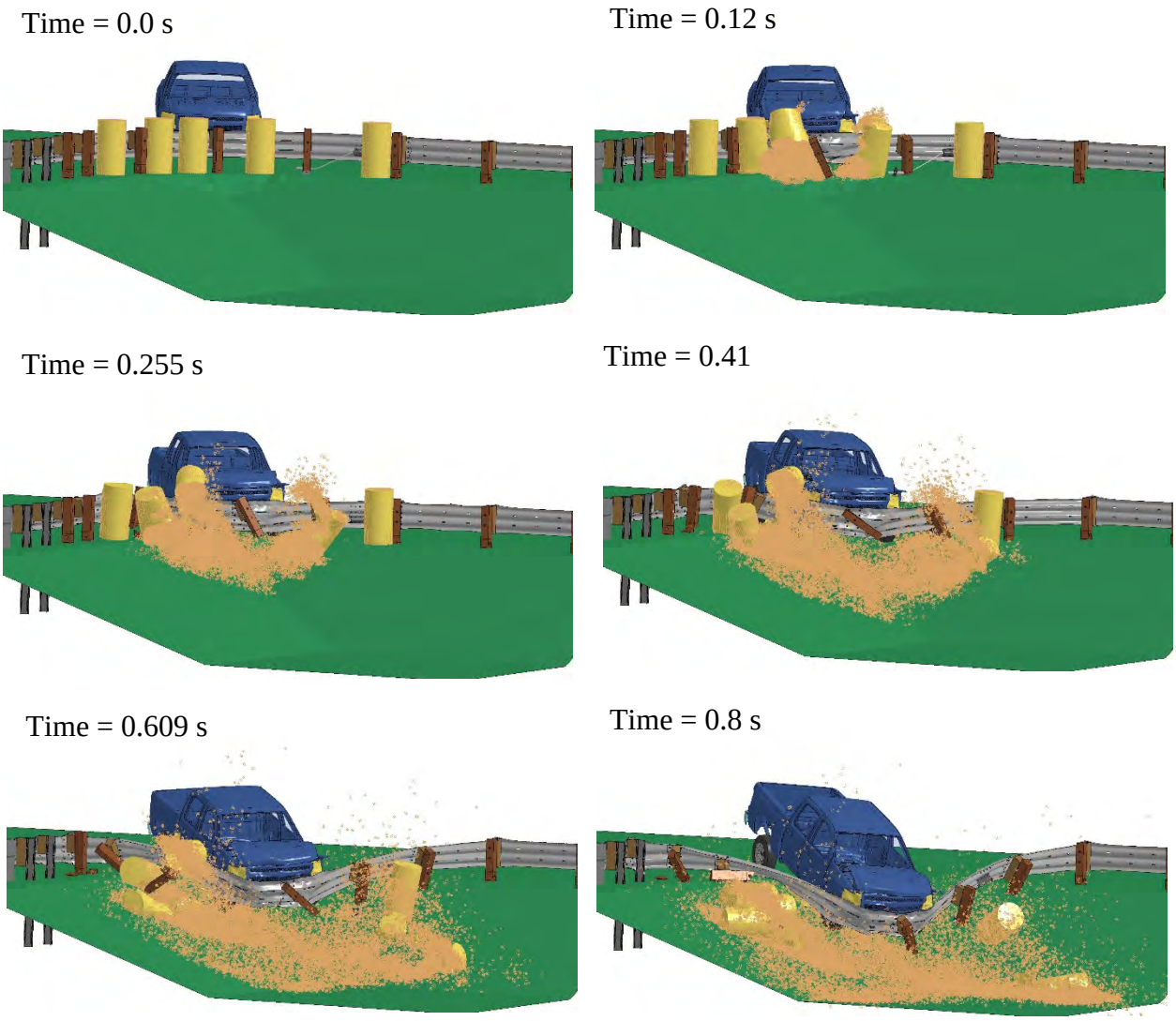


Figure 3.16. Sequential Images of Truck Simulation with Tension Cable and Five 700-lb Sand Drums.

Figures 3.17 and 3.18 display images of a closer view of the interaction between the truck and the system. The drums were removed from the images to have a clear view of the interaction.

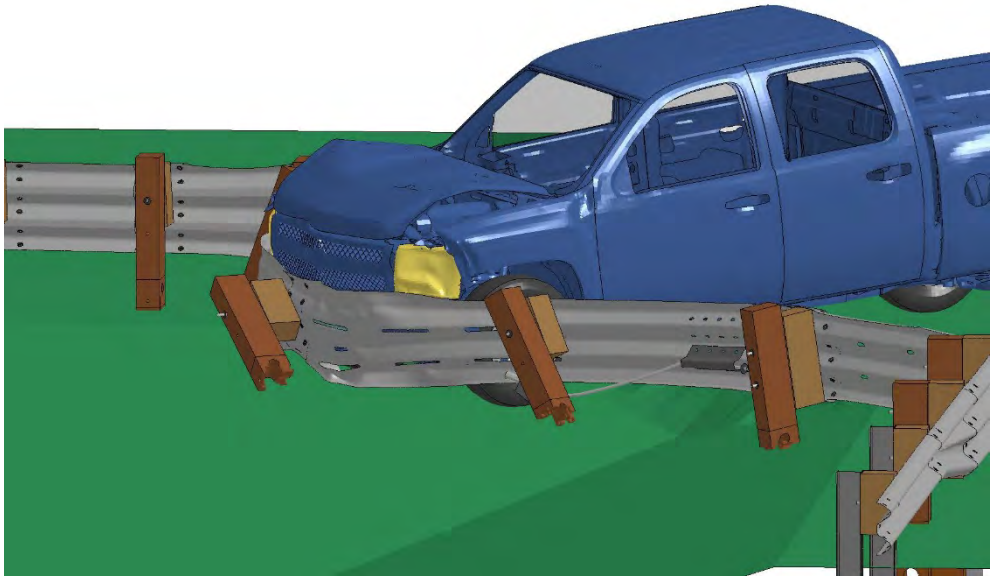


Figure 3.17. Interaction of Truck with System (No Drums Visible).

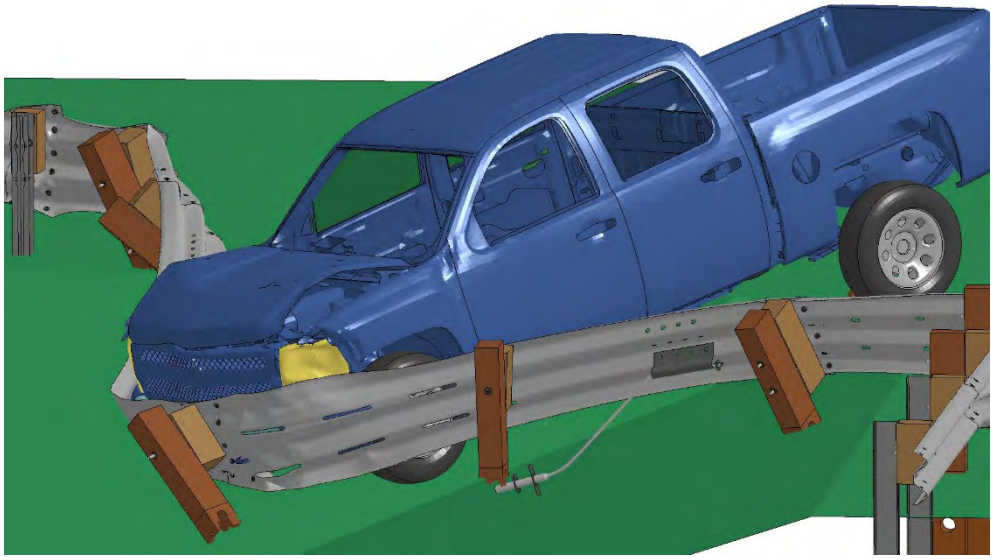


Figure 3.18. Final State of Truck (No Drums Visible).

Table 3.3 shows the TRAP results of the occupant risk factor for the simulation with the Tension Cable and spread out 700-lb sand drums.

Table 3.3. TRAP Summary Data of Simulation with Tension Cable and Five 700-lb Sand Drums.

TRAP Results: Truck Short Radius	
Impact Velocity, mph	43.5
Impact Angle (degrees)	25
Occupant Risk Factors	
OIV (ft/s)	
x-direction	29.2
y-direction	2.3
Occupant Ridedown Accelerations (g's)	
x-direction	−4.0
y-direction	−5.6
Max Roll, Pitch, and Yaw Angles (degrees)	
Roll	4.9
Pitch	−16.3
Yaw	−22.5

3.6 SIMULATION OF TRUCK IMPACTING SHORT RADIUS WITH TENSION CABLE AND SIX 700-LB SAND DRUMS

Figure 3.19 shows the system used for this simulation and the alignment of the truck to the system. For this simulation, the same layout was used with an additional drum. The system includes one short cable and a total of six drums spread along the rail. The drums are placed between posts 9 through 14. The short cable is on the secondary roadway placed between posts 9 and 10. It is attached to the thrie beam and terminates at post 10 at an angle.



Figure 3.19. Alignment of Truck with System.

Figure 3.20 presents the simulation of the truck. The first CRT post along the primary roadway broke, and by the end of the simulation three CRT posts were broken, one steel post was deformed, and the other stayed stable through the simulation. By 0.309 s, the driver side front wheel of the truck began to ride up onto the rail. The truck becomes unstable as early as 0.35 s.

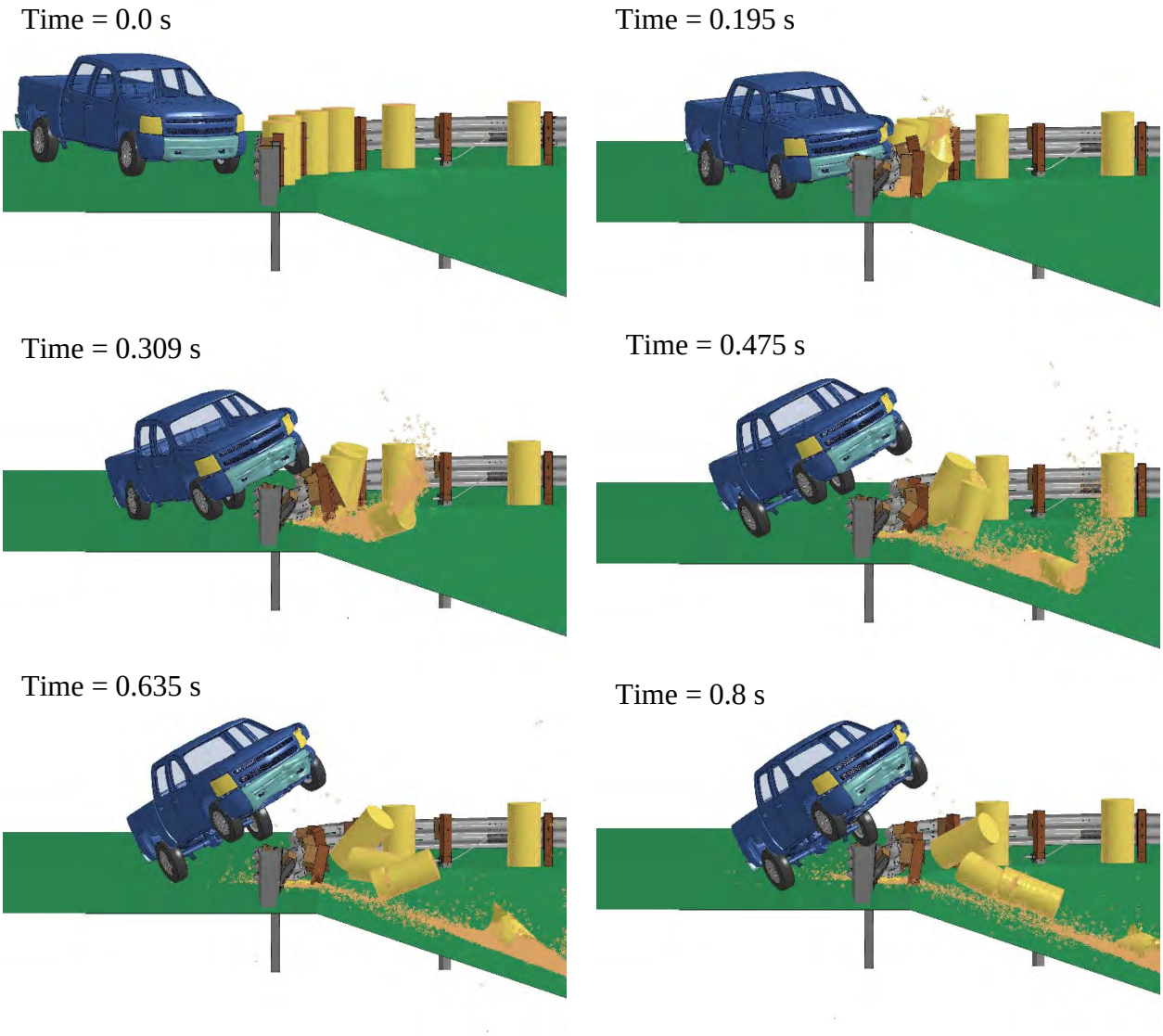


Figure 3.20. Sequential Images of Truck Simulation with Tension Cable and Six 700-lb Sand Drums.

Figures 3.21 and 3.22 display a closer view of the interaction. The drums were removed to show the deformation between the car and the rail.



Figure 3.21. Interaction of Truck with System.

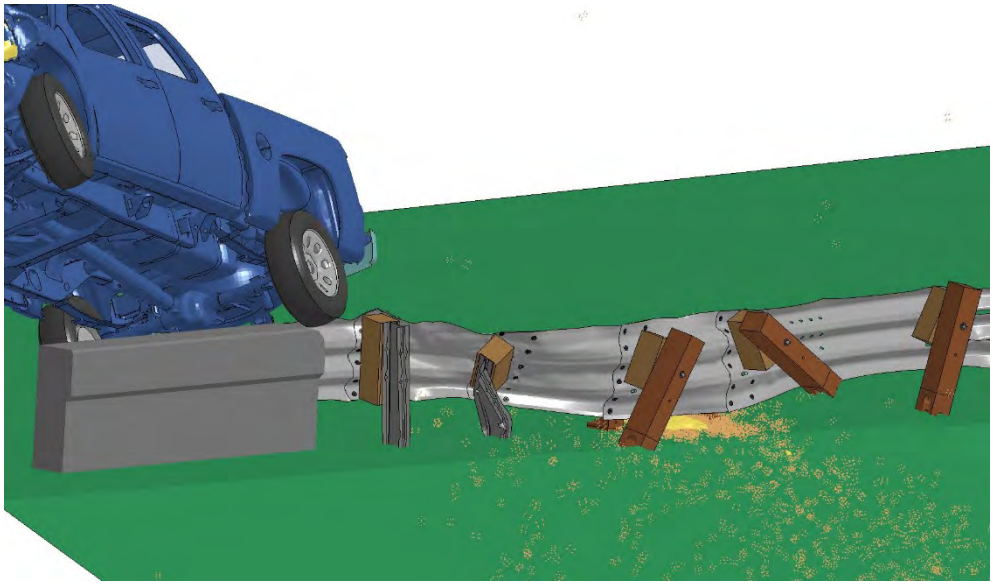


Figure 3.22. Final State of Truck.

Table 3.4 shows the TRAP results of the occupant risk factor for the simulation with the Tension Cable and spread out 700-lb sand drums.

Table 3.4. TRAP Summary Data of Simulation with Tension Cable and Six 700-lb Sand Drums.

TRAP Results: Truck Short Radius	
Impact Velocity, mph	43.5
Impact Angle (degrees)	25
Occupant Risk Factors	
OIV (ft/s)	
x-direction	26.2
y-direction	−7.2
Occupant Ridedown Accelerations (g's)	
x-direction	−7.6
y-direction	7.6
Max Roll, Pitch, and Yaw Angles (degrees)	
Roll	28.2
Pitch	16.7
Yaw	10.0

3.7 SIMULATION OF TRUCK IMPACTING SHORT RADIUS WITH TWO TENSION CABLES AND SIX 700-LB SAND DRUMS

Figure 3.23 presents the system layout used for the following simulation. The system includes two short cables and six drums spread along the rail. One of the cables is placed on the primary roadway between posts 12 and 13. It is attached to the thrie beam and terminates at post 12 at an angle. The second short cable is placed on the secondary roadway between posts 9 and 10. It is attached to the thrie beam and terminates at post 10. The six drums are placed between posts 9 through 15. Only one drum is placed between each post.

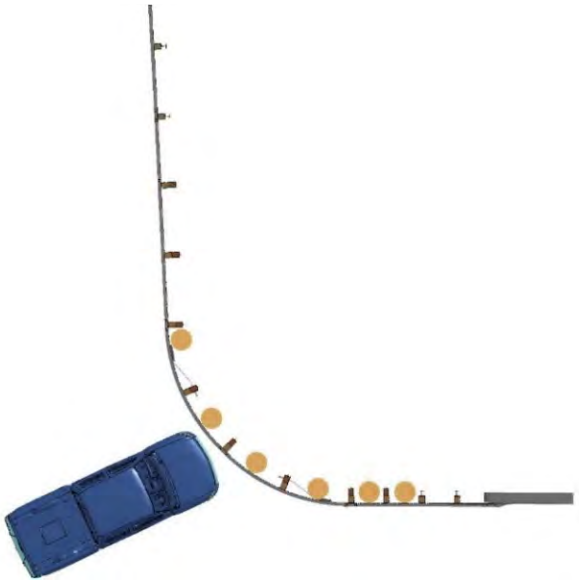


Figure 3.23. Alignment of Truck with System.

Figure 3.24 shows the sequential images of the simulation. In this simulation, the truck did not override the system. At 0.68 s, six of the wood posts broke and most of the drums dispersed the sand they were containing.

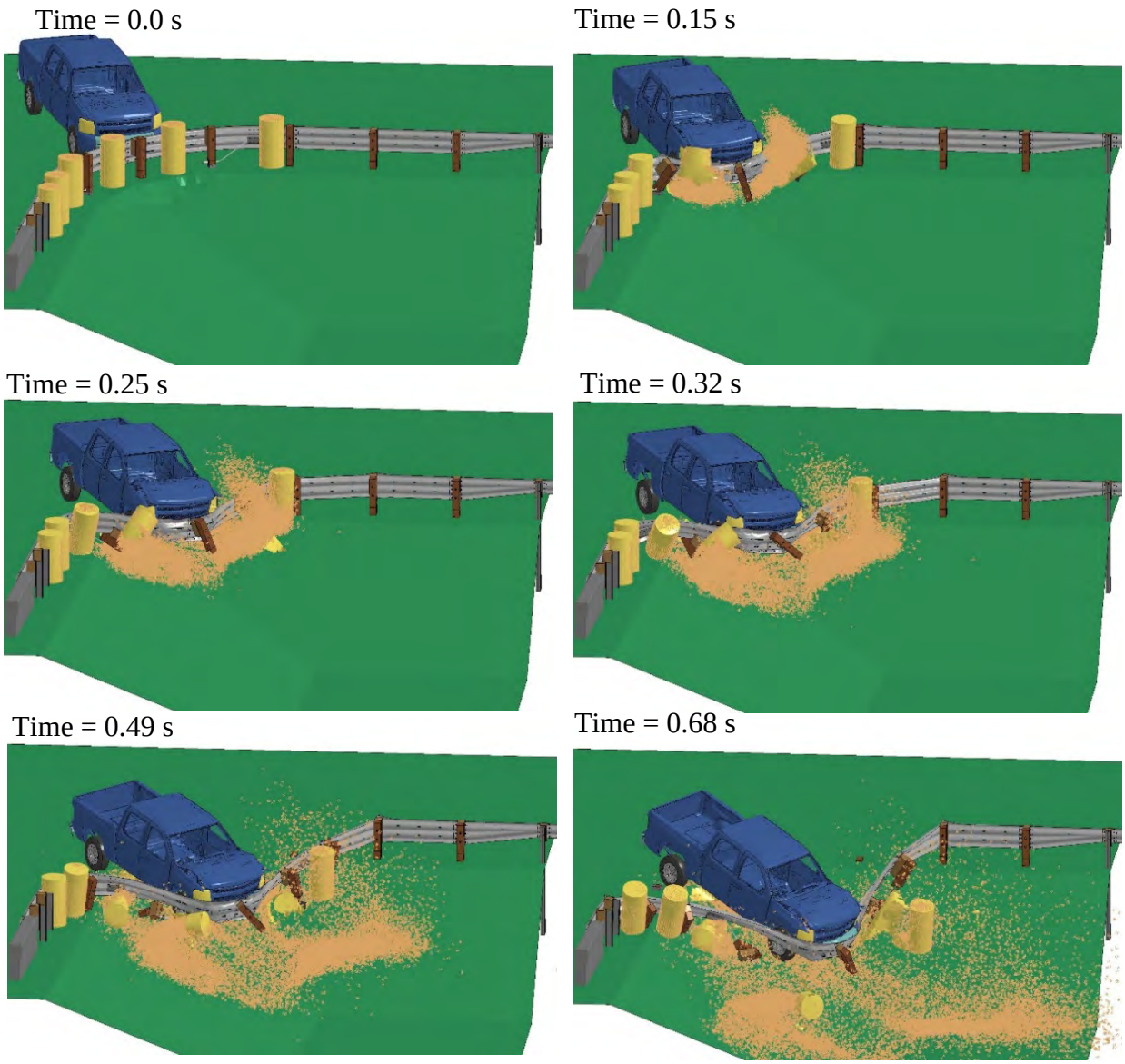


Figure 3.24. Sequential Images of Truck Simulation with Two Tension Cables and Six 700-lb Sand Drums.

Figures 3.25 and 3.26 are a closer view of the simulation. The drums were removed to show the deformation of the car and guardrail.

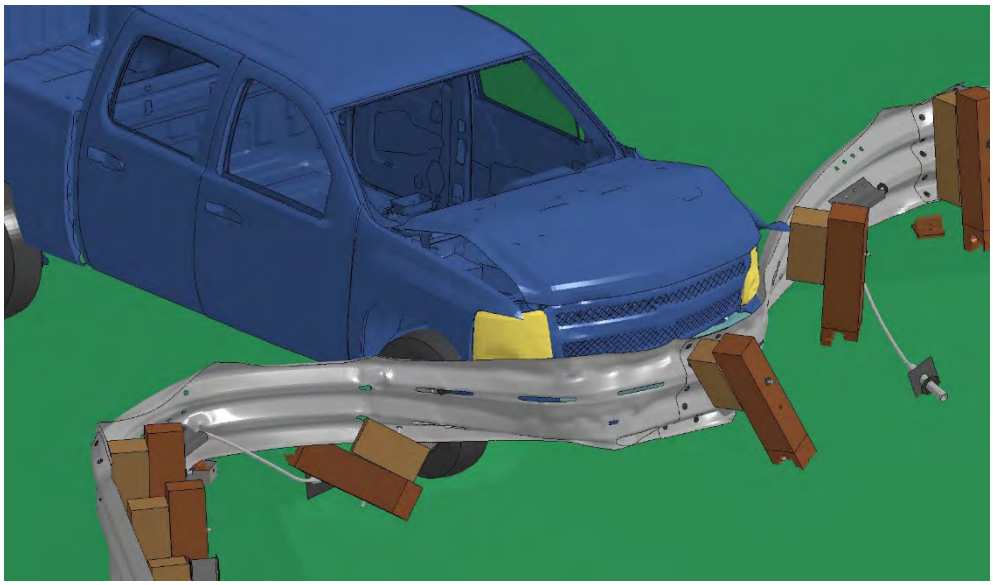


Figure 3.25. Interaction of Truck with System (No Drums Visible).

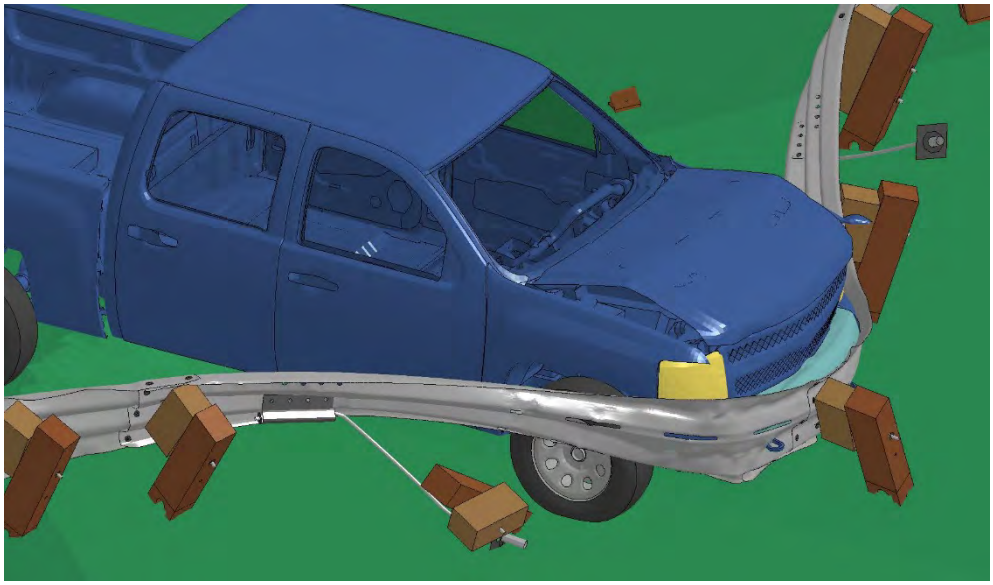


Figure 3.26. Final State of Truck Simulation (No Drums Visible).

Table 3.5 shows the TRAP results of the occupant risk factor for the simulation with the Tension Cable and spread out 700-lb sand drums.

Table 3.5. TRAP Summary Data of Simulation with Two Tension Cables and 700-lb Sand Drums.

TRAP Results: Truck Short Radius	
Impact Velocity, mph	43.5
Impact Angle (degrees)	25
Occupant Risk Factors	
OIV (ft/s)	
x-direction	25.9
y-direction	1.9
Occupant Ridedown Accelerations (g's)	
x-direction	−5.1
y-direction	−5.3
Max Roll, Pitch, and Yaw Angles (degrees)	
Roll	−5.7
Pitch	−15.5
Yaw	−29.0

3.8 SIMULATION OF TRUCK IMPACTING SHORT RADIUS WITH TENSION CABLE AND SIX 700-LB SAND DRUMS

For the following simulation, the truck was placed at a different position in the system. Figure 3.27 displays the system used and the alignment of the truck to the system. For this system, the cable from the preciously described system was removed. The truck is still at a 25° angle from the guardrail system, but this time it is impacting the guardrail system on the primary roadway.



Figure 3.27. Alignment of Truck with System.

Figure 3.28 shows the sequential images of the simulation. At 0.15 s, the truck has impacted the rail. The last image shows that the truck was not redirected away from the system. Instead, the front of the truck began to override the rail.

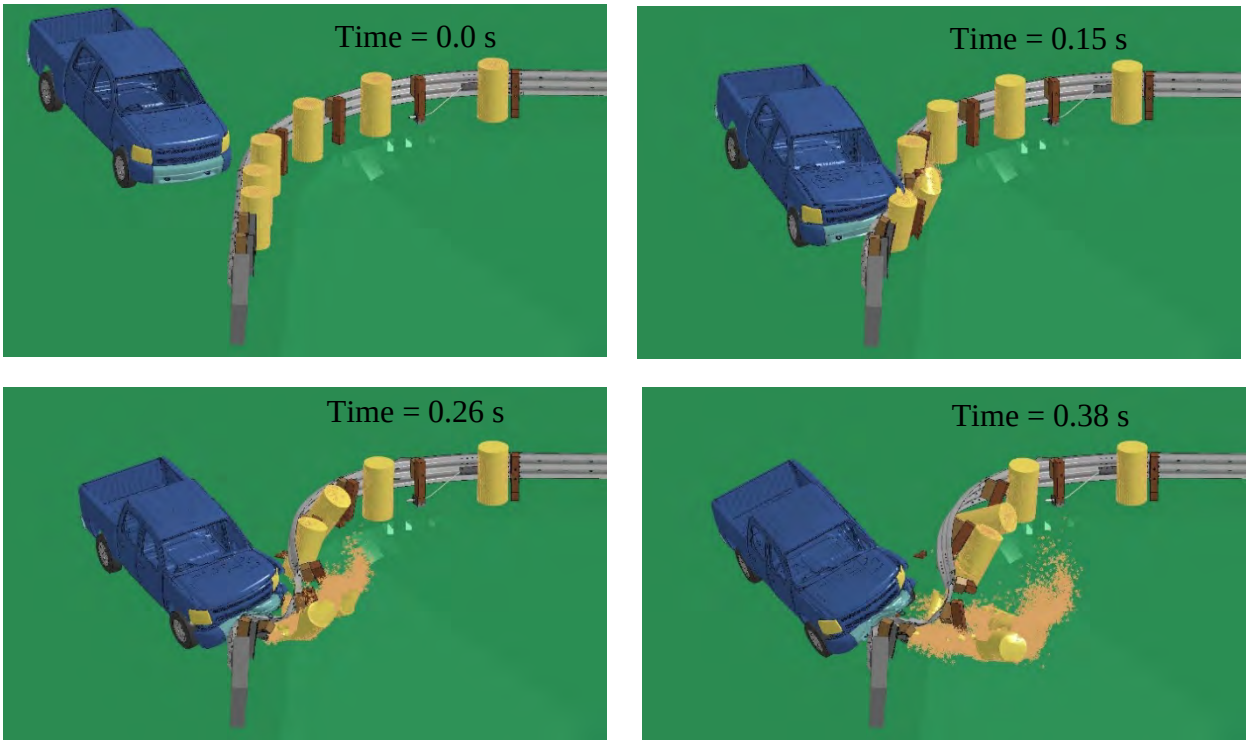


Figure 3.28. Sequential Images of Truck Simulation with Tension Cable and Six 700-lb Sand Drums.

Figures 3.29 and 3.30 show a close view of the deformation between the truck and the guardrail system. These two figures show different views of the truck at certain points in the simulation. As seen below, at approximately 0.3 s the front of the truck is lifted up. The drums were removed for clarity.

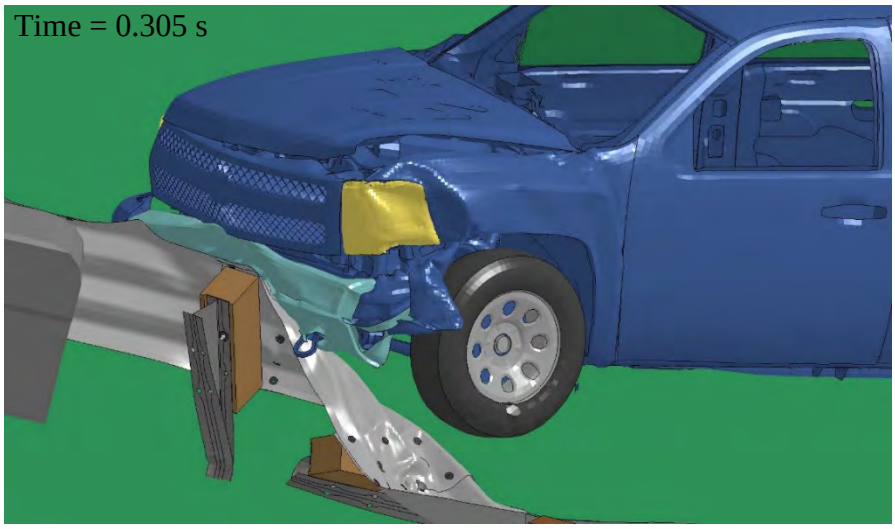


Figure 3.29. Interaction of Truck with System (No Drums Visible).

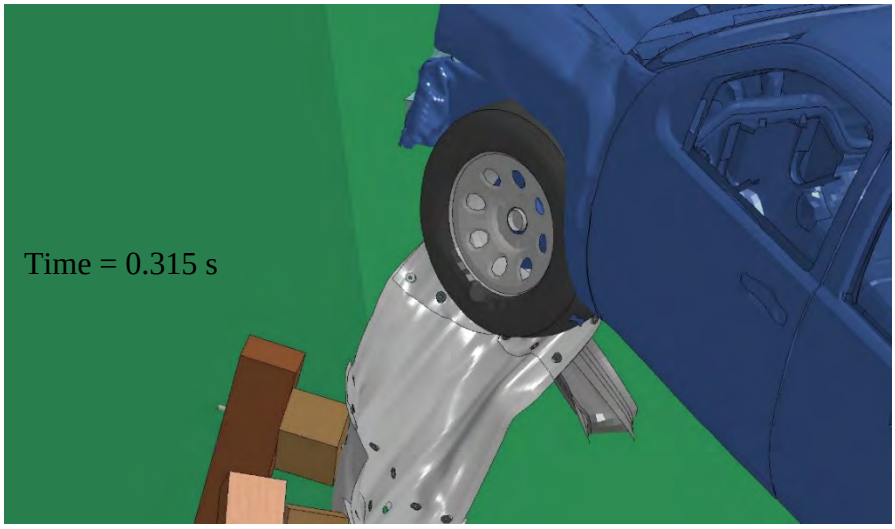


Figure 3.30. Interaction of Truck with System (No Drums Visible).

Table 3.6 shows the TRAP results of the occupant risk factor for the simulation with the Tension Cable and spread out 700-lb sand drums.

Table 3.6. TRAP Summary Data of Simulation with Tension Cable and Six 700-lb Sand Drums.

TRAP Results: Truck Short Radius	
Impact Velocity, mph	43.5
Impact Angle (degrees)	25
Occupant Risk Factors	
OIV (ft/s)	
x-direction	34.4
y-direction	−7.5
Occupant Ridedown Accelerations (g's)	
x-direction	−7.5
y-direction	5.2
Max Roll, Pitch, and Yaw Angles (degrees)	
Roll	21.8
Pitch	−3.5
Yaw	4.3

3.9 SIMULATION OF TRUCK IMPACTING SHORT RADIUS WITH TWO TENSION CABLES AND SIX 700-LB SAND DRUMS

Figure 3.31 displays the following system and position of the truck used for this simulation. Since the simulation described above did not satisfy the requirements, the cable was added back to the primary roadway.



Figure 3.31. Alignment of Truck with System.

Figure 3.32 shows the sequential images of this simulation. At 0.105 s, the truck pushed the rail into the interior of the system and the front left side of the truck deformed. The cable maintained tension capacity. By 0.4 s, the truck had been redirected. At 0.475 s, the left side corner of the truck interacted with the system. The last image displays the redirected truck after its interaction with the system was complete.

Figure 3.33 presents a closer view of the interaction. Deformation has occurred for both the truck and rail, leaving two broken CRT posts and one deformed steel post. The sand has been hidden from these images to better see the rail and truck.

Table 3.7 shows the TRAP results of the occupant risk factor for the simulation with one short cable and six spread out 700-lb sand drums.

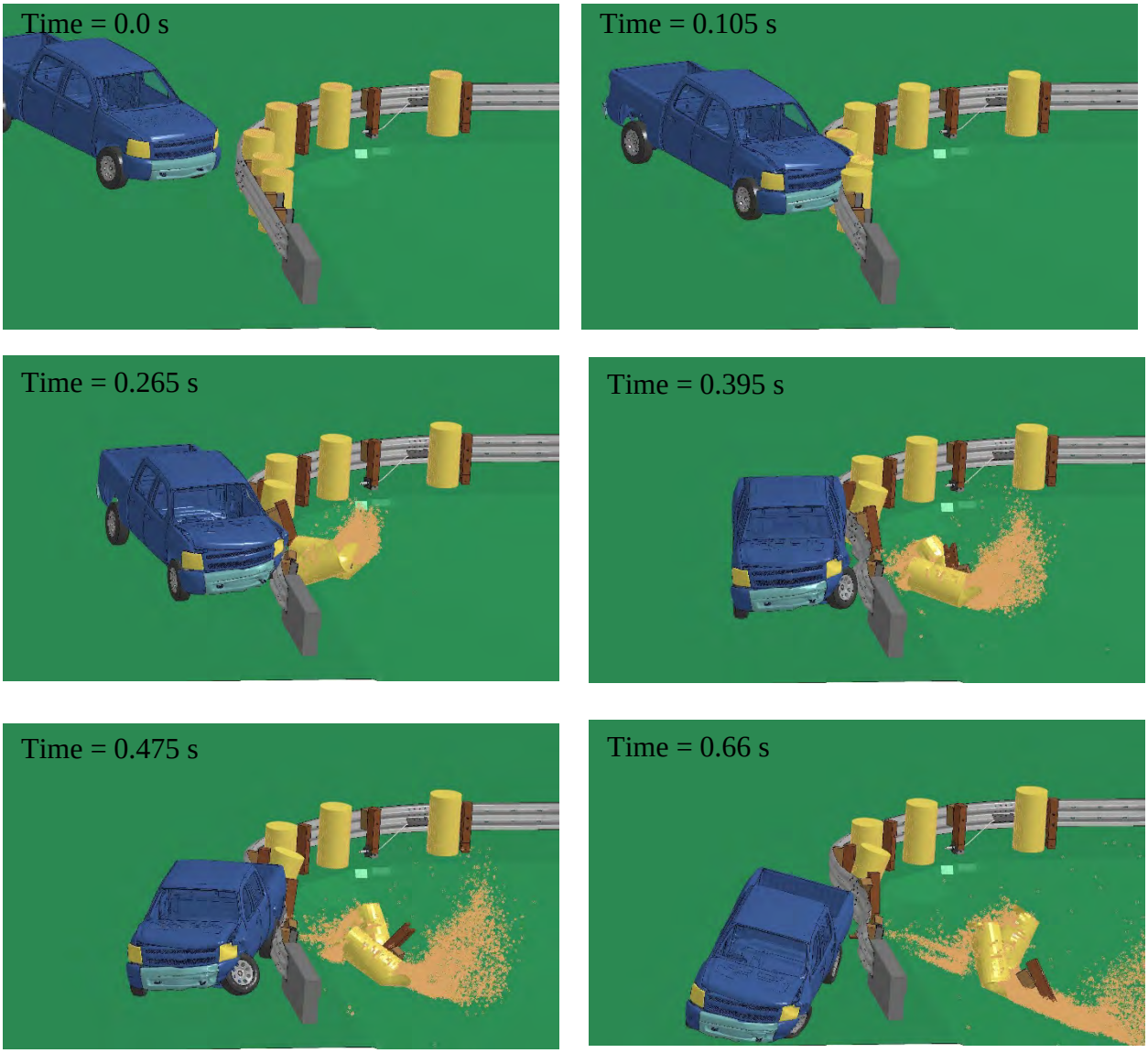


Figure 3.32. Sequential Images of Truck Simulation with Two Tension Cables and Six 700-lb Sand Drums.

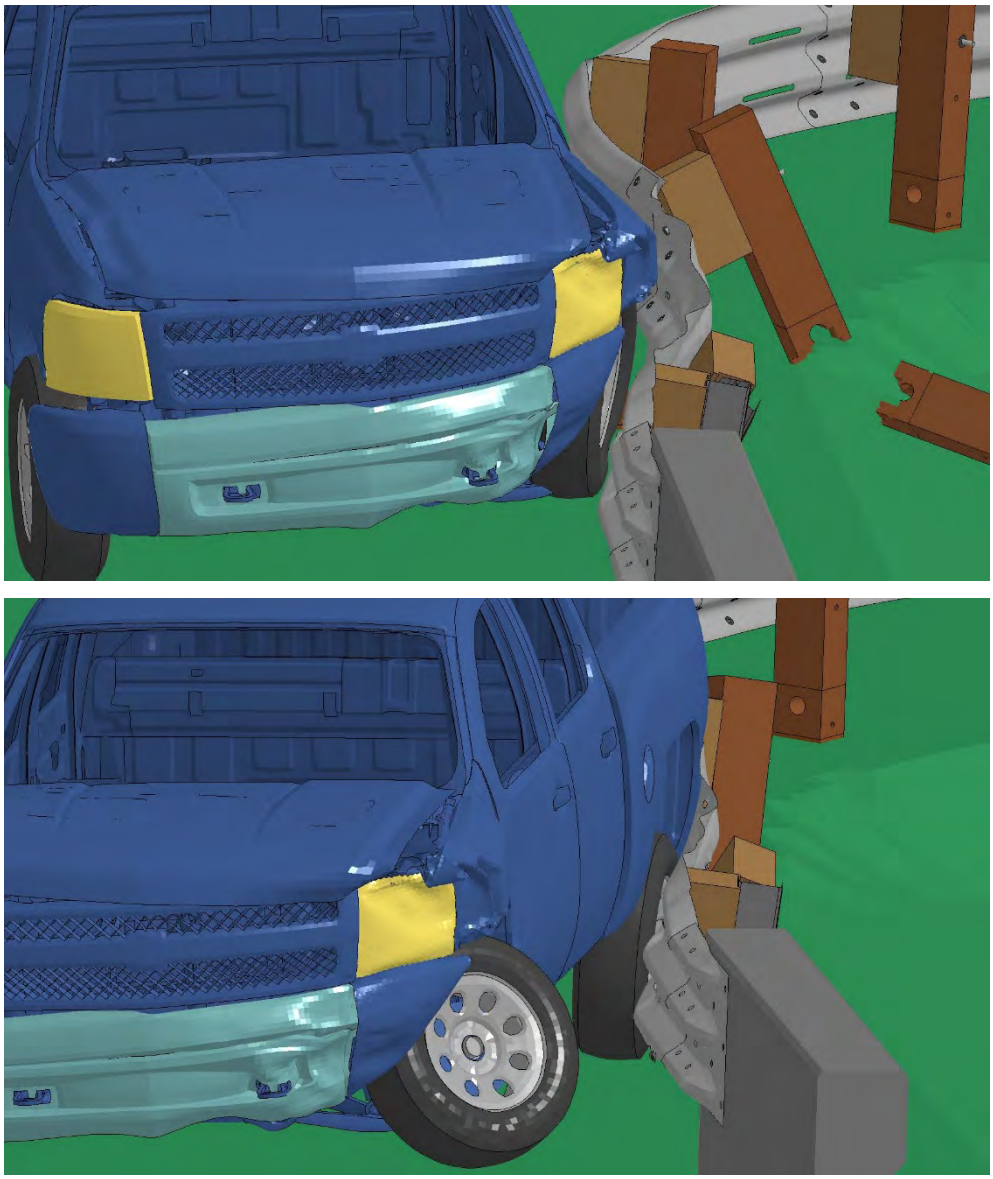


Figure 3.33. Interaction of Truck with System (No Drums Visible).

Table 3.7. TRAP Summary Data of Simulation with Two Tension Cables and Six 700-lb Sand Drums.

TRAP Results: Truck Short Radius	
Impact Velocity, mph	43.5
Impact Angle (degrees)	25
Occupant Risk Factors	
OIV (ft/s)	
x-direction	6.5
y-direction	−4.2
Occupant Ridedown Accelerations (g's)	
x-direction	−5.4
y-direction	7.0
Max Roll, Pitch, and Yaw Angles (degrees)	
Roll	−9.2
Pitch	−4.8
Yaw	48.5

3.10 SIMULATION OF TRUCK IMPACTING SHORT RADIUS WITH TWO TENSION CABLES AND SIX 700-LB SAND DRUMS

The following simulation includes the same system design with two tension cables and six 700-lb sand drums distributed behind the guardrail, from posts 9 to 15.

Figure 3.34 presents the sequential images depicting the performance of the system. The first image shows the initial position of the system. At 0.25 s, four wood posts surrounding the impact area broke. The wood posts continued to break consecutively. By the end of the simulation, all of the wood posts broke and one of steel posts had significant bending while the other one still remained intact.

Figures 3.36 and 3.36 show a closer view of the impact during the simulation and at the final state of the simulation. The drums were removed to have a clear view. Figure 3.36 displays a clear view of how the rail started to go under the front of the truck.

Table 3.8 shows the TRAP results of the occupant risk factor for the simulation with the Tension Cable and six spread out 700-lb sand drums.

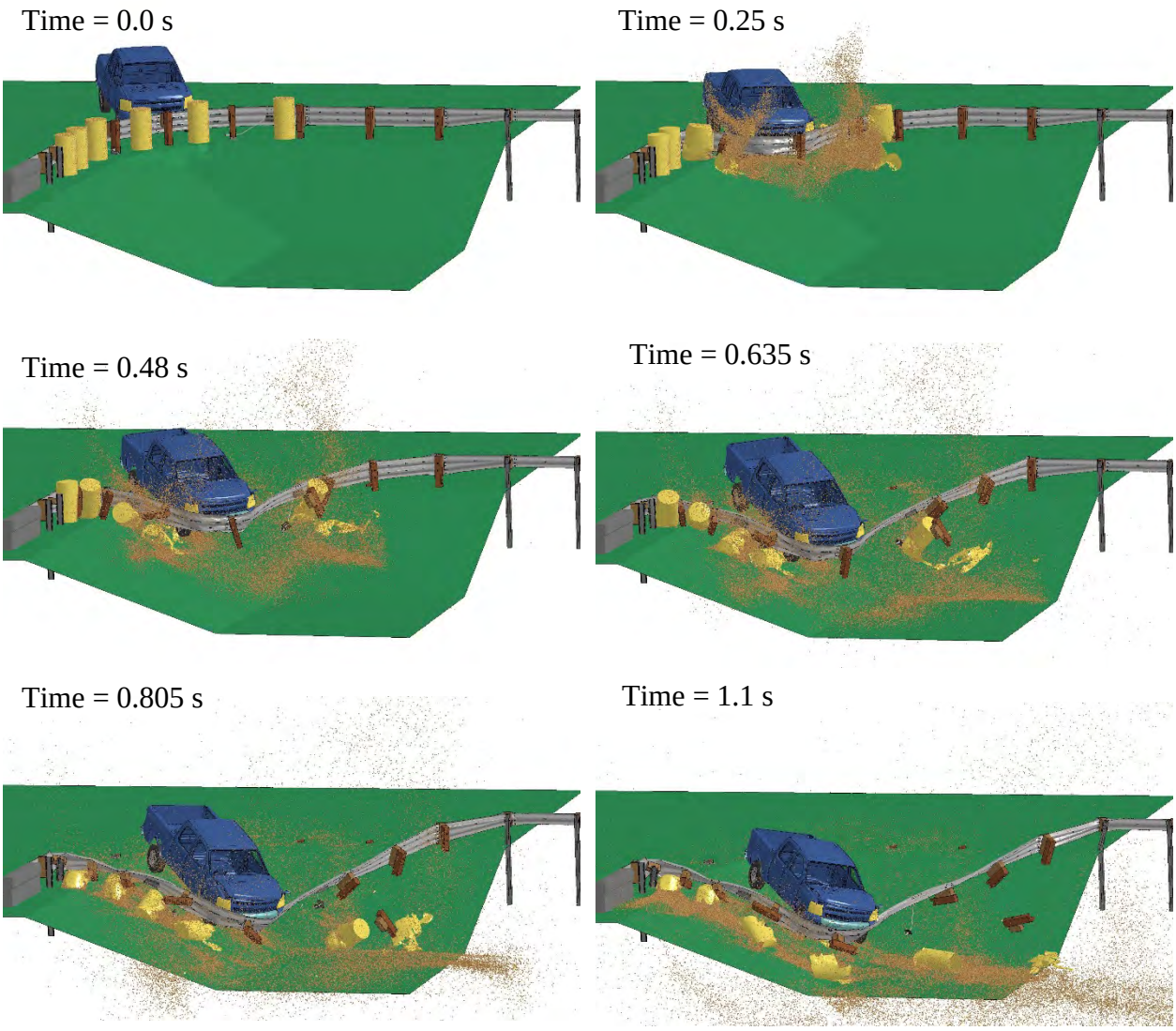


Figure 3.34. Sequential Images of Truck Simulation with Two Tension Cables and Six 700-lb Sand Drums.

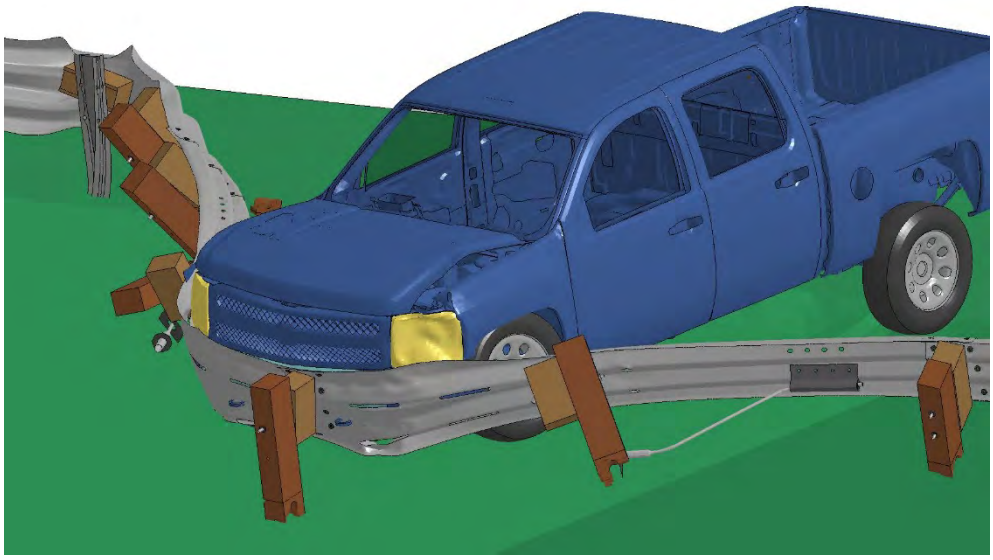


Figure 3.35. Interaction of Simulation with System (No Drums Visible).

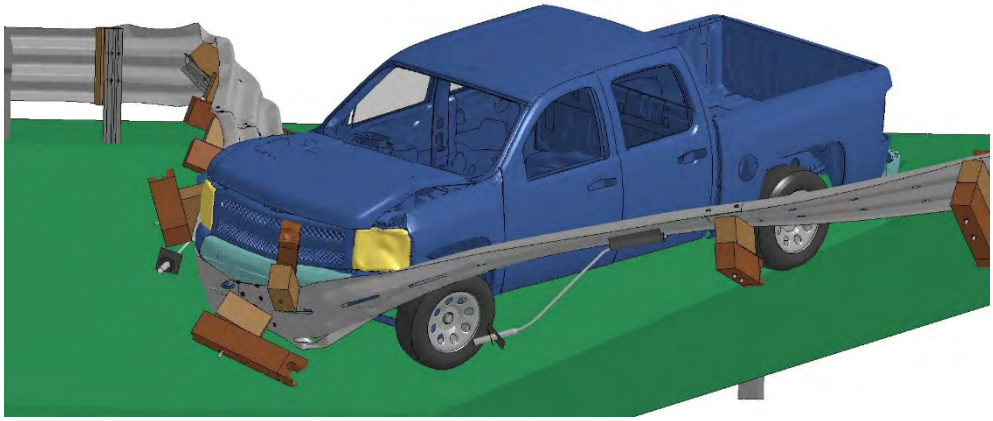


Figure 3.36. Final State of Truck (No Drums Visible).

Table 3.8. TRAP Summary Data of Simulation with Two Tension Cables and Six 700-lb Sand Drums.

TRAP Results: Truck Short Radius	
Impact Velocity, mph	43.5
Impact Angle (degrees)	25
Occupant Risk Factors	
OIV (ft/s)	
x-direction	21.3
y-direction	3.6
Occupant Ridedown Accelerations (g's)	
x-direction	−3.9
y-direction	−2.7
Max Roll, Pitch, and Yaw Angles (degrees)	
Roll	−12.6
Pitch	−17.5
Yaw	−16.6

3.11 SIMULATION OF TRUCK IMPACTING SHORT RADIUS WITH TWO TENSION CABLES AND SIX 700-LB SAND DRUMS

The same guardrail system of the truck presented above is used for this simulation. The goal of this simulation is to affirm that the truck is adequately captured within an acceptable distance behind the rail. Figure 3.37 shows the guardrail system and position of the truck for the simulation.

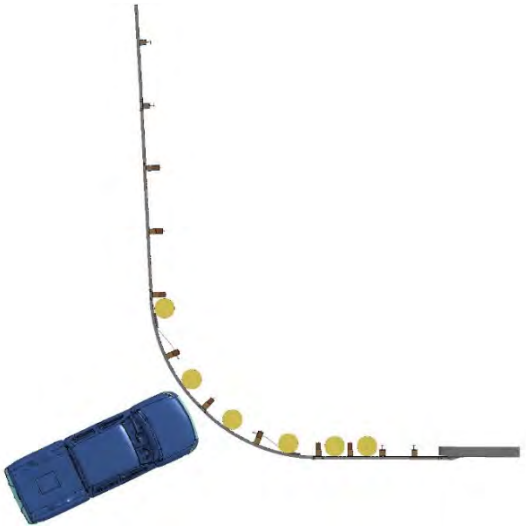


Figure 3.37. Two Tension Cables and 700-lb Sand Drums behind Radius.

Figure 3.38 depicts the truck throughout the simulation. The initial contact with the rail happened at 0.019 s. Before 0.20 s, two drums had dispersed the sand and two more drums were about to break as well. At approximately 0.45 s, the truck was riding up the rail. By 0.645 s, the

front two tires had completely gone over the rail. The last image shows the last state for the simulation where the truck had overridden the system.

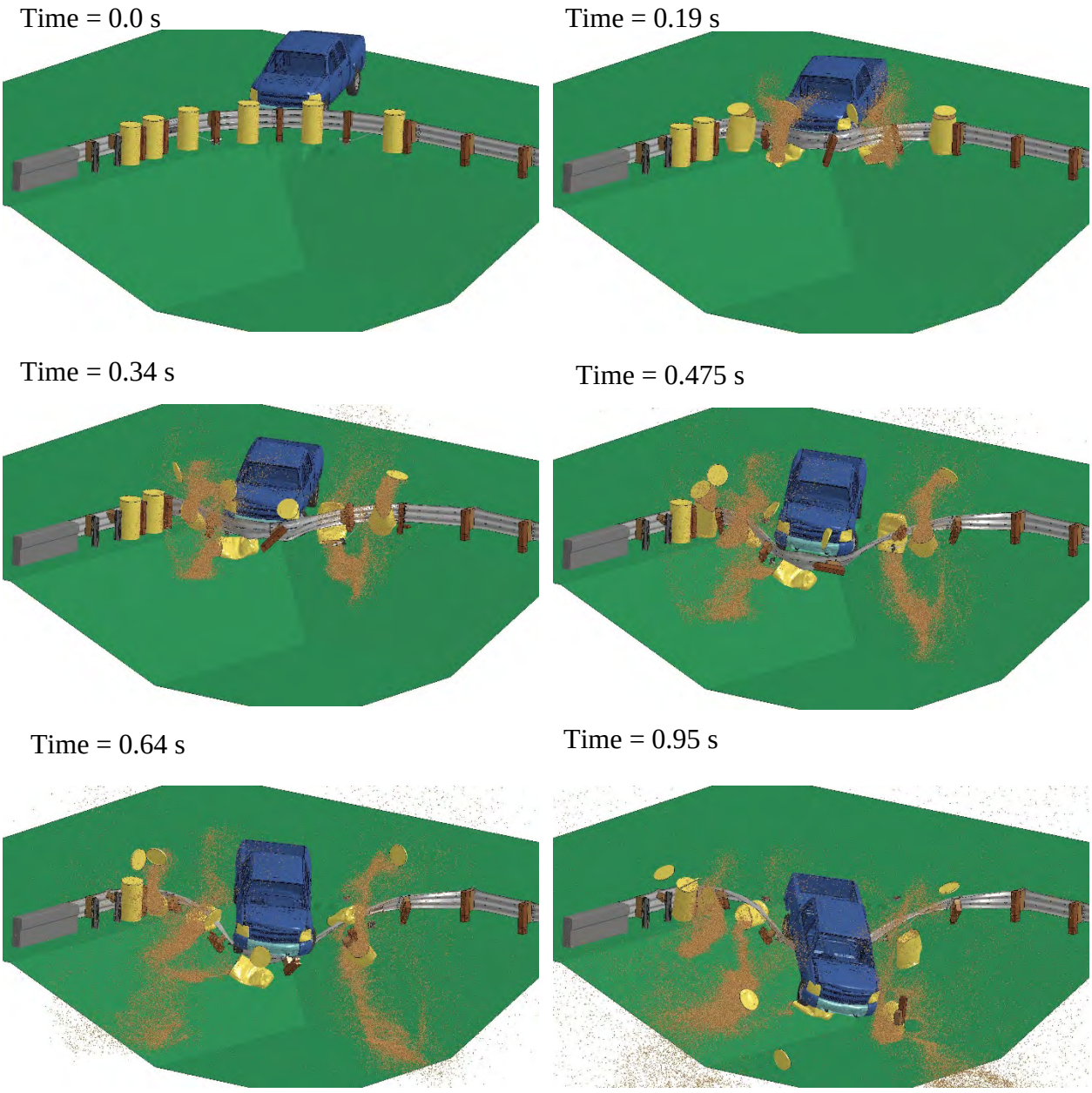


Figure 3.38. Sequential Images of Truck Simulation with Two Tension Cables and Six 700-lb Sand Drums.

Figures 3.39 and 3.40 demonstrates a closer view of the truck impacting the rail. The drums were removed from the simulation to have a clear view of the deformation of the truck and the guardrail. Figure 3.39 shows approximately the time before the truck begins to ride over the rail. Figure 3.40 shows the final state of the simulation.

Time = 0.45 s

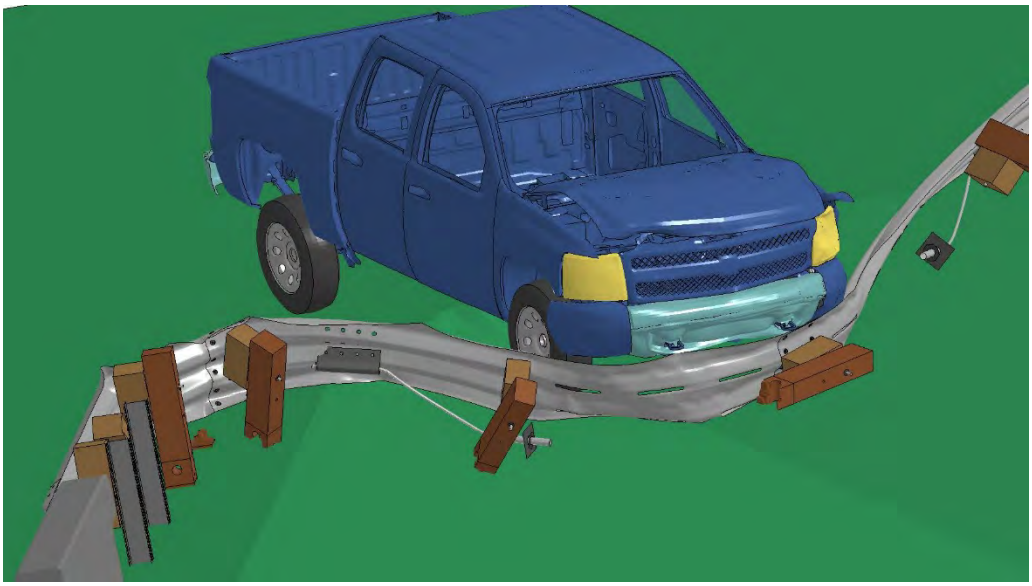


Figure 3.39. Interaction of Truck with System (No Drums Visible).

Time = 0.95 s

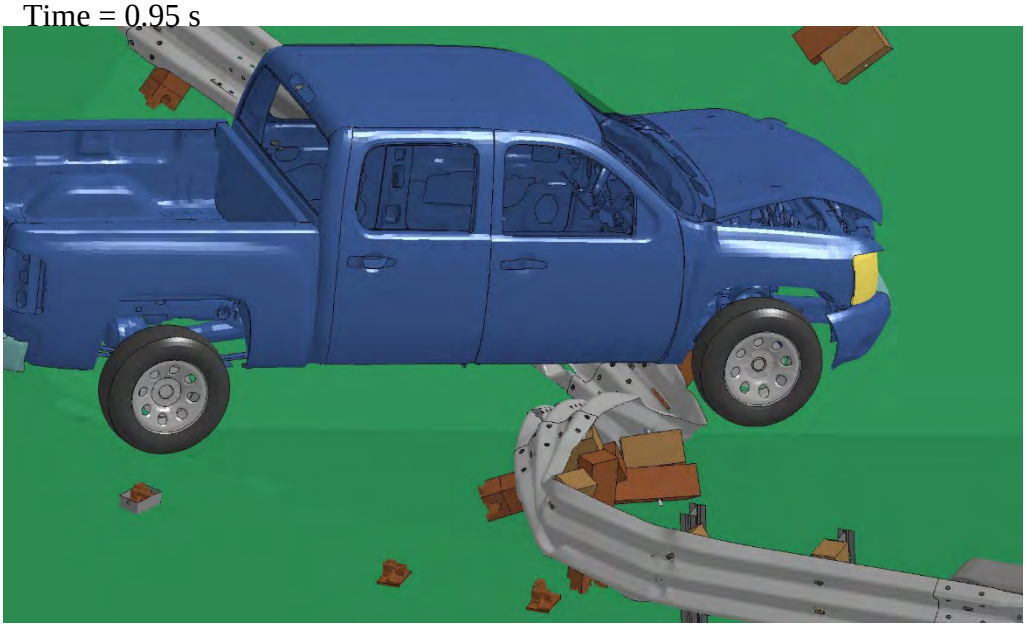


Figure 3.40. Final State of Simulation (No Drums Visible).

Table 3.9 shows the TRAP results of the occupant risk factor for the simulation with two short cables and six spread out 700-lb sand drums.

Table 3.9. TRAP Summary Data of Simulation with Two Tension Cables and Six 700-lb Sand Drums.

TRAP Results: Truck Short Radius	
Impact Velocity, mph	43.5
Impact Angle (degrees)	25
Occupant Risk Factors	
OIV (ft/s)	
x-direction	24.9
y-direction	1.9
Occupant Ridedown Accelerations (g's)	
x-direction	−3.4
y-direction	−2.8
Max Roll, Pitch, and Yaw Angles (degrees)	
Roll	−10.3
Pitch	−16.0
Yaw	−21.3

3.12 SIMULATION OF TRUCK IMPACTING SHORT RADIUS WITH TWO TENSION CABLES AND SIX 700-LB SAND DRUMS

The same system from the above simulations of the car was used for this simulation. It includes two short cables, one on the primary roadway and the other cable on the secondary roadway. Six drums were placed between posts 9 to 15. For this case, a truck was used instead of a small car. The goal of this simulation was to affirm that the truck is adequately captured within an acceptable distance behind the rail. Figure 3.41 shows the system and position of the truck used for this case.

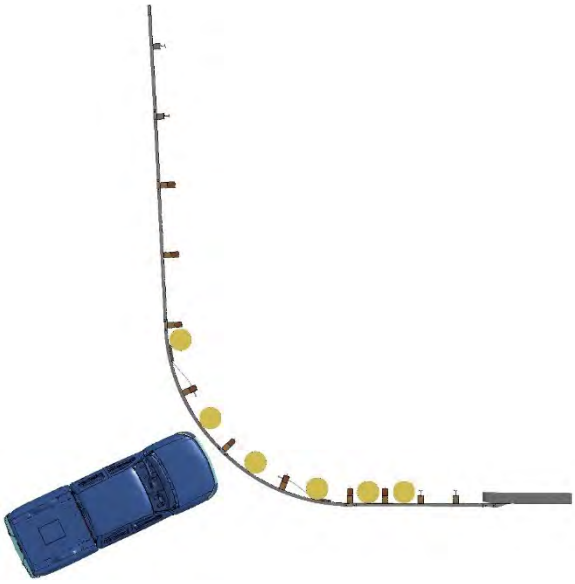


Figure 3.41. Alignment of Truck with System.

Figure 3.42 shows the sequential images of the simulation. The first image shows the initial position of the system and is followed by four images of the truck interacting with the rail. Before 0.235 s, the guardrail system was already deforming into the ditch. The last image of the simulation shows the truck being captured by the rail.

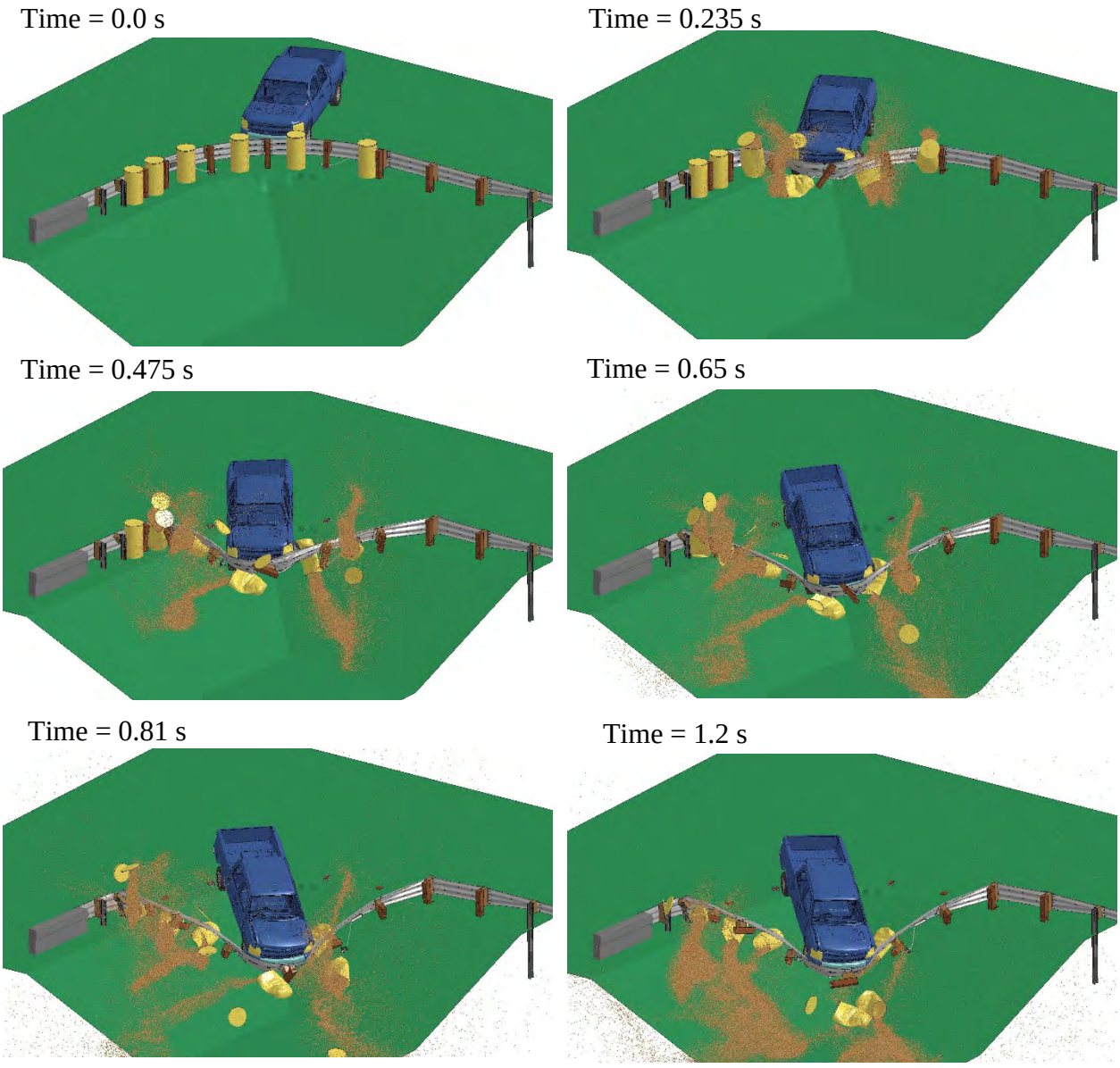


Figure 3.42. Sequential Images of Truck Simulation with Two Tension Cables and Six 700-lb Sand Drums.

Figures 3.43 and 3.44 show a closer view of the deformation between the guardrail system and the truck. The drums were removed from the figures to have a clear view of the deformation.

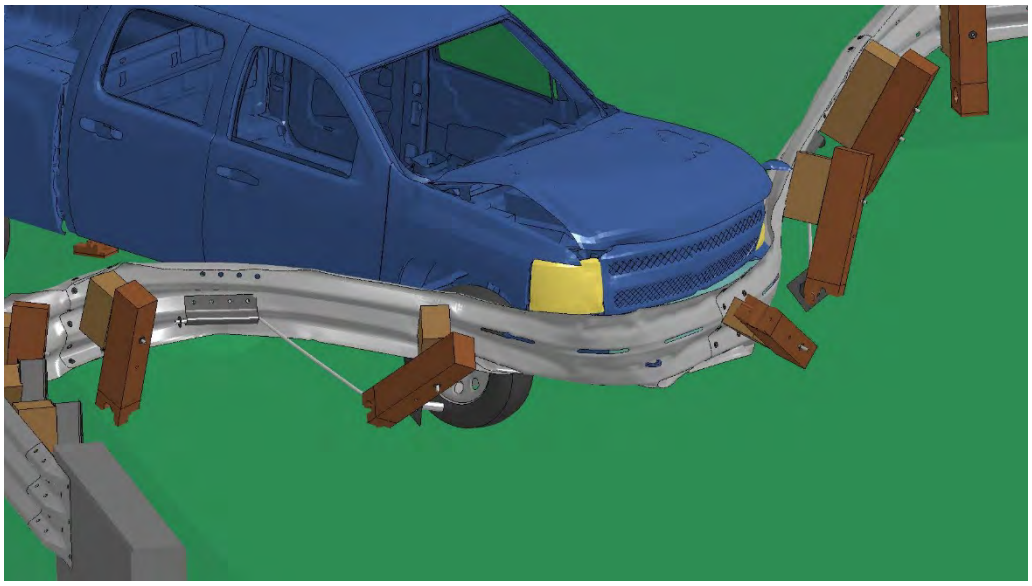


Figure 3.43. Interaction of Truck with System (No Drums Visible).

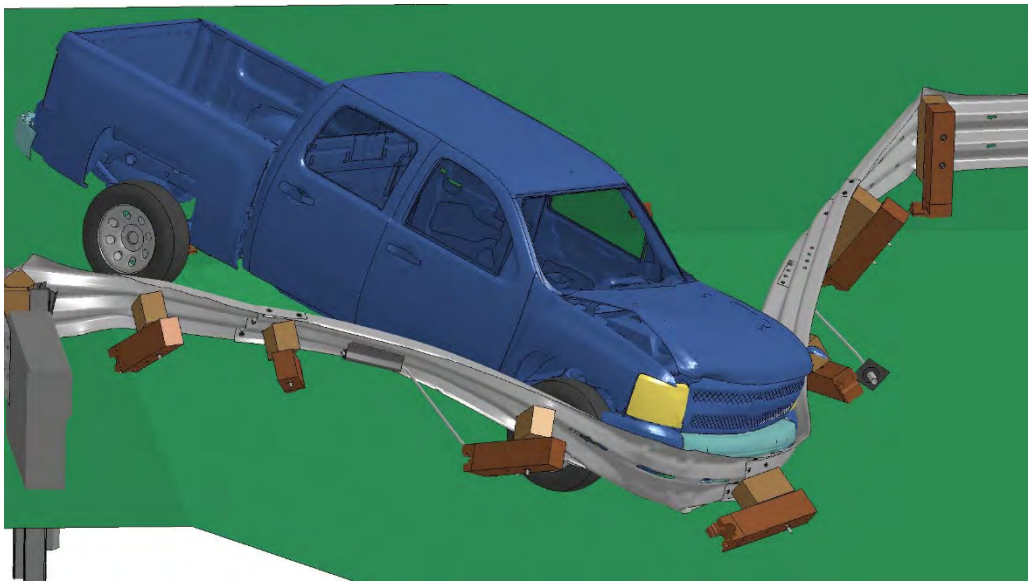


Figure 3.44. Final State of Simulation (No Drums Visible).

Table 3.10 shows the TRAP results of the occupant risk factor for the simulation with two short cables and six spread out 700-lb sand drums.

Table 3.10. TRAP Summary Data of Simulation with Two Tension Cables and Six 700-lb Sand Drums.

TRAP Results: Truck Short Radius	
Impact Velocity, mph	43.5
Impact Angle (degrees)	25
Occupant Risk Factors	
OIV (ft/s)	
x-direction	25.3
y-direction	3.9
Occupant Ridedown Accelerations (g's)	
x-direction	−3.0
y-direction	−3.5
Max Roll, Pitch, and Yaw Angles (degrees)	
Roll	−7.3
Pitch	−18.3
Yaw	−27.6

3.13 SIMULATION OF CAR IMPACTING SHORT RADIUS WITH TWO TENSION CABLES AND SIX 700-LB SAND DRUMS

Figure 3.45 presents the system layout for this simulation. The system includes two short cables and six drums spread along the rail. One of the cables was placed on the primary roadway between posts 12 and 13 at an angle; it is attached to the thrie beam and terminates at post 12. The second short cable is on the secondary roadway placed between posts 9 and 10. It is attached to the thrie beam and terminates at post 10. The drums are placed between posts 9 through 15. The drum placed between posts 9 and 10 is placed 17 inches from the center of drum to the center of post.

Figure 3.46 shows the placement of the car to the guardrail system. It is set at a 25° angle heading straight toward a drum at the curved section.

Figure 3.47 shows the sequential images throughout the simulation. The car remained stable during the simulation. The first image shows the initial position of the car and the system, and is followed by two images that depict the interaction of the car with the guardrail system and drums. At 0.27 s, the deformation from the car was present and three of the drums have broken and dispersed the sand. By 0.405 s, the car began to be captured by the rail. The last image displays the car being captured by the rail with three drums remaining intact and four out of the eight CRT posts broken.

Figures 3.48 and 3.49 display a closer view of the interaction of the car without the drums to have a clear view of the deformation between the car and the guardrail system.

Table 3.11 shows the TRAP results of the occupant risk factor for the simulation with two short cables and six spread out 700-lb sand drums.



Figure 3.45. Two Tension Cables and Six 700-lb Sand Drums behind Radius.

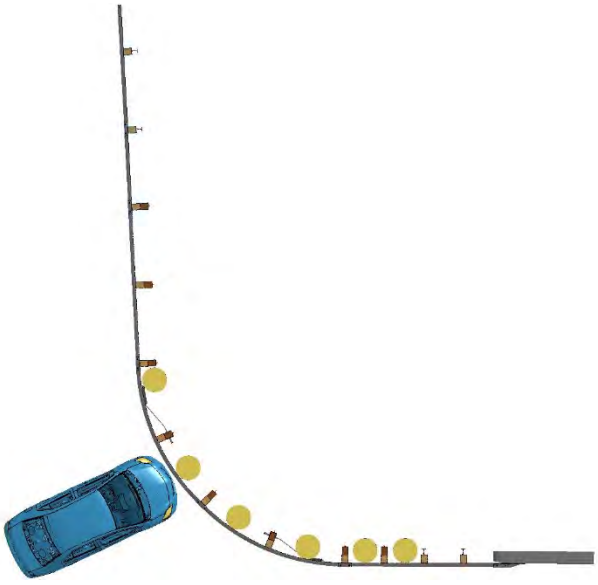
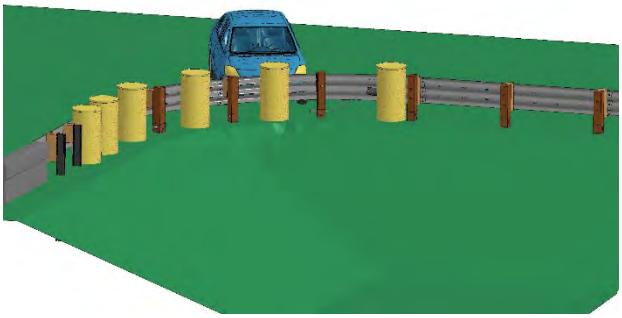
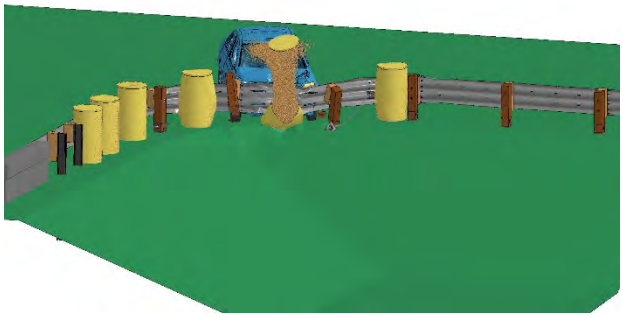


Figure 3.46. Alignment of Car with System.

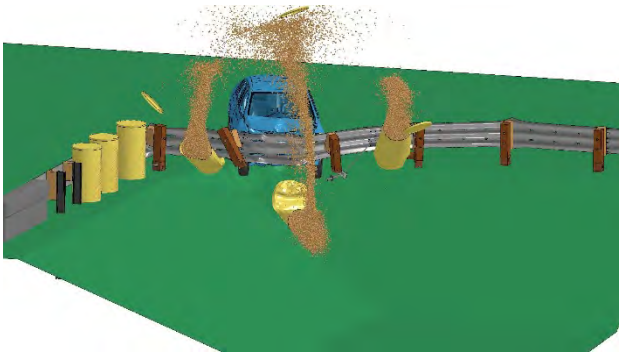
Time = 0.0 s



Time = 0.115 s



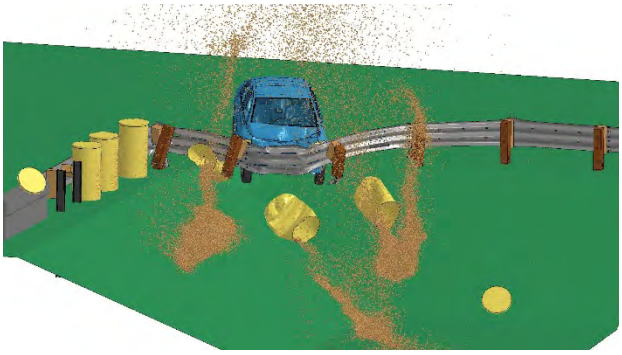
Time = 0.32 s



Time = 0.565 s



Time = 0.849 s



Time = 1.2 s

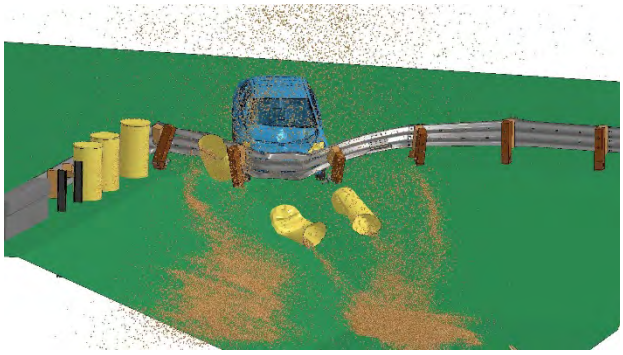


Figure 3.47. Sequential Images of Car Simulation with Two Tension Cables and Six 700-lb Sand Drums.

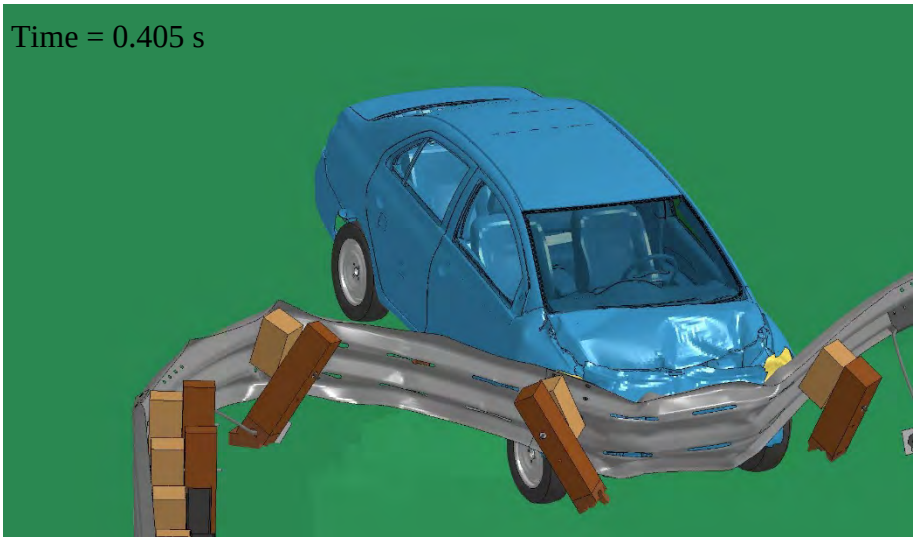


Figure 3.48. Interaction of Car with System (No Drums Visible).

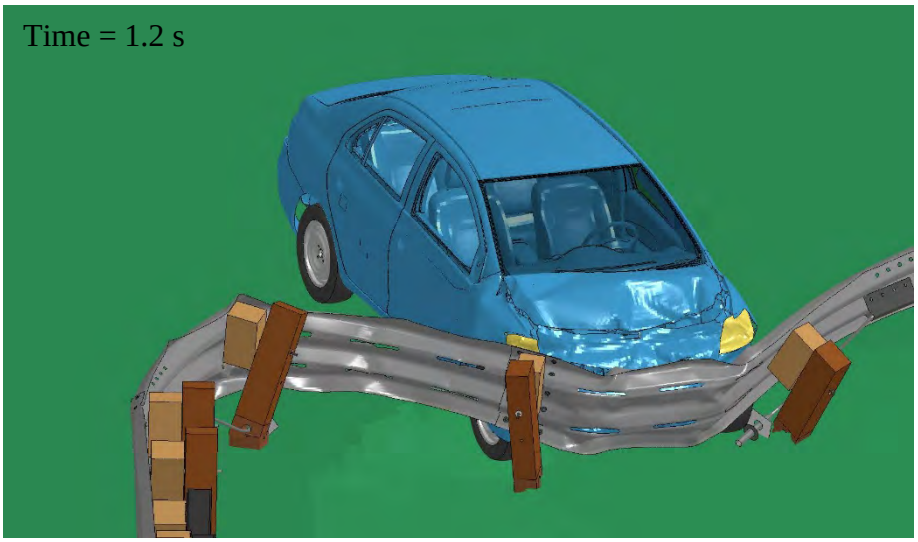


Figure 3.49. Final State of Simulation (No Drums Visible).

Table 3.11. TRAP Summary Data of Simulation with Two Tension Cables and Six 700-lb Sand Drums.

TRAP Results: Car Short Radius	
Impact Velocity, mph	43.5
Impact Angle (degrees)	25
Occupant Risk Factors	
OIV (ft/s)	
x-direction	31.5
y-direction	2.3
Occupant Ridedown Accelerations (g's)	
x-direction	−6.4
y-direction	−2.1
Max Roll, Pitch, and Yaw Angles (degrees)	
Roll	−3.3
Pitch	−8.2
Yaw	1.9

3.14 SIMULATION OF CAR IMPACTING SHORT RADIUS WITH TWO TENSION CABLES AND SIX 700-LB SAND DRUMS

The same guardrail system from the above simulation was used. The difference in this simulation is the position of the car. It is set to hit the rail directly instead of directly into a drum. Figure 3.50 shows the system and position of the car used in this simulation.

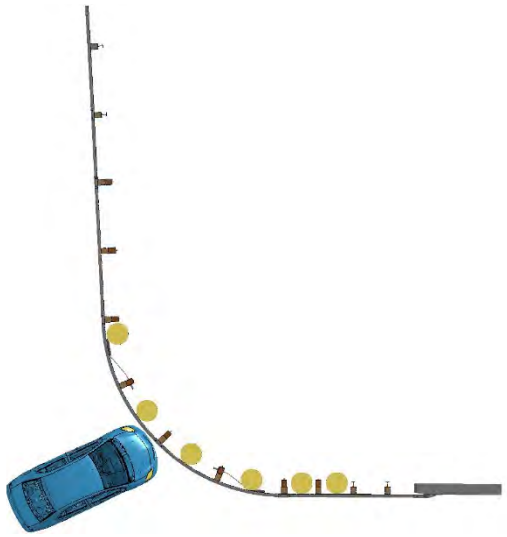


Figure 3.50. Alignment of Car with System.

Figure 3.51 shows the sequential images of the simulation. At 0.25 s, the hood of the car impacted the rail and deformed. Also, two of the drums broke and dispersed the sand. By 0.49 s, a third sand barrel had dispersed the sand while the car was being captured by the rail. The car

reached zero velocity at approximately 0.43 s and then began to rebound. The last image displays the end state of the position of the car.

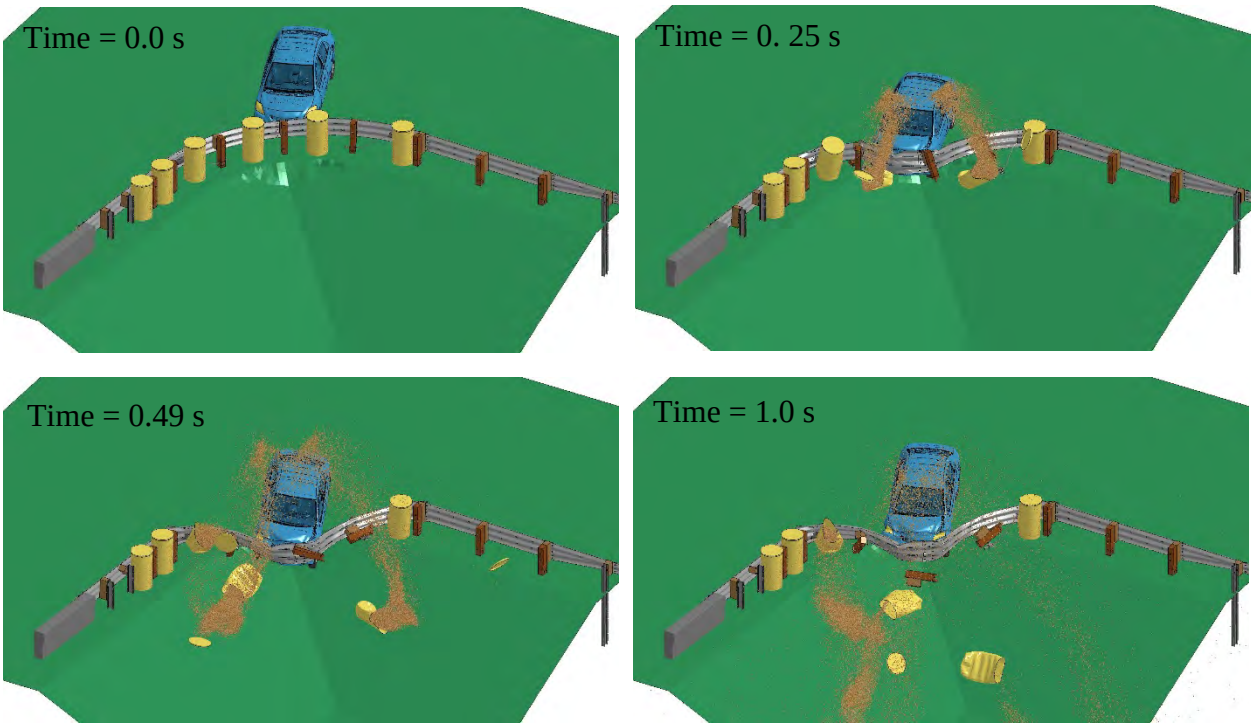


Figure 3.51. Sequential Images of Car Simulation with Two Tension Cables and Six 700-lb Sand Drums.

Figures 3.52 and 3.53 show a closer view of the impact between the guardrail and the car. The drums are removed to show a clear view of the deformation. Figure 3.52 shows the interaction of the rail with the car at 0.445 s, the approximate point at which the car reached zero velocity. Figure 3.53 shows the end state of the car in the simulation.

Table 3.12 shows the TRAP results of the occupant risk factor for the simulation with two short cables and six spread out 700-lb sand drums.

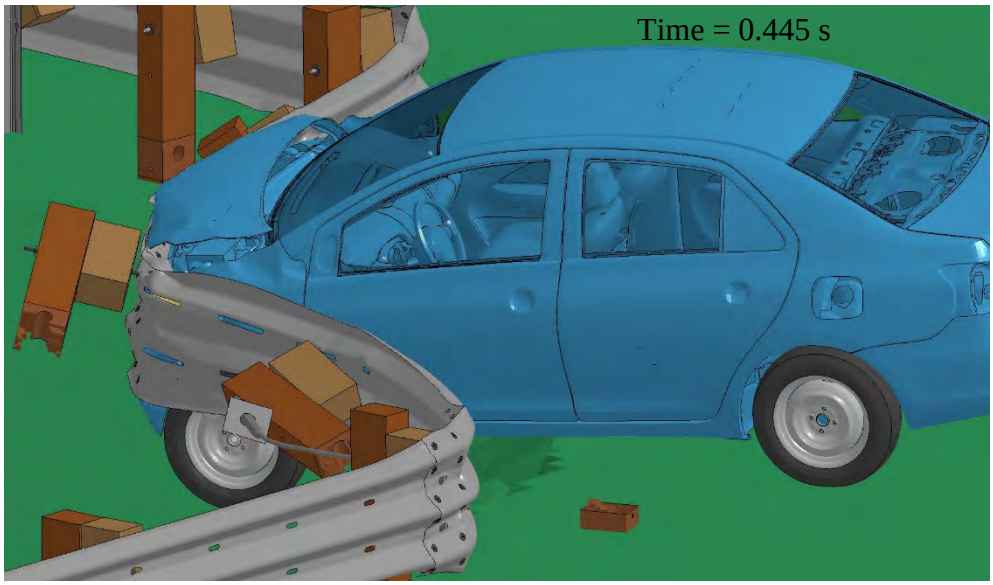


Figure 3.52. Interaction of Car with System (No Drums Visible).

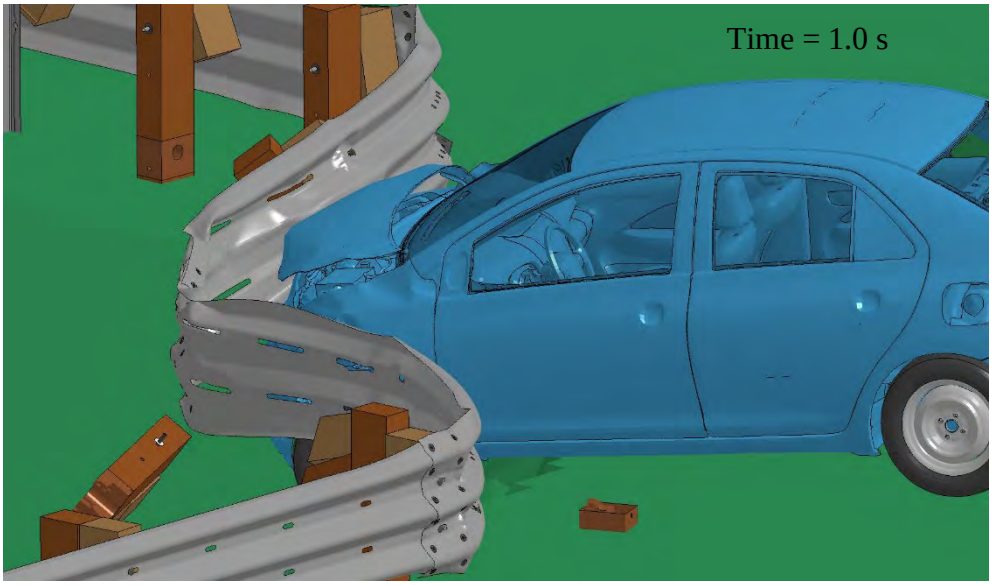


Figure 3.53. Final State of Simulation (No Drums Visible).

Table 3.12. TRAP Summary Data of Simulation with Two Tension Cables and Six 700-lb Sand Drums.

TRAP Results: Car Short Radius	
Impact Velocity, mph	43.5
Impact Angle (degrees)	25
Occupant Risk Factors	
OIV (ft/s)	
x-direction	35.1
y-direction	−0.6
Occupant Ridedown Accelerations (g's)	
x-direction	−4.5
y-direction	−3.2
Max Roll, Pitch, and Yaw Angles (degrees)	
Roll	−9.6
Pitch	−9.0
Yaw	−3.3

3.15 SIMULATION OF TRUCK IMPACTING SHORT RADIUS WITH TWO TENSION CABLES AND SIX 700-LB SAND DRUMS

For the following test case, the truck is aligned parallel with the primary roadway. Figure 3.54 shows the system used in this simulation. The system contains two short cables and six 700-lb sand drums spread out.

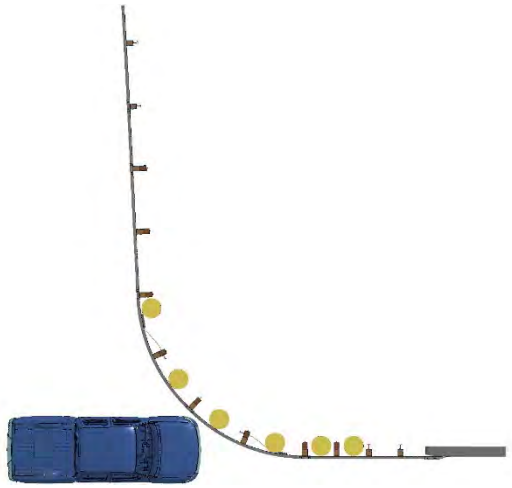


Figure 3.54. Alignment of System with Truck.

Figure 3.55 displays the truck in sequential images throughout the simulation. The first wood post at the center of the nose broke, as well as the CRT post on the primary roadway, at 0.075 s. At 0.155 s, the truck began to ride up the rail. The front left truck tire left the rail before 0.4 s, and the truck was unstable. By 0.88 s, all four tires were back on the ground.

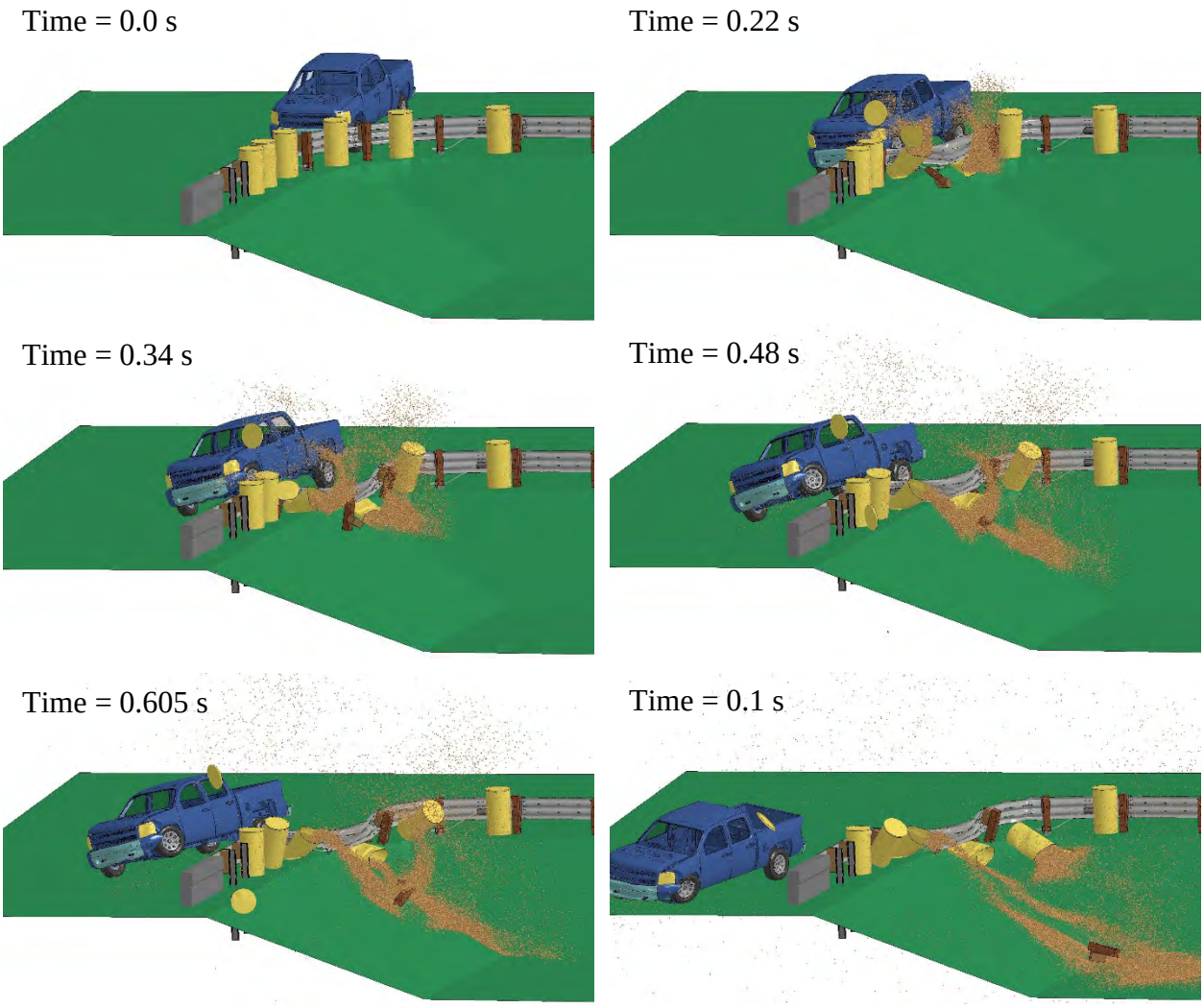
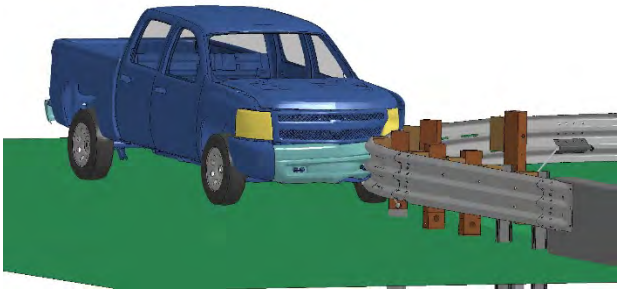


Figure 3.55. Sequential Images of Truck Simulation with Two Tension Cables and Six 700-lb Sand Drums.

The sequential images in Figure 3.56 show the trucks interaction with the rail. The sand has been hidden from these images to better see the rail and truck interaction. Figure 3.57 displays a closer view of the interaction from the back of the rail. Figure 3.57 shows the time when the truck had already gone up the rail and its interaction with the system was complete.

Time = 0.04 s



Time = 0.19 s



Time = 0.34 s

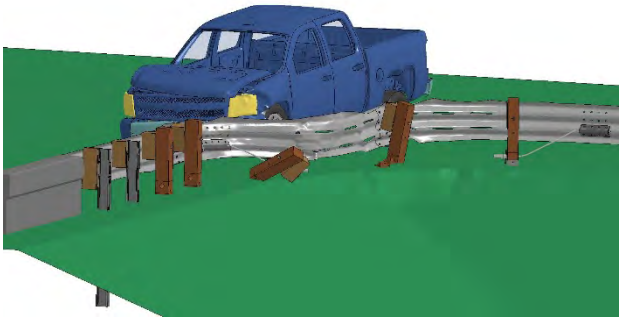


Time = 0.51 s



Figure 3.56. Sequential Images of Simulation from Front of Rail (No Drums Visible).

Time = 0.16 s



Time = 0.34 s

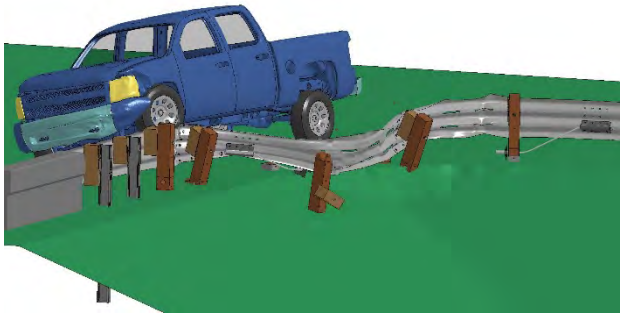


Figure 3.57. Images of Simulation from Back of Rail (No Drums Visible).

Table 3.13 shows the TRAP results of the occupant risk factor for the simulation with Tension Cable and spread out 700-lb sand drums. Table 3.13 shows the TRAP results of the occupant risk factor for the truck simulation with two short cables and six spread out 700-lb sand drums.

Table 3.13. TRAP Summary Data of Simulation with Two Tension Cables and Six 700-lb Sand Drums.

TRAP Results: Truck Short Radius	
Impact Velocity, mph	43.5
Impact Angle (degrees)	0
Occupant Risk Factors	
OIV (ft/s)	
x-direction	−9.8
y-direction	−9.8
Occupant Ridedown Accelerations (g's)	
x-direction	4.5
y-direction	4.5
Max Roll, Pitch, and Yaw Angles (degrees)	
Roll	17.0
Pitch	2.8
Yaw	22.5

3.16 SIMULATION OF CAR IMPACTING SHORT RADIUS WITH TWO TENSION CABLES AND SIX 700-LB SAND DRUMS

The next case involves a car impacting the same guardrail system. However, this case has the car positioned away from the center of the system and approximately 15-ft from the end of the parapet. Figure 3.58 shows the position of the car with the guardrail system. The car is still impacting the guardrail system at a 25° angle. This test was intended to evaluate the impact performance at a critical impact point where the car is being redirected. The impact point for this case is directly at a CRT post, post number 13 in the system.

Figures 3.59 and 3.60 display the car in sequential images throughout the simulation. At 0.095 s, the driver's door had deformed and popped open when impacting with the rail. At 0.4 s, the rear right side of the car made contact with the system. After 0.43 s, the car was redirected and its interaction with the system was complete. At the end of the simulation, only two CRT post and three drums were broken. Figures 3.61 and 3.62 show a closer view of the impact between the car and the guardrail system. The drums have been removed to have a clear view. The first image shows a closer view of what is happening with the deformation. It can be seen that the door opened when impacting at this alignment.

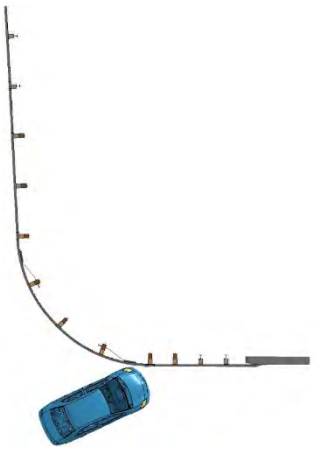


Figure 3.58. Alignment of Car with System (No Drums Visible).

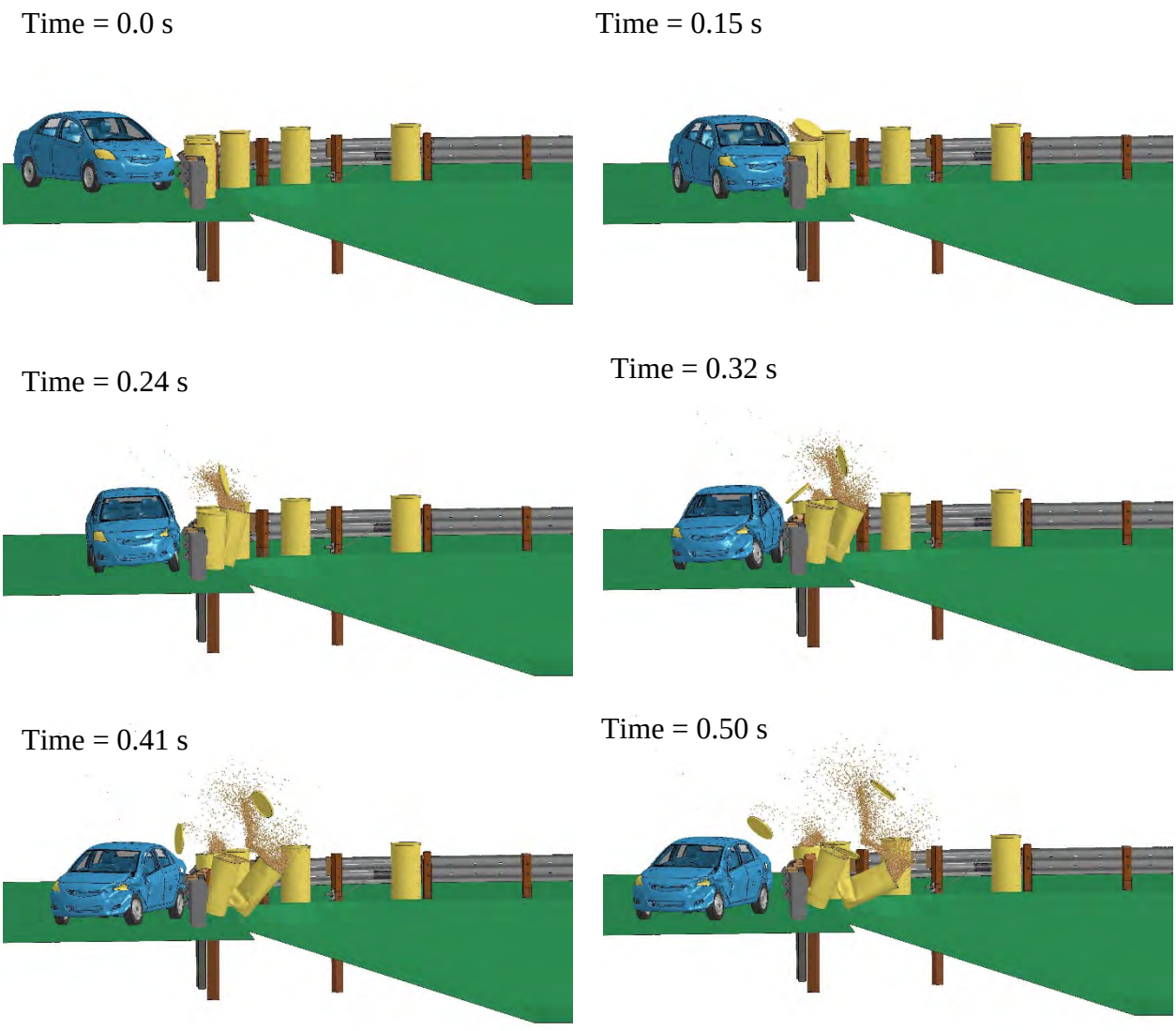


Figure 3.59. Sequential Images of Car Simulation with Two Tension Cables and Six 700-lb Sand Drums.

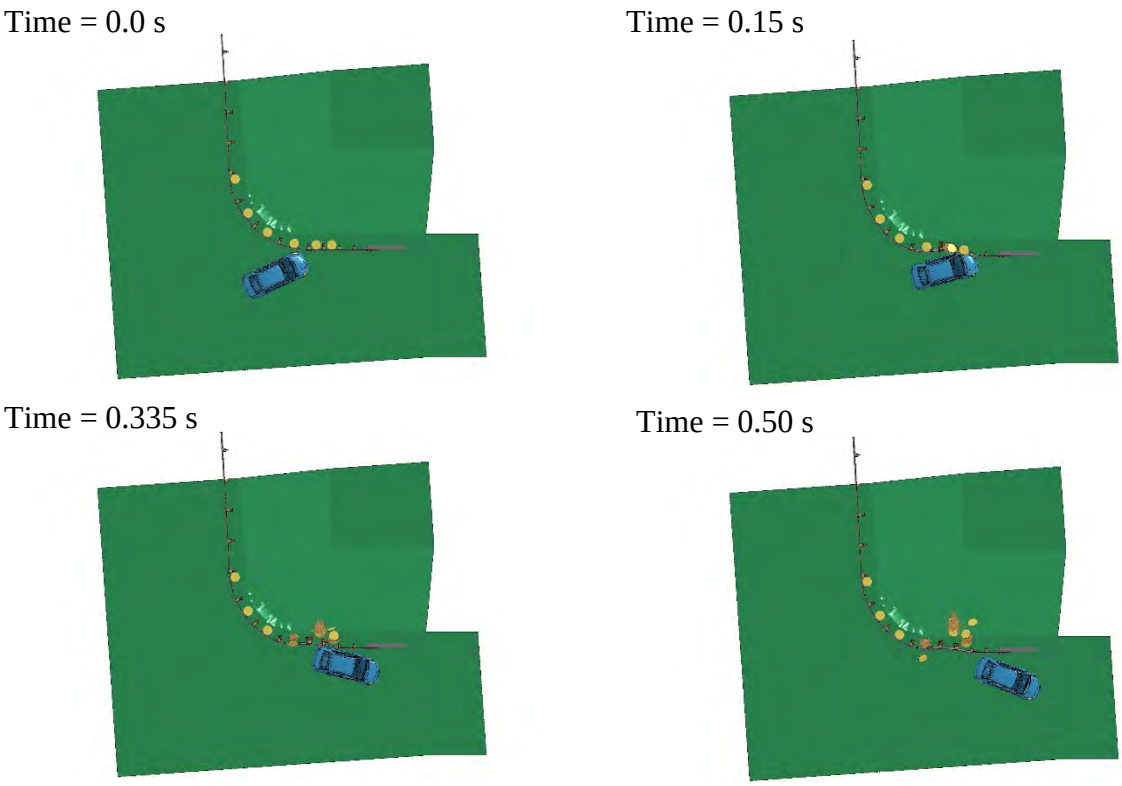


Figure 3.60. Sequential Images of Simulation (Top View).

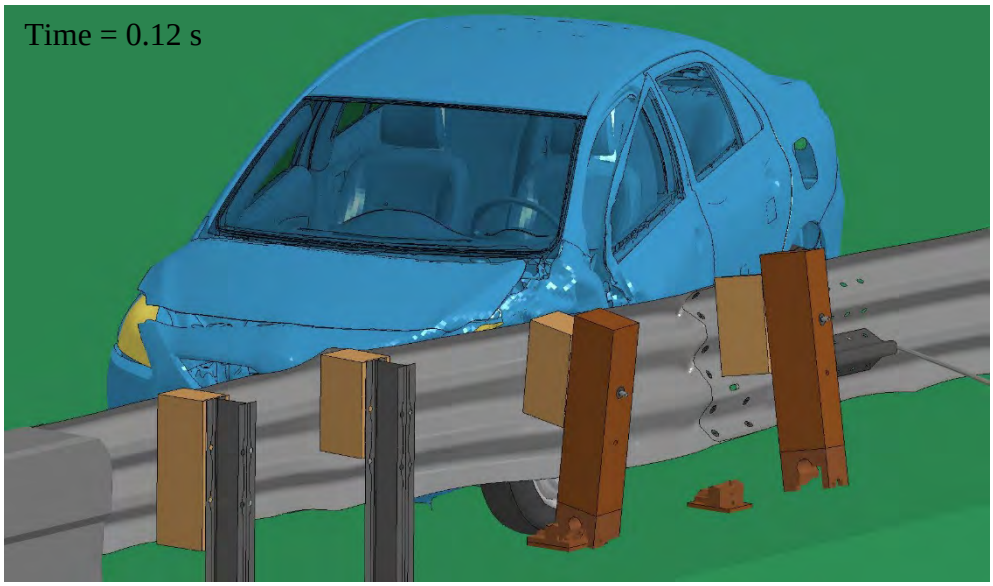


Figure 3.61. Interaction of Car with System (No Drums Visible).

Time = 0.50 s

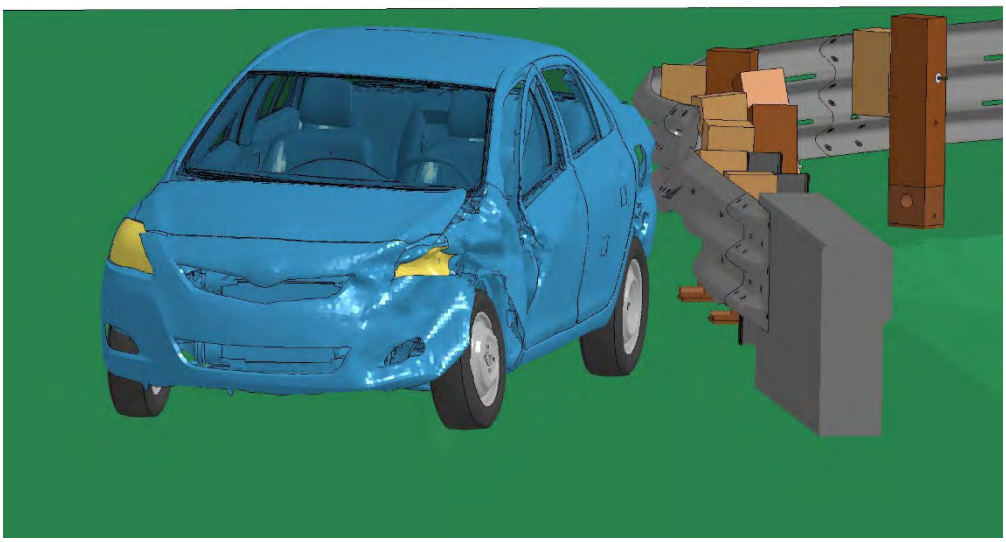


Figure 3.62. Interaction of Car with System (No Drums Visible).

Table 3.14 shows the TRAP results of the occupant risk factor for the car simulation with two short cables and six spread out 700-lb sand drums. Figures 3.63, 3.64, and 3.65 show the longitudinal accelerations in the X, Y, and Z direction, respectively. Figure 3.66 shows the roll, pitch, and yaw angles for the simulation.

Table 3.14. TRAP Summary Data of Simulation with Two Tension Cables and Six 700-lb Sand Drums.

TRAP Results: Truck Short Radius	
Impact Velocity, mph	43.5
Impact Angle (degrees)	25
Occupant Risk Factors	
OIV (ft/s)	
x-direction	21.9
y-direction	−17.0
Occupant Ridedown Accelerations (g's)	
x-direction	−6.8
y-direction	6.2
Max Roll, Pitch, and Yaw Angles (degrees)	
Roll	2.2
Pitch	−1.7
Yaw	45.9

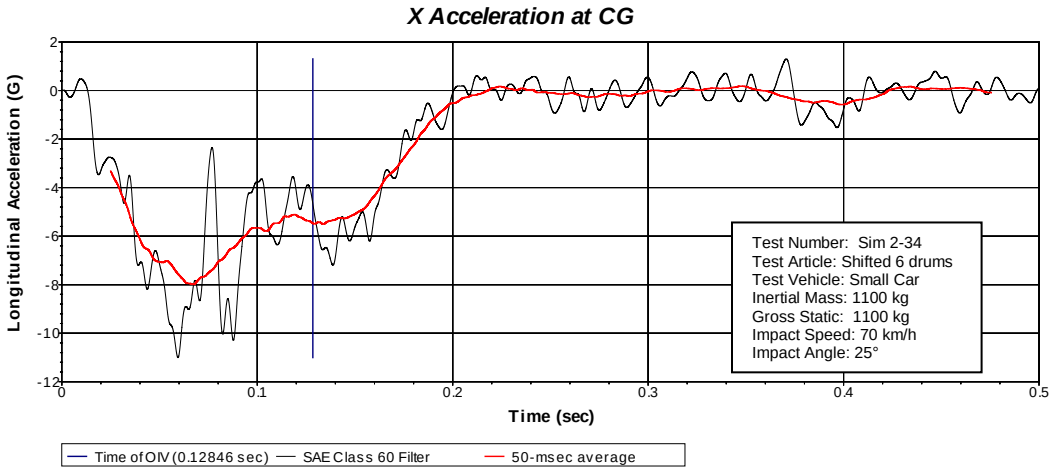


Figure 3.63. Longitudinal Acceleration of Car Impacting Short Radius with Two Tension Cables and Six 700-Lb Sand Drums.

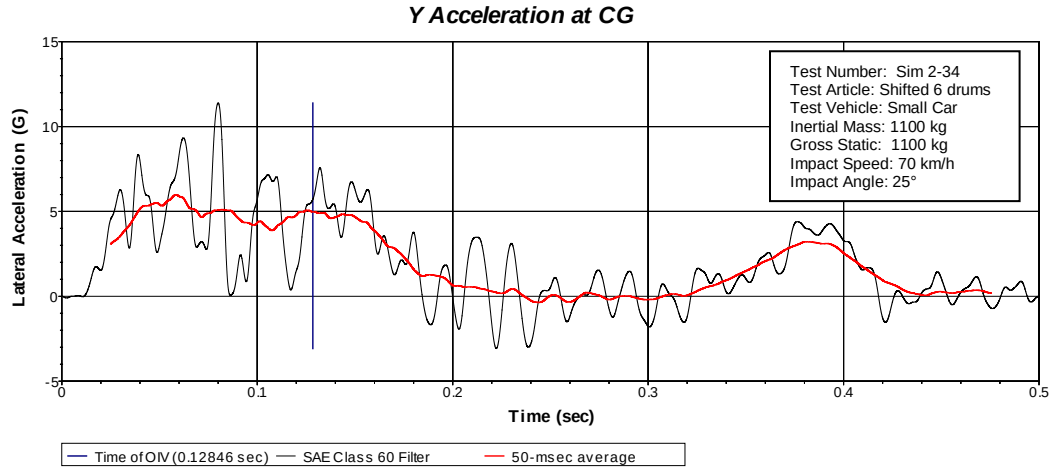


Figure 3.64. Longitudinal Acceleration of Car Impacting Short Radius with Two Tension Cables and Six 700-Lb Sand Drums.

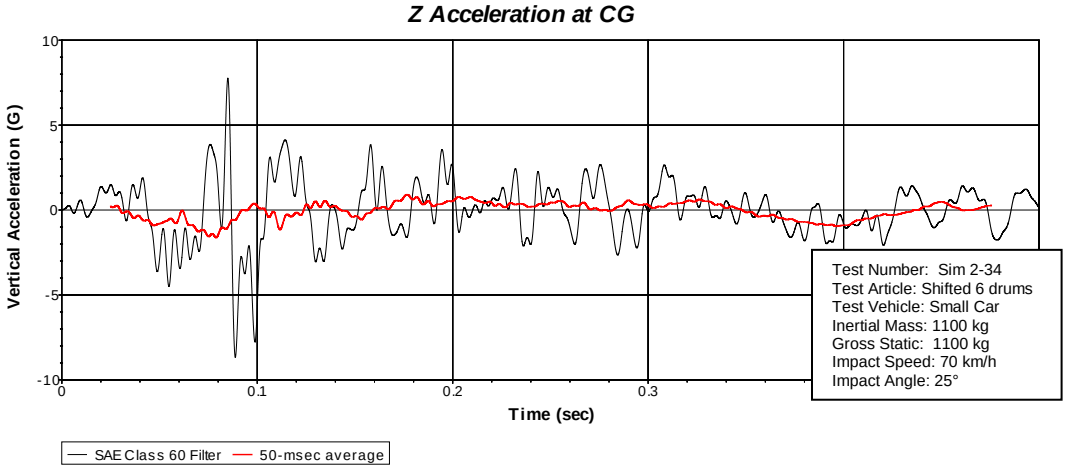


Figure 3.65. Longitudinal Acceleration of Car Impacting Short Radius with Two Tension Cables and Six 700-Lb Sand Drums.

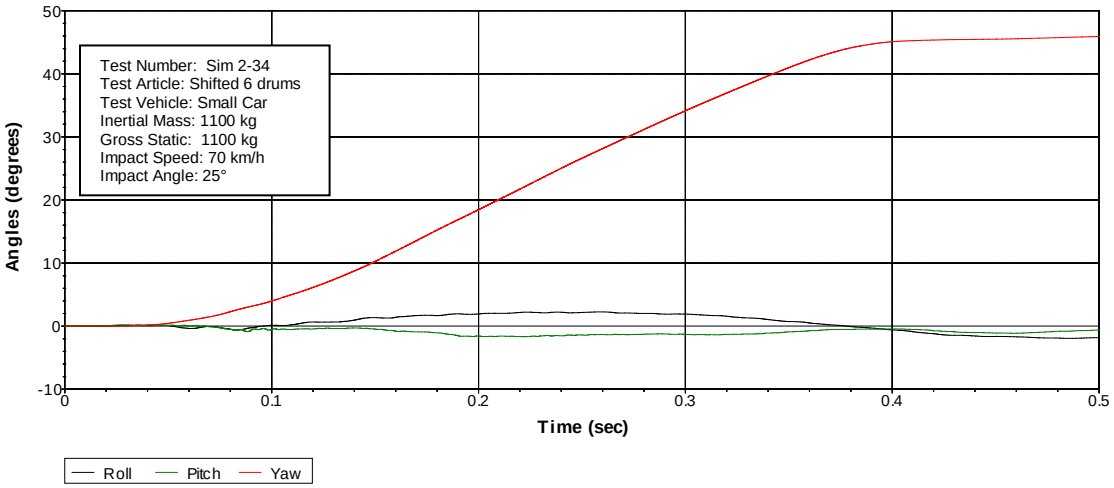


Figure 3.66. Roll, Pitch, and Yaw Angles for the Simulation of Car Impacting Short Radius with Two Tension Cables and Six 700-Lb Sand Drums.

3.17 SIMULATION OF CAR IMPACTING SHORT RADIUS WITH TWO TENSION CABLES AND SIX 700-LB SAND DRUMS

This simulation is also intended to evaluate the impact performance at a critical impact point where the car is being redirected. The only change made to this simulation is the position of the car, the guardrail system remains the same. The car was shifted 6-ft to the left from the simulation above, directly impacting the drum between posts 12 and 13. Figure 3.67 shows the alignment of the car with the system. The car impacts at a 25° angle and at a speed of 40 mph.

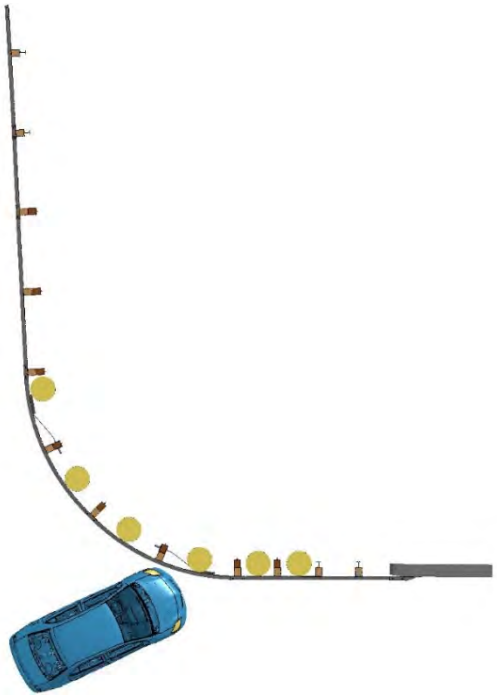


Figure 3.67. Alignment of Car with System.

Figure 3.68 displays the sequential images for the simulation. At approximately 0.07 s, the front left corner of the car had deformed. The car continued to have contact with the rail and instead of being redirected away from the guardrail system, the car ended up perpendicular to the primary roadway.

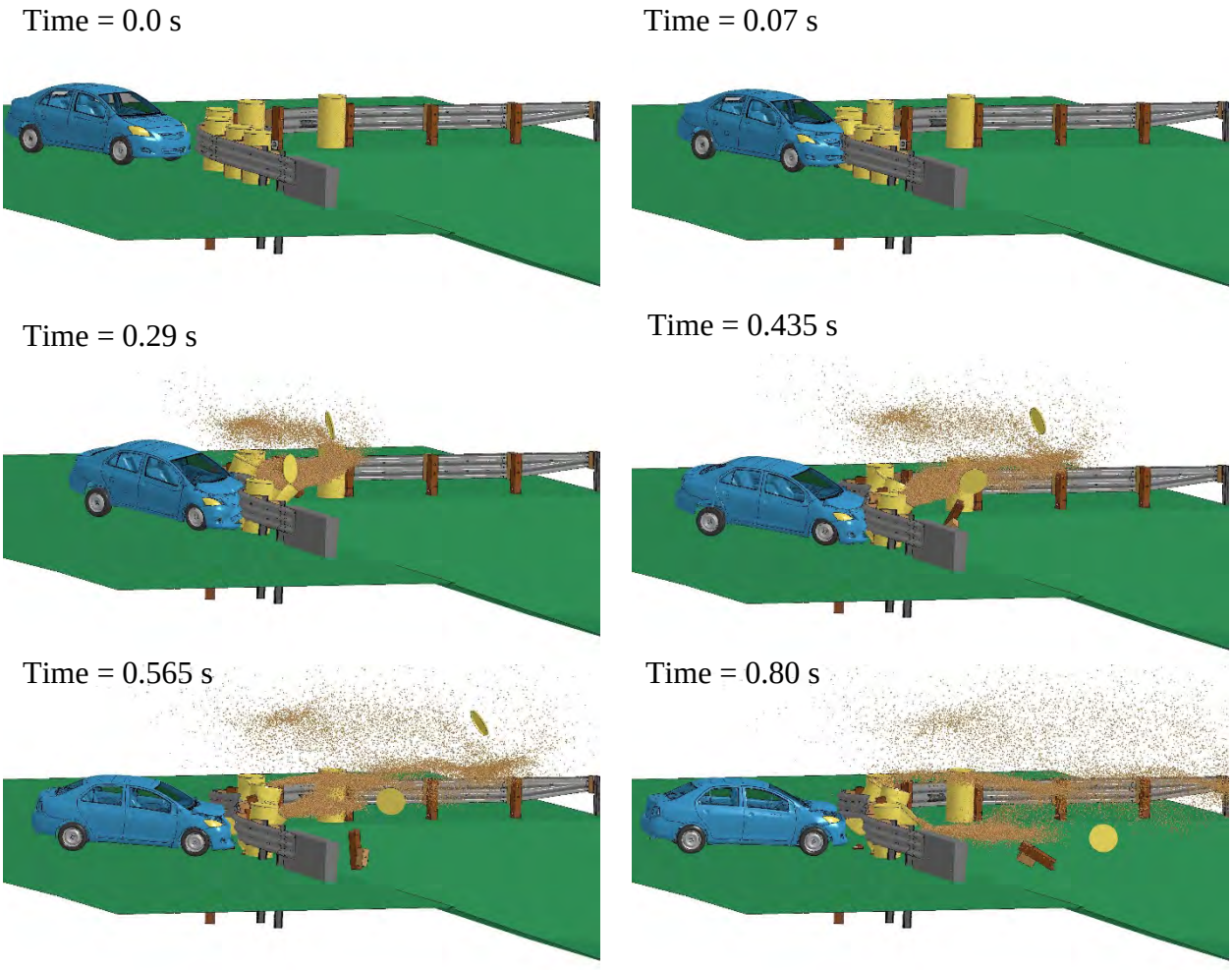


Figure 3.68. Sequential Images of Car Simulation with Two Tension Cables and Six 700-lb Sand Drums.

The following sequential images shown in Figure 3.69 display the top view. These images follow the positon of the car from the beginning state to the final state. Figures 3.70 and 3.71 show a closer view of the deformation caused in this simulation. The drums were removed from the images to have a clear view. The first image shows that most of the damage in the car was on the front left corner of the car.

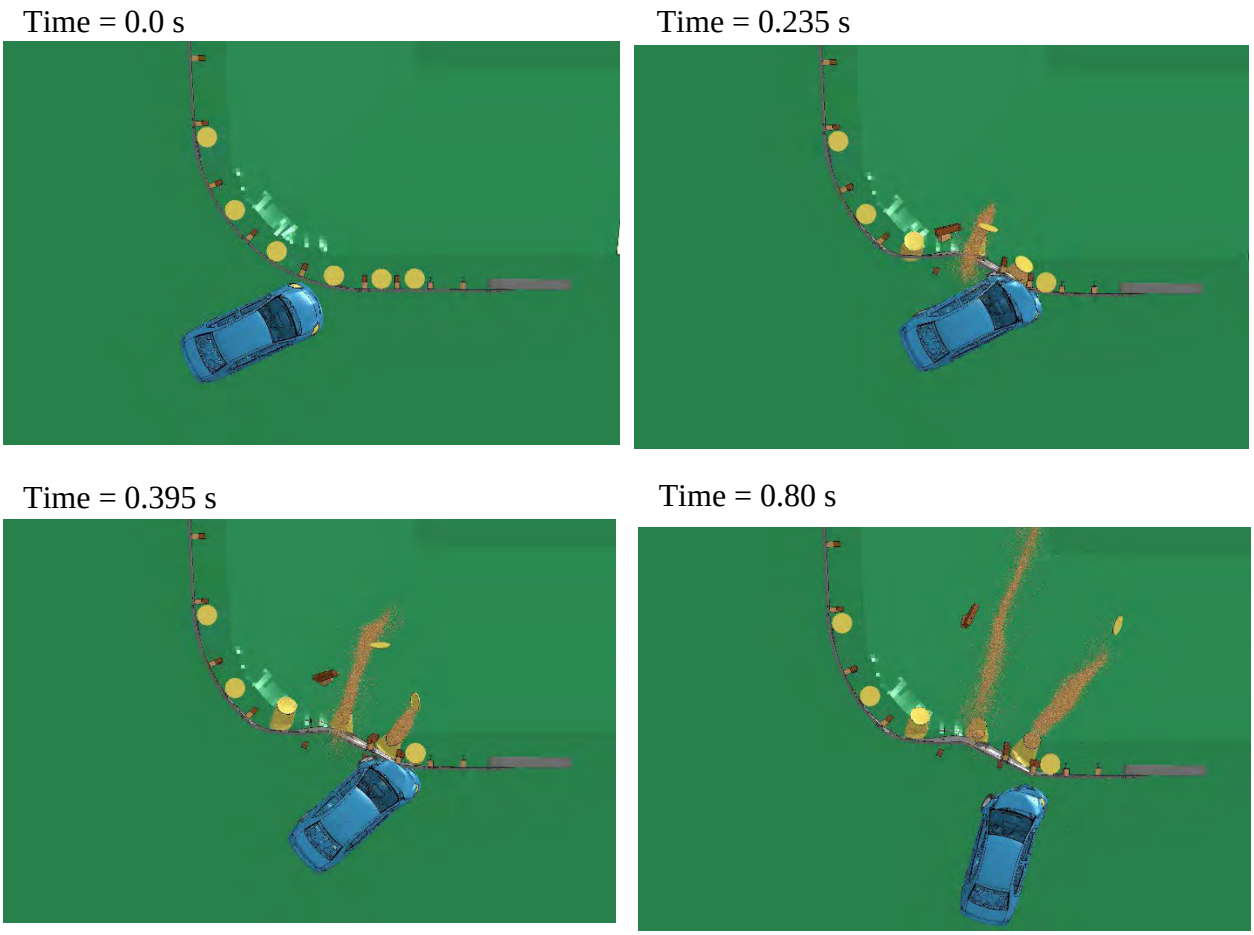


Figure 3.69. Sequential Images of Simulation (Top View).

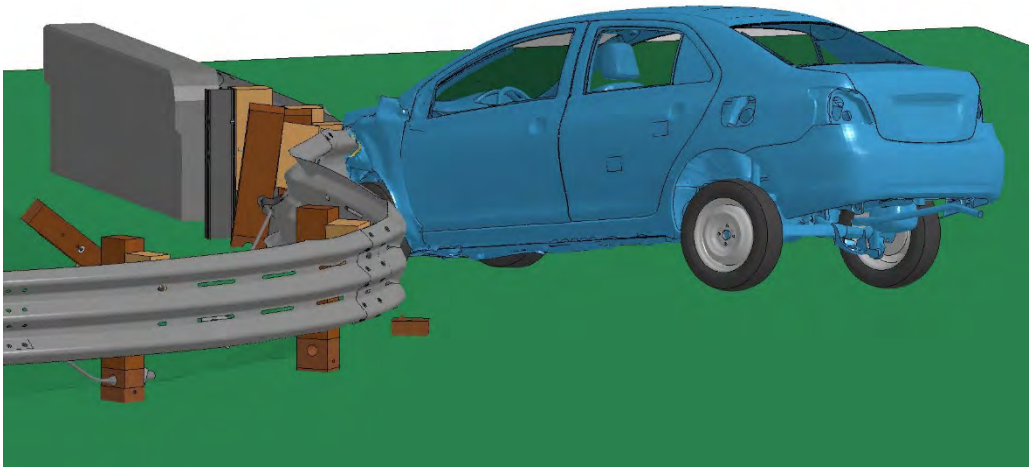


Figure 3.70. Interaction of Car with System (No Drums Visible).

Time = 0.80 s

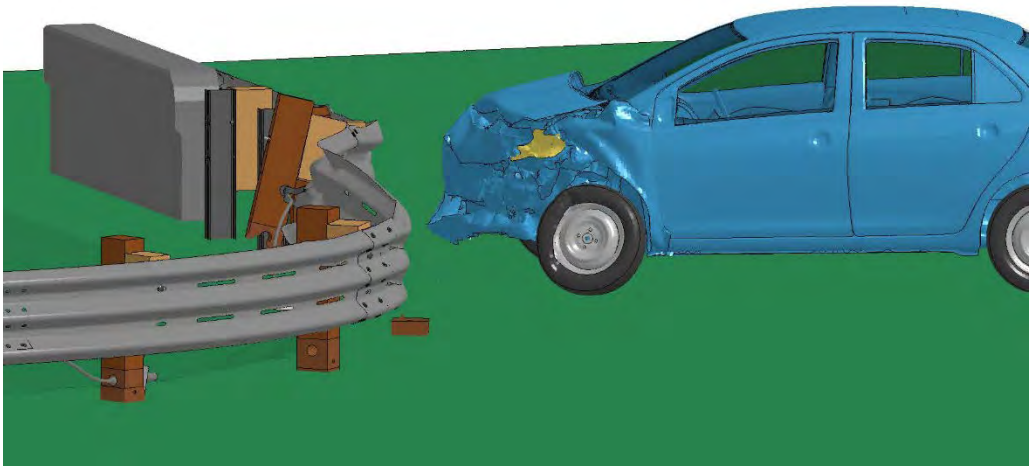


Figure 3.71. Final State of Simulation (No Drums Visible).

Table 3.15 shows the TRAP results of the occupant risk factor for the car simulation with two short cables and six spread out 700-lb sand drums. Figures 3.72, 3.73, and 3.74 show the longitudinal accelerations in the X, Y, and Z direction, respectively. Figure 3.75 shows the roll, pitch, and yaw angles for the simulation.

Table 3.15. TRAP Summary Data of Simulation with Two Tension Cables and Six 700-lb Sand Drums.

TRAP Results: Truck Short Radius	
Impact Velocity, mph	43.5
Impact Angle (degrees)	25
Occupant Risk Factors	
OIV (ft/s)	
x-direction	36.0
y-direction	−9.8
Occupant Ridedown Accelerations (g's)	
x-direction	−7.7
y-direction	4.0
Max Roll, Pitch, and Yaw Angles (degrees)	
Roll	7.5
Pitch	−6.1
Yaw	−49.9

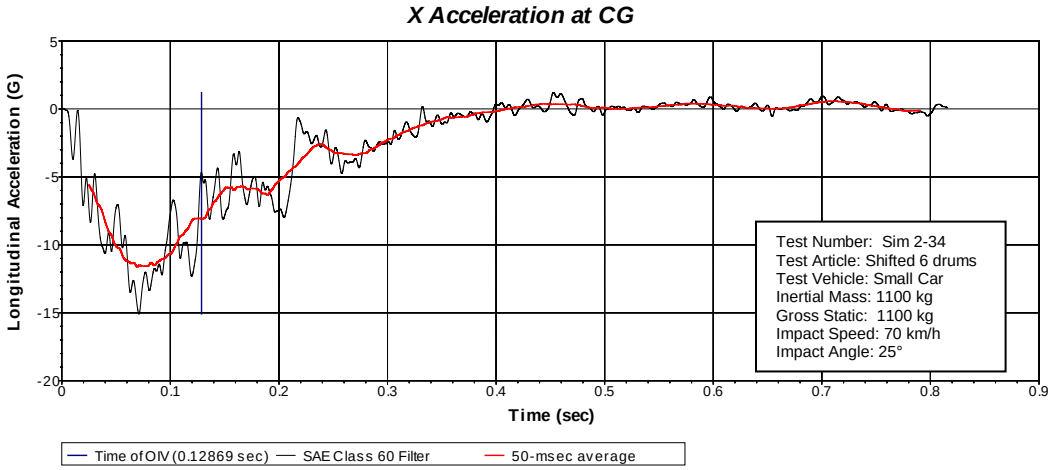


Figure 3.72. Longitudinal Acceleration of Car Impacting Short Radius with Two Tension Cables and Six 700-Lb Sand Drums.

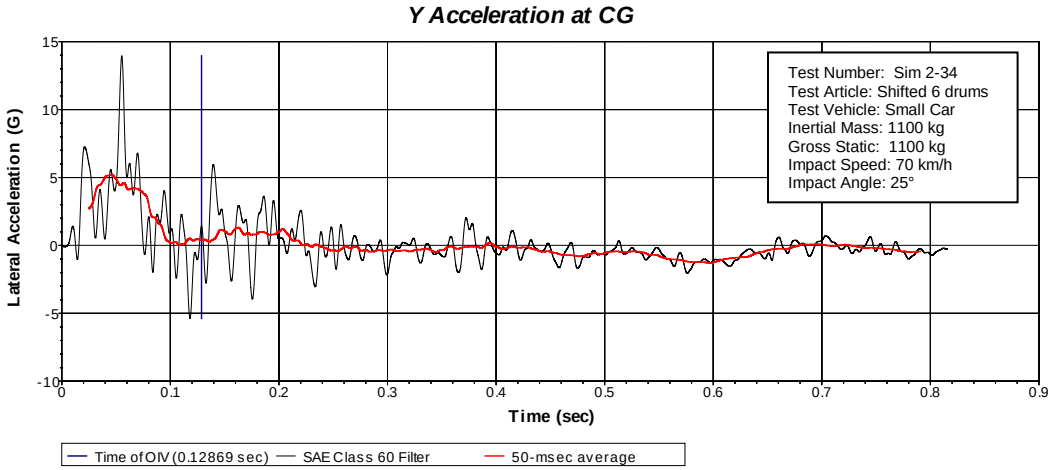


Figure 3.73. Longitudinal Acceleration of Car Impacting Short Radius with Two Tension Cables and Six 700-Lb Sand Drums.

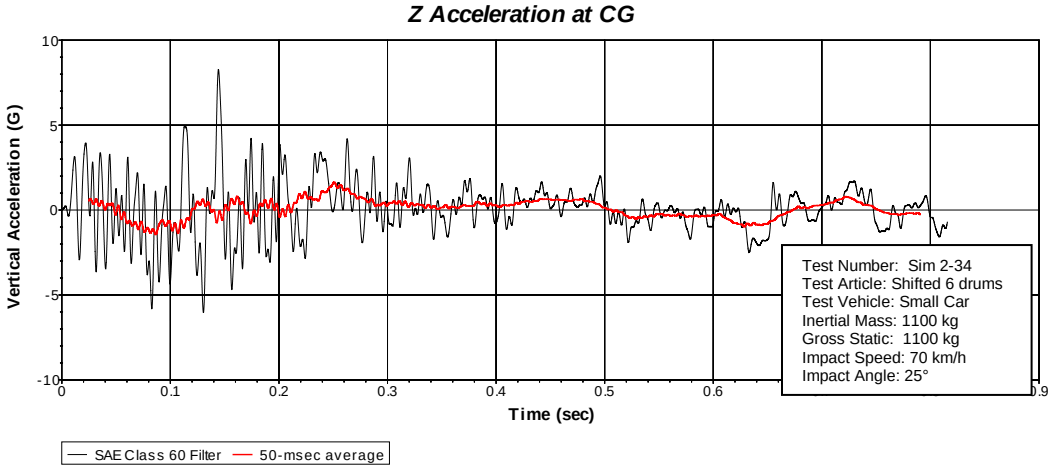


Figure 3.74. Longitudinal Acceleration of Car Impacting Short Radius with Two Tension Cables and Six 700-Lb Sand Drums.

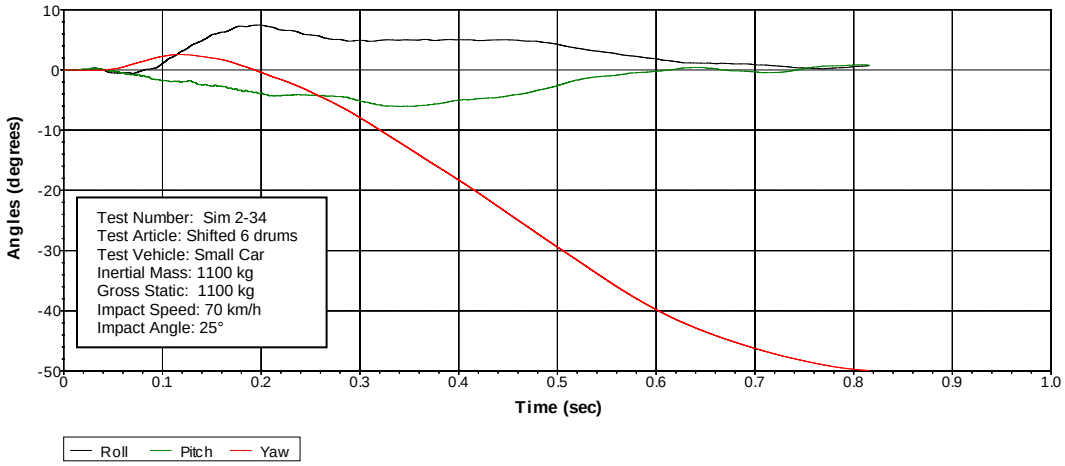


Figure 3.75. Roll, Pitch, and Yaw Angle of Car Impacting Short Radius with Two Tension Cables and Six 700-Lb Sand Drums.

3.18 SIMULATION OF CAR IMPACTING SHORT RADIUS WITH TWO TENSION CABLES AND SIX 700-LB SAND DRUMS

This simulation shared the intent of the previous two simulations: locating the critical impact point. The guardrail system was the same, but the car was shifted 6-ft to the left relative to the previous simulation. The front left corner of the bumper is positioned to impact the center of a drum, positioned between posts 11 and 12. Figure 3.76 shows the alignment of the car with the system. The car impacts at a 25° angle and at a speed of 40 mph.

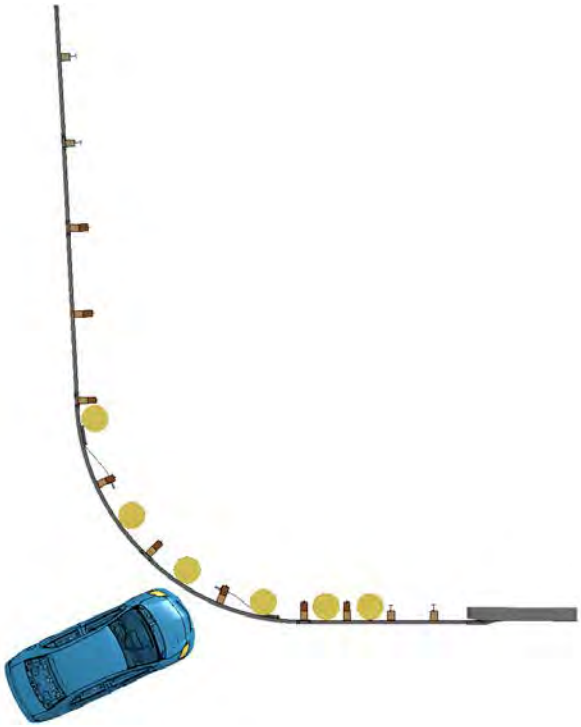


Figure 3.76. Alignment of Car with System.

Figure 3.77 displays sequential images of the simulation. By 0.05 s, the front left bumper was significantly deformed. At approximately 0.15 s, the surface area of the car in contact with the guardrail was maximized. By this point, the drums had been impacted and were starting to release sand. By 0.275 s, the front of the car was entirely deformed, and the majority of the car's kinetic energy had been dissipated; almost all of the sand from the relevant drums had been released. After this point, the car slowly rolled backward until rest. Figure 3.78 follows the position of the car from beginning state to the final state.

Table 3.16 shows the TRAP results of the occupant risk factor for the car simulation with two short cables and six spread out 700-lb sand drums. Figures 3.79, 3.80, and 3.81 show the longitudinal accelerations in the X, Y, and Z direction, respectively. Figure 3.82 shows the roll, pitch, and yaw angles for the simulation.

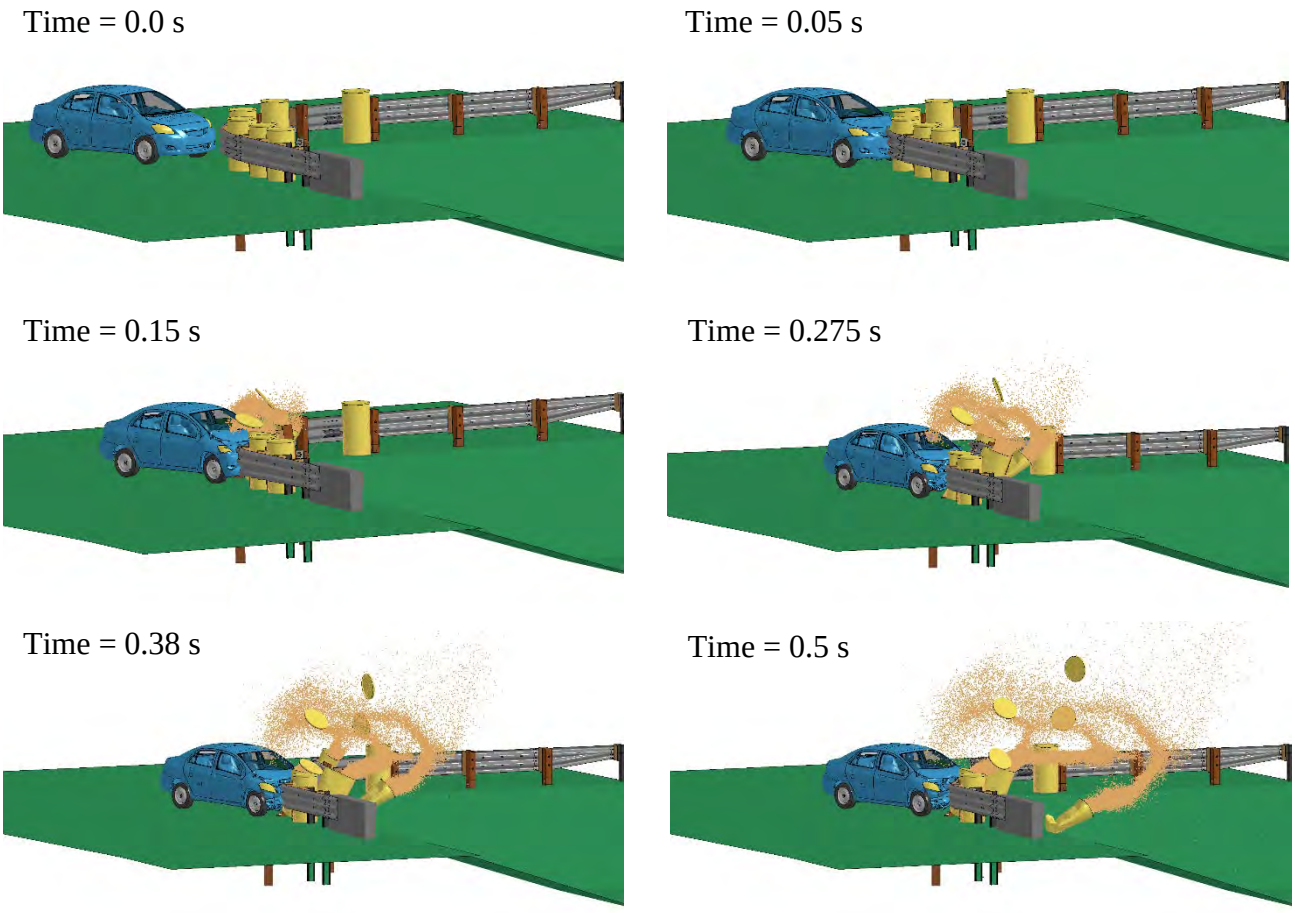
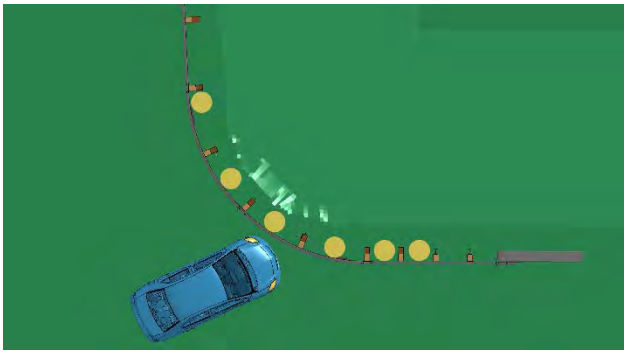
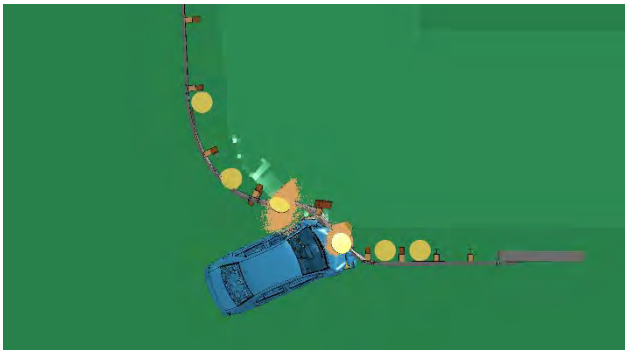


Figure 3.77. Sequential Images of Car Simulation with Two Tension Cables and Six 700-lb Sand Drums.

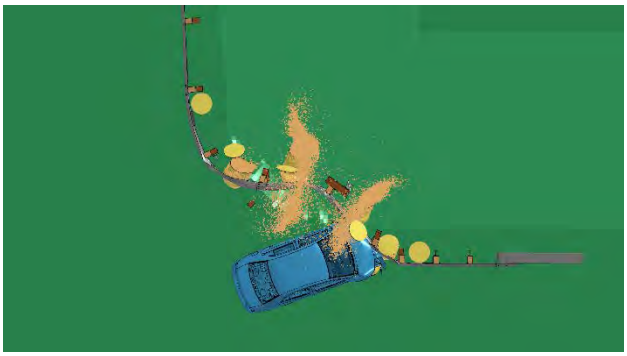
Time = 0.0 s



Time = 0.15 s



Time = 0.30 s



Time = 0.45 s

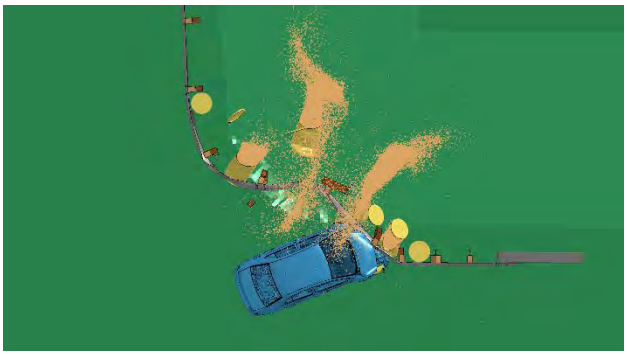


Figure 3.78. Sequential Images of Simulation (Top View).

Table 3.16. TRAP Summary Data of Simulation with Two Tension Cables and Six 700-lb Sand Drums.

TRAP Results: Truck Short Radius	
Impact Velocity, mph	43.5
Impact Angle (degrees)	25
Occupant Risk Factors	
OIV (ft/s)	
x-direction	32.5
y-direction	−8.8
Occupant Ridedown Accelerations (g's)	
x-direction	−7.7
y-direction	−2.2
Max Roll, Pitch, and Yaw Angles (degrees)	
Roll	2.0
Pitch	−1.7
Yaw	5.6

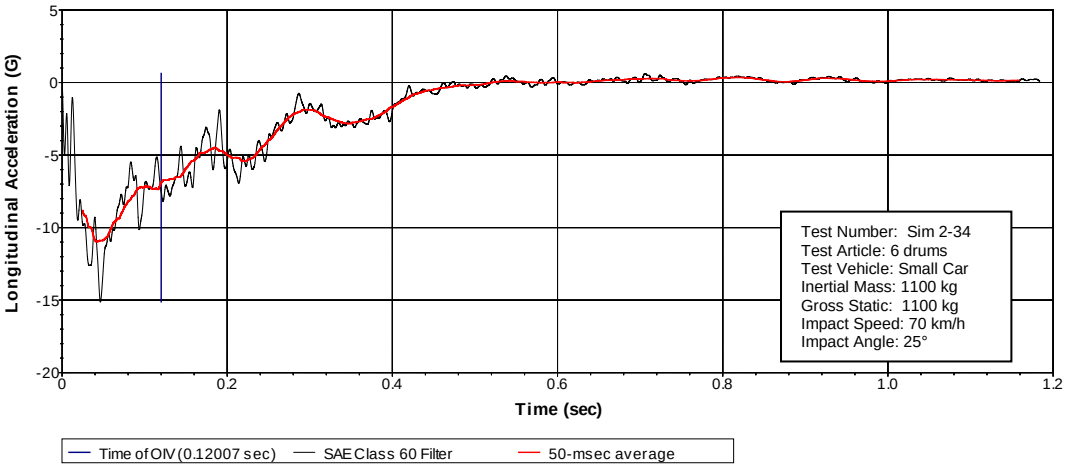


Figure 3.79. Longitudinal Acceleration of Car Impacting Short Radius with Two Tension Cables and Six 700-Lb Sand Drums.

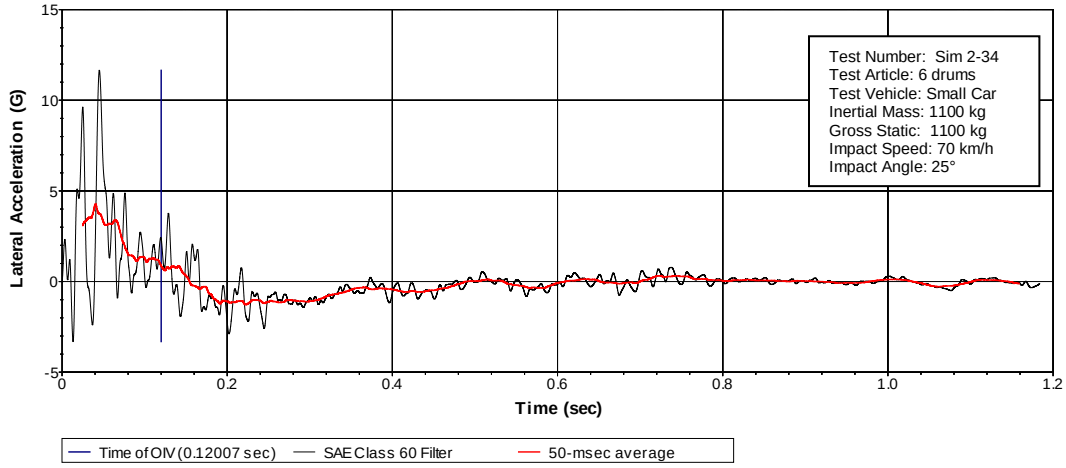


Figure 3.80. Lateral Acceleration of Car Impacting Short Radius with Two Tension Cables and Six 700-Lb Sand Drums.

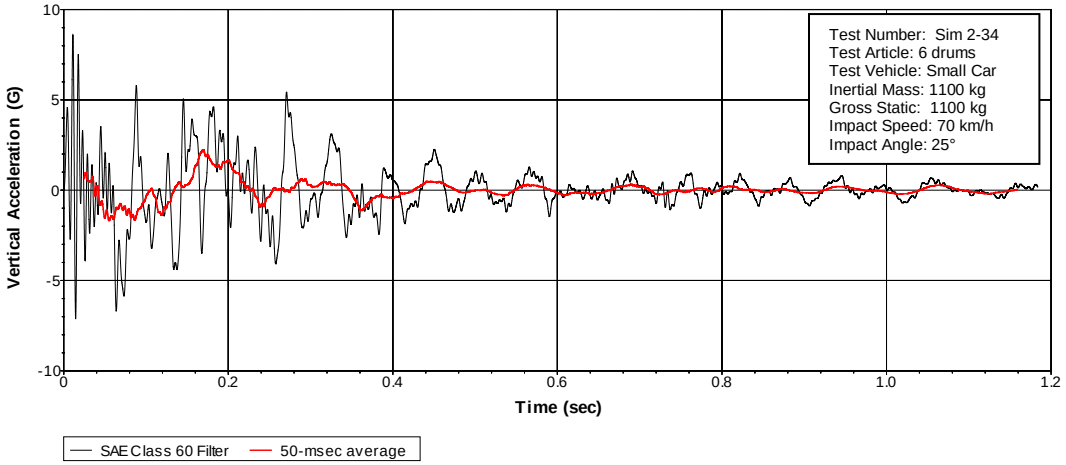


Figure 3.81. Vertical Acceleration of Car Impacting Short Radius with Two Tension Cables and Six 700-Lb Sand Drums.

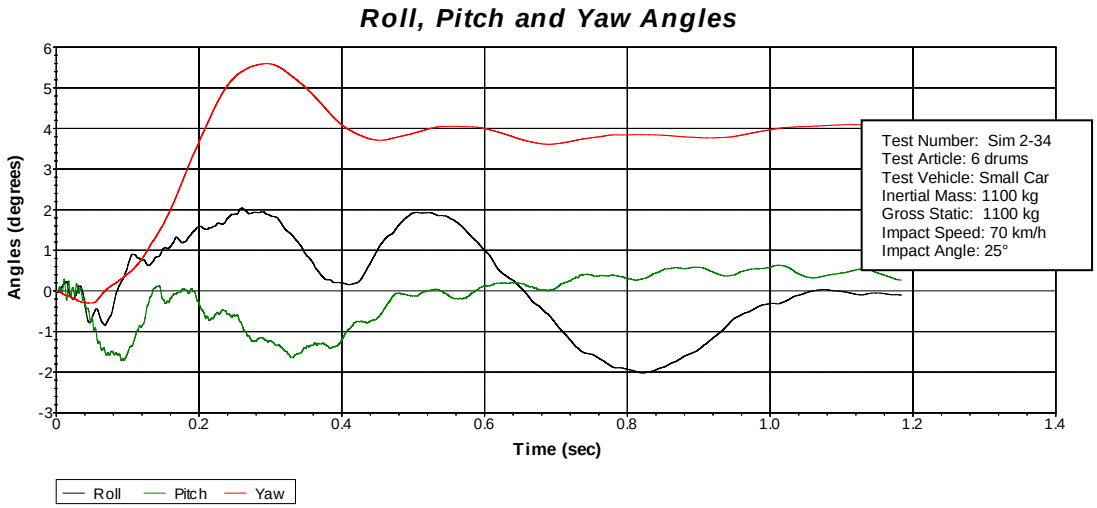


Figure 3.82. Roll, Pitch, and Yaw Angles of Car Impacting Short Radius with Two Tension Cables and Six 700-Lb Sand Drums.

3.19 CONCLUSIONS

The introduction of sand filled drums instead of sand filled barrels changed the course of the new system design. The first test, *MASH* test 2-33, included four 700-lb drums filled with sand and one tension cable. The simulation results show a positive outcome. For the next simulation, the truck was aligned parallel to the primary roadway; as a result, the truck was redirected away from the guardrail system with damage on the front corner of the driver's side.

One drum was added to the system design, which changed the results of the simulation. These results show that the truck was damaged up to the windshield. The following simulation showed the same system with the alignment of the truck impacting post 13. The results for the simulation show an unstable truck that has overridden the system.

Modifications were then done by adding another sand filled drum, making a total of six, with two tension cables one on the primary roadway and one on the secondary roadway. This modification gave positive results to the simulation by the truck not overriding the system. For the next case, the truck was aligned to hit post 13 at a 25°; this resulted in the truck being redirected away from the system. The tension cable that was placed on the primary was removed to understand which scenario gave an unreliable result. Without the tension cable, the truck was not successful in being redirected away from the system.

For *MASH* test 2-33, three simulations were created by making small changes for each. The first change made from the first simulation was the density of the drums that were modeled. The second change was a higher friction for the vehicle. The changes were made to improve the simulation and not having the truck override the system.

Once the design was cable of capturing the truck under *MASH* test 2-33 MOD conditions, *MASH* test 2-32 MOD (car) was then simulated to quantify occupant severity. *MASH* test 2-32 MOD gave favorable results for both simulated impact locations, between post 10 and post 11 and impact on post 11. Later, *MASH* test 2-31 (truck) was simulated, and the vehicle was redirected in a stable manner. Finally, the last three simulations for *MASH* test 2-34 MOD were conducted at three different impact locations to quantify the critical impact location, which resulted to be 6.3 inches downstream of post 12.

CHAPTER 4:
TEST ARTICLE DESIGN AND CONSTRUCTION

4.1 TEST ARTICLE AND INSTALLATION DETAILS

4.1.1 Guardrail

Each test installation consisted of a 31-inch tall, 87-ft long, thrie-beam short radius guardrail system constructed with an 11 ft-11 inch long primary-road leg (as measured along the guardrail) that transitioned to a section of bridge parapet, and a 50 ft-1 inch long secondary-road leg that terminated with a TxDOT GF (31) DAT-14 terminal. The curved 25-ft (post-to-post) arc length thrie-beam section (RTM02a) was rolled to a 16-ft inside radius. The primary-road side thrie-beam of the system was co-linear (parallel) to the parapet face, and the secondary-road side thrie-beam was perpendicular to the parapet face. Six sand drums were strategically placed on the inboard, field side of the installation between posts 9 and 15. The simulated parapet section was not designed for direct impact by a vehicle. See Appendix A, Sheets 1, 2, 3, 4, and 12 of 12 for overall installation details.

Post spacing was 6 ft-3 inches for each of posts 1 through 6. The post 6 to 7 spacing was 6 ft-4 inches. Posts 7 to 8 and posts 8 to 9 were spaced at 6 ft-3 inches. Each of posts 9 through 13 were spaced at 6 ft-3 inches as measured along the arc of the curved thrie-beam. The post 13 to 14 spacing was 3 ft-1½ inches, 14 to 15 spacing was 3 ft-½ inches, and 15 to 16 spacing was 3-ft 1½-inches. Post 16 to the end face of the concrete parapet was approximately 31½ inches. See Appendix A, Sheet 3 for details.

Several sections comprised the guardrail. Beginning with the DAT terminal at the secondary road, a rounded W-beam End Section (RWE03a) attached to post 1, and a 2-space, 9 ft-4½ inch long span W-beam DAT Terminal Rail Element connected post 1 to post 2. A standard W-beam, 4-space, 12 ft-6 inch span (RWM04a) connected posts 3 and 4. A 9 ft-4½ inch long span W-beam connected posts 5 and 6 to a 6 ft-4 inch long asymmetrical W- to thrie-beam transition section that connected posts 6 and 7. A thrie-beam, 4-space, 12 ft-6 inch span (RTM04a) connected posts 7, 8, and 9. Posts 9, 10, 11, 12, and 13 supported the two aforementioned curved 12 ft-6 inch arc length radiused thrie-beam sections (RTM02a). A final thrie-beam, 4-space, 12 ft-6 inch span (RWM04a) connected posts 13, 14, 15, and 16 to the parapet. Finally, a thrie-beam terminal connector (RTE01b) completed the transition from the guardrail to the parapet. All guardrail sections were galvanized standard 12-gauge material unless otherwise noted as “b.”

Posts 1 and 2 in the DAT terminal were each comprised of a timber post measuring 5½ inches × 7½ inches × 46 inches long. A 2½-inch diameter weakening hole was located 28½ inches from the top near grade. Each post was installed in a 72-inch long hollow structural section rectangular foundation tube socket (HSS 6 × 8 × ⅛ inch wall) embedded in the soil. See Appendix A, TxDOT Dwg GF (31) DAT-14 for post 1 and 2 details.

Posts 3 through 6 were 72-inch long W6×8.5 wide flange guardrail posts (PWE01). The guardrail was attached to each of posts 3 through 6 via a W-beam timber routered blockout (PDB01b, 6 inches × 8 inches × 14 inches tall; with a 4½-inch wide × ⅜-inch deep relief) and a

⅝-inch × 10-inch guardrail bolts (FBB03) and recessed guardrail nuts. Posts 3 through 6 were installed 40 inches deep into a drilled hole with compacted strong soil as per *MASH*.

Posts 7 and 8 were modified CRT timber posts (PDE09) 6 inches × 8 inches × 72 inches long. Two 3½-inch diameter weakening holes were located at 32 inches (grade level) and 47¾ inches below the top. The thrie-beam guardrail was attached to each of posts 7 and 8 via a 6-inch × 8-inch × 22-inch tall timber blockout (PDB02) and two ⅝ × 18-inch guardrail bolts (FBB04) and recessed guardrail nuts. Posts 7 and 8 were installed 40 inches deep into a drilled hole with compacted strong soil as per *MASH* and without a foundation tube. See Appendix A, Sheet 12 for details.

Posts 9 through 14 were modified BCT timber posts (PDF01) 5½ inches × 7½ inches × 48¼ inches long. A 2½-inch diameter weakening hole was located 30¾ inches from the top near grade. A ⅞-inch diameter hole was located 33¼ inches from the top through which to install a ⅝-inch × 10-inch A307 Grade 5 hex bolt, flat washer, and recessed guardrail nut that secured the post in the foundation tube. Each post's foundation tube was a 6-inch × 8-inch × $^{3}/_{16}$-inch thick ASTM A500 grade B steel HSS structural tube (PTE05), 72 inches long and embedded approximately 70 inches deep into drilled holes with compacted strong soil as per *MASH*. Two $^{13}/_{16}$-inch diameter holes were located 1 inch below the top of each tube (centered in the lateral direction) to secure the timber post in the tube as described above. The guardrail was attached to each post via a W-beam timber blockout (PDB01a) and a ⅝ × 18-inch guardrail bolt (FBB04) and recessed guardrail nut. See Appendix A, Sheets 4 and 12 for details.

Post 15 was a W6×8.5 wide flange guardrail post (PWE01), 72 inches long. The guardrail was attached to post 15 via a W-beam timber routered blockout (PDB01b) and a ⅝-inch × 10-inch guardrail bolt (FBB03) and recessed guardrail nut. Post 15 was installed 40 inches deep into a drilled hole with compacted strong soil as per *MASH.* See Appendix A, Sheet 4 for details.

Post 16 was a W6×8.5 wide flange guardrail posts (PWE01), 72 inches long. The guardrail was attached to post 16 via a thrie-beam timber routered blockout (6 inches × 8 inches × 18 inches tall; with a 4½-inch wide × ⅜-inch deep relief, similar to a PDB02) and one ⅝-inch × 10-inch guardrail bolt (FBB03) and recessed guardrail nut in the upper holes. Post 16 was installed 40 inches deep into a drilled hole with compacted strong soil as per *MASH*. See Appendix A, Sheet 4 for details.

A thrie-beam terminal connector (RTE01b) was utilized to connect and transition the thrie-beam to the parapet. Five A325 ⅞-inch diameter hex bolts, SAE flat washers, and heavy hex nuts secured the connector to the parapet: three 14-inch long bolts in the upper, wider part of the parapet, and two 12-inch long bolts in the lower, narrower part of the parapet. The terminal connector and thrie beam were joined with 12 sets of ⅝-inch diameter × 2-inch long guardrail bolts (FBB02), rectangular washers (FWR03), and recessed guardrail nuts. See Appendix A, Sheet 4 for details.

Two BCT anchor cables (FCA01) were integrated into each system. Refer to section 4.2 "Design Modification during Testing" for details and changes.

4.1.2 Parapet

A reinforced concrete bridge parapet was constructed by adding on to the existing concrete runway apron. The parapet base tapered from 60 to 56⅝ inches wide at the guardrail

attachment end (yielding a 2° offset angle) and was 8 ft long, 18 inches thick, and constructed of steel reinforced TxDOT Class C concrete with a minimum specified strength of 3600 psi. All reinforcing steel was ASTM A615 Grade 60, and unions of longitudinal, traverse, and vertical rebar were wire-tied on site. See Appendix A, Sheets 9 through 14 for details.

The parapet itself was 32 inches tall with a smooth vertical traffic side face and a stepped field side face. Its profile was 10½ inches wide at the base and transitioned with a 1½-inch chamfer to a 12-inch wide top portion beginning 18½ inches above grade. Exposed edges were chamfered ¾-inch. The traffic side face conformed to the 2° offset and was 24 inches from the edge of the runway on the upstream end, and 20⅝ inches from the edge of the runway on the guardrail end. On the traffic side, the width of the parapet tapered from 12 inches to 10 inches over the final 12 inches on the guardrail attachment end. Five 1-inch diameter holes were cast into the parapet at the time of the concrete pour to accommodate the thrie-beam terminal connector. See Appendix A, Sheet 9 for details.

Reinforcement in the parapet consisted of sixteen ½-inch nominal diameter reinforcing steel (#4 rebar) S-bars longitudinally spaced on 6-inch longitudinal centers and four 82-inch long #4 bent bars vertically spaced on 8-inch centers on the traffic side, and four 93-inch long #4 straight bars vertically spaced on 8-inch centers on the field side. The parapet was tied to the base with fifteen ½-inch nominal diameter reinforcing steel (#4 rebar) U-bars longitudinally spaced on 6-inch centers. Each 25½-inch tall U-bar extended from the bottom base mat to 10 inches into the lower portion of the parapet.

The base was secured to the runway apron with six ⅝-inch diameter (#5 rebar) × 24-inch long tie bars located on 16-inch horizontal centers. The tie bars were approximately 3 inches below the top surface, embedded 6 inches deep into holes drilled horizontally into the edge of the apron, and secured with Hilti RE200-A epoxy. See Appendix A, Sheet 11 for details.

Reinforcement in the base consisted of two mats of ⅝-inch nominal diameter reinforcing steel (#5 rebar) located approximately 1½ inches and 15 inches below the upper surface of the base. The upper mat rested on the new tie bars installed in the edge of the apron. The fifteen 53-inch long upper transverse bars were spaced on 6-inch centers and joined with seven 90-inch long longitudinal bars on 8-inch centers. The eight 53-inch lower transverse bars were spaced on 12-inch centers and joined with five 90-inch longitudinal bars on 12-inch centers. Five U-shaped support bars spaced on 18-inch centers provided structure and continuity between the upper and lower mats on the field side of the base.

4.1.3 Sand Drums

Six 55-gallon drums (Eagle Model #1656 with lid; High-Density Polyethylene), each filled with washed sand and weighing 715 ±10 lb, were strategically placed on the field side of the thrie-beam between posts 9 and 15. See Attachment A, Sheet 3 of 12 for placement geometry.

4.1.4 Ditch

A ditch was constructed on the field side of the installation. The upper edge of the ditch was located 2-ft behind, and parallel to, the inside of the curvature of the guardrail on the primary road parapet end, increasing to 3-ft behind, and parallel to, the inside of the curvature of

the guardrail on the secondary road terminal end. The ditch was 21-ft wide × 7-ft deep with a 3:1 slope on the faces.

Figure 4.1 presents overall information on the TxDOT low-speed short radius guardrail treatment, and Figure 4.2 provides photographs of the installation. Appendix A provides further details of the TxDOT low-speed short radius guardrail treatment.

4.2 DESIGN MODIFICATIONS DURING TESTING

Two BCT anchor cables were integrated into each system. One attached to post 10 at grade and terminated on the thrie-beam near post 9. The second attached to post 12 at grade and terminated on the thrie-beam near post 13.

Each anchor cable was a ¾-inch (6×19; or IWRC; AASHTO M-30; 46 kips min.) galvanized wire rope. Each anchor cable termination consisted of a standard swaged fitting with a 1-inch diameter threaded stud, washer, and nut; the swage was specified to exceed the breaking strength of the wire rope. Each weakening hole at posts 10 and 12 contained a 2-inch Sch 40 (0.1535-inch wall thickness) BCT post sleeve (FMM02) through which one terminal end of the anchor cable was secured via a 8-inch × 8-inch × ⅝-inch thick BCT bearing plate (FPB01), flat washer, and nut. The opposite end of each anchor cable was secured to the lower field side involute of the thrie-beam with a guardrail anchor bracket (FPA01) and, depending on the test installation as describe below, either four or eight ⅝-inch × 2-inch hex bolts with USS flat washers and recessed guardrail nuts. The swage stud nuts were tightened such that all slack was removed from the cable. See Appendix A, Sheet 3 for details.

For Test Nos. 469137-3-1 and -3-2 (*MASH* 2-33 and 2-32), standard BCT Anchor Cables (FCA01) measuring 6 ft-6¾ inches end to end, inclusive of terminal fittings, were used. Due to the cables being longer than required, the Guardrail Anchor Brackets (FPA01) were repositioned and attached to the thrie-beam with four bolts instead of eight.

For Test Nos. 469138-3-3, -3-4, and 469138-3-5 (*MASH* 2-31, 2-35, and 2-34, respectively), modified BCT Anchor Cables measuring 5 ft-5 inches end to end, inclusive of terminal fittings, were used. These shortened cables allowed the Guardrail Anchor Brackets (FPA01) to attach to the thrie-beam with eight bolts. See Appendix B, Sheets 3 and 13 for details.

Figure 4.3 shows the changes to the TxDOT low-speed short radius guardrail treatment for Test Nos. 469138-3-3, -3-4, and 469138-3-5, and Figure 4.4 provides photographs of the installation. Appendix B provides further details of the TxDOT low-speed short radius guardrail treatment.

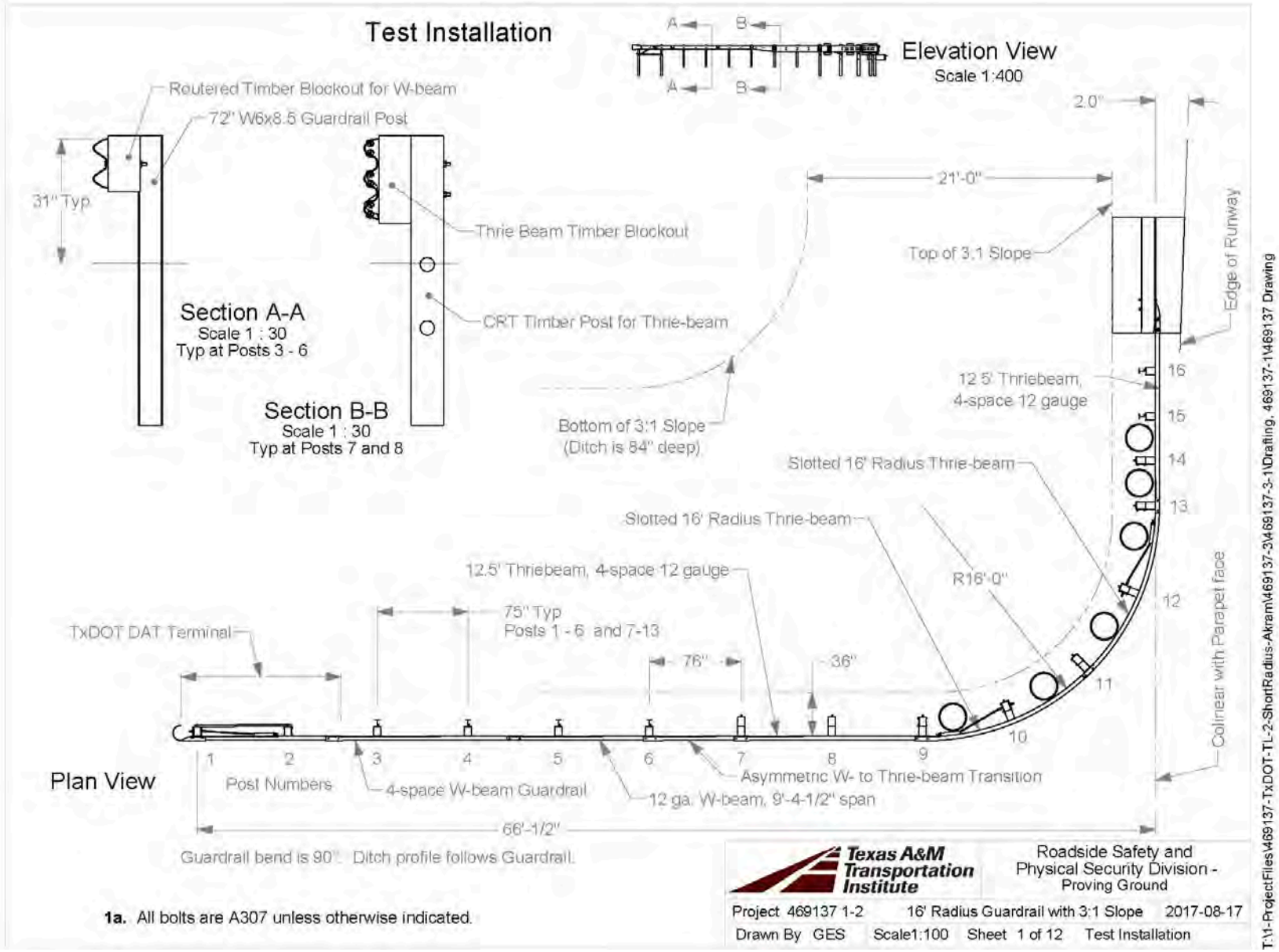


Figure 4.1. Overall Details of the TxDOT Low-Speed Short Radius Guardrail Treatment.



Figure 4.2. TxDOT Low-Speed Short Radius Guardrail Treatment prior to Test Nos. 469137-3-1 and 469138-3-4.

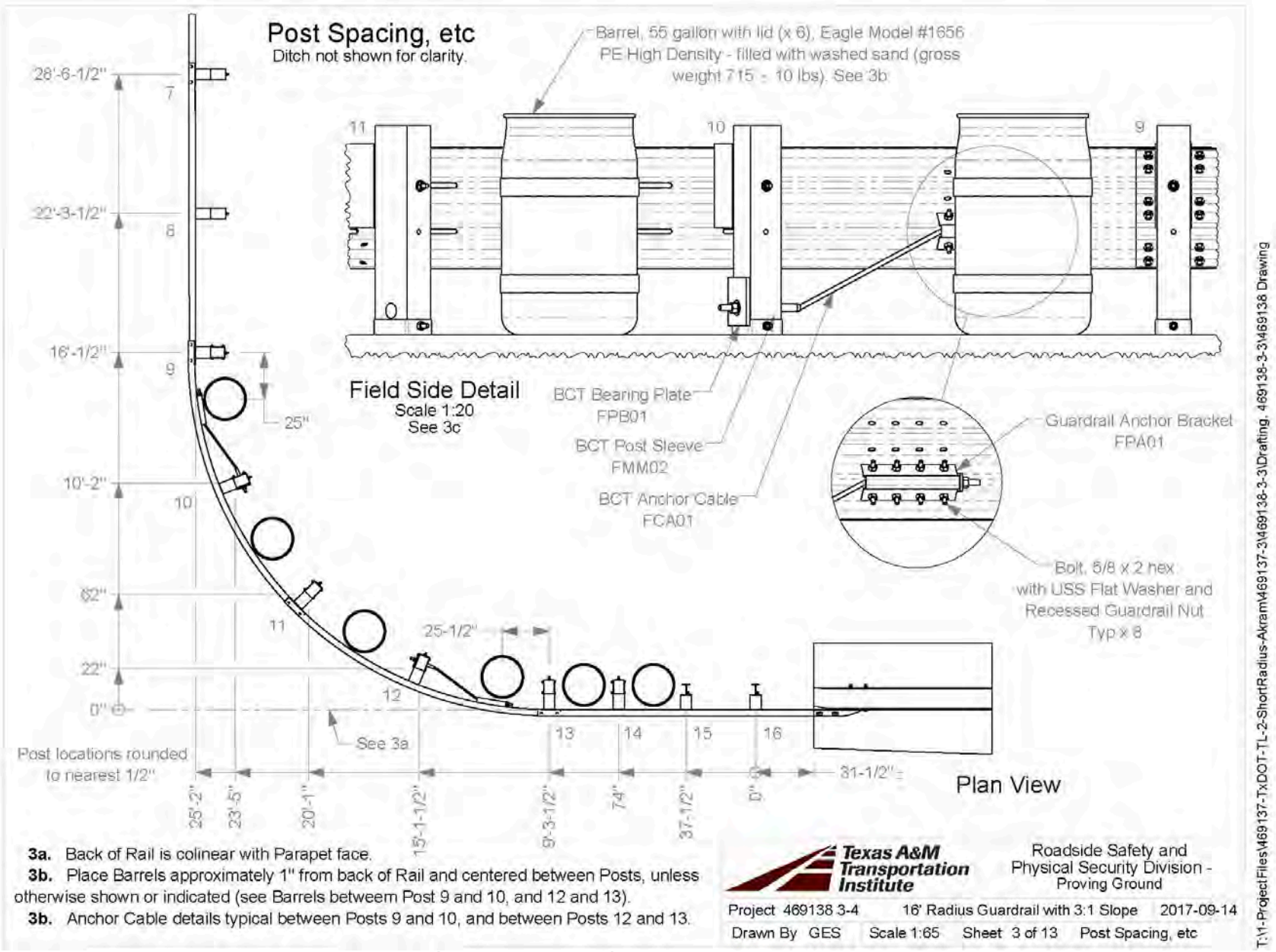


Figure 4.3. Details of the Cable used for Test Nos. 469138-3-3 and 469138-3-4.

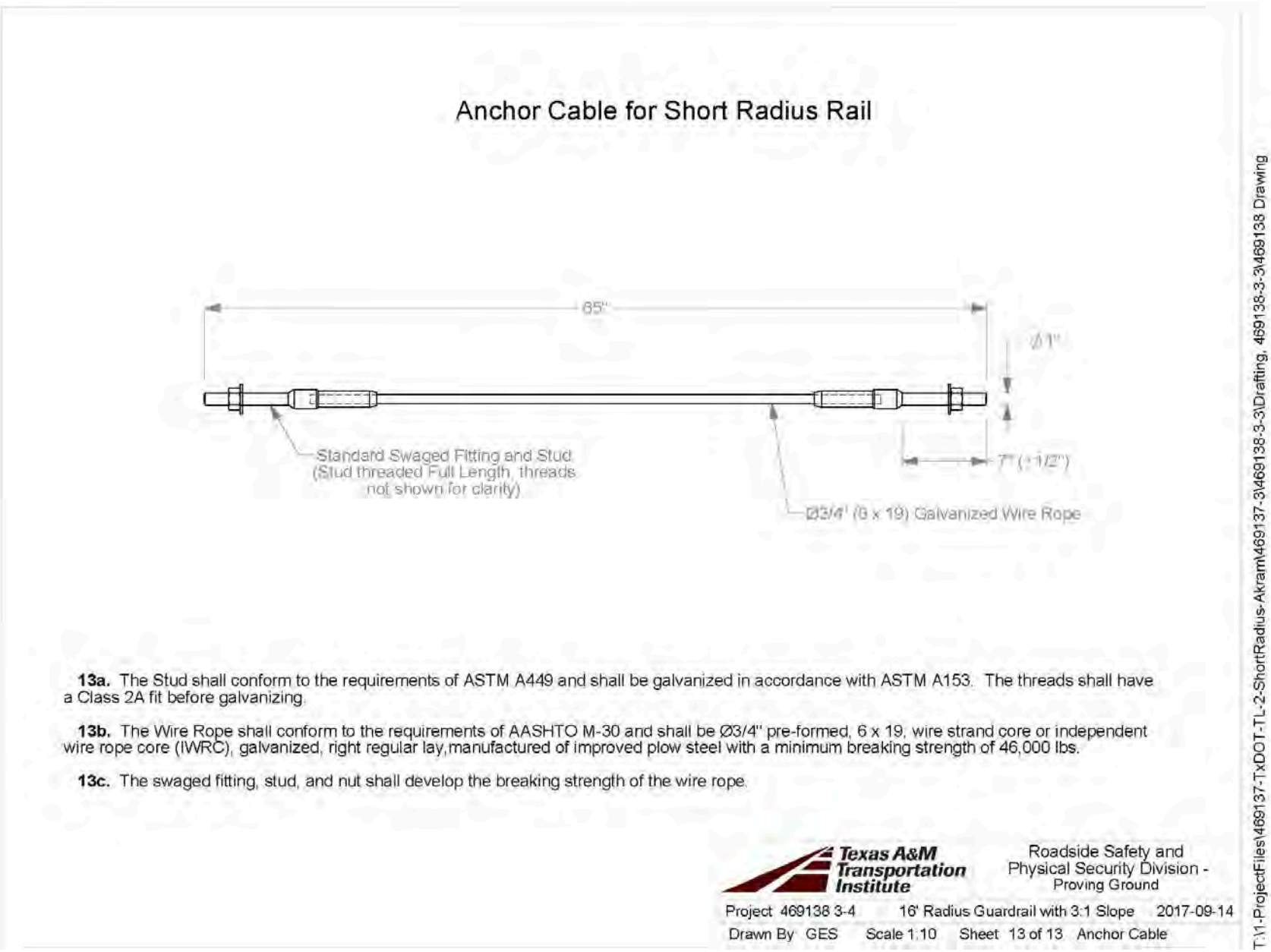


Figure 4.3. Details of the Cable used for Test Nos. 469138-3-3 and 469138-3-4 (Continued).



Figure 4.4. Cable prior to Test Nos. 469138-3-3 and 469138-3-4.

4.3 SOIL CONDITIONS

The test installation was installed in standard soil meeting AASHTO standard specifications for "Materials for Aggregate and Soil Aggregate Subbase, Base and Surface Courses," designated M147-65(2004), grading B.

In accordance with Appendix B of *MASH*, soil strength was measured the day of the crash test. During installation of the TxDOT low-speed short radius guardrail treatment for full-scale crash testing, two standard W6×16 posts were installed in the immediate vicinity of the installation, using the same fill materials and installation procedures used in the standard dynamic test was performed (see Table C.1 in Appendix C for establishment minimum soil strength properties in the dynamic test performed in accordance with *MASH* Appendix B).

As determined in the tests shown in Appendix C, Table C.1, the minimum post load required for deflections at 5 inches, 10 inches, and 15 inches, measured at a height of 25 inches, is 3940 lb, 5500 lb, and 6540 lb, respectively (90 percent of static load for the initial standard installation).

On the day of Test No. 469137-3-1, August 18, 2017, load on the post at deflections of 5 inches, 10 inches, and 15 inches was 9012 lbf, 9015 lbf, and 7540 lbf, respectively. In Appendix C, Table C.2 shows the strength of the backfill material in which the TxDOT low-speed short radius guardrail treatment was installed met minimum requirements.

On the day of Test No. 469137-3-2, September 5, 2017, load on the post at deflections of 5 inches, 10 inches, and 15 inches was 9646 lbf, 9343 lbf, and 8535 lbf, respectively. In Appendix C, Table C.3 shows the strength of the backfill material in which the TxDOT low-speed short radius guardrail treatment was installed met minimum requirements.

On the day of Test No. 469138-3-3, September 15, 2017, load on the post at deflections of 5 inches, 10 inches, and 15 inches was 8232 lbf, 8484 lbf, and 8585 lbf, respectively. In Appendix C, Table C.4 shows the strength of the backfill material in which the TxDOT low-speed short radius guardrail treatment was installed met minimum requirements.

On the day of Test No. 469138-3-4, September 28, 2017, load on the post at deflections of 5 inches, 10 inches, and 15 inches was 7626 lbf, 8989 lbf, and 10,050 lbf, respectively. In Appendix C, Table C.5 shows the strength of the backfill material in which the TxDOT low-speed short radius guardrail treatment was installed met minimum requirements.

On the day of Test No. 469138-3-5, December 14, 2017, load on the post at deflections of 5 inches, 10 inches, and 15 inches was 6060 lbf, 7272 lbf, and 7575 lbf, respectively. In Appendix C, Table C.6 shows the strength of the backfill material in which the TxDOT low-speed short radius guardrail treatment was installed met minimum requirements.

CHAPTER 5:
TEST REQUIREMENTS AND EVALUATION CRITERIA

5.1 CRASH TEST MATRIX

Table 5.1 shows the test conditions and evaluation criteria for *MASH* TL-2 non-gating end treatments. The target CIPs selected for the tests were determined according to the information provided in *MASH* Section 2.3.3 and *MASH* Figure 2-3A. The target CIP selected for each test is shown in Figures 5.1 through 5.5.

Table 5.1. Test Conditions and Evaluation Criteria Specified for *MASH* TL-2 Non-Gating End Treatments.

Test Article	Test Designation	Test Vehicle	Impact Conditions		Evaluation Criteria
			Speed	Angle	
Terminals and Redirective Crash Cushions	2-30	1100C	44 mi/h	0°	A, D, F, H, I
	2-31	2270P	44 mi/h	0°	A, D, F, H, I
	2-32	1100C	44 mi/h	5–15°	A, D, F, H, I
	2-33	2270P	44 mi/h	5–15°	A, D, F, H, I
	2-34	1100C	44 mi/h	15°	A, D, F, H, I
	2-35	2270P	44 mi/h	25°	A, D, F, H, I
	2-36	2270P	44 mi/h	25°	A, D, F, H, I
	2-37a	1100C	44 mi/h	25°	A, D, F, H, I
	2-37b	2270P			

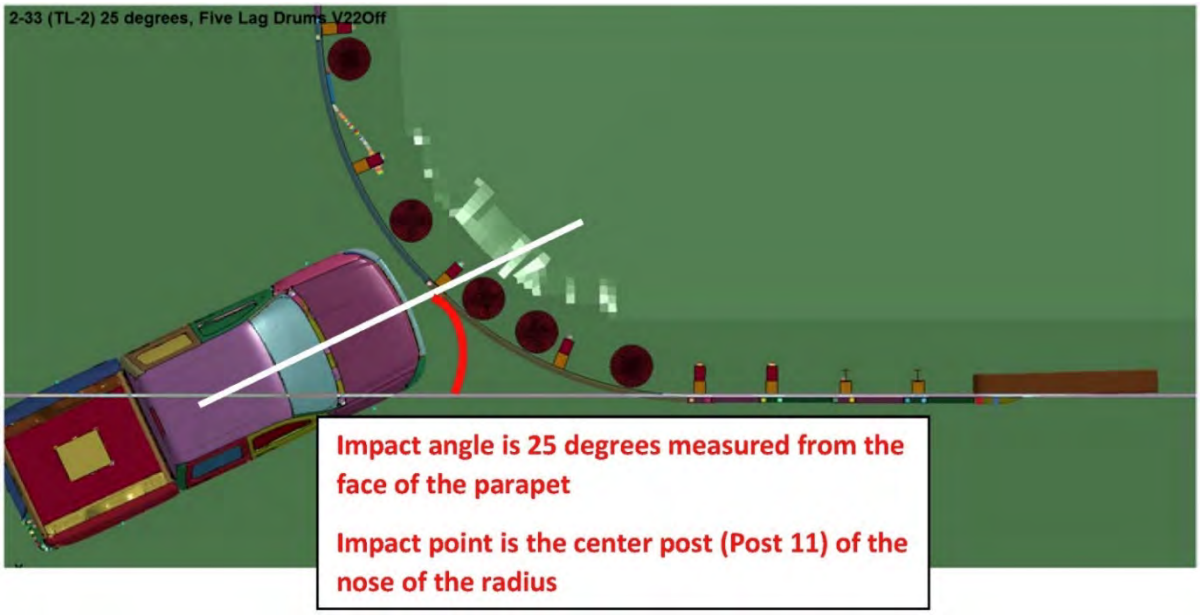


Figure 5.1. Target CIP for *MASH* Test 2-33 on the TxDOT Low-Speed Short Radius Guardrail Treatment.

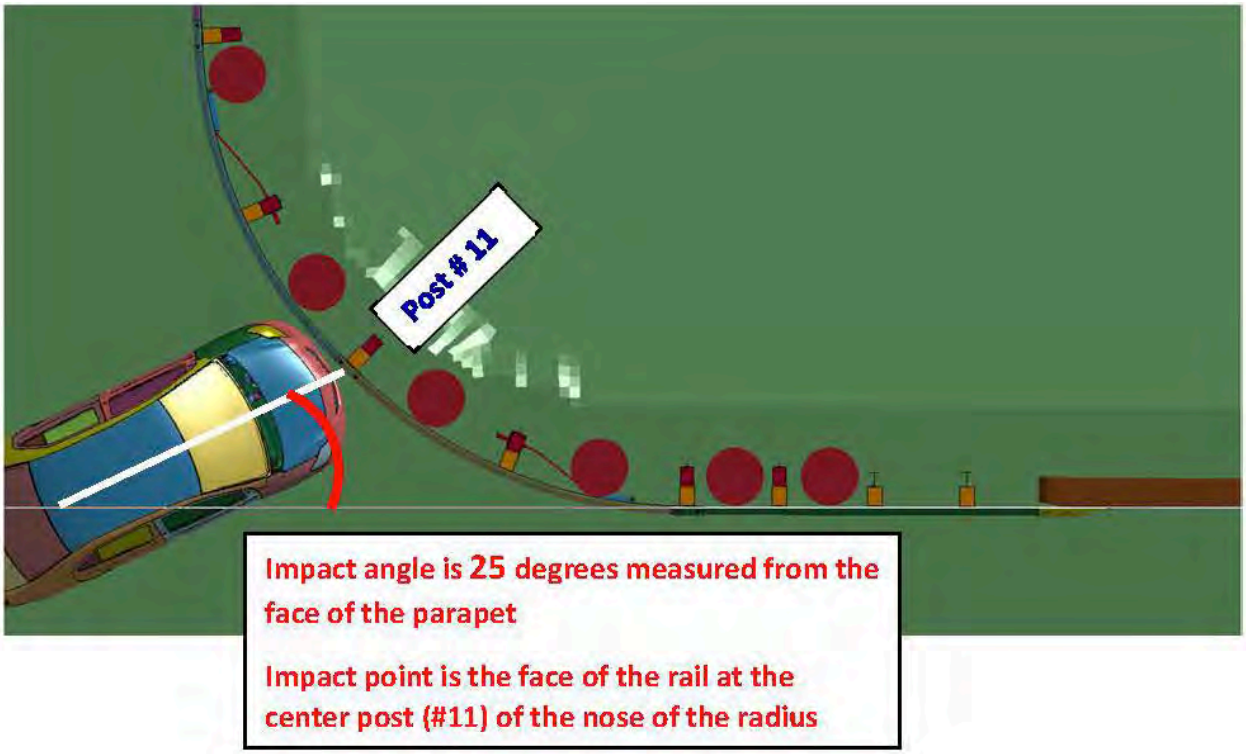


Figure 5.2. Target CIP for *MASH* Test 2-32 on the TxDOT Low-Speed Short Radius Guardrail Treatment.

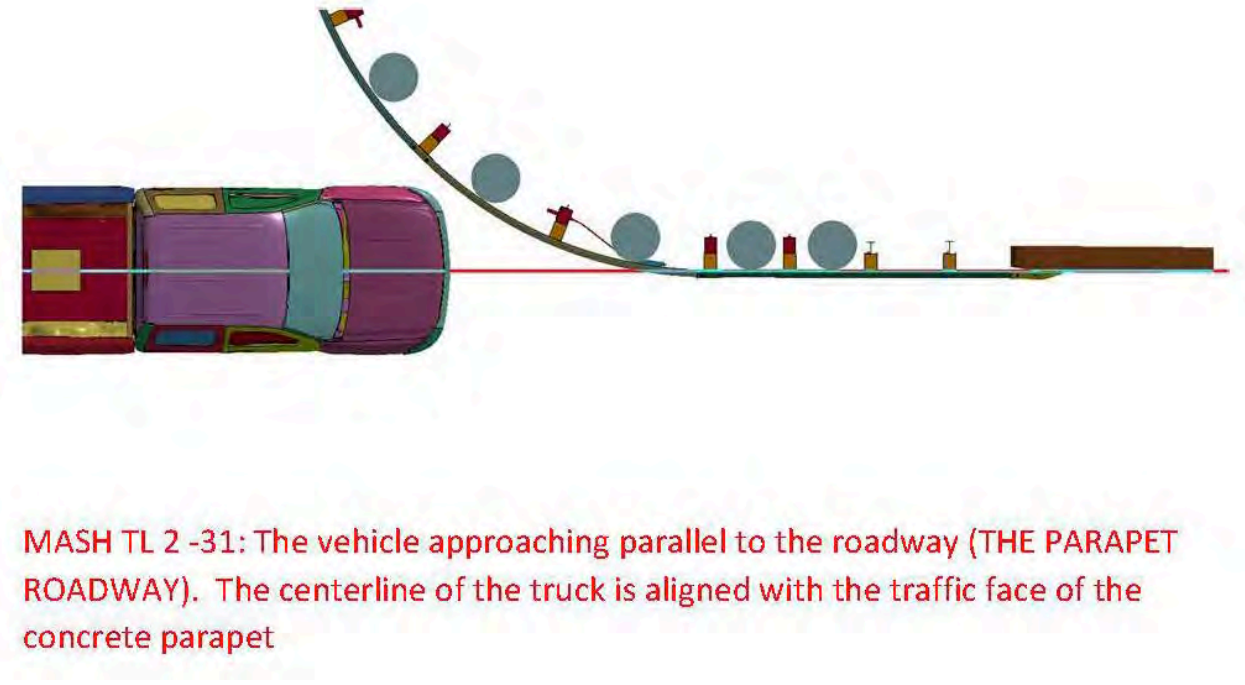


Figure 5.3. Target CIP for *MASH* Test 2-31 on the TxDOT Low-Speed Short Radius Guardrail Treatment.

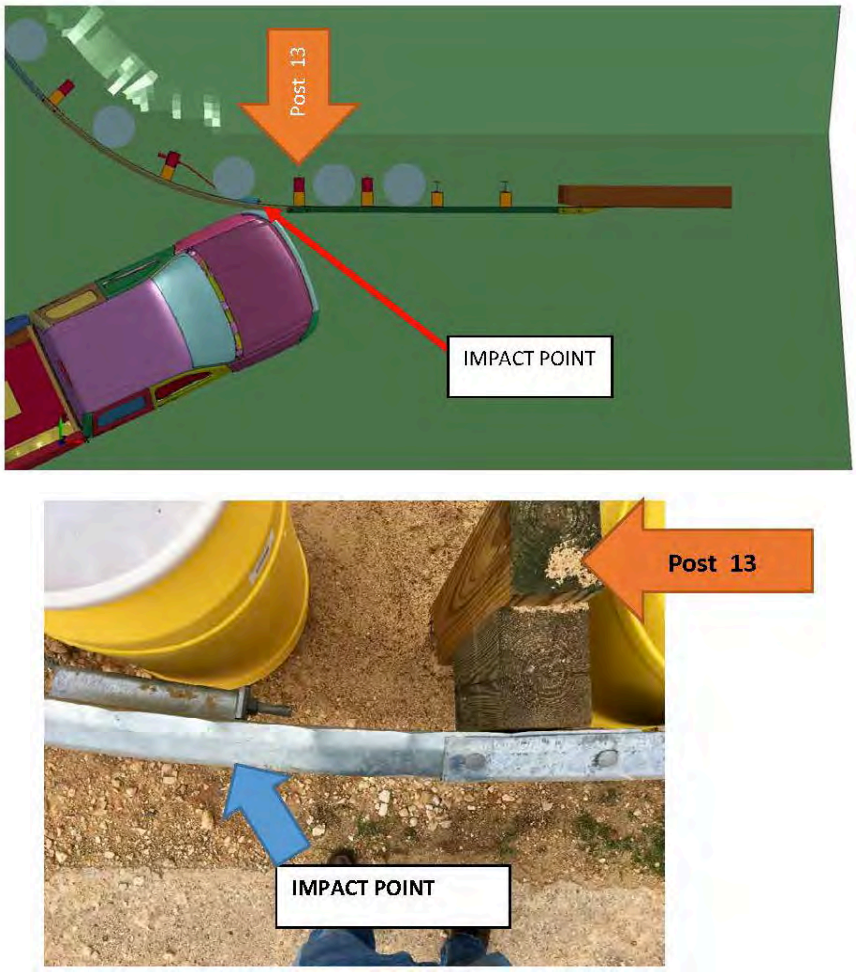


Figure 5.4. Target CIP for *MASH* Test 2-35 on the TxDOT Low-Speed Short Radius Guardrail Treatment.



Figure 5.5. Target CIP for Modified *MASH* Test 2-34 on the TxDOT Low-Speed Short Radius Guardrail Treatment.

The crash tests and data analysis procedures were in accordance with guidelines presented in *MASH*. Chapter 4 presents brief descriptions of these procedures.

5.2 EVALUATION CRITERIA

The appropriate safety evaluation criteria from Tables 2-3 and 5-1A through 5-1C of *MASH* were used to evaluate the crash tests reported herein. The test conditions and evaluation criteria required for *MASH* TL-2 non-gating end treatments are listed in Table 4.1, and the substance of the evaluation criteria in Table 5.2. An evaluation of the crash test results is presented in detail under the section Assessment of Test Results.

Table 5.2. Evaluation Criteria Required for *MASH* TL-2 Non-Gating End Treatments.

Evaluation Factors	Evaluation Criteria	
Structural Adequacy	*A.*	*Test article should contain and redirect the vehicle or bring the vehicle to a controlled stop; the vehicle should not penetrate, underride, or override the installation although controlled lateral deflection of the test article is acceptable.*
Occupant Risk	*D.*	*Detached elements, fragments, or other debris from the test article should not penetrate or show potential for penetrating the occupant compartment, or present undue hazard to other traffic, pedestrians, or personnel in a work zone.* *Deformations of, or intrusions into, the occupant compartment should not exceed limits set forth in Section 5.2.2 and Appendix E of MASH.*
	F.	*The vehicle should remain upright during and after collision. The maximum roll and pitch angles are not to exceed 75 degrees.*
	H.	*Occupant impact velocities (OIV) should satisfy the following limits: Preferred value of 30 ft/s, or maximum allowable value of 40 ft/s.*
	I.	*The occupant ridedown accelerations should satisfy the following: Preferred value of 15.0 g, or maximum allowable value of 20.49 g.*

CHAPTER 6:
TEST CONDITIONS

6.1 TEST FACILITY

The full-scale crash tests reported herein were performed at Texas A&M Transportation Institute (TTI) Proving Ground, an International Standards Organization (ISO)/International Electrotechnical Commission (IEC) 17025-accredited laboratory with American Association for Laboratory Accreditation (A2LA) Mechanical Testing Certificate 2821.01. The full-scale crash test was performed according to TTI Proving Ground quality procedures, and according to the *MASH* guidelines and standards.

The test facilities of the TTI Proving Ground are located on the Texas A&M University RELLIS Campus, which consists of a 2000-acre complex of research and training facilities situated 10 miles northwest of the flagship campus of Texas A&M University. The site, formerly a United States Army Air Corps base, has large expanses of concrete runways and parking aprons well suited for experimental research and testing in the areas of vehicle performance and handling, vehicle-roadway interaction, durability and efficacy of highway pavements, and evaluation of roadside safety hardware and perimeter protective devices. The site selected for construction and testing of the short radius guardrail treatment was along the edge of an out-of-service apron. The apron consists of an unreinforced jointed-concrete pavement in 12.5-ft × 15-ft blocks nominally 6 inches deep. The aprons were built in 1942, and the joints have some displacement, but are otherwise flat and level.

6.2 VEHICLE TOW AND GUIDANCE SYSTEM

Each test vehicle was towed into the test installation using a steel cable guidance and reverse tow system. A steel cable for guiding the test vehicle was tensioned along the path, anchored at each end, and threaded through an attachment to the front wheel of the test vehicle. An additional steel cable was connected to the test vehicle, passed around a pulley near the impact point, through a pulley on the tow vehicle, and then anchored to the ground such that the tow vehicle moved away from the test site. A 2:1 speed ratio between the test and tow vehicle existed with this system. Just prior to impact with the installation, the test vehicle was released and ran unrestrained. The vehicle remained freewheeling (i.e., no steering or braking inputs) until it cleared the immediate area of the test site (no sooner than 2 s after impact), after which the brakes were activated, if needed, to bring the test vehicle to a safe and controlled stop.

6.3 DATA ACQUISITION SYSTEMS

6.3.1 Vehicle Instrumentation and Data Processing

Each test vehicle was instrumented with a self-contained, on-board data acquisition system. The signal conditioning and acquisition system is a 16-channel, Tiny Data Acquisition System (TDAS) Pro produced by Diversified Technical Systems, Inc. The accelerometers, which measure the x, y, and z axis of vehicle acceleration, are strain gauge type with linear millivolt output proportional to acceleration. Angular rate sensors, measuring vehicle roll, pitch, and yaw

rates, are ultra-small, solid state units designed for crash test service. The TDAS Pro hardware and software conform to the latest SAE J211, Instrumentation for Impact Test. Each of the 16 channels is capable of providing precision amplification, scaling, and filtering based on transducer specifications and calibrations. During the test, data are recorded from each channel at a rate of 10,000 values per second with a resolution of one part in 65,536. Once data are recorded, internal batteries back these up inside the unit should the primary battery cable be severed. Initial contact of the pressure switch on the vehicle bumper provides a time zero mark and initiates the recording process. After each test, the data are downloaded from the TDAS Pro unit into a laptop computer at the test site. The Test Risk Assessment Program (TRAP) software then processes the raw data to produce detailed reports of the test results.

Each of the TDAS Pro units is returned to the factory annually for complete recalibration and all instrumentation used in the vehicle conforms to all specifications outlined by SAE J211. All accelerometers are calibrated annually by means of an ENDEVCO® 2901, precision primary vibration standard. This standard and its support instruments are checked annually and receive a National Institute of Standards Technology (NIST) traceable calibration. The rate transducers used in the data acquisition system receive a calibration via a Genisco Rate-of-Turn table. The subsystems of each data channel are also evaluated annually, using instruments with current NIST traceability, and the results are factored into the accuracy of the total data channel, per SAE J211. Calibrations and evaluations are also made any time data are suspect. Acceleration data are measured with an expanded uncertainty of ±1.7 percent at a confidence factor of 95 percent (k=2).

TRAP uses the data from the TDAS Pro to compute occupant/compartment impact velocities, time of occupant/compartment impact after vehicle impact, and the highest 10-millisecond (ms) average ridedown acceleration. TRAP calculates change in vehicle velocity at the end of a given impulse period. In addition, maximum average accelerations over 50-ms intervals in each of the three directions are computed. For reporting purposes, the data from the vehicle-mounted accelerometers are filtered with a 60-Hz low-pass digital filter, and acceleration versus time curves for the longitudinal, lateral, and vertical directions are plotted using TRAP.

TRAP uses the data from the yaw, pitch, and roll rate transducers to compute angular displacement in degrees at 0.0001-s intervals, then plots yaw, pitch, and roll versus time. These displacements are in reference to the vehicle-fixed coordinate system with the initial position and orientation of the vehicle-fixed coordinate systems being initial impact. Rate of rotation data is measured with an expanded uncertainty of ±0.7 percent at a confidence factor of 95 percent (k=2).

6.3.2 Anthropomorphic Dummy Instrumentation

An Alderson Research Laboratories Hybrid II, 50th percentile male anthropomorphic dummy, restrained with lap and shoulder belts, was placed in the front seat on the impact side of the 1100C vehicle. The dummy was not instrumented.

According to *MASH*, use of a dummy in the 2270P vehicle is optional, and no dummy was used in the test.

6.3.3 Photographic Instrumentation and Data Processing

Photographic coverage of the test included three high-speed cameras:

- One overhead with a field of view perpendicular to the ground and directly over the impact point.
- One placed behind the installation at an angle.
- A third placed to have a field of view parallel to and aligned with the installation at the downstream end.

A flashbulb on the impacting vehicle was activated by a pressure-sensitive tape switch to indicate the instant of contact with the short radius guardrail treatment. The flashbulb was visible from each camera. The video files from these digital high-speed cameras were analyzed to observe phenomena occurring during the collision and to obtain time-event, displacement, and angular data. A digital camera recorded and documented conditions of each test vehicle and the installation before and after the test.

CHAPTER 7:
MASH TEST 2-33 (CRASH TEST NO. 469137-3-1)

7.1 TEST DESIGNATION AND ACTUAL IMPACT CONDITIONS

MASH Test 2-33 involves a 2270P vehicle weighing 5000 lb ±110 lb impacting the nose of the short radius guardrail at an impact speed of 44 mi/h ±2.5 mi/h and an angle of 5–15° ±1.5°. TTI researchers determined the most critical impact angle to be 25° measured from the face of the parapet. The target impact point for *MASH* Test 2-33 on the short radius guardrail was centerline of the vehicle with the centerline of post 11 of the nose of the radius ±1 ft.

The 2011 Dodge RAM 1500 pickup truck used in the test weighed 5039 lb, and the actual impact speed and angle were 44.8 mi/h and 25.5°, respectively. The actual impact point was centerline of the vehicle aligned with the centerline of post 11. Minimum target kinetic energy (KE) was 291 kip-ft, and actual KE was 338 kip-ft.

7.2 WEATHER CONDITIONS

The test was performed on the morning of August 18, 2017. Weather conditions at the time of testing were as follows: wind speed: 8 mi/h; wind direction: 189° (vehicle was traveling in a northwesterly direction); temperature: 89°F; relative humidity: 67 percent.

7.3 TEST VEHICLE

The 2011 Dodge RAM 1500 pickup truck, shown in Figures 7.1 and 7.2, was used for the crash test. The vehicle's test inertia weight was 5039 lb, and its gross static weight was 5039 lb. The height to the lower edge of the vehicle bumper was 11.0 inches, and height to the upper edge of the bumper was 26.5 inches. The height to the center of gravity of the vehicle was 28.38 inches. Tables D.1 and D.2 in Appendix D.1 give additional dimensions and information on the vehicle. The vehicle was directed into the installation using the cable reverse tow and guidance system, and was released to be freewheeling and unrestrained just prior to impact.



Figure 7.1. TxDOT Low-Speed Short Radius Guardrail Treatment/Test Vehicle Geometrics for Test No. 469137-3-1.



Figure 7.2. Test Vehicle before Test No. 469137-3-1.

7.4 TEST DESCRIPTION

The test vehicle, traveling at an impact speed of 44.8 mi/h, contacted the TxDOT low-speed short radius guardrail treatment with the centerline of the vehicle aligned with the centerline of post 11 at an impact angle of 25.5°. Table 7.1 lists times and significant events that occurred during Test No. 469137-3-1. Figures D.1 and D.2 in Appendix D.2 present sequential photographs during the test.

After loss of contact with the barrier, the vehicle came to rest 260 ft downstream of the impact.

7.5 DAMAGE TO TEST INSTALLATION

Figures 7.3 through 7.6 show the damage to the TxDOT low-speed short radius guardrail treatment. The soil around post 1 was slightly disturbed. Post 5 was displaced 0.75 inch through the soil toward the field side. Post 6 was displaced 8.5 inches through the soil toward the field side. Posts 7, 9, and 13 fractured at ground level but remained attached to the rail element. Posts 8, 10, 11, 12, and 14 fractured at ground level and separated from the rail element. Post 15 was displaced through the soil 5.5 inches toward the field side and 6.0 inches toward the parapet. Post 16 was displaced 1.0 inch through the soil toward the field side. Maximum dynamic deflection during the test was 24.2 ft, and maximum permanent deformation was 20.5 ft.

7.6 DAMAGE TO TEST VEHICLE

Figure 7.7 shows the damage the vehicle sustained. The front bumper, grill, headlights, right and left front fenders, radiator support, and right front door were damaged. Maximum exterior crush to the vehicle was 6.0 inches in the front plane at the both front corners at bumper height. No occupant compartment deformation or intrusion occurred. Figure 7.8 shows the interior of the vehicle. Tables D.3 and D.4 in Appendix D.1 provides exterior crush and occupant compartment measurements.

Table 7.1. Events during Test No. 469137-3-1.

Time (s)	Event
0.005	Thrie-beam impacts drum at posts #10-11
0.015	Thrie-beam contacts drum #2 between posts #10-11
0.022	Anchor cable at post #10 loses tension
0.027	Thrie-beam contacts drum #3
0.030	Post #11 fully fractured
0.033	Anchor cable at post #12 loses tension
0.047	Post #10 begins to fracture
0.069	Thrie-beam contacts drum #1
0.080	Vehicle begins to redirect
0.105	Post #12 begins to fracture
0.137	Thrie-beam contacts drum #4
0.137	Right front wheel lifts off of soil
0.145	Vehicle begins to pitch upward
0.147	Post #12 fully fractured
0.196	Post #9 begins to fracture
0.217	Post #13 begins to fracture
0.224	Thrie-beam forms kink and begins to fold about post #8
0.224	Thrie-beam forms kink and begins to fold about post #14
0.227	Thrie-beam contacts drum #5
0.235	Post #9 fully fractured
0.271	Post #12 fully fractured
0.400	Vehicle begins to pitch downward into hole
0.426	Thrie-beam forms kink and begins to fold about post #15
0.433	Post #8 detaches from thrie-beam and fractures below grade
0.440	Thrie-beam contacts drum #6
0.440	Post #8 (already fractured below grade) begins to pull out of soil
0.450	Thrie-beam forms kink and begins to fold about post #15
0.676	Post #15 begins to rotate, lean, and displace through soil
0.716	Thrie-beam forms kink and begins to fold about post #16
0.821	Thrie-beam begins to slide up post #15
1.200	Vehicle loses contact with installation; exit speed/angle not obtainable

7.7 OCCUPANT RISK FACTORS

Data from the accelerometer, located at the vehicle center of gravity, were digitized for evaluation of occupant risk and are shown in Table 7.2. Figure 7.9 summarizes these data and other pertinent information from the test. Figure D.3 in Appendix D.3 shows the vehicle angular displacements, and Figures D.4 through D.9 in Appendix D.4 show accelerations versus time traces.



Figure 7.3. TxDOT Low-Speed Short Radius Guardrail Treatment after Test No. 469137-3-1.



Figure 7.4. Damage to Rail Section Perpendicular to Roadway after Test No. 469137-3-1.



Figure 7.5. Damage to Nose after Test No. 469137-3-1.



Figure 7.6. Damage to Rail Section Parallel to Roadway after Test No. 469137-3-1.



Figure 7.7. Test Vehicle after Test No. 469137-3-1.



Before Test



After Test

Figure 7.8. Interior of Test Vehicle for Test No. 469137-3-1.

Table 7.2. Occupant Risk Factors for Test No. 469137-3-1.

Occupant Risk Factor	Value	Time
OIV		
Longitudinal	**23.6 ft/s**	at 0.1459 s on front of interior
Lateral	**2.3 ft/s**	
Occupant Ridedown Accelerations		
Longitudinal	**4.2 g**	0.1938–0.2038 s
Lateral	**4.1 g**	0.1670–0.1770 s
Theoretical Head Impact Velocity (THIV)	**26.4 km/h** **7.3 m/s**	at 0.1462 s on front of interior
Post Head Deceleration (PHD)	**4.3 g**	0.1937–0.2037 s
Acceleration Severity Index (ASI)	**0.70**	0.0366–0.0866 s
Maximum 50-ms Moving Average		
Longitudinal	**−8.0 g**	0.0157–0.0657 s
Lateral	**−2.5 g**	0.1422–0.1922 s
Vertical	**2.7 g**	0.2467–0.2967 s
Maximum Roll, Pitch, and Yaw Angles		
Roll	**7.7°**	0.6998 s
Pitch	**21.3°**	0.9231 s
Yaw	**23.1°**	0.6729 s

7.8 ASSESSMENT OF TEST RESULTS

An assessment of the test based on the applicable safety evaluation criteria for *MASH* Test 2-33 is provided in Table 7.3.



0.000 s



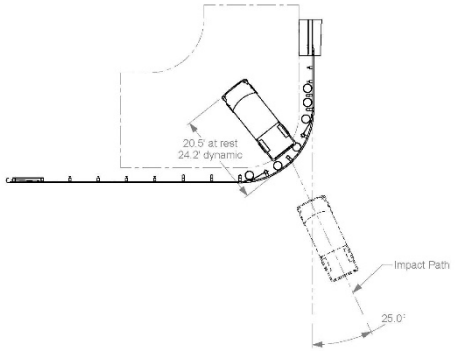
0.200 s

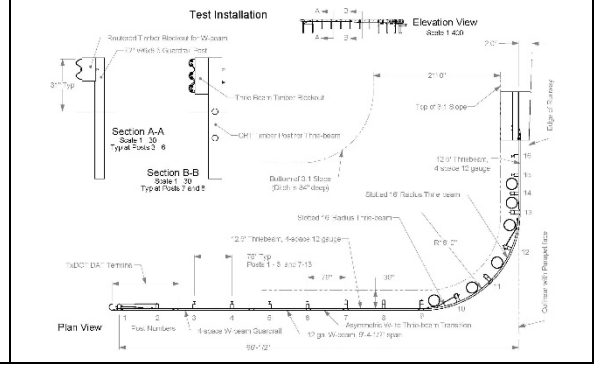


0.400 s



1.000 s





General Information
- Test Agency ..... Texas A&M Transportation Institute (TTI)
- Test Standard Test No. ..... MASH Test 2-33
- TTI Test No. 469137-3-1
- Test Date 2017-08-18

Test Article
- Type ..... Short Radius Guardrail Treatment
- Name ..... TxDOT Low-Speed Short Radius
- Installation Length ..... 66 ft-½ inch
- Material or Key Elements ... 31-inch tall, 87-ft long, thrie-beam short radius guardrail system with curved 25-ft arc length thrie-beam section rolled to a 16-ft inside radius
- **Soil Type and Condition** ..... AASHTO M147-65(2004), grading B Soil (crushed limestone), Damp

Test Vehicle
- Type/Designation 2270P
- Make and Model ..... 2011 Dodge RAM 1500
- Curb ..... 5157 lb
- Test Inertial ..... 5039 lb
- Dummy ..... No dummy
- Gross Static ..... 5039 lb

Impact Conditions
- Speed ..... 44.8 mi/h
- Angle ..... 25.5°
- Location/Orientation ..... Centerline post 11

Kinetic Energy ..... 338 kip-ft

Exit Conditions
- Speed ..... Not obtainable
- Angle ..... Not obtainable

Occupant Risk Values
- Longitudinal OIV ..... 23.6 ft/s
- Lateral OIV ..... 2.3 ft/s
- Longitudinal Ridedown ..... 4.2 g
- Lateral Ridedown ..... 4.1 g
- THIV ..... 26.4 km/h
- PHD ..... 4.3 g
- ASI 0.70

Max. 0.050-s Average
- Longitudinal ..... –8.0 g
- Lateral ..... –2.5 g
- Vertical ..... –.7 g

Post-Impact Trajectory
- Stopping Distance ..... 25 ft downstream

Vehicle Stability
- Maximum Yaw Angle ..... 23°
- Maximum Pitch Angle ..... 21°
- Maximum Roll Angle ..... 8°

Test Article Deflections
- Dynamic ..... 24.2 ft
- Permanent ..... 20.5 ft

Vehicle Damage
- VDS 12FD3
- CDC 12FDEW3
- Max. Exterior Deformation ..... 6.0 inches
- OCDI FS0000000
- Max. Occupant Compartment Deformation ..... None

Figure 7.9. Summary of Results for *MASH* Test 2-33 on the TxDOT Low-Speed Short Radius Guardrail Treatment.

Table 7.3. Performance Evaluation Summary for *MASH* Test 2-33 on the TxDOT Low-Speed Short Radius Guardrail Treatment.

Test Agency: Texas A&M Transportation Institute Test No.: 469137-3-1 Test Date: 2017-08-18

***MASH* Test 2-33 Evaluation Criteria**	**Test Results**	**Assessment**
Structural Adequacy		
A. Test article should contain and redirect the vehicle or bring the vehicle to a controlled stop; the vehicle should not penetrate, underride, or override the installation although controlled lateral deflection of the test article is acceptable	The TxDOT low-speed short radius guardrail treatment contained the 2270P vehicle. The vehicle did not penetrate, underride, or override the installation. Maximum dynamic deflection during the test was 24.2 ft.	Pass
Occupant Risk		
D. Detached elements, fragments, or other debris from the test article should not penetrate or show potential for penetrating the occupant compartment, or present an undue hazard to other traffic, pedestrians, or personnel in a work zone.	Posts 8, 10, 11, 12, and 14 fractured at ground level and separated from the rail element. However, these detached elements did not penetrate or show potential for penetrating the occupant compartment, or present hazard to others in the area.	Pass
Deformations of, or intrusions into, the occupant compartment should not exceed limits set forth in Section 5.3 and Appendix E of MASH.	No occupant compartment deformation or intrusion occurred.	
F. The vehicle should remain upright during and after collision. The maximum roll and pitch angles are not to exceed 75 degrees.	The 2270P vehicle remained upright during and after the collision event. The maximum roll and pitch angles were 8° and 21°, respectively	Pass
H. Occupant impact velocities (OIV) should satisfy the following limits: Preferred value of 30 ft/s, or maximum allowable value of 40 ft/s.	Longitudinal OIV was 23.6 ft/s, and lateral OIV was 2.3 ft/s.	Pass
I. The occupant ridedown accelerations should satisfy the following limits: Preferred value of 15.0 g, or maximum allowable value of 20.49 g.	Maximum longitudinal occupant ridedown acceleration was 4.2 g, and maximum lateral occupant ridedown acceleration was 4.1 g.	Pass

CHAPTER 8:
MASH TEST 2-32 (CRASH TEST NO. 469137-3-2)

8.1 TEST DESIGNATION AND ACTUAL IMPACT CONDITIONS

MASH Test 2-32 involves an 1100C vehicle weighing 2420 lb ±55 lb impacting the nose of the short radius guardrail at an impact speed of 44 mi/h ±2.5 mi/h and an angle of 5–15° ±1.5°. TTI researchers determined the most critical impact angle to be 25° measured from the face of the parapet. The target impact point for *MASH* Test 2-32 on the short radius guardrail treatment was face of the rail at the center post (post 11) of the nose of the radius ±1 ft.

The 2011 Kia Rio used in the test weighed 2456 lb, and the actual impact speed and angle were 45.3 mi/h and 25.5°, respectively. The actual impact point was face of the rail at the center post (post 11) of the nose of the radius. Minimum target KE was 141 kip-ft, and actual KE was 168 kip-ft.

8.2 WEATHER CONDITIONS

The test was performed on the morning of September 5, 2017. Weather conditions at the time of testing were as follows: wind speed: 5 mi/h; wind direction: 250° (vehicle was traveling in a northwesterly direction); temperature: 82°F; relative humidity: 83 percent.

8.3 TEST VEHICLE

The 2011 Kia Rio, shown in Figures 8.1 and 8.2, was used for the crash test. The vehicle's test inertia weight was 2456 lb, and its gross static weight was 2621 lb. The height to the lower edge of the vehicle bumper was 7.75 inches, and height to the upper edge of the bumper was 21.00 inches. Table E.1 in Appendix E.1 gives additional dimensions and information on the vehicle. The vehicle was directed into the installation using the cable reverse tow and guidance system, and was released to be freewheeling and unrestrained just prior to impact.



Figure 8.1. TxDOT Low-Speed Short Radius Guardrail Treatment/Test Vehicle Geometrics for Test No. 469137-3-2.

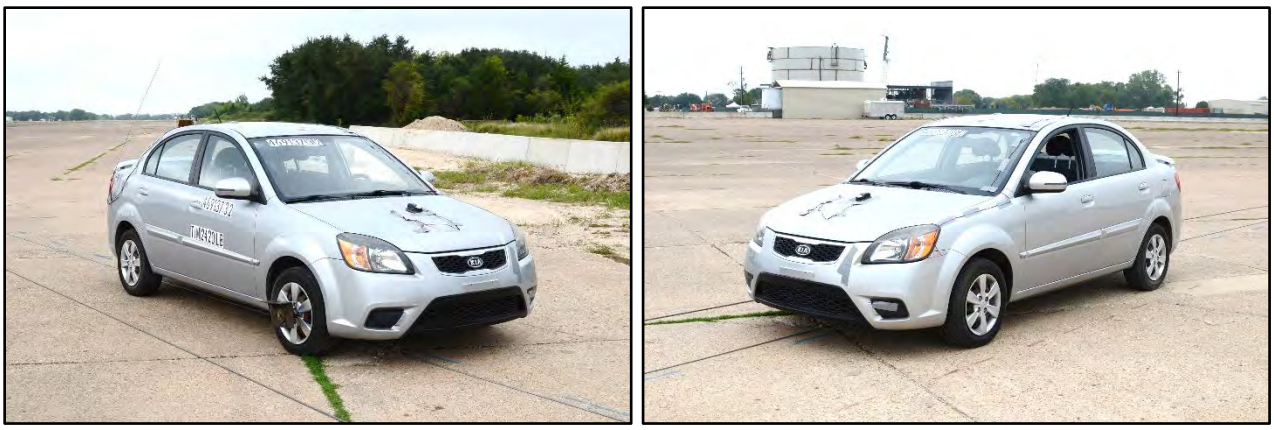


Figure 8.2. Test Vehicle before Test No. 469137-3-2.

8.4 TEST DESCRIPTION

The test vehicle, traveling at an impact speed of 45.3 mi/h, contacted the TxDOT low-speed short radius guardrail treatment at the face of the rail at the center post (post 11) of the nose of the radius at an impact angle of 25.5°. Table 8.1 lists times and significant events that occurred during Test No. 469137-3-2. Figures E.1 and E.2 in Appendix E.2 present sequential photographs during the test.

Table 8.1. Events during Test No. 469137-3-2.

TIME (s)	EVENT
0.007	Post #11 begins to deflect to field side
0.011	Thrie-Beam impacts drum at Posts #10-11
0.012	Post #10 begins to deflect to field side
0.012	Post #12 begins to deflect to traffic side
0.019	Thrie-beam contacts drum #2 between posts #10-11
0.020	Anchor cable at post #10 loses tension
0.023	Thrie-beam displaces away from drums 5 and 6
0.026	Thrie-beam contacts drum #3
0.029	Vehicle begins to redirect
0.032	Anchor cable at post #12 loses tension
0.035	Post #11 begins to fracture
0.044	Post #12 begins to rebound toward field side
0.045	Post #11 fully fractured
0.049	Post #10 foundation tube begins to deflect through soil to field
0.059	Post #9 begins to deflect to field side
0.075	Thrie-beam and cable bracket contact drum #1
0.078	Post #9 foundation tube begins to deflect through soil to field
0.081	Thrie-beam contacts drum #1 between Posts #9-10
0.094	Post #12 begins to fracture

Table 8.1. Events during Test No. 469137-3-2 (Continued).

TIME (s)	EVENT
0.106	Post #10 begins to fracture
0.116	Post #13 begins to deflect to field side
0.117	Vehicle begins to pitch upward as front wheels cross foundation tubes
0.141	Thrie-beam and anchor bracket contact drum #4
0.146	Post #10 fully fractured
0.150	Thrie-beam contacts drum #4
0.157	Post #12 fully fractured
0.170	Thrie-beam forms kink and begins to fold about Post #9
0.172	Post #14 begins to deflect to field side
0.190	Thrie-beam forms kink and begins to fold about Post #13
0.357	Vehicle begins to drop into ditch
0.377	Post #13 begins to fracture
0.502	Vehicle came to rest at 44.8°

After loss of contact with the barrier, the vehicle came to rest 8.3 ft downstream of the point of impact.

8.5 DAMAGE TO TEST INSTALLATION

Figures 8.3 through 8.6 show the damage to the TxDOT low-speed short radius guardrail treatment. No disturbance of the soil around posts 1 through 6 was noted. Post 7 was displaced through the soil 1.0 inch toward field side. Post 8 was displaced through the soil 2.38 inches toward the field side and was leaning 85° toward the field side. Post 9 was displaced through the soil 9.25 inches toward the field side and was leaning 80° toward the field side. The ground tube for post 10 was displaced through the soil 3.75 inches, and the post fractured at the top of the ground tube. The ground tube for post 11 was displaced through the soil 0.25 inches, and the post fractured at the top of the ground tube. The ground tube for post 12 was displaced through the soil 0.38 inches, and the post fractured at the top of the ground tube. The ground tube for post 13 was displaced through the soil 0.12 inches, and the post fractured at the top of the ground tube. The soil was disturbed around post 14, and the rail element separated from the blockout. No disturbance of the soil around posts 15 and 16 was noted. Drums 1–4 were resting in the ditch, and drum 5 was pushed toward the field side 3.0 inches. Working width was 2.5 ft, and height of working width was below grade (vehicle in ditch). Maximum dynamic deflection during the test was 10.5 ft, and maximum permanent deformation was 10.5 ft.



Figure 8.3. TxDOT Low-Speed Short Radius Guardrail Treatment and Test Vehicle after Test No. 469137-3-2.



Figure 8.4. Test Article after Test No. 469137-3-2.



Figure 8.5. Field Side of Test Article after Test No. 469137-3-2.



Figure 8.6. Damage to Cables after Test No. 469137-3-2.

8.6 VEHICLE DAMAGE

Figure 8.7 shows the damage sustained by the vehicle. The front bumper, hood, grill, radiator, radiator support, headlights, and right and left front fenders were damaged. Maximum exterior crush to the vehicle was 5.0 inches in the front plane at the left corner at bumper height. No occupant compartment deformation or intrusion occurred. Figure 8.8 shows the interior of the vehicle. Tables E.2 and E.3 in Appendix E.1 provide exterior crush and occupant compartment measurements.



Figure 8.7. Test Vehicle after Test No. 469137-3-2.



Figure 8.8. Interior of Test Vehicle for Test No. 469137-3-2.

8.7 OCCUPANT RISK FACTORS

Data from the accelerometer, located at the vehicle center of gravity, were digitized for evaluation of occupant risk and are shown in Table 8.2. Figure 8.9 summarizes these data and other pertinent information from the test. Figure E.3 in Appendix E.3 shows the vehicle angular displacements, and Figures E.4 through E.9 in Appendix E.4 show accelerations versus time traces.

Table 8.2. Occupant Risk Factors for Test No. 469137-3-2.

Occupant Risk Factor	Value	Time
OIV		
Longitudinal	**33.1 ft/s**	at 0.1079 s on front of interior
Lateral	**3.0 ft/s**	
Occupant Ridedown Accelerations		
Longitudinal	**5.1 g**	0.1105–0.1205 s
Lateral	**3.2 g**	0.1096–0.1196 s
THIV	**37.5 km/h** **10.4 m/s**	at 0.1082 s on front of interior
PHD	**6.0 g**	0.1100–0.1200 s
ASI	**1.19**	0.0429–0.0929 s
Maximum 50-ms Moving Average		
Longitudinal	**−13.4 g**	0.0191–0.0691 s
Lateral	**−3.0 g**	0.0660–0.1160 s
Vertical	**−3.0 g**	0.0396–0.0896 s
Maximum Roll, Pitch, and Yaw Angles		
Roll	**4.2**	0.2052 s
Pitch	**7.7**	0.5928 s
Yaw	**22.2**	0.9998 s

8.8 ASSESSMENT OF TEST RESULTS

An assessment of the test based on the applicable safety evaluation criteria for *MASH* Test 2-32 is provided in Table 8.3.



0.000 s



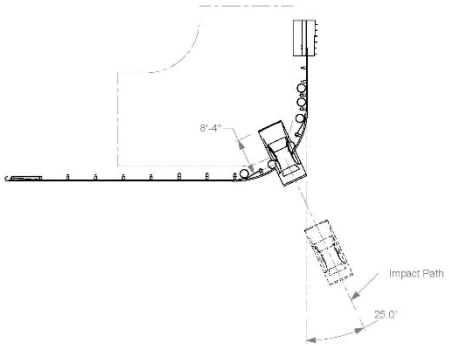
0.200 s

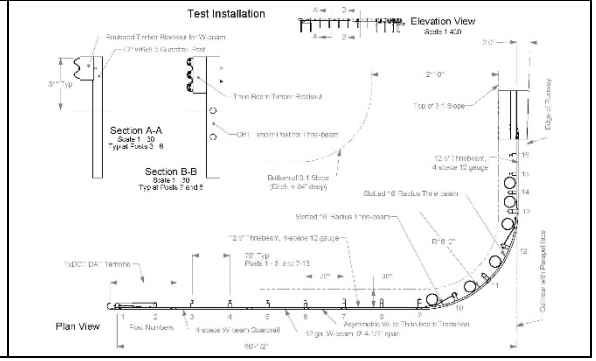


0.400 s



0.600 s





General Information
- Test Agency ..... Texas A&M Transportation Institute (TTI)
- Test Standard Test No. ..... MASH Test 2-32
- TTI Test No. 469137-3-2
- Test Date 2017-09-05

Test Article
- Type ..... Short Radius Guardrail Treatment
- Name ..... TxDOT Low-Speed Short Radius
- Installation Length ..... 66 ft-½ inch
- Material or Key Elements ... 31-inch tall, 87-ft long, thrie-beam short radius guardrail system with curved 25-ft arc length thrie-beam section rolled to a 16-ft inside radius
- **Soil Type and Condition** ..... AASHTO M147-65(2004), grading B Soil (crushed limestone), Damp

Test Vehicle
- Type/Designation 1100C
- Make and Model ..... 2011 Kia Rio
- Curb ..... 2495 lb
- Test Inertial ..... 2456 lb
- Dummy ..... 165 lb
- Gross Static ..... 2621 lb

Impact Conditions
- Speed ..... 45.3 mi/h
- Angle ..... 25.5°
- Location/Orientation ..... Centerline post 11

Kinetic Energy ..... 168 kip-ft

Exit Conditions
- Speed ..... Stopped
- Angle ..... 44.8°

Occupant Risk Values
- Longitudinal OIV ..... 33.1 ft/s
- Lateral OIV ..... 3.0 ft/s
- Longitudinal Ridedown ..... 5.1 g
- Lateral Ridedown ..... 3.2 g
- THIV ..... 37.5 km/h
- PHD ..... 6.0 g
- ASI 1.19

Max. 0.050-s Average
- Longitudinal ..... −13.4 g
- Lateral ..... −3.0 g
- Vertical ..... −3.0 g

Post-Impact Trajectory
- Stopping Distance ..... 8.3 ft

Vehicle Stability
- Maximum Yaw Angle ..... 22°
- Maximum Pitch Angle ..... 8°
- Maximum Roll Angle ..... 4°

Test Article Deflections
- Dynamic ..... 10.5 ft
- Permanent ..... 10.5 ft
- Working Width ..... 2.5 ft
- Height of Working Width ..... Vehicle in ditch

Vehicle Damage
- VDS 12FD4
- CDC 12FDEW3
- Max. Exterior Deformation ..... 5.0 inches
- OCDI FS0000000
- Max. Occupant Compartment Deformation ..... None

Figure 8.9. Summary of Results for *MASH* Test 2-32 on TxDOT Low-Speed Short Radius Guardrail Treatment.

Table 8.3. Performance Evaluation Summary for *MASH* Test 2-32 on the TxDOT Low-Speed Short Radius Guardrail Treatment.

Test Agency: Texas A&M Transportation Institute Test No.: 469137-3-2 Test Date: 2017-09-05

***MASH* Test 2-32 Evaluation Criteria**	**Test Results**	**Assessment**
Structural Adequacy		
A. Test article should contain and redirect the vehicle or bring the vehicle to a controlled stop; the vehicle should not penetrate, underride, or override the installation although controlled lateral deflection of the test article is acceptable	The TxDOT low-speed short radius guardrail treatment contained the 1100C vehicle. The vehicle did not penetrate, underride, or override the installation. Maximum dynamic deflection during the test was 10.5 ft.	Pass
Occupant Risk		
D. Detached elements, fragments, or other debris from the test article should not penetrate or show potential for penetrating the occupant compartment, or present an undue hazard to other traffic, pedestrians, or personnel in a work zone.	Posts 10 through 13 fractured at ground. These fractured posts remained near the installation and did not penetrate or show potential for penetrating the occupant compartment, or present hazard to others in the area.	Pass
Deformations of, or intrusions into, the occupant compartment should not exceed limits set forth in Section 5.3 and Appendix E of MASH.	No occupant compartment deformation or intrusion occurred.	
F. The vehicle should remain upright during and after collision. The maximum roll and pitch angles are not to exceed 75 degrees.	The 1100C vehicle remained upright during and after the collision event. The maximum roll and pitch angles were 4° and 8°, respectively	Pass
H. Occupant impact velocities (OIV) should satisfy the following limits: Preferred value of 30 ft/s, or maximum allowable value of 40 ft/s.	Longitudinal OIV was 33.1 ft/s, and lateral OIV was 3.0 ft/s.	Pass
I. The occupant ridedown accelerations should satisfy the following limits: Preferred value of 15.0 g, or maximum allowable value of 20.49 g.	Maximum longitudinal occupant ridedown acceleration was 10.1 g, and maximum lateral occupant ridedown acceleration was 0.9 g.	Pass

CHAPTER 9:
MASH TEST 2-31 (CRASH TEST NO. 469138-3-3)

9.1 TEST DESIGNATION AND ACTUAL IMPACT CONDITIONS

MASH Test 2-31 involves a 2270P vehicle weighing 5000 lb ±110 lb impacting the nose of the short radius guardrail at an impact speed of 44 mi/h ±2.5 mi/h and an angle of 0° ±1.5°. The target impact point for *MASH* Test 2-31 on the short radius guardrail was centerline of the truck aligned with the traffic face of the parapet ±1 ft.

The 2012 Dodge RAM 1500 pickup truck used in the test weighed 5034 lb, and the actual impact speed and angle were 44.0 mi/h and 0.2°, respectively. The actual impact point was centerline of the vehicle with the traffic face of the parapet. Minimum target KE was 291 kip-ft, and actual KE was 326 kip-ft.

9.2 WEATHER CONDITIONS

The test was performed on the morning of September 15, 2017. Weather conditions at the time of testing were as follows: wind speed: 12 mi/h; wind direction: 171° (vehicle was traveling in a northwesterly direction); temperature: 83°F; relative humidity: 72 percent.

9.3 TEST VEHICLE

The 2012 Dodge RAM 1500 pickup truck, shown in Figures 9.1 and 9.2, was used for the crash test. The vehicle's test inertia weight was 5034 lb, and its gross static weight was 5034 lb. The height to the lower edge of the vehicle bumper was 11.0 inches, and height to the upper edge of the bumper was 26.5 inches. The height to the center of gravity of the vehicle was 28.25 inches. Tables F.1 and F.2 in Appendix F.1 give additional dimensions and information on the vehicle. The vehicle was directed into the installation using the cable reverse tow and guidance system, and was released to be freewheeling and unrestrained just prior to impact.



Figure 9.1. TxDOT Low-Speed Short Radius Guardrail Treatment/Test Vehicle Geometrics for Test No. 469138-3-3.



Figure 9.2. Test Vehicle before Test No. 469138-3-3.

9.4 TEST DESCRIPTION

The test vehicle, traveling at an impact speed of 44.0 mi/h, contacted the nose of the TxDOT low-speed short radius guardrail treatment centerline of the vehicle with the traffic face of the parapet at an impact angle of 0.2°. Table 9.1 lists times and significant events that occurred during Test No. 469138-3-3. Figures F.1 and F.2 in Appendix F.2 present sequential photographs during the test.

Table 9.1. Events during Test No. 469138-3-3.

TIME (s)	EVENT
0.012	Thrie-beam begins to displace to field at drum #3
0.015	Post #12 begins to deflect to field side
0.016	Post #11 begins to deflect to traffic side
0.017	Post #14 begins to deflect to traffic side
0.019	Post #10 begins to deflect to traffic side
0.020	Thrie-beam contacts drum #3
0.021	Post #10 and thrie-beam begin to displace to traffic side
0.029	Post #9 begins to deflect to traffic side
0.056	Anchor cable at post #12 loses tension
0.060	Vehicle begins to redirect
0.059	Thrie-beam forms kink and begins to fold upstream of post #11
0.064	Left front wheel leaves pavement
0.078	Thrie-beam contacts drum #4
0.092	Thrie-beam forms kink and begins to fold upstream of post #13
0.121	Thrie-beam contacts drum #5
0.136	Thrie-beam forms kink and begins to fold about post #14
0.566	Vehicle exited installation while traveling at 31.1 mi/h and 23.6°

After loss of contact with the barrier, the vehicle came to rest 123 ft downstream of the impact and 15 ft toward traffic lanes.

9.5 DAMAGE TO TEST INSTALLATION

Figures 9.3 through 9.6 show the damage to the TxDOT low-speed short radius guardrail treatment. The soil around posts 1 through 10 showed no signs of movement. Post 11 was displaced through the soil 0.62 inch toward the field side and leaning 86° toward the field side. Posts 12 and 13 fractured at the top of the foundation tube. Post 12 separated from the rail element and came to rest in the ditch. Post 13 separated from the rail but remained attached to the rail element. Post 14 was displaced through the soil 0.12 inch toward the field side. The soil around posts 15 and 16 showed no signs of movement. Working width was 1.5 ft, and the height of maximum working width was 2.5 ft. Maximum dynamic deflection during the test was 3.8 ft, and maximum permanent deformation was 2.9 ft.



Figure 9.3. TxDOT Low-Speed Short Radius Guardrail Treatment after Test No. 469138-3-3.



Figure 9.4. Damage to Rail Section Perpendicular to Roadway after Test No. 469138-3-3.



Figure 9.5. Damage to Rail Section Parallel to Roadway after Test No. 469138-3-3.



Figure 9.6. Damage to Cable and Post 12 after Test No. 469138-3-3.

9.6 DAMAGE TO TEST VEHICLE

Figure 9.7 shows the damage the vehicle sustained. The front bumper, grill, left front fender, left tire and rim, left rear rim, left rear exterior bed, and left rear bumper were damaged. Maximum exterior crush to the vehicle was 9.0 inches in the front plane at the left front corner at

bumper height. No occupant compartment deformation or intrusion occurred. Figure 9.8 shows the interior of the vehicle. Tables F.3 and F.4 in Appendix F.1 provide exterior crush and occupant compartment measurements.



Figure 9.7. Test Vehicle after Test No. 469138-3-3.



Before Test After Test

Figure 9.8. Interior of Test Vehicle for Test No. 469138-3-3.

9.7 OCCUPANT RISK FACTORS

Data from the accelerometer, located at the vehicle center of gravity, were digitized for evaluation of occupant risk and are shown in Table 9.2. Figure 9.9 summarizes these data and other pertinent information from the test. Figure F.3 in Appendix F.3 shows the vehicle angular displacements, and Figures F.4 through F.9 in Appendix F.4 show accelerations versus time traces.

Table 9.2. Occupant Risk Factors for Test No. 469138-3-3.

Occupant Risk Factor	Value	Time
OIV		
Longitudinal	**13.1 ft/s**	at 0.1625 s on left side of interior
Lateral	**11.5 ft/s**	
Occupant Ridedown Accelerations		
Longitudinal	**2.1 g**	0.4041–0.4141 s
Lateral	**3.1 g**	0.4661–0.4761 s
THIV	**18.4 km/h** **5.1 m/s**	at 0.1551 s on left side of interior
PHD	**3.2 g**	0.3972–0.4072 s
ASI	**0.50**	0.0440–0.0940 s
Maximum 50-ms Moving Average		
Longitudinal	**−3.8 g**	0.0171–0.0671 s
Lateral	**3.6 g**	0.0248–0.0748 s
Vertical	**−2.5 g**	0.6601–0.7101 s
Maximum Roll, Pitch, and Yaw Angles		
Roll	**11.5°**	0.3371 s
Pitch	**6.0°**	1.4146 s
Yaw	**26.7°**	0.4846 s

9.8 ASSESSMENT OF TEST RESULTS

An assessment of the test based on the applicable safety evaluation criteria for *MASH* Test 2-31 is provided in Table 8.3.



0.000 s



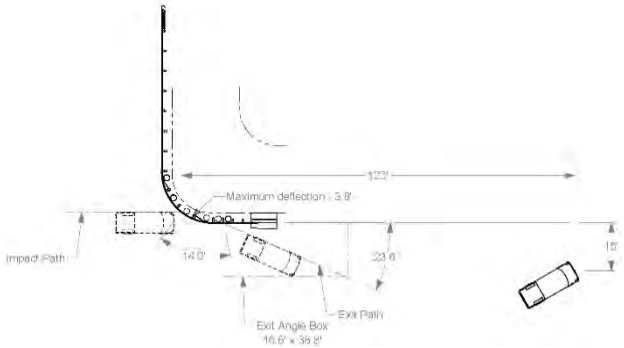
0.200 s

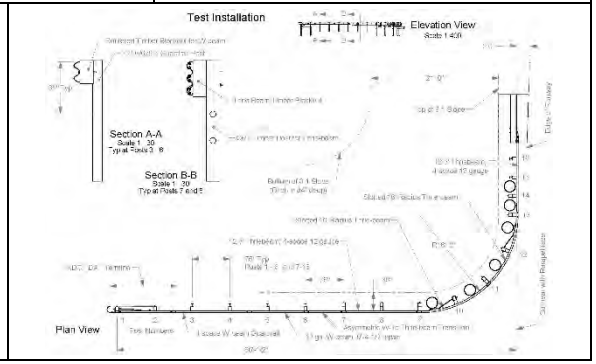


0.400 s



0.600 s





General Information
- Test Agency..... Texas A&M Transportation Institute (TTI)
- Test Standard Test No..... MASH Test 2-31
- TTI Test No. 469138-3-3
- Test Date 2017-09-15

Test Article
- Type ..... Short Radius Guardrail Treatment
- Name..... TxDOT Low-Speed Short Radius
- Installation Length..... 66 ft-½ inch
- Material or Key Elements ... 31-inch tall, 87-ft long, thrie-beam short radius guardrail system with curved 25-ft arc length thrie-beam section rolled to a 16-ft inside radius
- **Soil Type and Condition** ..... AASHTO M147-65(2004), grading B Soil (crushed limestone), Damp

Test Vehicle
- Type/Designation..... 2270P
- Make and Model ..... 2012 Dodge RAM 1500
- Curb..... 5114 lb
- Test Inertial..... 5034 lb
- Dummy ..... No dummy
- Gross Static ..... 5034 lb

Impact Conditions
- Speed ..... 44.0 mi/h
- Angle ..... 0.2°
- Location/Orientation ..... Centerline of vehicle w/traffic face parapet
- **Kinetic Energy**..... 326 kip-ft

Exit Conditions
- Speed ..... 31.1 mi/h
- Angle ..... 23.6°

Occupant Risk Values
- Longitudinal OIV ..... 13.1 ft/s
- Lateral OIV..... 11.5 ft/s
- Longitudinal Ridedown..... 2.1 g
- Lateral Ridedown ..... 3.1 g
- THIV ..... 18.4 km/h
- PHD..... 3.2 g
- ASI..... 0.50

Max. 0.050-s Average
- Longitudinal ..... −3.8 g
- Lateral..... 3.9 g
- Vertical..... −2.5 g

Post-Impact Trajectory
- Stopping Distance..... 123 ft downstream 15 ft twd traffic

Vehicle Stability
- Maximum Yaw Angle ..... 27°
- Maximum Pitch Angle ..... 6°
- Maximum Roll Angle..... 12°

Test Article Deflections
- Dynamic..... 3.8 ft
- Permanent..... 2.9 ft
- Working Width..... 1.5 ft
- Height of Working Width ..... 2.5 ft

Vehicle Damage
- VDS..... 11LFQ3
- CDC..... 11FLEW3
- Max. Exterior Deformation..... 9.0 inches
- OCDI..... FL0000000
- Max. Occupant Compartment Deformation ..... None

Figure 9.9. Summary of Results for *MASH* Test 2-31 on the TxDOT Low-Speed Short Radius Guardrail Treatment.

Table 9.3. Performance Evaluation Summary for *MASH* Test 2-31 on the TxDOT Low-Speed Short Radius Guardrail Treatment.

Test Agency: Texas A&M Transportation Institute Test No.: 469138-3-3 Test Date: 2017-09-15

***MASH* Test 2-31 Evaluation Criteria**	**Test Results**	**Assessment**
Structural Adequacy		
A. Test article should contain and redirect the vehicle or bring the vehicle to a controlled stop; the vehicle should not penetrate, underride, or override the installation although controlled lateral deflection of the test article is acceptable	The TxDOT low-speed short radius guardrail treatment contained the 2270P vehicle. The vehicle did not penetrate, underride, or override the installation. Maximum dynamic deflection during the test was 3.8 ft.	Pass
Occupant Risk		
D. Detached elements, fragments, or other debris from the test article should not penetrate or show potential for penetrating the occupant compartment, or present an undue hazard to other traffic, pedestrians, or personnel in a work zone.	Posts 13 and 14 fractured at ground level and separated from the rail element. However, these detached elements did not penetrate or show potential for penetrating the occupant compartment, or present hazard to others in the area.	Pass
Deformations of, or intrusions into, the occupant compartment should not exceed limits set forth in Section 5.3 and Appendix E of MASH.	No occupant compartment deformation or intrusion occurred.	
F. The vehicle should remain upright during and after collision. The maximum roll and pitch angles are not to exceed 75 degrees.	The 2270P vehicle remained upright during and after the collision event. The maximum roll and pitch angles were 12° and 6°, respectively.	Pass
H. Occupant impact velocities (OIV) should satisfy the following limits: Preferred value of 30 ft/s, or maximum allowable value of 40 ft/s.	Longitudinal OIV was 13.1 ft/s, and lateral OIV was 11.5 ft/s.	Pass
I. The occupant ridedown accelerations should satisfy the following limits: Preferred value of 15.0 g, or maximum allowable value of 20.49 g.	Maximum longitudinal occupant ridedown acceleration was 2.1 g, and maximum lateral occupant ridedown acceleration was 3.1 g.	Pass

CHAPTER 10:
MASH TEST 2-35 (CRASH TEST NO. 469138-3-4)

10.1 TEST DESIGNATION AND ACTUAL IMPACT CONDITIONS

MASH Test 2-35 involves a 2270P vehicle weighing 5000 lb ±110 lb impacting the beginning of the length of need of the short radius guardrail at an impact speed of 44 mi/h ±2.5 mi/h and an angle of 0° ±1.5°. The target impact point for *MASH* Test 2-31 the left front corner of the bumper impacting the point on the rail where the downstream end of the cable bracket is attached to the rail south of post 13 ±1 ft.

The 2012 Dodge RAM 1500 pickup truck used in the test weighed 5022 lb, and the actual impact speed and angle were 45.9 mi/h and 24.9°, respectively. The actual impact point was 29 inches upstream of post 13. Minimum target IS was 52 kip-ft, and actual IS was 63 kip-ft.

10.2 WEATHER CONDITIONS

The test was performed on the morning of September 28, 2017. Weather conditions at the time of testing were as follows: wind speed: 4 mi/h; wind direction: 26° (vehicle was traveling in a northwesterly direction); temperature: 83°F; relative humidity: 80 percent.

10.3 TEST VEHICLE

The 2012 Dodge RAM 1500 pickup truck, shown in Figures 10.1 and 10.2, was used for the crash test. The vehicle's test inertia weight was 5022 lb, and its gross static weight was 5022 lb. The height to the lower edge of the vehicle bumper was 11.25 inches, and height to the upper edge of the bumper was 26.5 inches. The height to the center of gravity of the vehicle was 28.62 inches. Tables G.1 and G.2 in Appendix G.1 give additional dimensions and information on the vehicle. The vehicle was directed into the installation using the cable reverse tow and guidance system, and was released to be freewheeling and unrestrained just prior to impact.



Figure 10.1. TxDOT Low-Speed Short Radius Guardrail Treatment/Test Vehicle Geometrics for Test No. 469138-3-4.



Figure 10.2. Test Vehicle before Test No. 469138-3-4.

10.4 TEST DESCRIPTION

The test vehicle, traveling at an impact speed of 45.9 mi/h, contacted the TxDOT low-speed short radius guardrail treatment 29 inches upstream of post 13 at an impact angle of 24.9°. Table 10.1 lists times and significant events that occurred during Test No. 469138-3-3. Figures G.1 and G.2 in Appendix G.2 present sequential photographs during the test.

Table 10.1. Events during Test No. 469138-3-4.

TIME (s)	EVENT
0.013	Post #13 and #14 begin to deflect to field side
0.016	Post #12 begins to deflect to field side
0.026	Thrie-beam contacts drum #5
0.033	Thrie-beam contacts drum #4
0.044	Thrie-beam forms kink and begins to fold upstream of post #15
0.045	Vehicle begins to redirect
0.086	Post #15 begins to deflect to field side and rotate
0.103	Thrie-beam impacts drum #3
0.106	Thrie-beam forms kink and begins to fold at post #16
0.163	Sand drums #4, 5, and 6 begin to accelerate away from guardrail to ditch
0.165	Post #16 begins to deflect to field side
0.187	Thrie-beam and terminal connector begin to form kinks
0.216	Vehicle front bumper at upstream end of parapet
0.280	Vehicle traveling parallel with parapet
0.313	Rear bumper impacts guardrail at the anchor bracket at Post #13
0.382	Post #12 fractures at grade and deflect to traffic side
0.453	Max Deflection of rail at post #14 (rear bumper backslap)
0.857	Vehicle loses contact with installation while traveling at an exit speed and angle of 26.4 mi/h and 6.5°, respectively

After loss of contact with the barrier, the vehicle came to rest 116 ft downstream of the impact and 5 ft toward traffic lanes.

10.5 DAMAGE TO TEST INSTALLATION

Figures 10.3 through 10.6 show the damage to the TxDOT low-speed short radius guardrail treatment. The soil around posts 1 through 9 showed no signs of movement, and the soil around post 10 was disturbed. Post 11 fractured at the top of the foundation tube and leaning 83° toward the field side, but remained in place, and the tube was displaced through the soil 0.12 inch toward the field side. Posts 12 fractured at the top of the foundation tube, separated from the rail element, and resting toward the field side adjacent to the tube; the tube was displaced 0.5 inch toward the field side. Posts 13 fractured at the top of the foundation tube, remained attached to the rail element, and was resting 21.5 inches toward the field side. Post 14 fractured at the top of the foundation tube, separated from the rail element, and was resting 36 inches toward the field side. Post 15 was leaning 38° toward the parapet and 69° toward the field side. Post 16 was leaning 67° toward the parapet and 88° toward the field side and displaced through the soil 0.38 inch toward the field side. Working width was greater than 20 ft, and the height of maximum working width was 3.5 ft. Maximum dynamic deflection during the test was 2.6 ft, and maximum permanent deformation was 1.8 ft.



Figure 10.3. TxDOT Low-Speed Short Radius Guardrail Treatment after Test No. 469138-3-4.



Figure 10.4. Damage to Rail Section Parallel to Roadway after Test No. 469138-3-4.

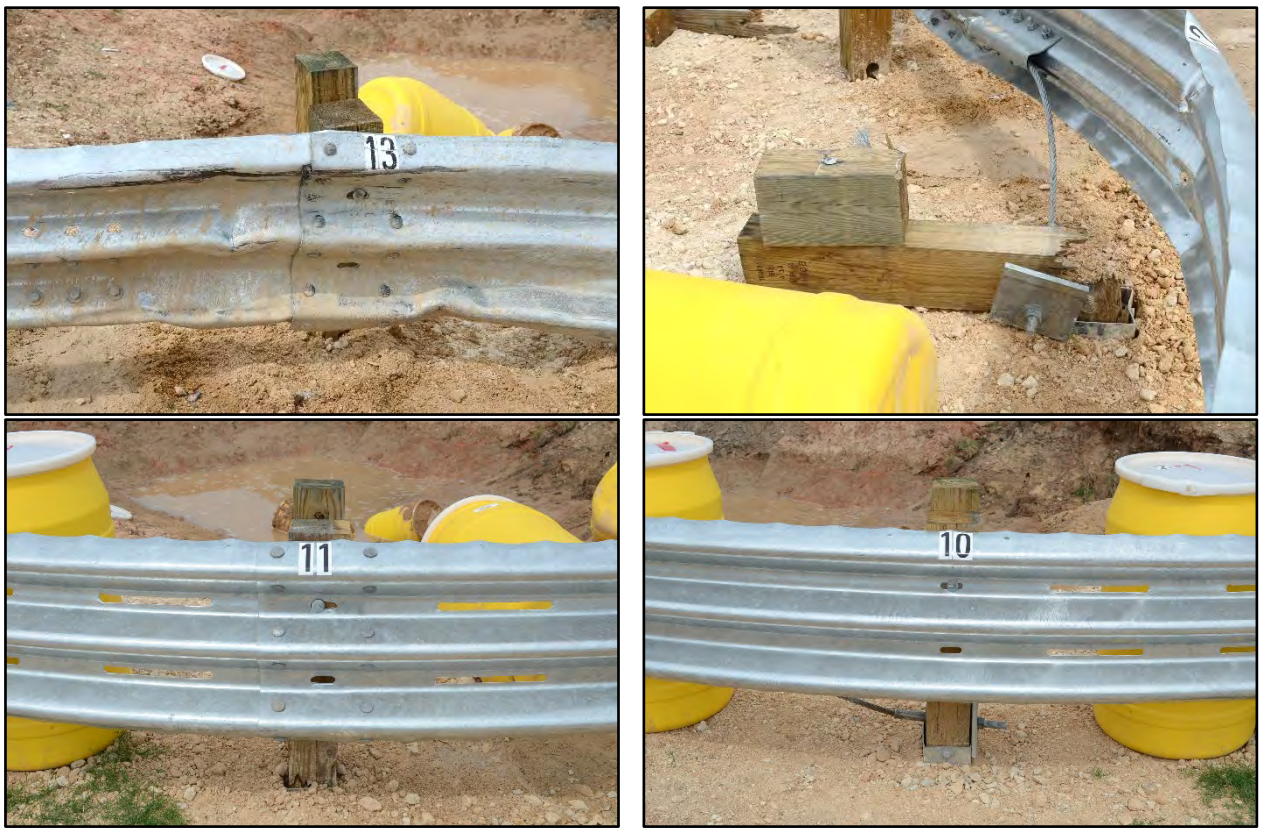


Figure 10.5. Damage to Post 13 through 10 after Test No. 469138-3-4.

10.6 DAMAGE TO TEST VEHICLE

Figure 10.6 shows the damage the vehicle sustained. The front bumper, grill, radiator support, left front fender, and left tire and rim were damaged. Maximum exterior crush to the vehicle was 10.0 inches in the front plane at the left front corner at bumper height. No occupant compartment deformation or intrusion occurred. Figure 10.7 shows the interior of the vehicle. Tables G.3 and G.4 in Appendix G.1 provide exterior crush and occupant compartment measurements.

10.7 OCCUPANT RISK FACTORS

Data from the accelerometer, located at the vehicle center of gravity, were digitized for evaluation of occupant risk and are shown in Table 10.2. Figure 10.8 summarizes these data and other pertinent information from the test. Figure G.3 in Appendix G.3 shows the vehicle angular displacements, and Figures G.4 through G.9 in Appendix G.4 show accelerations versus time traces.



Figure 10.6. Test Vehicle after Test No. 469138-3-4.



Before Test After Test

Figure 10.7. Interior of Test Vehicle for Test No. 469138-3-4.

Table 10.2. Occupant Risk Factors for Test No. 469138-3-4.

Occupant Risk Factor	Value	Time
OIV		
Longitudinal	**16.7 ft/s**	at 0.1507 s on left side of interior
Lateral	**14.1 ft/s**	
Occupant Ridedown Accelerations		
Longitudinal	**11.3 g**	0.5555–0.5655 s
Lateral	**3.4 g**	1.1461–1.1561 s
THIV	**23.6 km/h** **6.6 m/s**	at 0.1432 s on left side of interior
PHD	**11.3 g**	0.5556–0.5656 s
ASI	**0.60**	0.0711–0.1211 s
Maximum 50-ms Moving Average		
Longitudinal	**−5.0 g**	0.0798–0.1298 s
Lateral	**4.3 g**	0.0362–0.0862 s
Vertical	**−3.3 g**	1.1327–1.1827 s
Maximum Roll, Pitch, and Yaw Angles		
Roll	**32.0°**	0.8939 s
Pitch	**11.8°**	0.4417 s
Yaw	**55.2°**	1.2161 s

10.8 ASSESSMENT OF TEST RESULTS

An assessment of the test based on the applicable safety evaluation criteria for *MASH* Test 2-35 is provided in Table 10.3.



0.000 s



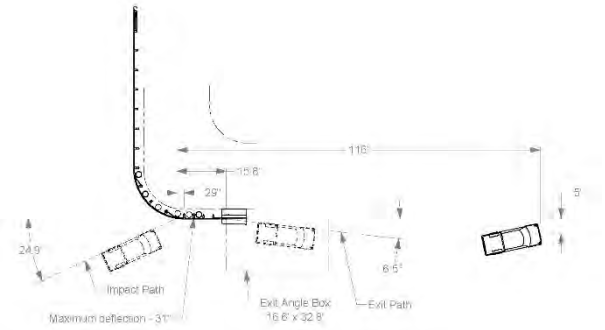
0.250 s

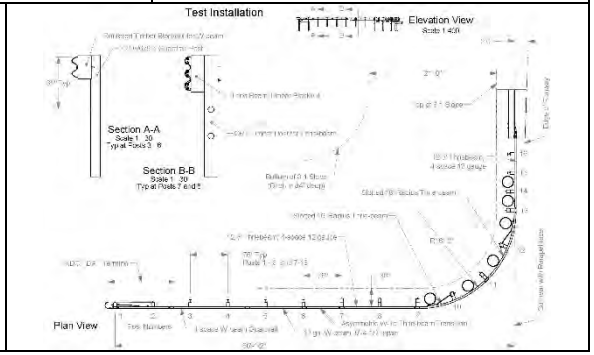


0.500 s



0.875 s





General Information
- Test Agency ..... Texas A&M Transportation Institute (TTI)
- Test Standard Test No. ..... MASH Test 2-35
- TTI Test No. 469138-3-4
- Test Date 2017-09-28

Test Article
- Type ..... Short Radius Guardrail Treatment
- Name ..... TxDOT Low-Speed Short Radius
- Installation Length ..... 66 ft-½ inch
- Material or Key Elements ... 31-inch tall, 87 ft long, thrie-beam short radius guardrail system with curved 25-ft arc length thrie-beam section rolled to a 16-ft inside radius
- **Soil Type and Condition** ..... AASHTO M147-65(2004), grading B Soil (crushed limestone), Damp

Test Vehicle
- Type/Designation 2270P
- Make and Model ..... 2012 Dodge RAM 1500 Pickup
- Curb ..... 4899 lb
- Test Inertial ..... 5022 lb
- Dummy ..... No dummy
- Gross Static ..... 5022 lb

Impact Conditions
- Speed ..... 45.9 mi/h
- Angle ..... 24.9°
- Location/Orientation ..... 29 inches upstream of post 13
- **Impact Severity** ..... 63 kip-ft

Exit Conditions
- Speed ..... 26.4 mi/h
- Angle ..... 6.4°

Occupant Risk Values
- Longitudinal OIV ..... 16.7 ft/s
- Lateral OIV ..... 14.1 ft/s
- Longitudinal Ridedown ..... 11.3 g
- Lateral Ridedown ..... 3.4 g
- THIV ..... 23.6 km/h
- PHD ..... 11.3 g
- ASI 0.60

Max. 0.050-s Average
- Longitudinal ..... −5.0 g
- Lateral ..... 4.3 g
- Vertical ..... −3.3 g

Post-Impact Trajectory
- Stopping Distance ..... 116 ft downstream 5 ft twd traffic

Vehicle Stability
- Maximum Yaw Angle ..... 55°
- Maximum Pitch Angle ..... 12°
- Maximum Roll Angle ..... 32°

Test Article Deflections
- Dynamic ..... 2.6 ft
- Permanent ..... 1.8 ft
- Working Width ..... >20 ft
- Height of Working Width ..... 3.5 ft

Vehicle Damage
- VDS 11LF3
- CDC 11FLEW3
- Max. Exterior Deformation ..... 10.0 inches
- OCDI FL0000000
- Max. Occupant Compartment Deformation ..... None

Figure 10.8. Summary of Results for *MASH* Test 2-35 on the TxDOT Low-Speed Short Radius Guardrail Treatment.

Table 10.3. Performance Evaluation Summary for *MASH* Test 2-35 on the TxDOT Low-Speed Short Radius Guardrail Treatment.

Test Agency: Texas A&M Transportation Institute Test No.: 469138-3-4 Test Date: 2017-09-28

***MASH* Test 2-35 Evaluation Criteria**	**Test Results**	**Assessment**
Structural Adequacy		
A. Test article should contain and redirect the vehicle or bring the vehicle to a controlled stop; the vehicle should not penetrate, underride, or override the installation although controlled lateral deflection of the test article is acceptable	The TxDOT low-speed short radius guardrail treatment contained the 2270P vehicle. The vehicle did not penetrate, underride, or override the installation. Maximum dynamic deflection during the test was 2.6 ft.	Pass
Occupant Risk		
D. Detached elements, fragments, or other debris from the test article should not penetrate or show potential for penetrating the occupant compartment, or present an undue hazard to other traffic, pedestrians, or personnel in a work zone.	Several posts fractured at ground level and separated from the rail element. However, these detached elements did not penetrate or show potential for penetrating the occupant compartment, or present hazard to others in the area.	Pass
Deformations of, or intrusions into, the occupant compartment should not exceed limits set forth in Section 5.3 and Appendix E of MASH.	No occupant compartment deformation or intrusion occurred.	
F. The vehicle should remain upright during and after collision. The maximum roll and pitch angles are not to exceed 75 degrees.	The 2270P vehicle remained upright during and after the collision event. The maximum roll and pitch angles were 12° and 32°, respectively.	Pass
H. Occupant impact velocities (OIV) should satisfy the following limits: Preferred value of 30 ft/s, or maximum allowable value of 40 ft/s.	Longitudinal OIV was 16.7 ft/s, and lateral OIV was 14.1 ft/s.	Pass
I. The occupant ridedown accelerations should satisfy the following limits: Preferred value of 15.0 g, or maximum allowable value of 20.49 g.	Maximum longitudinal occupant ridedown acceleration was 11.3 g, and maximum lateral occupant ridedown acceleration was 3.4 g.	Pass

CHAPTER 11:
MODIFIED *MASH* TEST 2-34 (CRASH TEST NO. 469138-3-5)

11.1 TEST DESIGNATION AND ACTUAL IMPACT CONDITIONS

MASH Test 2-34 involves an 1100C vehicle weighing 2420 lb ±55 lb impacting the CIP of the short radius guardrail at an impact speed of 44 mi/h ±2.5 mi/h and an angle of 15° ±1.5°. However, the impact angle was increased to 25° for this test. The CIP for *MASH* Test 2-34 on the guardrail was 6.3 inches ±1 ft downstream of post 12.

The 2009 Kia Rio used in the test weighed 2444 lb, and the actual impact speed and angle were 44.6 mi/h and 24.8°, respectively. The actual impact point was 6.5 inches downstream of post 12. Minimum target impact severity was 9 kip-ft, and actual IS was 29 kip-ft.

11.2 WEATHER CONDITIONS

The test was performed on the morning of December 14, 2017. Weather conditions at the time of testing were as follows: wind speed: 4 mi/h; wind direction: 309° (vehicle was traveling in a northwesterly direction); temperature: 58°F; relative humidity: 58 percent.

11.3 TEST VEHICLE

The 2009 Kia Rio, shown in Figures 11.1 and 11.2, was used for the crash test. The vehicle's test inertia weight was 2444 lb, and its gross static weight was 2609 lb. The height to the lower edge of the vehicle bumper was 7.75 inches, and height to the upper edge of the bumper was 21.0 inches. Table H.1 in Appendix H1 gives additional dimensions and information on the vehicle. The vehicle was directed into the installation using the cable reverse tow and guidance system, and was released to be freewheeling and unrestrained just prior to impact.



Figure 11.1. TxDOT Low-Speed Short Radius Guardrail /Test Vehicle Geometrics for Test No. 469138-3-5.



Figure 11.2. Test Vehicle before Test No. 469138-3-5.

11.4 TEST DESCRIPTION

The test vehicle, traveling at an impact speed of 44.6 mi/h, contacted the TxDOT low-speed short radius guardrail treatment 6.5 inches downstream of post 12 at an impact angle of 24.8°. Table 11.1 lists times and significant events that occurred during Test No. 469138-3-5. Figure H.1 in Appendix H2 presents sequential photographs during the test.

Table 11.1. Events during Test No. 469138-3-5.

TIME (s)	EVENTS
0.0070	Rail element begins to deflect toward field side
0.0090	Post #12 begins to deflect toward field side
0.0160	Post #11 begins to deflect toward field side
0.0240	Post #13 begins to deflect toward field side/Rear of rail contacts drum #3
0.0280	Post #14 begins to deflect toward field side
0.0310	Rear of rail contacts drum #4
0.0350	Rear of rail contacts drum #5
0.0380	Left front bumper contacts drum #4
0.0400	Vehicle begins to redirect
0.0410	Drum #3 and #4 begin to deflect toward slope
0.0740	Kink in rail begins to form just upstream of post #14
0.0770	Center front bumper contacts post #13
0.0850	Post 13 contacts drum #5/drum #5 begins to deflect toward slope
0.1680	Center front bumper contacts post #14
0.2150	Drum #6 begins to deflect toward slope
0.3200	Vehicle begins to yaw counterclockwise
0.3670	Left front corner of bumper contacts post #15

For longitudinal barriers, it is desirable that the vehicle redirects and exits the barrier within the exit box criteria (not less than 32.8 ft downstream from impact for cars and pickups).

The 1100C vehicle exited within the exit box criteria defined in *MASH*. The vehicle came to rest 20 ft downstream of the impact adjacent to the traffic face of the rail at post 15.

11.5 DAMAGE TO TEST INSTALLATION

Figure 11.3 shows the damage to the TxDOT low-speed short radius guardrail treatment. The soil around post 10 was disturbed, and post 11 was fractured near ground level and leaning 84° toward the field side. Posts 12–14 fractured at ground level and separated from the rail element. Posts 15 and 16 were pushed toward the field side 0.25 inch and 0.12 inch, respectively. Drums 1 and 2 were undisturbed, and drums 3 and 6 were overturned. Drums 4 and 5 were resting at the bottom of the slope. Working width was 5.8 ft at a height of 3.2 ft. Maximum dynamic deflection during the test was 5.0 ft, and maximum permanent deformation was 3.7 ft.



Figure 11.3. TxDOT Low-Speed Short Radius Guardrail/Test Vehicle after Test No. 469138-3-5.



Figure 11.4. TxDOT Low-Speed Short Radius Guardrail after Test No. 469138-3-5.



Figure 11.5. Rear of Installation after Test No. 469138-3-5.

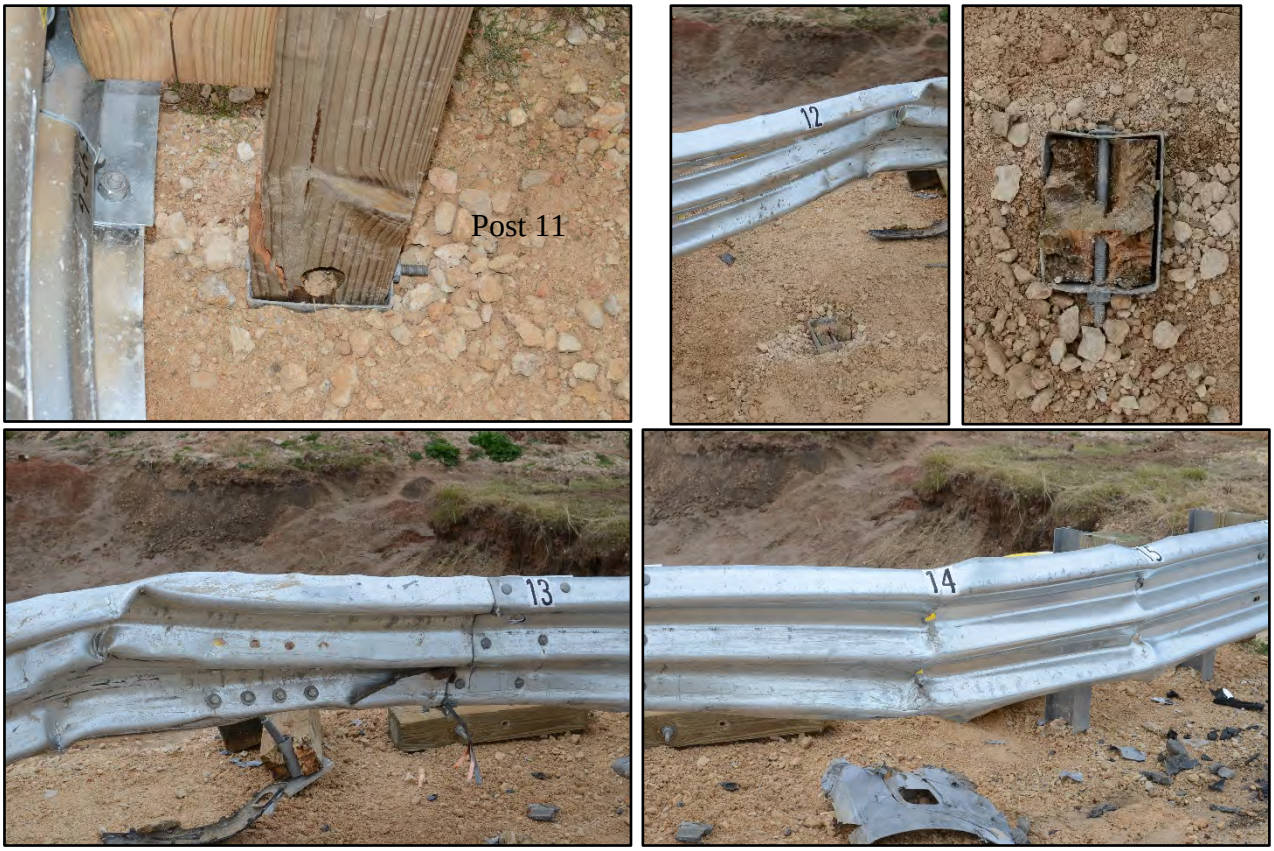


Figure 11.6. Posts 11 through 14 after Test No. 469138-3-5.

11.6 VEHICLE DAMAGE

Figure 11.4 shows the damage sustained by the vehicle. The front bumper, grill, radiator and support, hood, left and right front fender, left front tire and rim, and left front subframe were damaged. Maximum exterior crush to the vehicle was 26.0 inches in the front plane at the left front corner at bumper height. No occupant compartment deformation or intrusion was noted.

Figure 11.5 shows the interior of the vehicle. Tables H.2 and H.3 in Appendix H1 provide exterior crush and occupant compartment measurements.



Figure 11.7. Test Vehicle after Test No. 469138-3-5.



Figure 11.8. Interior of Test Vehicle for Test No. 469138-3-5.

11.7 OCCUPANT RISK FACTORS

Data from the accelerometer, located at the vehicle center of gravity, were digitized for evaluation of occupant risk and are shown in Table 11.2. Figure 11.6 summarizes these data and other pertinent information from the test. Figure H.2 in Appendix H3 shows the vehicle angular displacements, and Figures H.3 through H.8 in Appendix H4 show accelerations versus time traces.

11.8 ASSESSMENT OF TEST RESULTS

An assessment of the test based on the applicable safety evaluation criteria for *MASH* Test 2-34 is provided in Table 11.3.

Table 11.2. Occupant Risk Factors for Test No. 469138-3-5.

Occupant Risk Factor	Value	Time
OIV		
Longitudinal	**31.8 ft/s**	at 0.1340 s on front of interior
Lateral	**12.5 ft/s**	
Occupant Ridedown Accelerations		
Longitudinal	**10.0 g**	0.1978–0.2078 s
Lateral	**3.4 g**	0.1959–0.2059 s
THIV	**35.8 km/h** **9.9 m/s**	at 0.1283 s on left side of interior
PHD	**10.3 g**	0.1977–0.2077 s
ASI	**0.97**	0.0610–0.1110 s
Maximum 50-ms Moving Average		
Longitudinal	**−9.6 g**	0.0340–0.0840 s
Lateral	**4.9 g**	0.0246–0.0746 s
Vertical	**7.0 g**	0.2952–0.3452 s
Maximum Roll, Pitch, and Yaw Angles		
Roll	**5.2**	0.9089 s
Pitch	**7.9**	0.6494 s
Yaw	**16.6**	0.3684 s



0.000 s



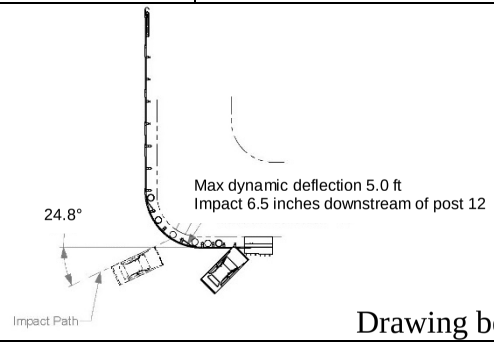
0.200 s



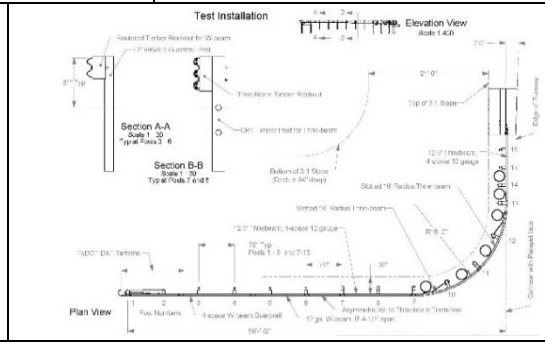
0.400 s



0.800 s



Drawing being corrected



General Information
- Test Agency ..... Texas A&M Transportation Institute (TTI)
- Test Standard Test No. ..... Modified MASH Test 2-34
- TTI Test No. 469138-3-5
- Test Date 2017-12-14

Test Article
- Type ..... Short Radius Guardrail Treatment
- Name ..... TxDOT Low-Speed Short Radius
- Installation Length ..... 66 ft-½ inch
- Material or Key Elements ... 31-inch tall, 87 ft long, thrie-beam short radius guardrail system with curved 25-ft arc length thrie-beam section rolled to a 16-ft inside radius
- **Soil Type and Condition** ..... AASHTO M147-65(2004), grading B Soil (crushed limestone), Damp

Test Vehicle
- Type/Designation 1100C
- Make and Model ..... 2009 Kia Rio
- Curb ..... 2483 lb
- Test Inertial ..... 2444 lb
- Dummy ..... 165 lb
- Gross Static ..... 2609 lb

Impact Conditions
- Speed ..... 44.6 mi/h
- Angle ..... 24.8°
- Location/Orientation ..... 6.5 inches dwnstrm of post 12

Impact Severity ..... 29 kip-ft

Exit Conditions
- Speed ..... Stopped
- Angle ..... 41.9°

Occupant Risk Values
- Longitudinal OIV ..... 31.8 ft/s
- Lateral OIV ..... 12.5 ft/s
- Longitudinal Ridedown ..... 10.0 g
- Lateral Ridedown ..... 3.4 g
- THIV ..... 35.8 km/h
- PHD ..... 10.3 g
- ASI 0.97

Max. 0.050-s Average
- Longitudinal ..... –9.6 g
- Lateral ..... 4.9 g
- Vertical ..... 7.0 g

Post-Impact Trajectory
- Stopping Distance ..... 20 ft downstream

Vehicle Stability
- Maximum Yaw Angle ..... 17°
- Maximum Pitch Angle ..... 8°
- Maximum Roll Angle ..... 5°
- Vehicle Snagging ..... No
- Vehicle Pocketing ..... No

Test Article Deflections
- Dynamic ..... 5.0 ft
- Permanent ..... 3.7 ft
- Working Width ..... 5.8 ft
- Height of Working Width ..... 3.2 ft

Vehicle Damage
- VDS 11LFQ4
- CDC 11FLEW3
- Max. Exterior Deformation ..... 26.0 inches
- OCDI FL0000000
- Max. Occupant Compartment Deformation ..... None

Figure 11.9. Summary of Results for *MASH* Test 2-34 on the TxDOT Low-Speed Short Radius Guardrail Treatment.

Table 11.3. Performance Evaluation Summary for Modified *MASH* Test 2-34 on the TxDOT Low-Speed Short Radius Guardrail Treatment.

Test Agency: Texas A&M Transportation Institute Test No.: 469138-3-5 Test Date: 2017-12-14

***MASH* Test 2-32 Evaluation Criteria**	**Test Results**	**Assessment**
Structural Adequacy		
A. Test article should contain and redirect the vehicle or bring the vehicle to a controlled stop; the vehicle should not penetrate, underride, or override the installation although controlled lateral deflection of the test article is acceptable	The TxDOT low-speed short radius guardrail treatment contained the 1100C vehicle. The vehicle did not penetrate, underride, or override the installation. Maximum dynamic deflection during the test was 5.0 ft.	Pass
Occupant Risk		
D. Detached elements, fragments, or other debris from the test article should not penetrate or show potential for penetrating the occupant compartment, or present an undue hazard to other traffic, pedestrians, or personnel in a work zone.	Three posts fractured and released from the installation, however did not penetrate or show potential for penetrating the occupant compartment, or to present undue hazard to others in the area.	Pass
Deformations of, or intrusions into, the occupant compartment should not exceed limits set forth in Section 5.3 and Appendix E of MASH.	No occupant compartment deformation or intrusion occurred.	
F. The vehicle should remain upright during and after collision. The maximum roll and pitch angles are not to exceed 75 degrees.	The 1100C vehicle remained upright during and after the collision event. The maximum roll and pitch angles were 5° and 8°, respectively	Pass
H. Occupant impact velocities (OIV) should satisfy the following limits: Preferred value of 30 ft/s, or maximum allowable value of 40 ft/s.	Longitudinal OIV was 31.8 ft/s, and lateral OIV was 12.5 ft/s.	Pass
I. The occupant ridedown accelerations should satisfy the following limits: Preferred value of 15.0 g, or maximum allowable value of 20.49 g.	Maximum longitudinal occupant ridedown acceleration was 10.0 g, and maximum lateral occupant ridedown acceleration was 3.4 g.	Pass

CHAPTER 12:
SUMMARY AND CONCLUSIONS

12.1 SUMMARY OF RESULTS

12.1.1 *MASH* Test 2-33

The TxDOT low-speed short radius guardrail treatment contained the 2270P vehicle. The vehicle did not penetrate, underride, or override the installation. Maximum dynamic deflection during the test was 24.2 ft. Posts 8, 10, 11, 12, and 14 fractured at ground level and separated from the rail element. However, these detached elements did not penetrate or show potential for penetrating the occupant compartment, or present hazard to others in the area. No occupant compartment deformation or intrusion occurred. The 2270P vehicle remained upright during and after the collision event. Occupant risk factors were within the preferred limits of *MASH*.

12.1.2 *MASH* Test 2-32

The TxDOT low-speed short radius guardrail treatment contained the 1100C vehicle. The vehicle did not penetrate, underride, or override the installation. Maximum dynamic deflection during the test was 10.5 ft. Posts 10 through 13 fractured at ground level. These fractured posts remained near the installation and did not penetrate or show potential for penetrating the occupant compartment, or present hazard to others in the area. No occupant compartment deformation or intrusion occurred. The 1100C vehicle remained upright during and after the collision event. Occupant risk factors were within the required limits of *MASH*.

12.1.3 *MASH* Test 2-31

The TxDOT low-speed short radius guardrail treatment contained the 2270P vehicle. The vehicle did not penetrate, underride, or override the installation. Maximum dynamic deflection during the test was 3.8 ft. Posts 13 and 14 fractured at ground level and separated from the rail element. However, these detached elements did not penetrate or show potential for penetrating the occupant compartment, or present hazard to others in the area. No occupant compartment deformation or intrusion occurred. The 2270P vehicle remained upright during and after the collision event. Occupant risk factors were within the preferred limits of *MASH*.

12.1.3 *MASH* Test 2-35

The TxDOT low-speed short radius guardrail treatment contained the 2270P vehicle. The vehicle did not penetrate, underride, or override the installation. Maximum dynamic deflection during the test was 2.6 ft. Several posts fractured at ground level and separated from the rail element. However, these detached elements did not penetrate or show potential for penetrating the occupant compartment, or present hazard to others in the area. No occupant compartment deformation or intrusion occurred. The 2270P vehicle remained upright during and after the collision event. Occupant risk factors were within the preferred limits of *MASH*.

12.1.4 Modified *MASH* Test 2-34

The TxDOT low-speed short radius guardrail treatment contained the 1100C vehicle. The vehicle did not penetrate, underride, or override the installation. Maximum dynamic deflection during the test was 5.0 ft. Three posts fractured and released from the installation, however, did not penetrate or show potential for penetrating the occupant compartment, or to present undue hazard to others in the area. No occupant compartment deformation or intrusion occurred. Occupant risk factors were within the required limits of *MASH*.

12.2 CONCLUSIONS

Table 12.1 shows the TxDOT low-speed short radius guardrail treatment performed acceptably for *MASH* Tests 2-33, 2-32, 2-31, 2-35, and modified 2-34.

Table 12.1. Assessment Summary for *MASH* TL-2 Testing on the TxDOT Low-Speed Short Radius Guardrail Treatment.

Evaluation Factors	Evaluation Criteria	Test No. 469137-3-1	Test No. 469137-3-2	Test No. 469138-3-3	Test No. 469138-3-4	Test No. 469138-3-5
Structural Adequacy	A	S*	S	S	S	S
Occupant Risk	D	S	S	S	S	S
	F	S	S	S	S	S
	H	S	S	S	S	S
	I	S	S	S	S	S
Test No.		***MASH* Test 2-33**	***MASH* Test 2-32**	***MASH* Test 2-31**	***MASH* Test 2-35**	**Modified *MASH* Test 2-34**
Pass/Fail		Pass	Pass	Pass	Pass	Pass

* S = Satisfactory
U = Unsatisfactory

CHAPTER 13:
IMPLEMENTATION STATEMENT[1]

A 31-inch tall short radius system was developed and tested per *MASH* TL-2 modified conditions, by increasing the impact angle to 25° from 15°, and is considered *MASH* complaint per the *MASH* evaluation criteria. This new short radius system requires a thrie-beam guardrail system constructed along the primary roadway that transitioned to a section of bridge parapet. The thrie-beam is curved at the nose section and then is attached to a w-beam rail via an asymmetric thrie to w-beam connector. The w-beam rail is attached with a TxDOT GF (31) DAT-14 terminal at the secondary roadway end. The curved 25-ft arc length thrie-beam section was rolled to a 16-ft inside radius, and it has 11-inch long slots on the nose section of the curved thrie-rail. Six sand drums were strategically placed on the inboard, field side of the installation between posts 9 and 15 as illustrated in the test installation drawings. The impact performance of the short radius guardrail system with a 3H:1V slope was evaluated using modified *MASH* Tests 2-33, 2-32 2-31, 2-35, and 2-34 that were conducted successfully.

This system can be implemented in the field provided that a minimum of 3-ft of flat ground is made available behind it to accommodate the placement of the six 700-lb drums filled with sand positioned per the supplied drawings. A slope of 3H:1V or flatter can be placed after the 3-ft flat area to accommodate ditches in the field side. The successfully tested installation provides for the minimum length of the system. However, a longer primary roadway rail can be implemented provided that it starts past post 16 with the proper crash worthy transition section toward its end. Similarly, a longer secondary roadway can be implemented provided that it starts beyond post 5 away from the nose section and terminated with a crashworthy terminal. This implementation applies only to *MASH* TL-2 roadways.

[1] The opinions/interpretations identified/expressed in this section are outside the scope of TTI Proving Ground's A2LA Accreditation.

REFERENCES

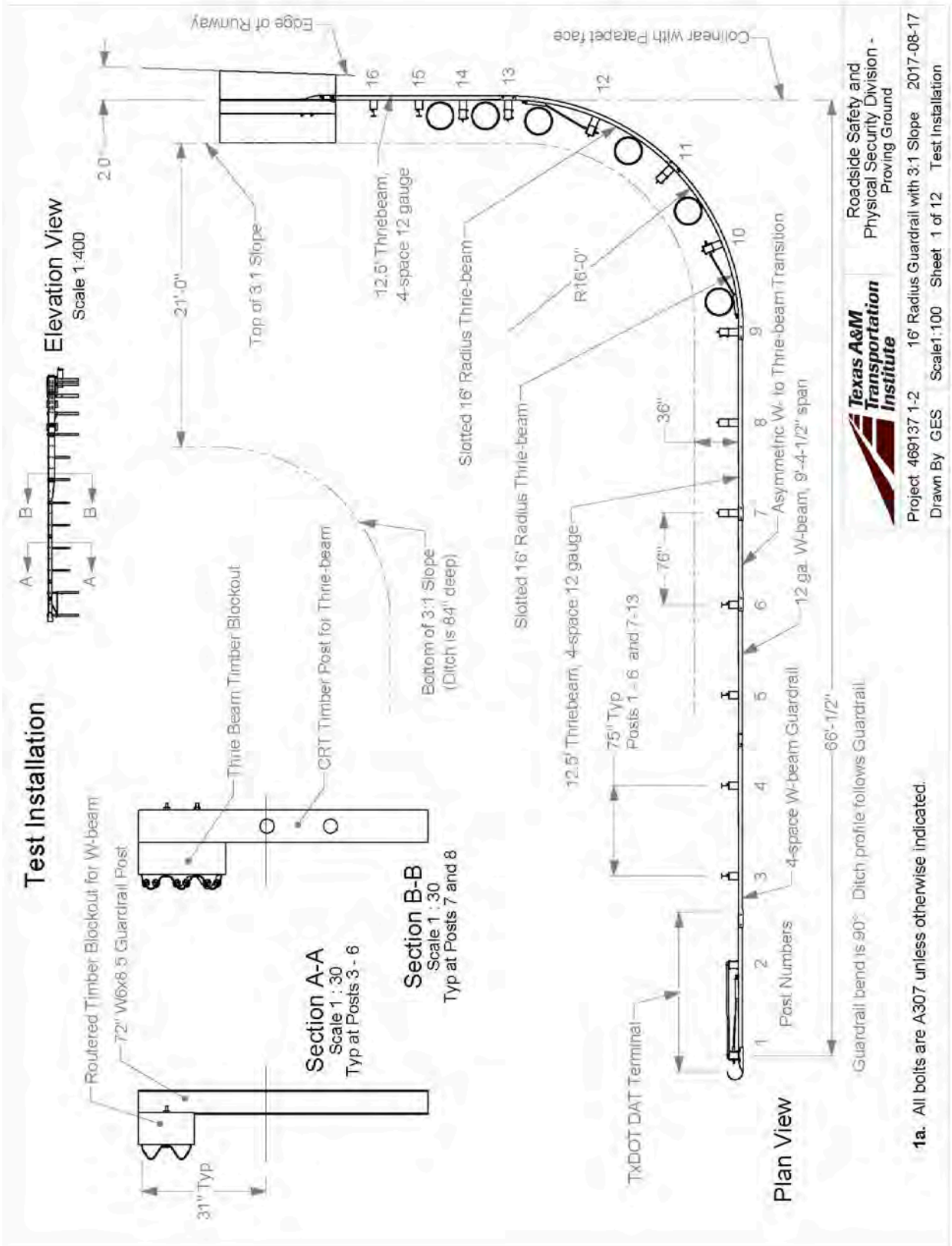
1. AASHTO. *Manual for Assessing Roadside Safety Hardware.* Second Edition, 2016, American Association of State Highway and Transportation Officials: Washington, D.C.

2. LS-DYNA KEYWORD USER'S MANUAL, LIVERMORE SOFTWARE TECHNOLOGY CORPORATION (LSTC), Livermore, California, August 2016.

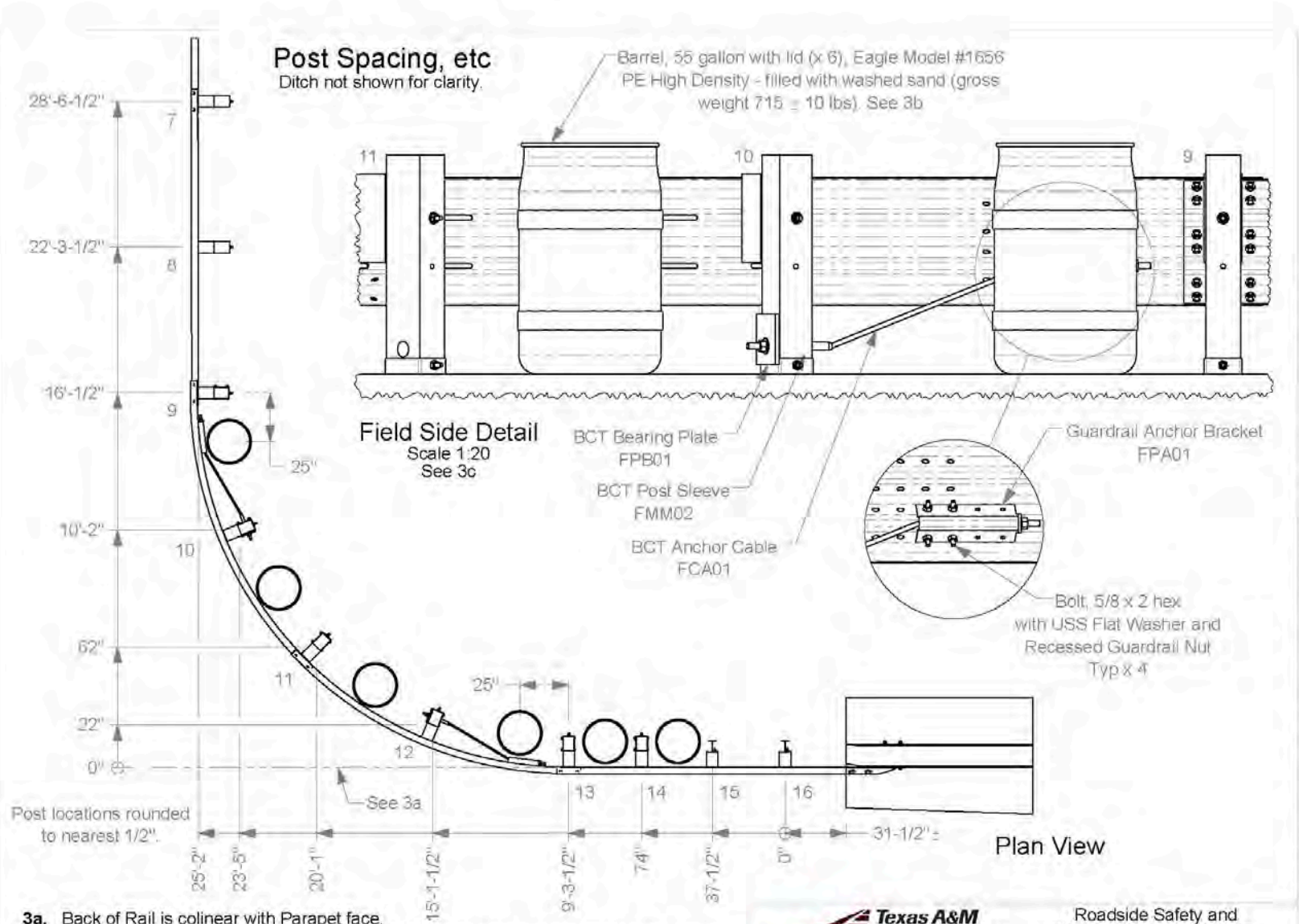
3. Akram Y. Abu-Odeh, Katherine McCaskey, Roger P. Bligh, Wanda L. Menges, and Darrell L. Kuhn. *Crash Test and MASH TL-3 Evaluation of the TxDOT Short Radius Guardrail.* Texas A&M Transportation Institute, March 2015.

4. Roger P. Bligh, Dusty R. Arrington, and Wanda L. Menges. *Development of a MASH TL-2 Guardrail-to-Bridge Rail Transition Compatible with 31- Inch Guardrail.* Texas A&M Transportation Institute, December 2011.

APPENDIX A. DETAILS OF THE GUARDRAIL TREATMENT FOR TEST NOS. 469137-3-1 AND 469137-3-2



T:\1-ProjectFiles\469137-TxDOT-TL-2-ShortRadius-Akram\469137-3\469137-3-1\Drafting\469137-1\469137 Drawing



3a. Back of Rail is colinear with Parapet face.

3b. Place Barrels approximately 1" from back of Rail and centered between Posts, unless otherwise shown or indicated (see Barrels betweem Post 9 and 10, and 12 and 13).

3b. Anchor Cable details typical between Posts 9 and 10, and between Posts 12 and 13.

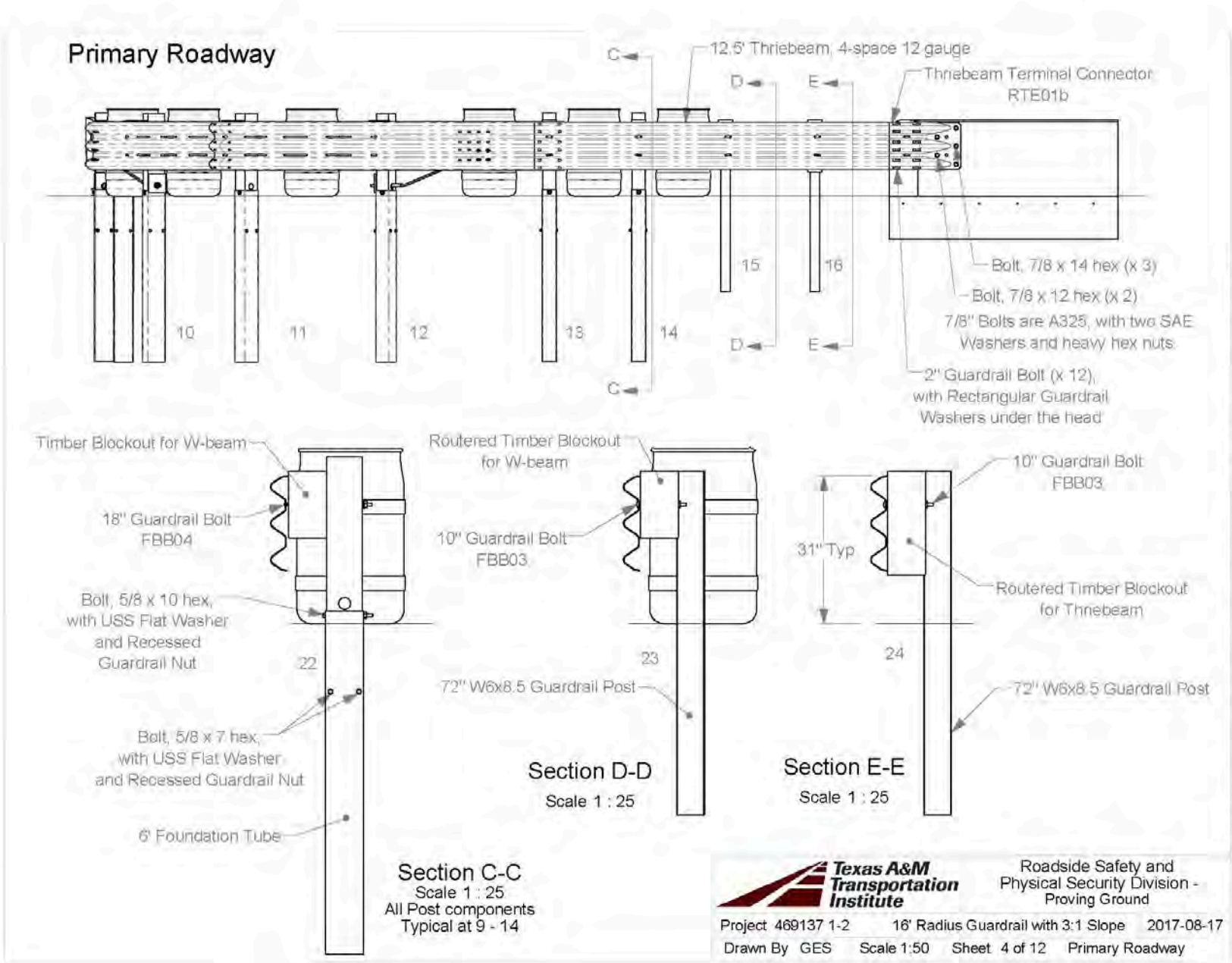
Texas A&M Transportation Institute

Roadside Safety and Physical Security Division - Proving Ground

Project 469137 1-2 16' Radius Guardrail with 3:1 Slope 2017-08-17

Drawn By GES Scale 1:65 Sheet 3 of 12 Post Spacing, etc

T:\1-ProjectFiles\469137-TxDOT-TL-2-ShortRadius-Akram\469137-3\469137-3-1\Drafting, 469137-1\469137 Drawing


Primary Roadway
12.5' Thriebeam, 4-space 12 gauge
Thriebeam Terminal Connector RTE01b
Bolt, 7/8 x 14 hex (x 3)
Bolt, 7/8 x 12 hex (x 2)
7/8" Bolts are A325, with two SAE Washers and heavy hex nuts
2" Guardrail Bolt (x 12), with Rectangular Guardrail Washers under the head
10
11
12
13
14
15
16
C
D
E
Timber Blockout for W-beam
18" Guardrail Bolt FBB04
Bolt, 5/8 x 10 hex, with USS Flat Washer and Recessed Guardrail Nut
Bolt, 5/8 x 7 hex, with USS Flat Washer and Recessed Guardrail Nut
6' Foundation Tube
22
Routered Timber Blockout for W-beam
10" Guardrail Bolt FBB03
72" W6x8.5 Guardrail Post
23
Section D-D
Scale 1 : 25
31" Typ
10" Guardrail Bolt FBB03
Routered Timber Blockout for Thriebeam
72" W6x8.5 Guardrail Post
24
Section E-E
Scale 1 : 25
Section C-C
Scale 1 : 25
All Post components Typical at 9 - 14
Texas A&M Transportation Institute
Roadside Safety and Physical Security Division - Proving Ground
Project 469137 1-2
16' Radius Guardrail with 3:1 Slope
2017-08-17
Drawn By GES
Scale 1:50
Sheet 4 of 12
Primary Roadway
T:\1-ProjectFiles\469137-TxDOT-TL-2-ShortRadius-Akram\469137-3\469137-3-1\Drafting, 469137-1\469137 Drawing

T:\1-ProjectFiles\469137-TxDOT-TL-2-ShortRadius-Akram\469137-3\469137-3-1\Drafting, 469137-1\469137 Drawing
Concrete
Plan View
Elevation View
Section F-F
Scale 1 : 20
Edge of Runway
Ground Line
3/4" chamfer exposed edges
1-1/2" both ways
Ø 1" holes (x 5) cored or cast
R6"
96"
24"
60"
10"
88.0°
56-5/8"
32"
20"
0"
18"
12"
28"
20"
12"
8"
0"
28-5/8"
24-13/16"
21"
17-3/16"
13-3/8"
Texas A&M Transportation Institute
Roadside Safety and Physical Security Division - Proving Ground
Project 469137 1-2 16' Radius Guardrail with 3:1 Slope 2017-08-17
Drawn By GES Scale 1:30 Sheet 5 of 12 Concrete
5a. Concrete is TxDOT Class C (3600 psi).

T:\1-Project Files\469137-TxDOT-TL-2-ShortRadius-Akram\469137-3\469137-3-1\Drafting, 469137-1\469137 Drawing

T:\1-ProjectFiles\469137-TxDOT-TL-2-ShortRadius-Akram\469137-3\469137-3-1\Drafting, 469137-1\469137 Drawing

T:\1-ProjectFiles\469137-TxDOT-TL-2-ShortRadius-Akram\469137-3\469137-3-1\Drafting, 469137-1\469137 Drawing

Rebar Details-3
(End View)

Texas A&M Transportation Institute

Roadside Safety and Physical Security Division - Proving Ground

Project 469137 1-2 16' Radius Guardrail with 3:1 Slope 2017-08-17

Drawn By GES Scale 1:12 Sheet 8 of 12 Rebar Details-3

PARTS	
Part Name	QTY.
S-3 Bar	1
S-2 Bar	1
S-1 Bar	14
U-bar	15
Bent Bar	4
Longitudinal Bar, Parapet	4
Longitudinal Bar, Deck	12
Transverse Bar	23
Tie Bar	6
Support Bar	5

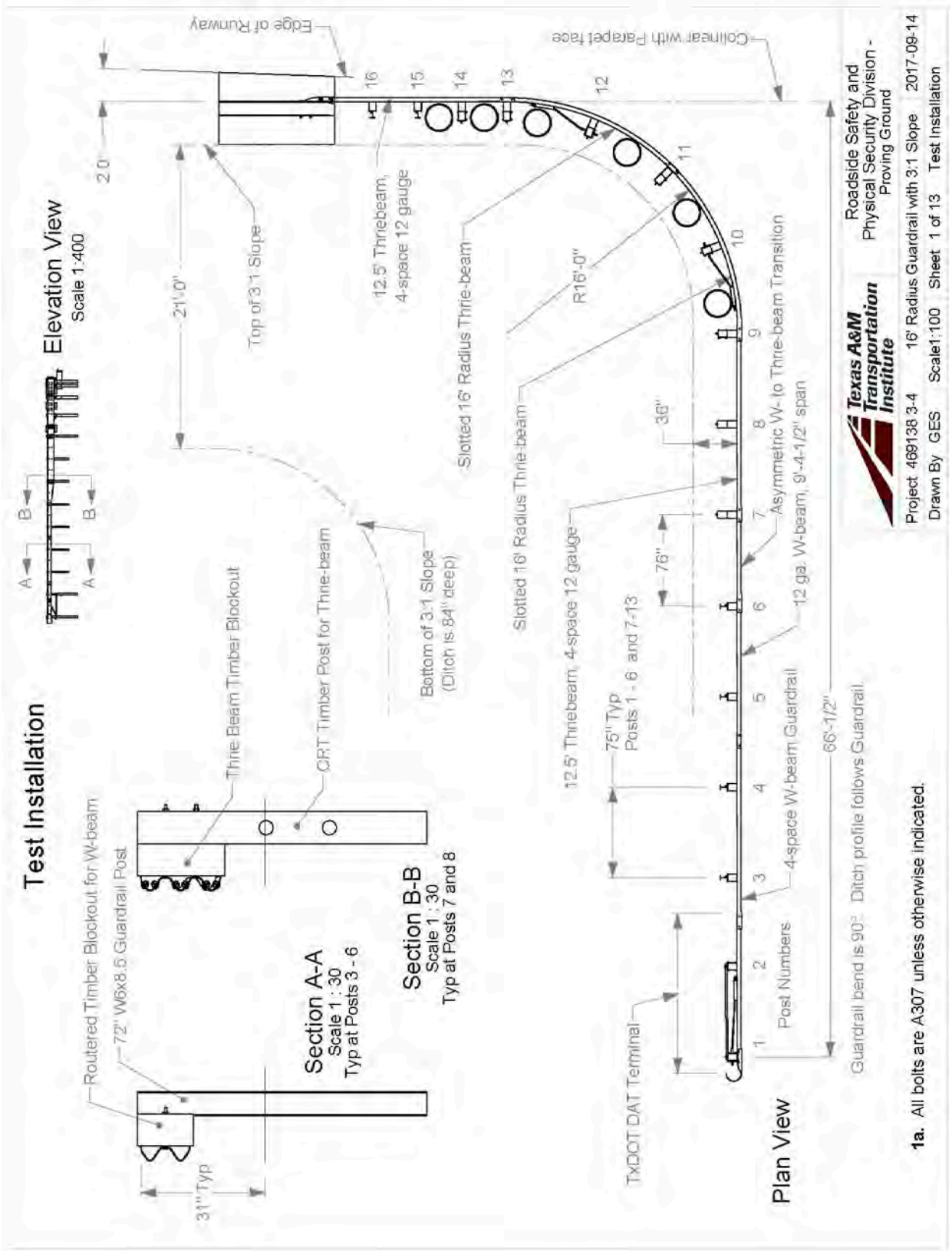
9a. All rebar is grade 60.

T:\1-Project Files\469137-TxDOT-TL-2-ShortRadius-Akram\469137-3\469137-3-1\Drafting\469137-1\469137 Drawing
Roadside Safety and
Physical Security Division -
Proving Ground
Texas A&M
Transportation
Institute
Project 469137 1-2 16' Radius Guardrail with 3:1 Slope 2017-08-17
Drawn By GES Scale 1:10 Sheet 10 of 12 Rebar-2
Bent Bar
Longitudinal Bar, Parapet
Longitudinal Bar, Deck
Transverse Bar
Tie Bar
82"
11-1/4"
2"
3"
93"
90"
53"
24"
#5/8"
#1/2"

11a. See Thrie-beam Guardrail (TF# RTM02a) for all dimensions not shown here.

T:\1-Project Files\469137-TxDOT-TL-2-ShortRadius-Akram\469137-3\469137-3-1\Drafting, 469137-1\469137 Drawing
Roadside Safety and Physical Security Division - Proving Ground
Texas A&M Transportation Institute
Project 469137 1-2 16' Radius Guardrail with 3:1 Slope 2017-08-17
Drawn By GES Scale 1:10 Sheet 12 of 12 Timber Posts
CRT Timber Post for Thrie Beam
Modified BCT Timber Post
Ø 3/4" x 2
Ø 7/8"
Ø 2-1/2"
Ø 3-1/2" x 2
Ø 3/4" x 2
0"
10"
17-5/8"
30-3/4"
33-1/4"
48-1/4"
5-1/2"
7-1/2"
8"
0"
7"
14-5/8"
32"
47-3/4"
72"
8"

APPENDIX B. DETAILS OF THE GUARDRAIL TREATMENT FOR TEST NOS. 469138-3-3 THROUGH 469138-3-5



T:\1-ProjectFiles\469137-TxDOT-TL-2-ShortRadius-Akram\469137-3\469138-3-3\Drafting\469138-3-3\469138 Drawing

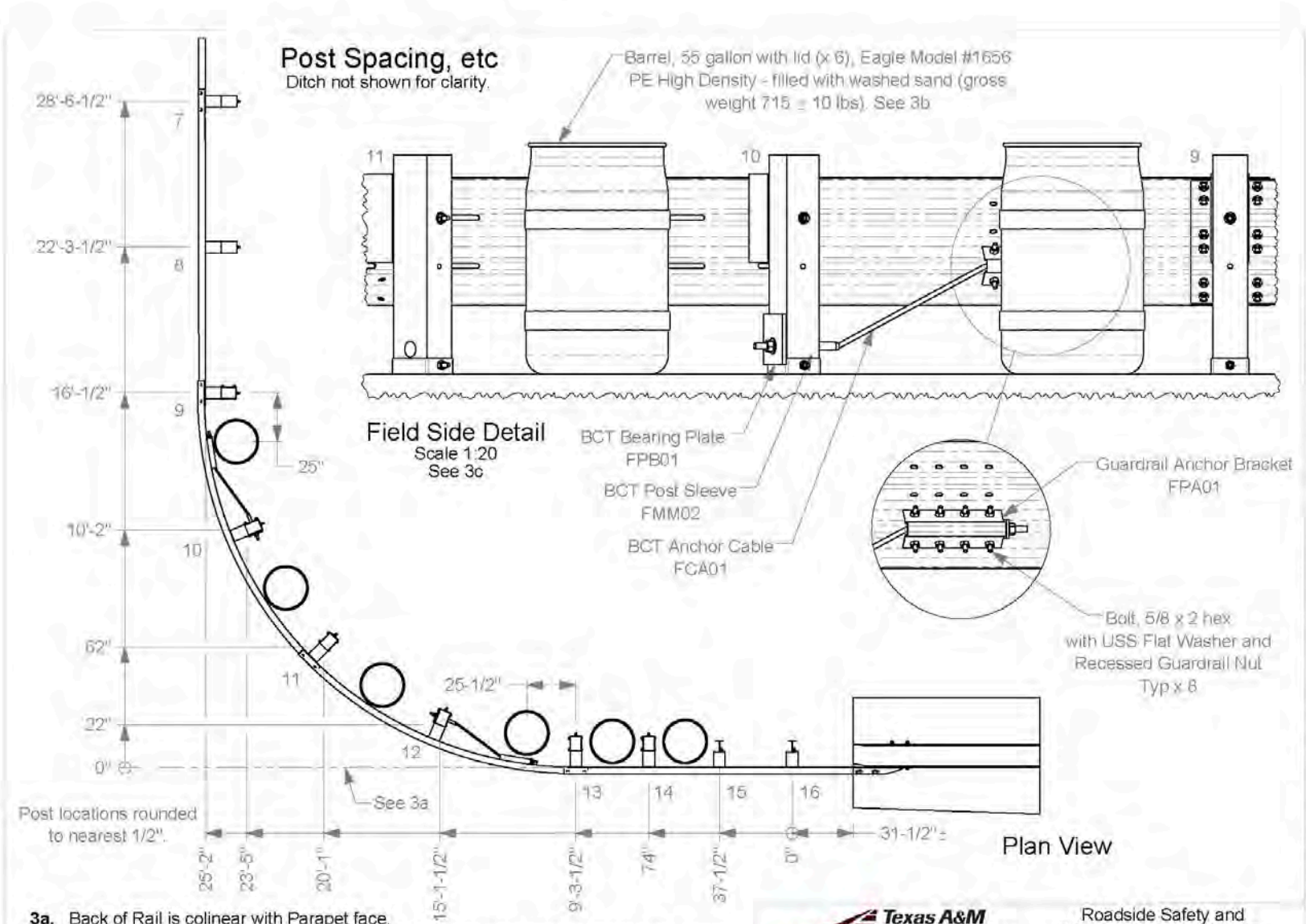
Isometric Views

Texas A&M Transportation Institute

Roadside Safety and Physical Security Division - Proving Ground

Project 469138 3-4 16' Radius Guardrail with 3:1 Slope 2017-09-14

Drawn By GES Scale 1:60 Sheet 2 of 13 Isometric Views



3a. Back of Rail is colinear with Parapet face.

3b. Place Barrels approximately 1" from back of Rail and centered between Posts, unless otherwise shown or indicated (see Barrels betweem Post 9 and 10, and 12 and 13).

3b. Anchor Cable details typical between Posts 9 and 10, and between Posts 12 and 13.

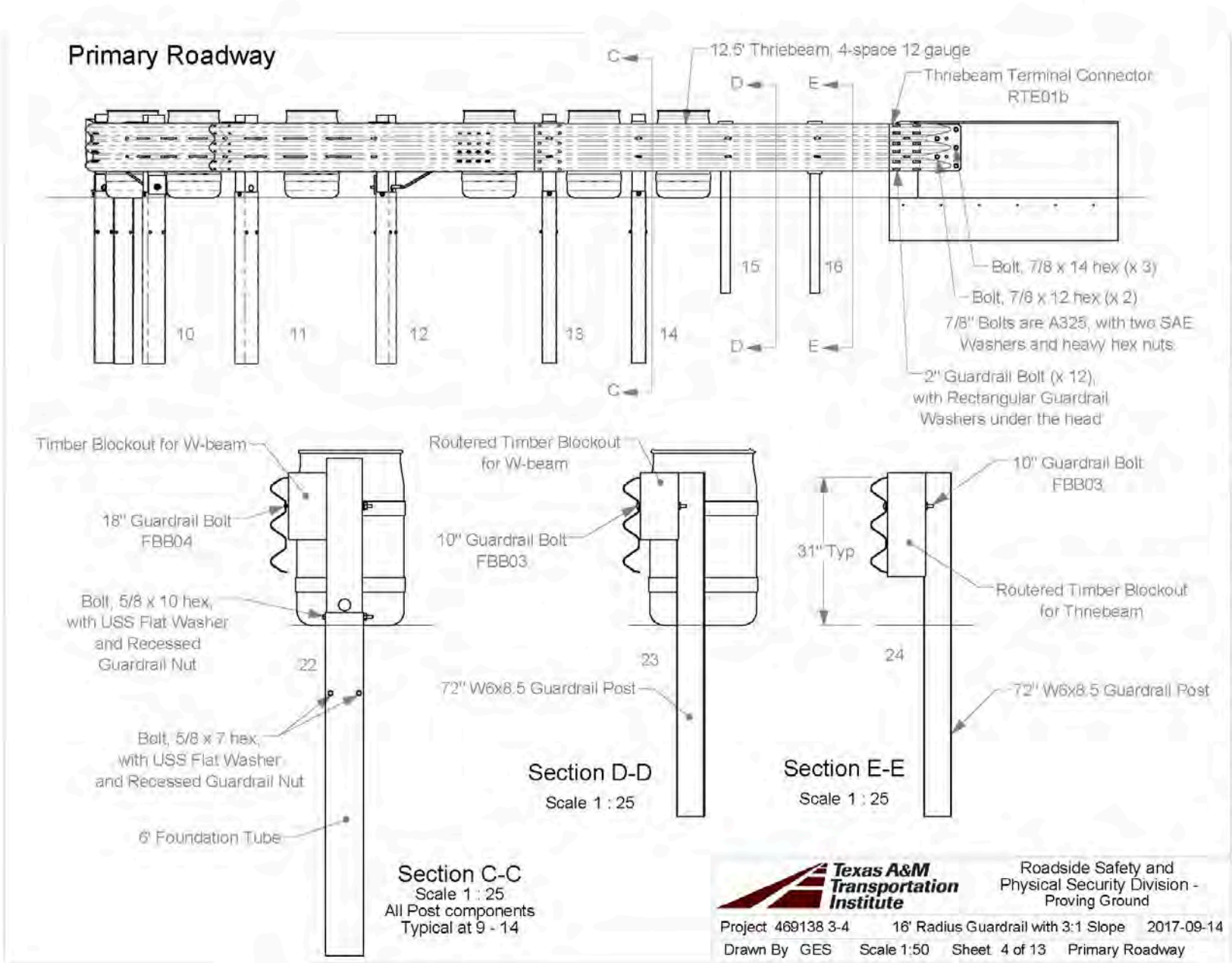
Texas A&M Transportation Institute

Roadside Safety and Physical Security Division - Proving Ground

Project 469138 3-4 | 16' Radius Guardrail with 3:1 Slope | 2017-09-14

Drawn By GES | Scale 1:65 | Sheet 3 of 13 | Post Spacing, etc

T:\1-ProjectFiles\469137-TxDOT-TL-2-ShortRadius-Akram\469137-3\469138-3-3\Drafting. 469138-3-3\469138 Drawing


Primary Roadway
12.5' Thriebeam, 4-space 12 gauge
Thriebeam Terminal Connector RTE01b
Bolt, 7/8 x 14 hex (x 3)
Bolt, 7/8 x 12 hex (x 2)
7/8" Bolts are A325, with two SAE Washers and heavy hex nuts
2" Guardrail Bolt (x 12), with Rectangular Guardrail Washers under the head
10
11
12
13
14
15
16
C
D
E
Timber Blockout for W-beam
18" Guardrail Bolt FBB04
Bolt, 5/8 x 10 hex, with USS Flat Washer and Recessed Guardrail Nut
Bolt, 5/8 x 7 hex, with USS Flat Washer and Recessed Guardrail Nut
6' Foundation Tube
22
Section C-C
Scale 1 : 25
All Post components Typical at 9 - 14
Routered Timber Blockout for W-beam
10" Guardrail Bolt FBB03
72" W6x8.5 Guardrail Post
23
Section D-D
Scale 1 : 25
31" Typ
10" Guardrail Bolt FBB03
Routered Timber Blockout for Thriebeam
72" W6x8.5 Guardrail Post
24
Section E-E
Scale 1 : 25
Texas A&M Transportation Institute
Roadside Safety and Physical Security Division - Proving Ground
Project 469138 3-4 16' Radius Guardrail with 3:1 Slope 2017-09-14
Drawn By GES Scale 1:50 Sheet 4 of 13 Primary Roadway
T:\1-ProjectFiles\469137-TxDOT-TL-2-ShortRadius-Akram\469137-3\469138-3-3\Drafting, 469138-3-3\469138 Drawing

T:\1-Project Files\469137-TxDOT-TL-2-ShortRadius-Akram\469137-3\469138-3-3\Drafting\469138-3-3\469138 Drawing
Concrete
Plan View
Edge of Runway
96"
24"
60"
10"
88.0°
56-5/8"
Section F-F
Scale 1 : 20
3/4" chamfer exposed edges
12"
1-1/2" both ways
32"
20"
0"
18"
Elevation View
Ground Line
Ø1" holes (x 5) cored or cast
R6"
28"
20"
12"
8"
0"
28-5/8"
24-13/16"
21"
17-3/16"
13-3/8"
Texas A&M Transportation Institute
Roadside Safety and Physical Security Division - Proving Ground
Project 469138 3-4 16' Radius Guardrail with 3:1 Slope 2017-09-14
Drawn By GES Scale 1:30 Sheet 5 of 13 Concrete
5a. Concrete is TxDOT Class C (3600 psi).

T:\1-ProjectFiles\469137-TxDOT-TL-2-ShortRadius-Akram\469137-3\469138-3-3\Drafting\469138-3-3\469138 Drawing

T:\1-Project Files\469137-TxDOT-TL-2-ShortRadius-Akram\469137-3\469138-3-3\Drafting, 469138-3-3\469138 Drawing

T:\1-ProjectFiles\469137-TxDOT-TL-2-ShortRadius-Akram\469137-3\469138-3-3\Drafting, 469138-3-3\469138 Drawing

PARTS	
Part Name	QTY.
S-3 Bar	1
S-2 Bar	1
S-1 Bar	14
U-bar	15
Bent Bar	4
Longitudinal Bar, Parapet	4
Longitudinal Bar, Deck	12
Transverse Bar	23
Tie Bar	6
Support Bar	5

9a. All rebar is grade 60.

T:\1-Project Files\469137-TxDOT-TL-2-ShortRadius-Akram\469137-3\469138-3-3\Drafting\469138-3-3\469138 Drawing
Roadside Safety and
Physical Security Division -
Proving Ground
Texas A&M
Transportation
Institute
Project 469138 3-4 16' Radius Guardrail with 3:1 Slope 2017-09-14
Drawn By GES Scale 1:10 Sheet 10 of 13 Rebar-2
Bent Bar
Longitudinal Bar, Parapet
Longitudinal Bar, Deck
Transverse Bar
Tie Bar
82"
11-1/4"
2"
3"
93"
90"
53"
24"
#3
#5/8"
#1/2"

T:\1-ProjectFiles\469137-TxDOT-TL-2-ShortRadius-Akram\469137-3\469138-3-3\Drafting, 469138-3-3\469138 Drawing

11a. See Thrie-beam Guardrail (TF# RTM02a) for all dimensions not shown here.

T:\1-Project Files\469137-TxDOT-TL-2-ShortRadius-Akram\469137-3\469138-3-3\Drafting\469138-3-3\469138 Drawing
Roadside Safety and Physical Security Division - Proving Ground
Texas A&M Transportation Institute
Project 469138 3-4 16' Radius Guardrail with 3:1 Slope 2017-09-14
Drawn By GES Scale 1:10 Sheet 12 of 13 Timber Posts
CRT Timber Post for Thrie Beam
Modified BCT Timber Post
5-1/2"
7-1/2"
0"
10"
17-5/8"
30-3/4"
33-1/4"
48-1/4"
Ø 2-1/2"
Ø 3/4" x 2
Ø 7/8"
8"
Ø 3-1/2" x 2
0"
7"
14-5/8"
32"
47-3/4"
72"
8"
Ø 3/4" x 2

Anchor Cable for Short Radius Rail



13a. The Stud shall conform to the requirements of ASTM A449 and shall be galvanized in accordance with ASTM A153. The threads shall have a Class 2A fit before galvanizing.

13b. The Wire Rope shall conform to the requirements of AASHTO M-30 and shall be Ø3/4" pre-formed, 6 x 19, wire strand core or independent wire rope core (IWRC), galvanized, right regular lay, manufactured of improved plow steel with a minimum breaking strength of 46,000 lbs.

13c. The swaged fitting, stud, and nut shall develop the breaking strength of the wire rope.

Texas A&M Transportation Institute

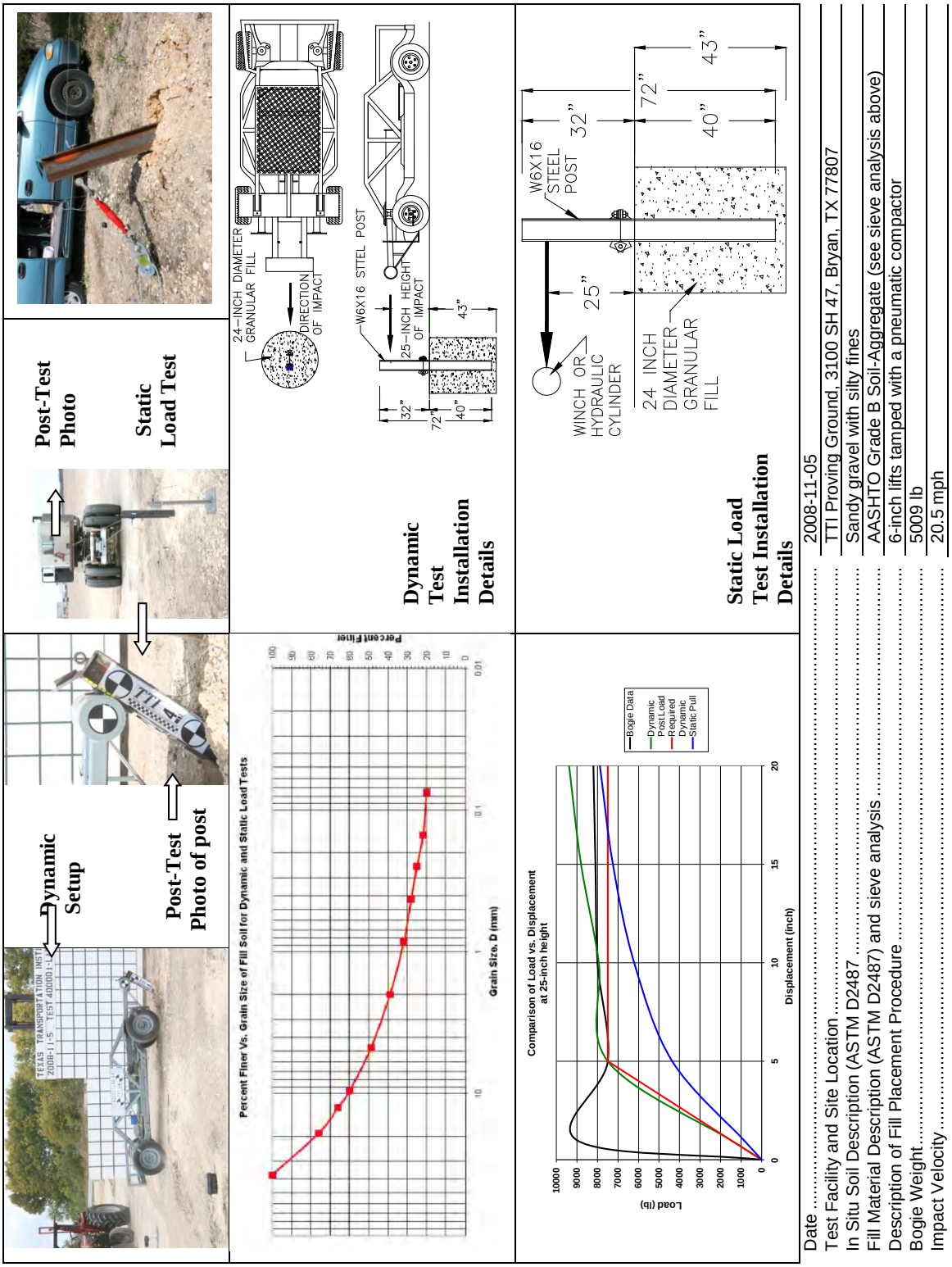
Roadside Safety and Physical Security Division - Proving Ground

Project 469138 3-4 16' Radius Guardrail with 3:1 Slope 2017-09-14

Drawn By GES Scale 1:10 Sheet 13 of 13 Anchor Cable

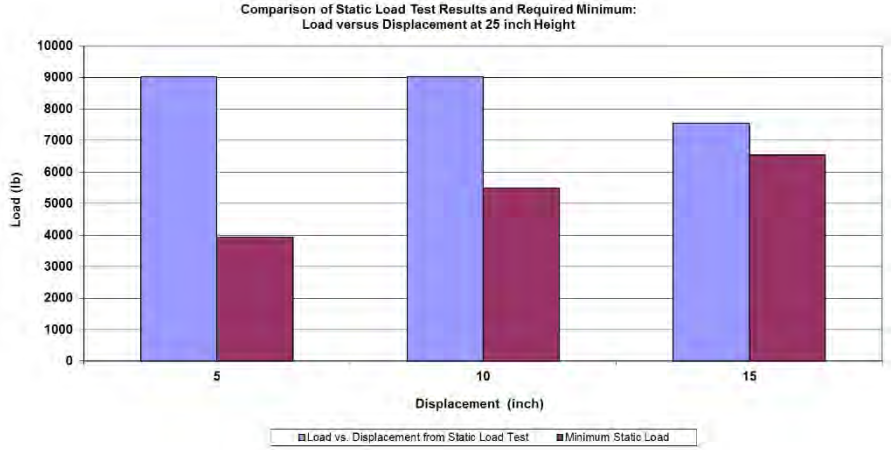
T:\1-ProjectFiles\469137-TxDOT-TL-2-ShortRadius-Akram\469137-3\469138-3-3\Drafting, 469138-3-3\469138 Drawing

Table C.1. Summary of Strong Soil Test Results for Establishing Installation Procedure.



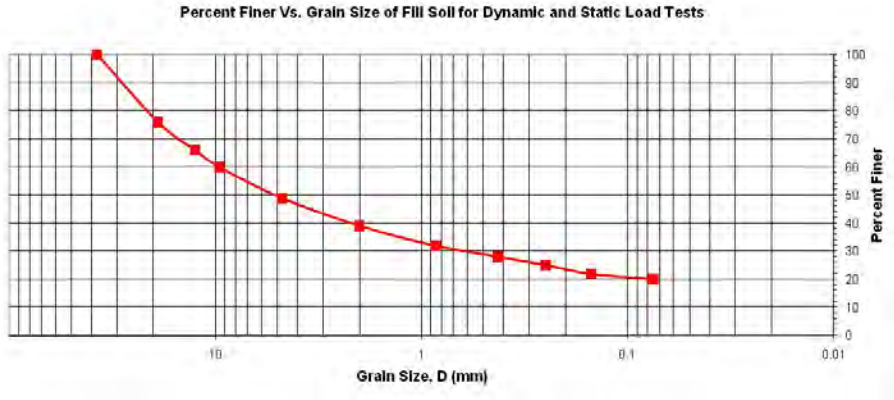
Date	2008-11-05
Test Facility and Site Location	TTI Proving Ground, 3100 SH 47, Bryan, TX 77807
In Situ Soil Description (ASTM D2487	Sandy gravel with silty fines
Fill Material Description (ASTM D2487) and sieve analysis	AASHTO Grade B Soil-Aggregate (see sieve analysis above)
Description of Fill Placement Procedure	6-inch lifts tamped with a pneumatic compactor
Bogie Weight	5009 lb
Impact Velocity	20.5 mph

Table C.2. Test Day Static Soil Strength Documentation for Test No. 469137-3-1.





Static Load Setup

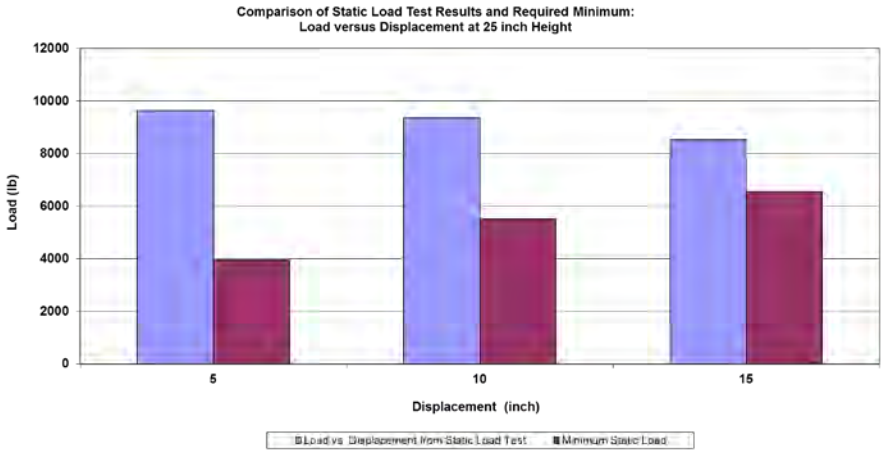




Post-Test Photo of Post

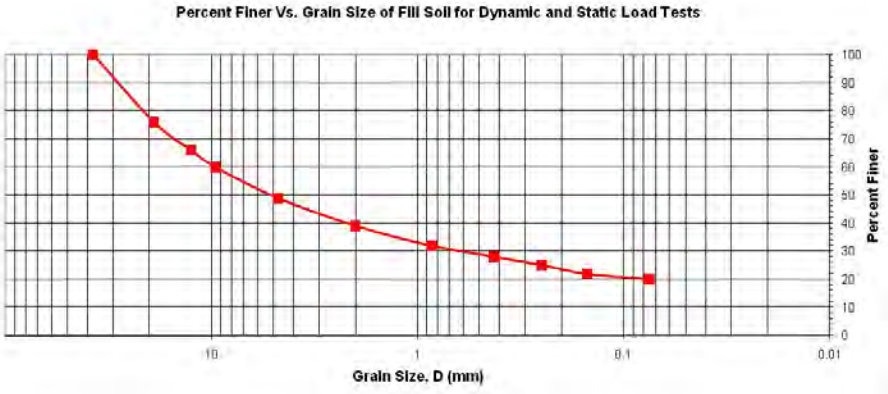
Date.....	2017-08-18
Test Facility and Site Location	TTI Proving Ground – 3100 SH 47, Bryan, Tx
In Situ Soil Description (ASTM D2487)	Sandy gravel with silty fines
Fill Material Description (ASTM D2487) and sieve analysis ..	AASHTO Grade B Soil-Aggregate (see sieve analysis)
Description of Fill Placement Procedure	6-inch lifts tamped with a pneumatic compactor

Table C.3. Test Day Static Soil Strength Documentation for Test No. 469137-3-2.





Static Load Setup

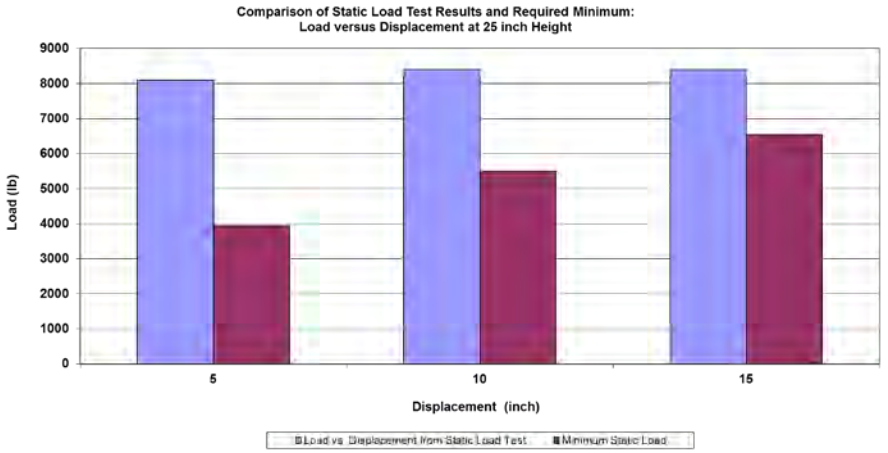




Post-Test Photo of Post

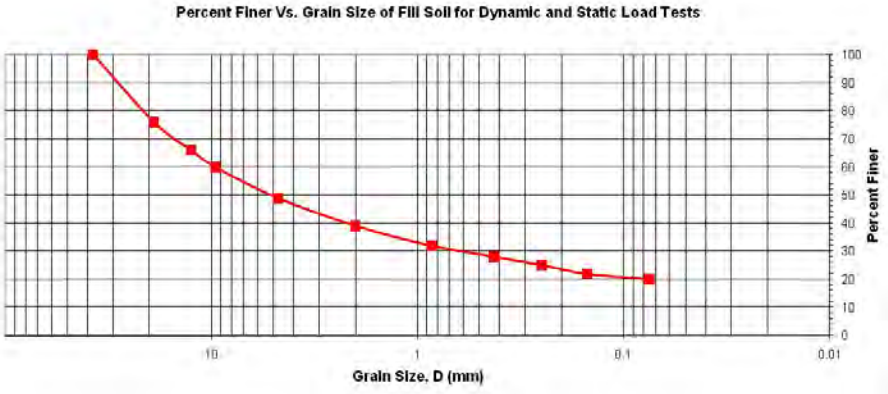
Date	2017-09-05
Test Facility and Site Location	TTI Proving Ground – 3100 SH 47, Bryan, Tx
In Situ Soil Description (ASTM D2487)	Sandy gravel with silty fines
Fill Material Description (ASTM D2487) and sieve analysis	AASHTO Grade B Soil-Aggregate (see sieve analysis)
Description of Fill Placement Procedure	6-inch lifts tamped with a pneumatic compactor

Table C.4. Test Day Static Soil Strength Documentation for Test No. 469138-3-3.





Static Load Setup

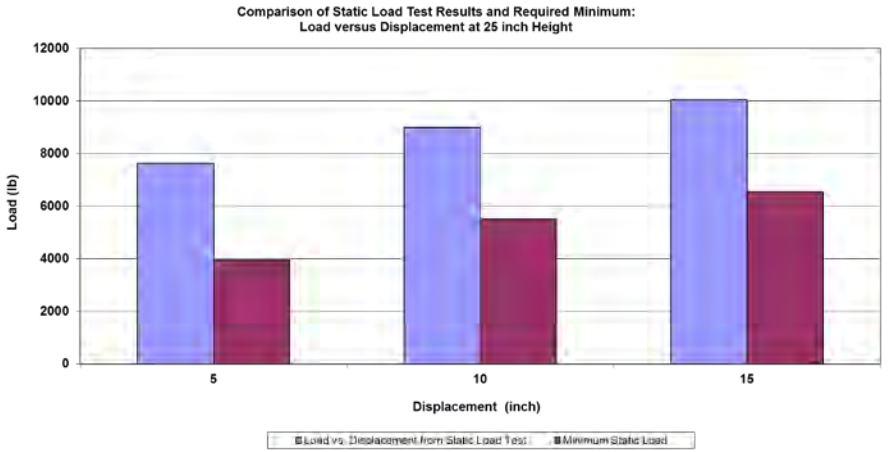




Post-Test Photo of Post

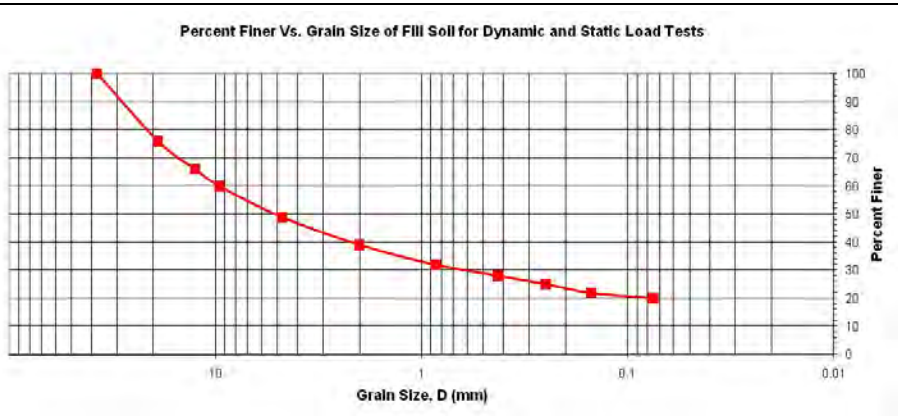
Date.....	2017-09-15
Test Facility and Site Location	TTI Proving Ground – 3100 SH 47, Bryan, Tx
In Situ Soil Description (ASTM D2487)	Sandy gravel with silty fines
Fill Material Description (ASTM D2487) and sieve analysis ..	AASHTO Grade B Soil-Aggregate (see sieve analysis)
Description of Fill Placement Procedure	6-inch lifts tamped with a pneumatic compactor

Table C.5. Test Day Static Soil Strength Documentation for Test No. 469138-3-4.





Static Load Setup





Post-Test Photo of Post

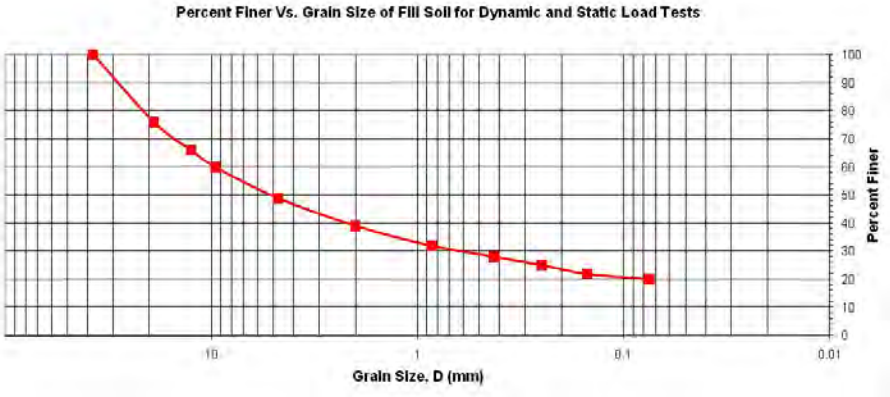
Date.....	2017-09-28
Test Facility and Site Location	TTI Proving Ground – 3100 SH 47, Bryan, Tx
In Situ Soil Description (ASTM D2487)	Sandy gravel with silty fines
Fill Material Description (ASTM D2487) and sieve analysis ..	AASHTO Grade B Soil-Aggregate (see sieve analysis)
Description of Fill Placement Procedure	6-inch lifts tamped with a pneumatic compactor

Table C.6. Test Day Static Soil Strength Documentation for Test No. 469138-3-5.





Static Load Setup



Post-Test Photo of Post

Date.....	2017-12-14
Test Facility and Site Location	TTI Proving Ground – 3100 SH 47, Bryan, Tx
In Situ Soil Description (ASTM D2487)	Sandy gravel with silty fines
Fill Material Description (ASTM D2487) and sieve analysis ..	AASHTO Grade B Soil-Aggregate (see sieve analysis)
Description of Fill Placement Procedure	6-inch lifts tamped with a pneumatic compactor

APPENDIX D. *MASH* TEST 2-33 (CRASH TEST NO. 469137-3-1)

D.1 VEHICLE PROPERTIES AND INFORMATION

Table D.1. Vehicle Properties for Test No. 469137-3-1.

Date: 2017-08-18 Test No.: 469137-3-1 VIN No.: 1D7RB1GP7BS526827

Year: 2011 Make: Dodge Model: RAM 1500

Tire Size: 265/70R17 Tire Inflation Pressure: 35 psi

Tread Type: Highway Odometer: 405188

Note any damage to the vehicle prior to test: None

• Denotes accelerometer location.

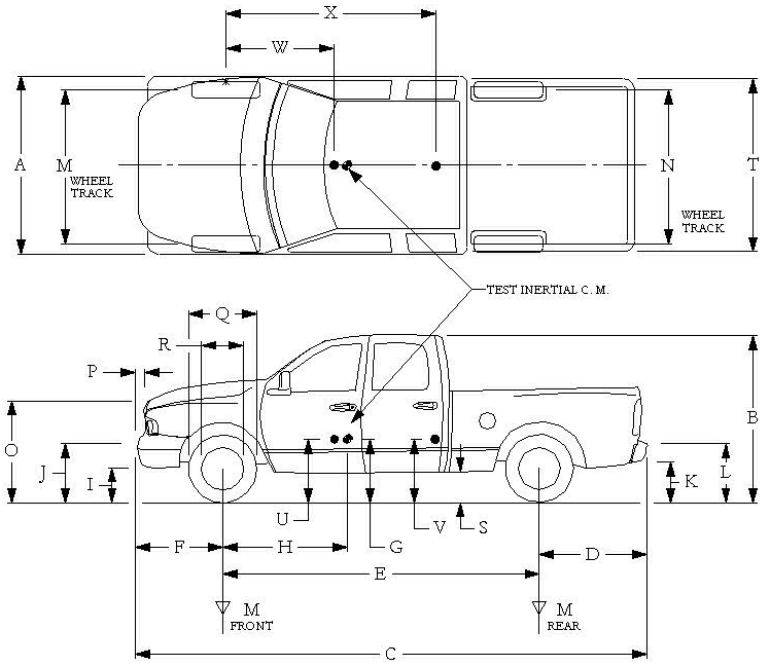
NOTES: None

Engine Type: V-8
Engine CID: 4.7 liter

Transmission Type:
x Auto or ___ Manual
___ FWD x RWD ___ 4WD

Optional Equipment:
None

Dummy Data:
Type: None
Mass: NA
Seat Position: NA



Geometry: inches

A	78.50	F	40.00	K	20.75	P	3.00	U	27.25
B	75.00	G	28.38	L	29.50	Q	30.50	V	30.25
C	227.50	H	62.00	M	68.50	R	18.00	W	62.00
D	47.00	I	11.00	N	68.00	S	13.25	X	77.00
E	140.50	J	26.50	O	46.00	T	77.00		

Wheel Center Height Front	14.75	Wheel Well Clearance (Front)	6.00	Bottom Frame Height - Front	17.00
Wheel Center Height Rear	14.75	Wheel Well Clearance (Rear)	9.25	Bottom Frame Height - Rear	25.50

GVWR Ratings:		**Mass:** lb	Curb	Test Inertial	Gross Static
Front	3700	M_{front}	2907	2813	------
Back	3900	M_{rear}	2250	2226	------
Total	6700	M_{Total}	5157	5039	------

(Allowable Range for TIM and GSM = 5000 lb ±110 lb)

Mass Distribution:
lb LF: 1403 RF: 1410 LR: 1112 RR: 1114

Table D.2. Measurements of Vehicle Vertical CG for Test No. 469137-3-1.

Date: 2017-08-18 Test No.: 469137-3-1 VIN: 1D7RB1GP7BS526827

Year: 2011 Make: Dodge Model: RAM 1500

Body Style: Quad Cab Mileage: 405188

Engine: 4.7 liter V-8 Transmission: Automatic

Fuel Level: Empty Ballast: 207 lb (440 lb max)

Tire Pressure: Front: 35 psi Rear: 35 psi Size: 265/70R17

Measured Vehicle Weights: (lb)

LF:	1403	RF:	1410	Front Axle:	2813
LR:	1112	RR:	1114	Rear Axle:	2226
Left:	2515	Right:	2524	Total:	5039
					5000 ±110 lb allowed

Wheel Base: 140.5 inches (148 ±12 inches allowed) Track: F: 68.5 inches R: 68 inches

Track = (F+R)/2 = 67 ±1.5 inches allowed

Center of Gravity, SAE J874 Suspension Method

X:	62.07 inches	Rear of Front Axle	(63 ±4 inches allowed)
Y:	0.06 inches	Left - Right +	of Vehicle Centerline
Z:	28.375 inches	Above Ground	(minumum 28.0 inches allowed)

Hood Height: 46.00 inches (43 ±4 inches allowed) Front Bumper Height: 26.50 inches

Front Overhang: 40.00 inches (39 ±3 inches allowed) Rear Bumper Height: 29.50 inches

Overall Length: 227.50 inches (237 ±13 inches allowed)

Table D.3. Exterior Crush Measurements of Vehicle for Test No. 469137-3-1.

Date: 2017-08-18 Test No.: 469137-3-1 VIN No.: 1D7RB1GP7BS526827

Year: 2011 Make: Dodge Model: RAM 1500

VEHICLE CRUSH MEASUREMENT SHEET[1]

Complete When Applicable	
End Damage	Side Damage
Undeformed end width _____ Corner shift: A1 _____ A2 _____ End shift at frame (CDC) (check one) < 4 inches _____ ≥ 4 inches _____	Bowing: B1 _____ X1 _____ B2 _____ X2 _____ Bowing constant $\frac{X1+X2}{2}$ = _____

Note: Measure C_1 to C_6 from Driver to Passenger Side in Front or Rear impacts – Rear to Front in Side Impacts.

Specific Impact Number	Plane* of C-Measurements	Direct Damage		Field L**	C_1	C_2	C_3	C_4	C_5	C_6	±D
		Width** (CDC)	Max*** Crush								
1	Front plane at bumper ht	72	6	72	6	3	2.5	2.5	3	6	0
	Measurements recorded										
	in inches										

[1]Table taken from National Accident Sampling System (NASS).

*Identify the plane at which the C-measurements are taken (e.g., at bumper, above bumper, at sill, above sill, at beltline, etc.) or label adjustments (e.g., free space).

Free space value is defined as the distance between the baseline and the original body contour taken at the individual C locations. This may include the following: bumper lead, bumper taper, side protrusion, side taper, etc.
Record the value for each C-measurement and maximum crush.

**Measure and document on the vehicle diagram the beginning or end of the direct damage width and field L (e.g., side damage with respect to undamaged axle).

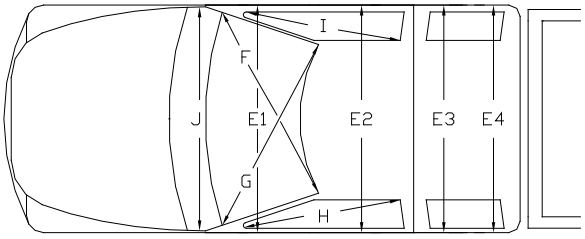
***Measure and document on the vehicle diagram the location of the maximum crush.

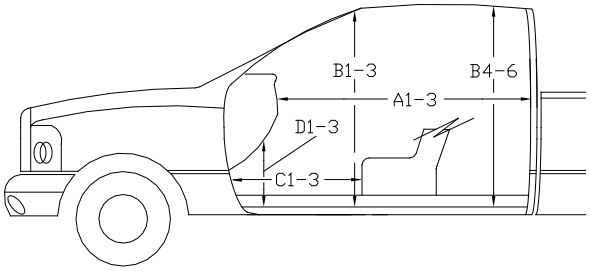
Note: Use as many lines/columns as necessary to describe each damage profile.

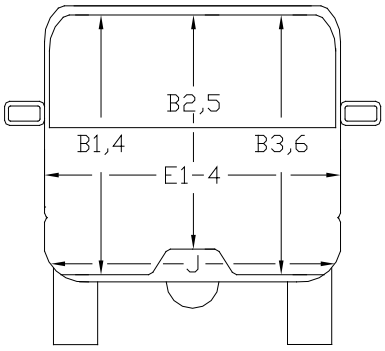
Table D.4. Occupant Compartment Measurements of Vehicle for Test No. 469137-3-1.

Date: 2017-08-18 Test No.: 469137-3-1 VIN No.: 1D7RB1GP7BS526827

Year: 2011 Make: Dodge Model: RAM 1500







*Lateral area across the cab from driver's side kickpanel to passenger's side kickpanel.

OCCUPANT COMPARTMENT DEFORMATION MEASUREMENT

	Before	After (inches)	Differ.
A1	65.25	65.25	0
A2	63.25	63.25	0
A3	65.50	65.50	0
B1	44.50	44.50	0
B2	38.00	38.00	0
B3	44.50	44.50	0
B4	39.50	39.50	0
B5	43.00	43.00	0
B6	39.50	39.50	0
C1	26.00	26.00	0
C2	-----	-----	-
C3	26.00	26.00	0
D1	11.50	11.50	0
D2	-----	-----	-
D3	11.50	11.50	0
E1	58.75	58.75	0
E2	63.50	63.50	0
E3	63.50	63.50	0
E4	63.50	63.50	0
F	59.00	59.00	0
G	59.00	59.00	0
H	37.50	37.50	0
I	37.50	37.50	0
J*	23.25	23.25	0

D.2 SEQUENTIAL PHOTOGRAPHS

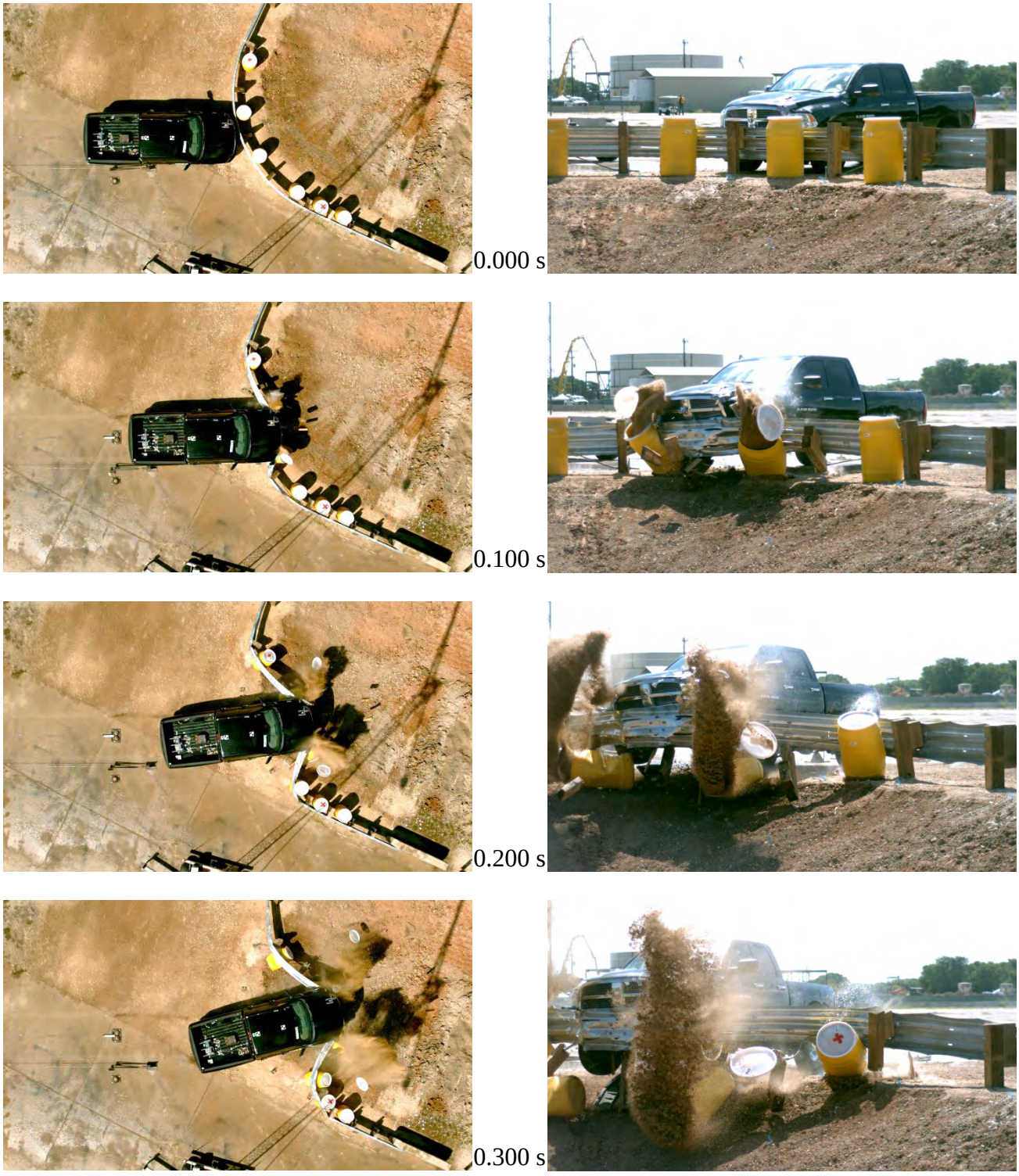
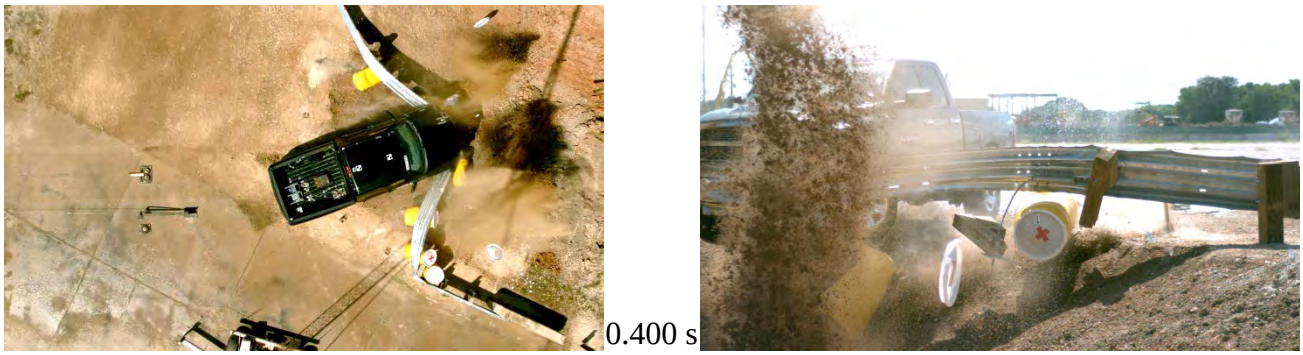
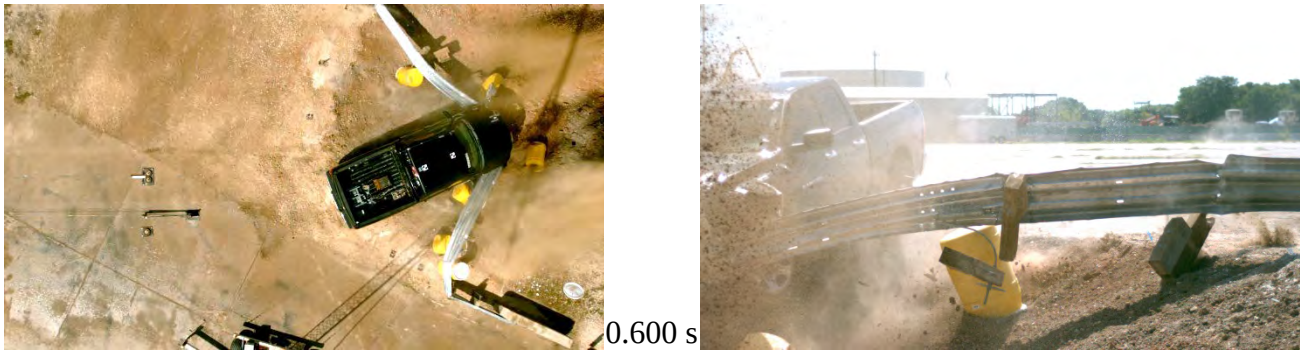
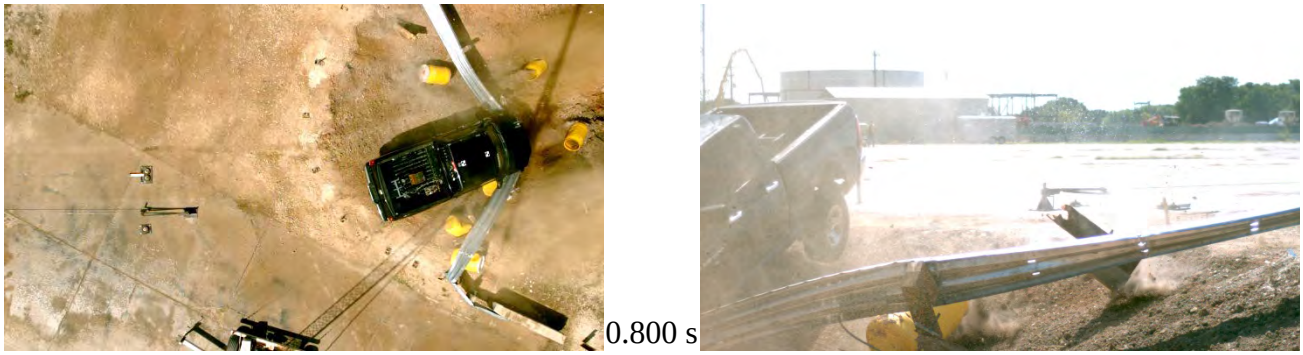


Figure D.1. Sequential Photographs for Test No. 469137-3-1 (Overhead and Rear Views).


0.400 s


0.600 s


0.800 s

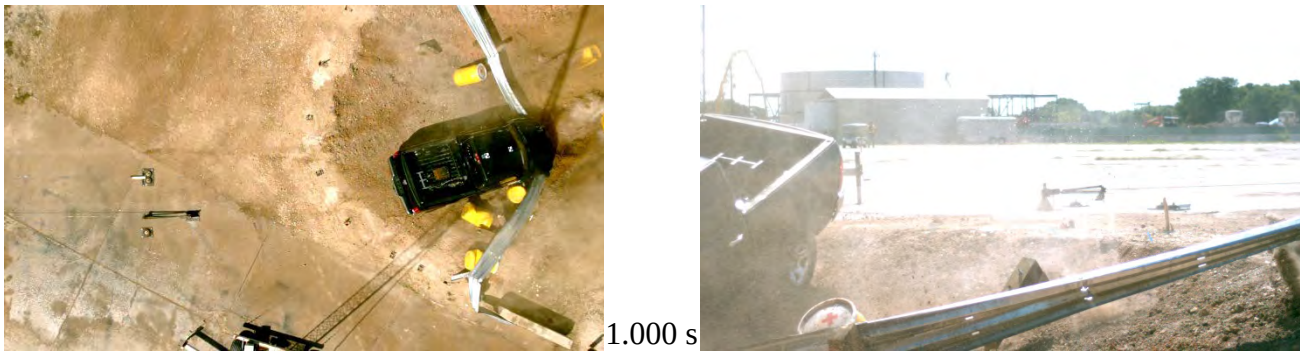

1.000 s

Figure D.1. Sequential Photographs for Test No. 469137-3-1 (Overhead and Rear Views) (Continued).

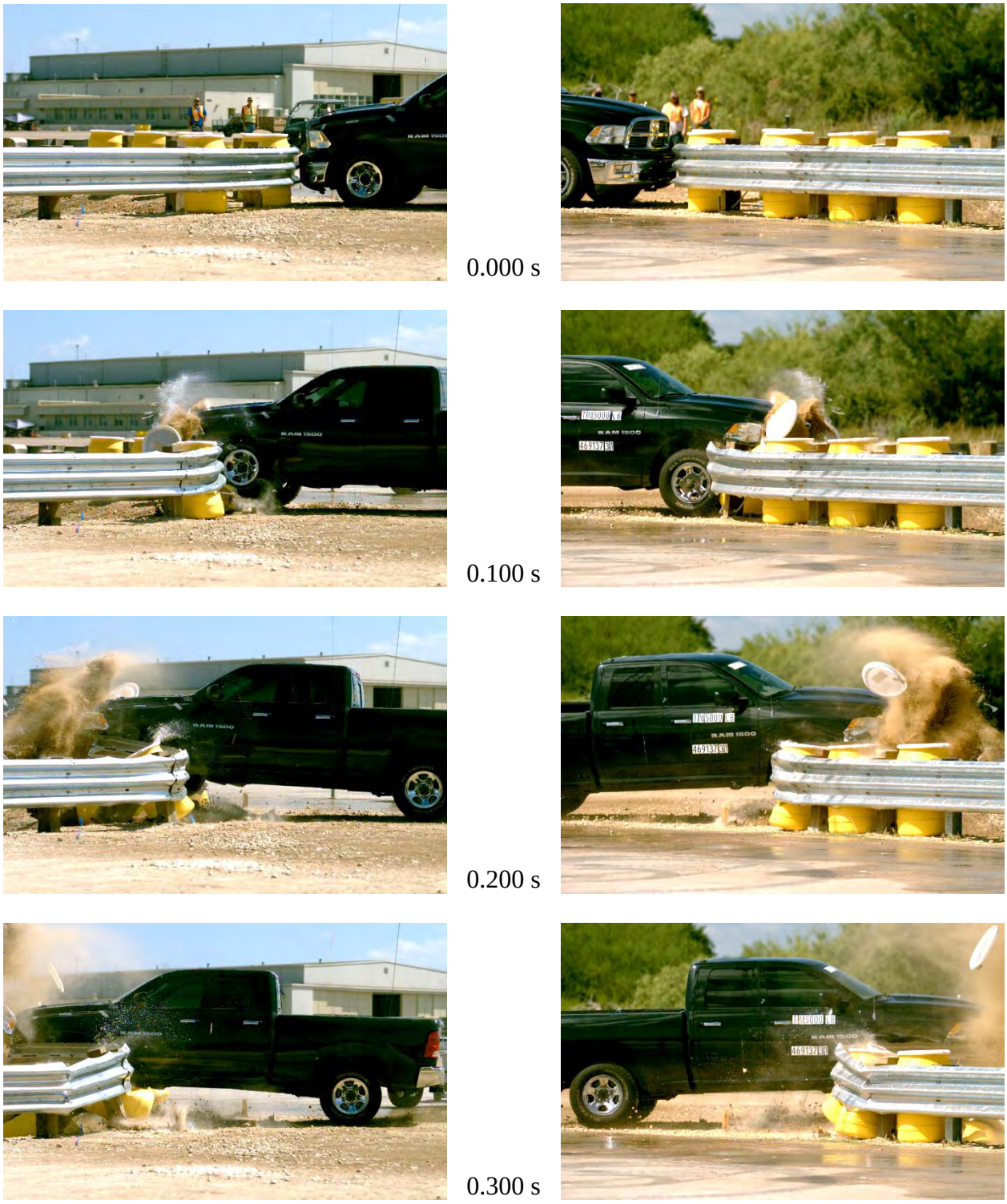
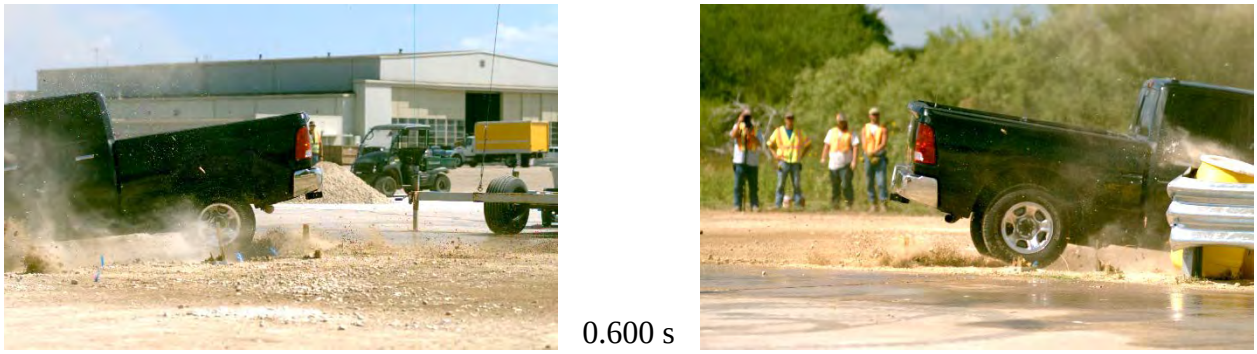
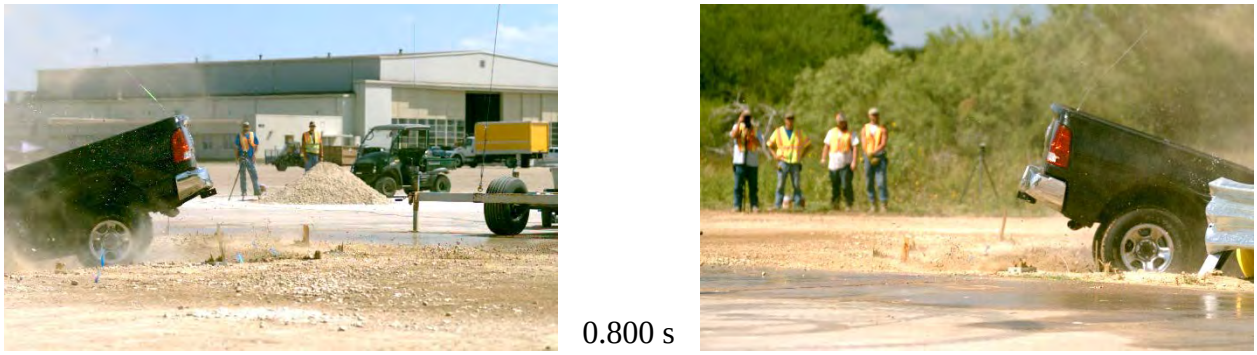


Figure D.2. Sequential Photographs for Test No. 469137-3-1 (Perpendicular Views).







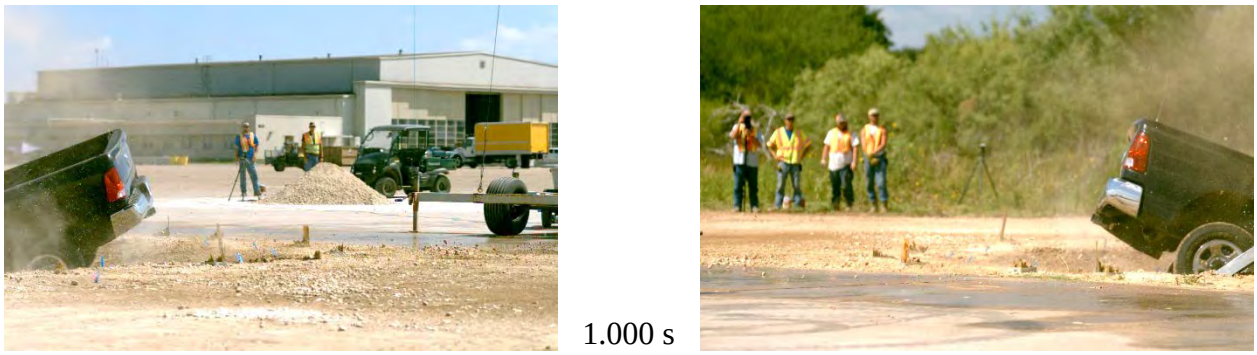


Figure D.2. Sequential Photographs for Test No. 469137-3-1 (Perpendicular Views) (Continued).

D.3 VEHICLE ANGULAR DISPLACEMENT

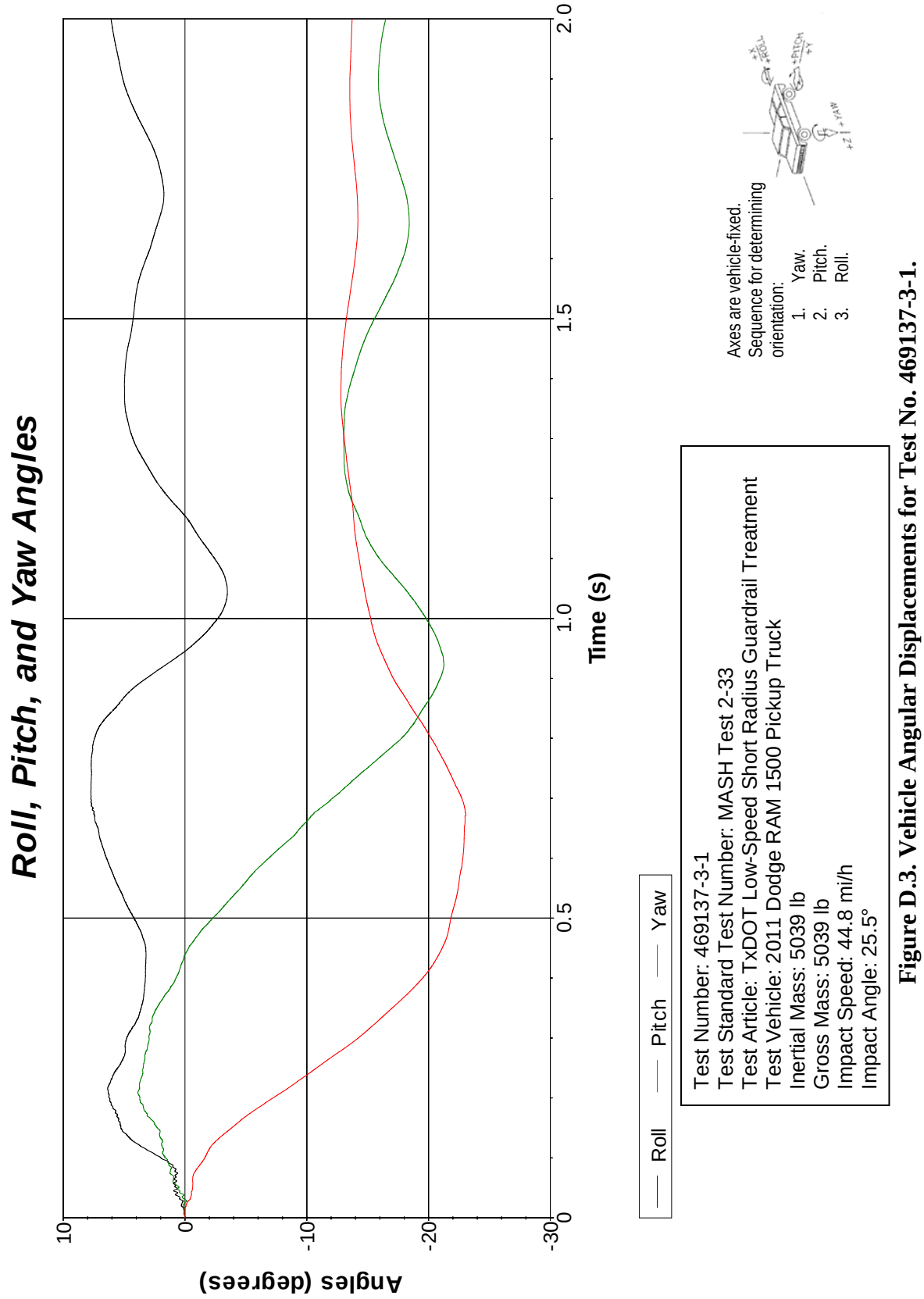


Figure D.3. Vehicle Angular Displacements for Test No. 469137-3-1.

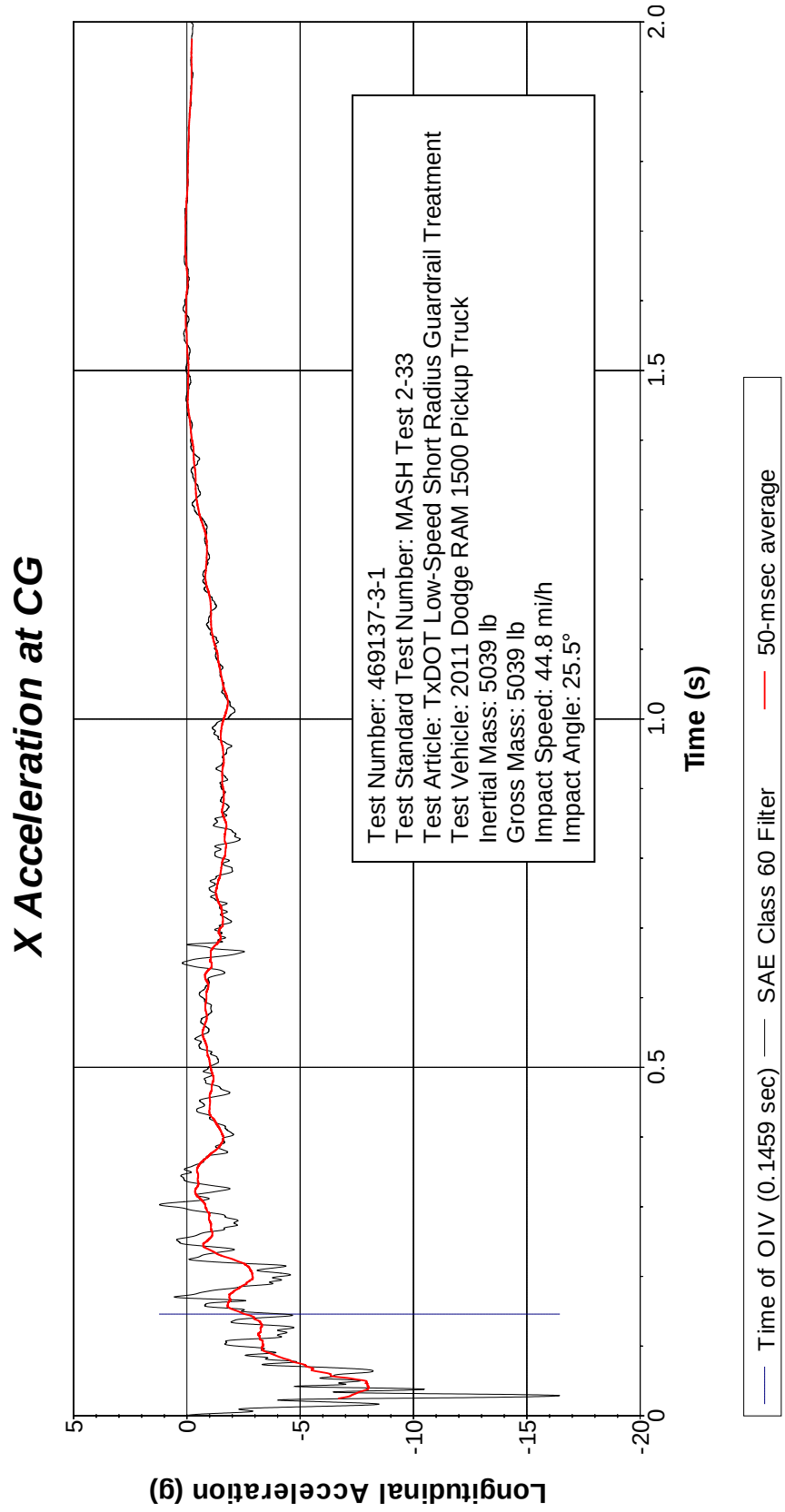


Figure D.4. Vehicle Longitudinal Accelerometer Trace for Test No. 469137-3-1 (Accelerometer Located at Center of Gravity).

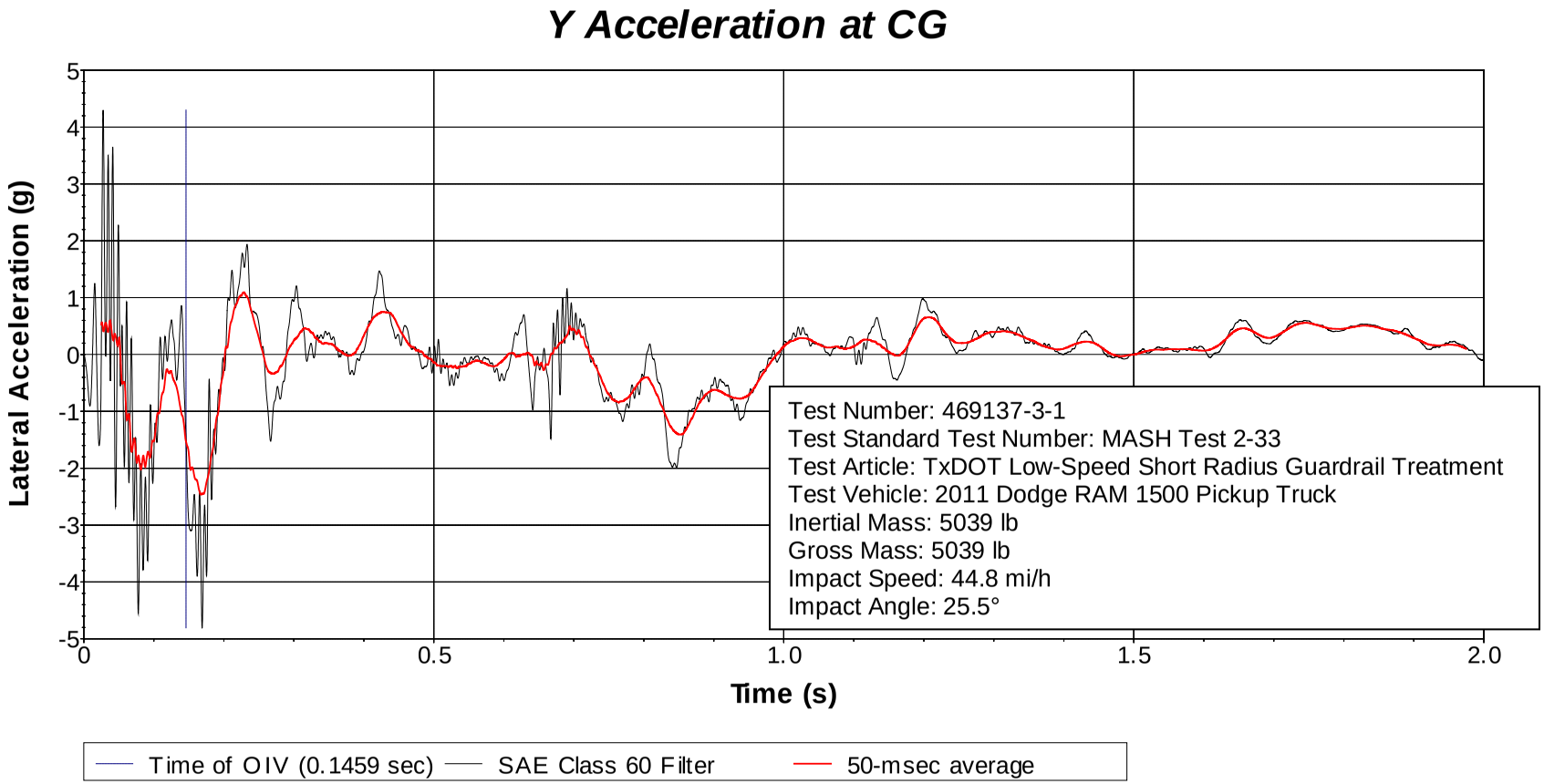


Figure D.5. Vehicle Lateral Accelerometer Trace for Test No. 469137-3-1 (Accelerometer Located at Center of Gravity).

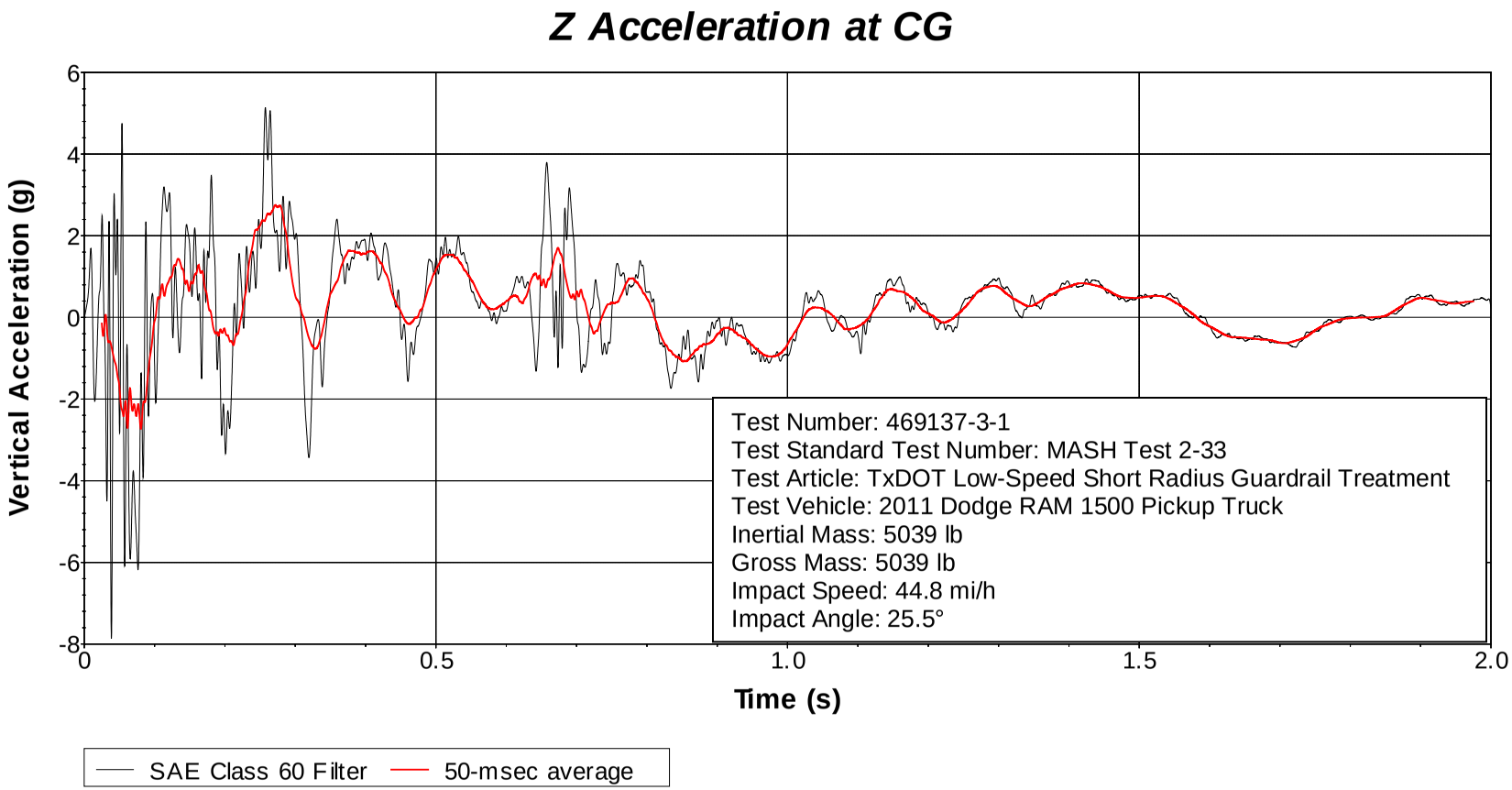


Figure D.6. Vehicle Vertical Accelerometer Trace for Test No. 469137-3-1 (Accelerometer Located at Center of Gravity).

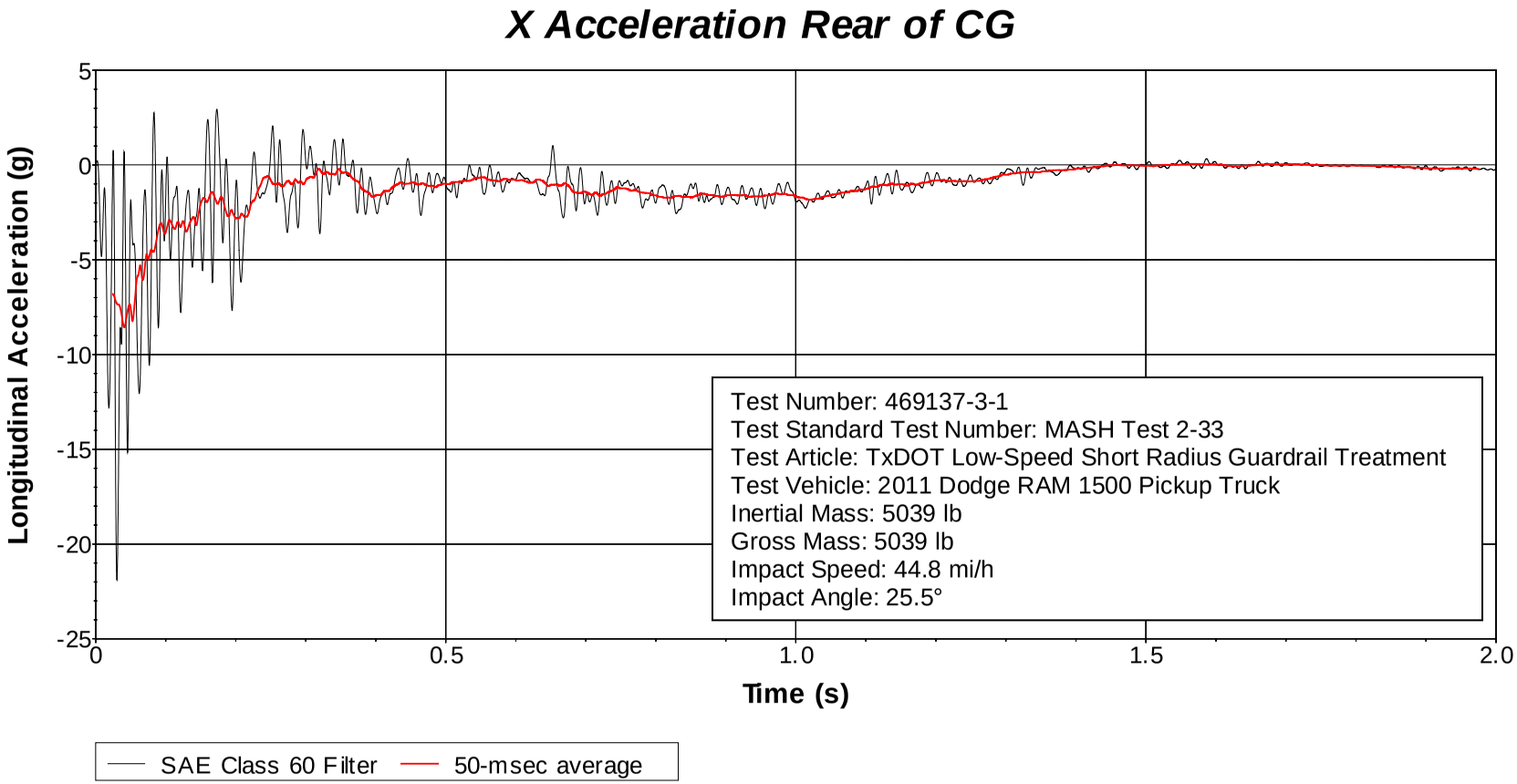


Figure D.7. Vehicle Longitudinal Accelerometer Trace for Test No. 469137-3-1 (Accelerometer Located Rear of Center of Gravity).

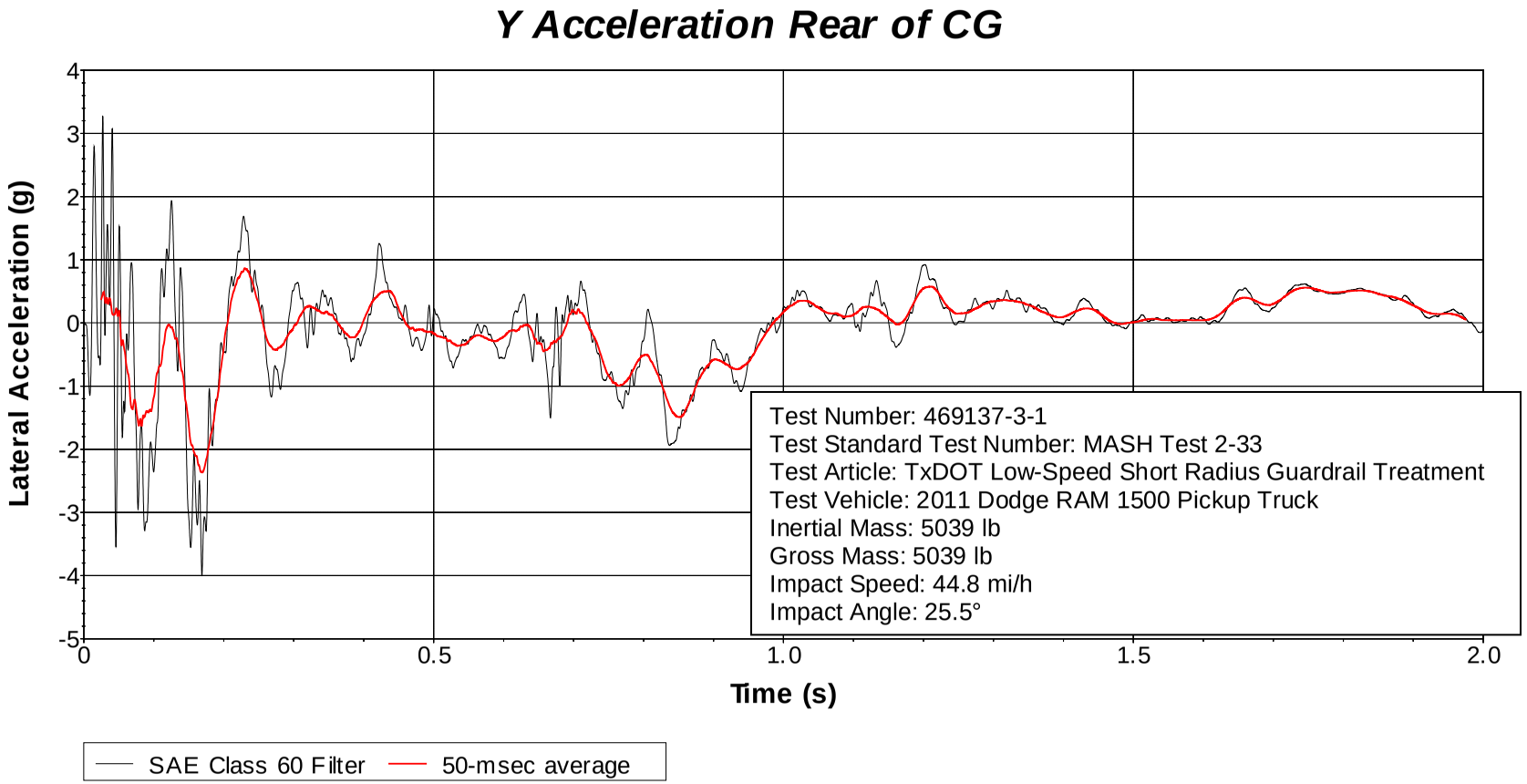


Figure D.8. Vehicle Lateral Accelerometer Trace for Test No. 469137-3-1 (Accelerometer Located Rear of Center of Gravity).

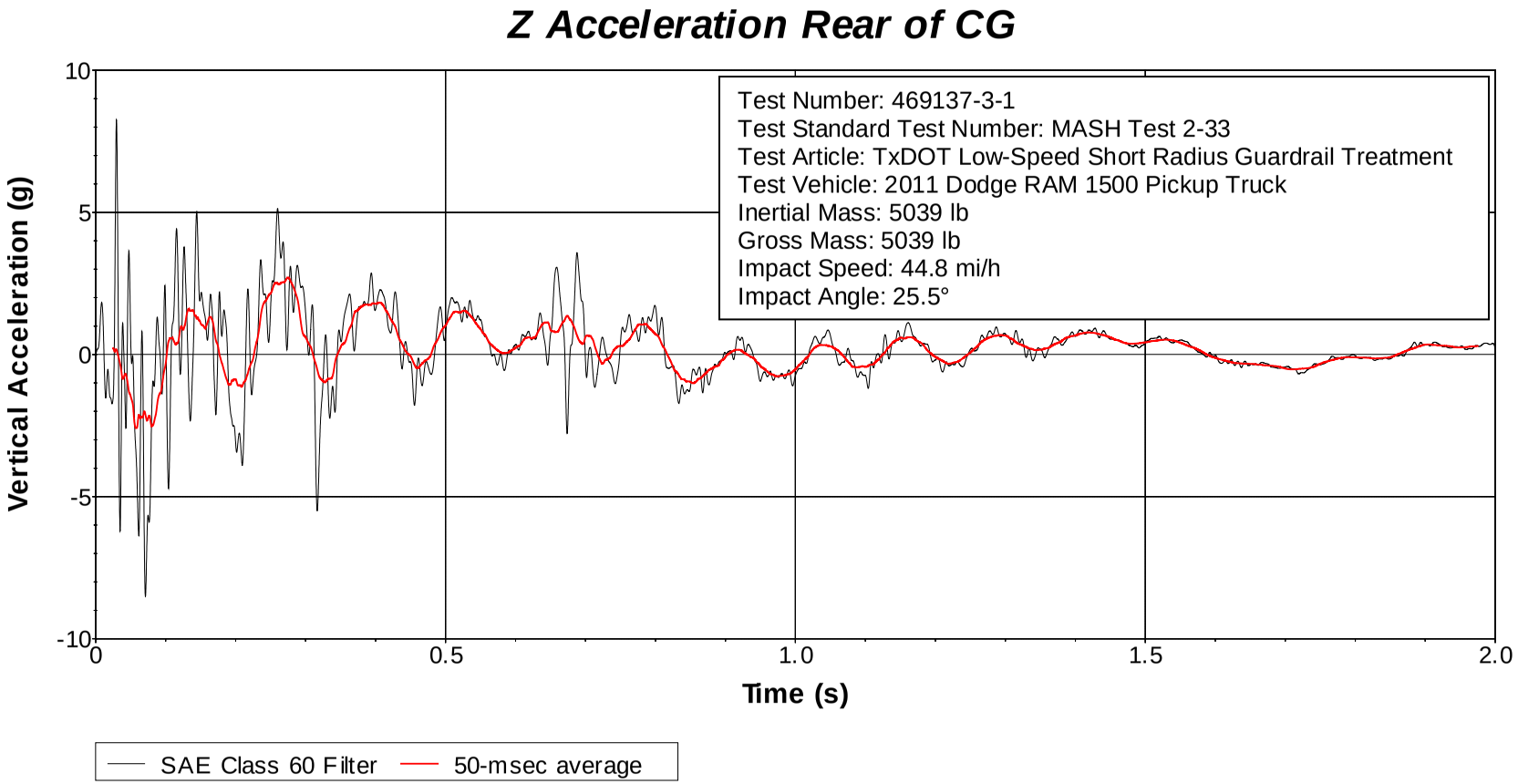


Figure D.9. Vehicle Vertical Accelerometer Trace for Test No. 469137-3-1 (Accelerometer Located Rear of Center of Gravity).

APPENDIX E. *MASH* TEST 2-32 (CRASH TEST NO. 469137-3-2)

E.1 VEHICLE PROPERTIES AND INFORMATION

Table E.1. Vehicle Properties for Test No. 469137-3-2.

Date: 2017-09-05 Test No.: 469137-3-2 VIN No.: KNADH4A38B6960769

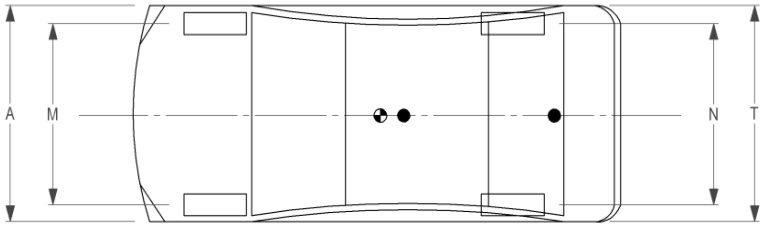
Year: 2011 Make: Kia Model: Rio

Tire Inflation Pressure: 32 psi Odometer: 101676 Tire Size: 185/65R14

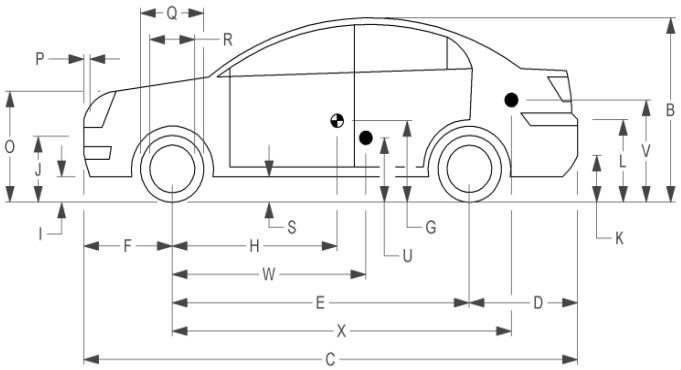
Describe any damage to the vehicle prior to test: None

• Denotes accelerometer location.

NOTES: None



Engine Type: 4 cylinder
Engine CID: 1.6 liter
Transmission Type:
x Auto or ____ Manual
x FWD ____ RWD ____ 4WD
Optional Equipment:
None



Dummy Data:
Type: 50th Percentile Male
Mass: 165 lb
Seat Position: Driver

Geometry: inches

A	66.38	F	33.00	K	10.50	P	4.12	U	15.25
B	58.00	G	-----	L	24.50	Q	22.50	V	20.38
C	165.75	H	35.66	M	57.75	R	15.50	W	35.66
D	34.00	I	7.75	N	57.70	S	9.00	X	107.40
E	98.75	J	21.00	O	28.00	T	66.20		
Wheel Center Ht Front		11.00		Wheel Center Ht Rear		11.00	W-H	0	

GVWR Ratings:		**Mass:** lb	Curb	Test Inertial	Gross Static
Front	1718	M_{front}	1581	1569	1654
Back	1874	M_{rear}	914	887	967
Total	3638	M_{Total}	2495	2456	2621

Mass Distribution:
lb LF: 799 RF: 770 LR: 448 RR: 439

Table E.2. Exterior Crush Measurements for Test No. 469137-3-2.

Date: 2017-09-05 Test No.: 469137-3-2 VIN No.: KNADH4A38B6960769

Year: 2011 Make: Kia Model: Rio

VEHICLE CRUSH MEASUREMENT SHEET[1]

Complete When Applicable	
End Damage	Side Damage
Undeformed end width _____ Corner shift: A1 _____ A2 _____ End shift at frame (CDC) (check one) < 4 inches _____ ≥ 4 inches _____	Bowing: B1 _____ X1 _____ B2 _____ X2 _____ Bowing constant $\frac{X1+X2}{2}$ = _____

Note: Measure C_1 to C_6 from Driver to Passenger Side in Front or Rear impacts – Rear to Front in Side Impacts.

Specific Impact Number	Plane* of C-Measurements	Direct Damage		Field L**	C_1	C_2	C_3	C_4	C_5	C_6	±D
		Width** (CDC)	Max*** Crush								
1	Front plane at bumper ht	60	5	60	5	4.75	3.75	3.25	3	4	0
	Measurements recorded										
	in inches										

[1]Table taken from National Accident Sampling System (NASS).

*Identify the plane at which the C-measurements are taken (e.g., at bumper, above bumper, at sill, above sill, at beltline, etc.) or label adjustments (e.g., free space).

Free space value is defined as the distance between the baseline and the original body contour taken at the individual C locations. This may include the following: bumper lead, bumper taper, side protrusion, side taper, etc. Record the value for each C-measurement and maximum crush.

**Measure and document on the vehicle diagram the beginning or end of the direct damage width and field L (e.g., side damage with respect to undamaged axle).

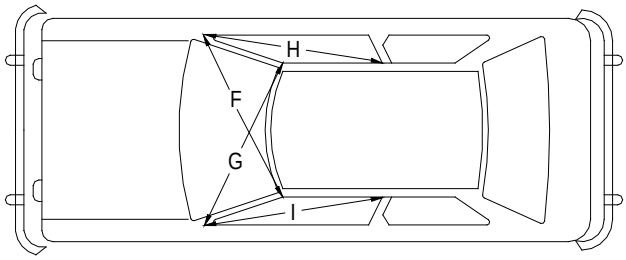
***Measure and document on the vehicle diagram the location of the maximum crush.

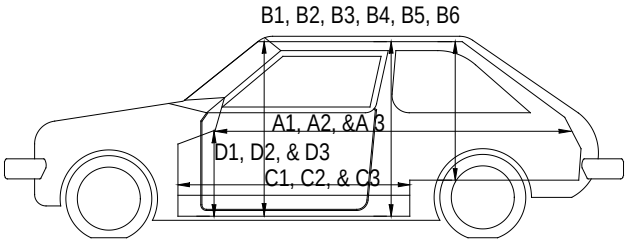
Note: Use as many lines/columns as necessary to describe each damage profile.

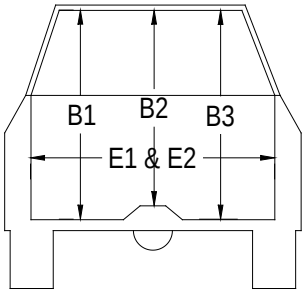
Table E.3. Occupant Compartment Measurements for Test No. 469137-3-2.

Date: 2017-09-05 Test No.: 469137-3-2 VIN No.: KNADH4A38B6960769

Year: 2011 Make: Kia Model: Rio







OCCUPANT COMPARTMENT DEFORMATION MEASUREMENT

	Before	After (inches)	Differ.
A1	67.50	67.50	0
A2	67.50	67.50	0
A3	67.75	67.75	0
B1	40.50	40.50	0
B2	36.75	36.75	0
B3	40.50	40.50	0
B4	36.25	36.25	0
B5	35.75	35.75	0
B6	36.25	36.25	0
C1	26.00	26.00	0
C2	-----	-----	-
C3	26.00	26.00	0
D1	9.50	9.50	0
D2	-----	-----	-
D3	9.75	9.75	0
E1	51.50	51.50	0
E2	51.00	51.00	0
F	51.00	51.00	0
G	51.00	51.00	0
H	38.00	38.00	0
I	38.00	38.00	0
J*	51.00	51.00	0

*Lateral area across the cab from
driver's side kickpanel to passenger's side kickpanel.

E.2 SEQUENTIAL PHOTOGRAPHS

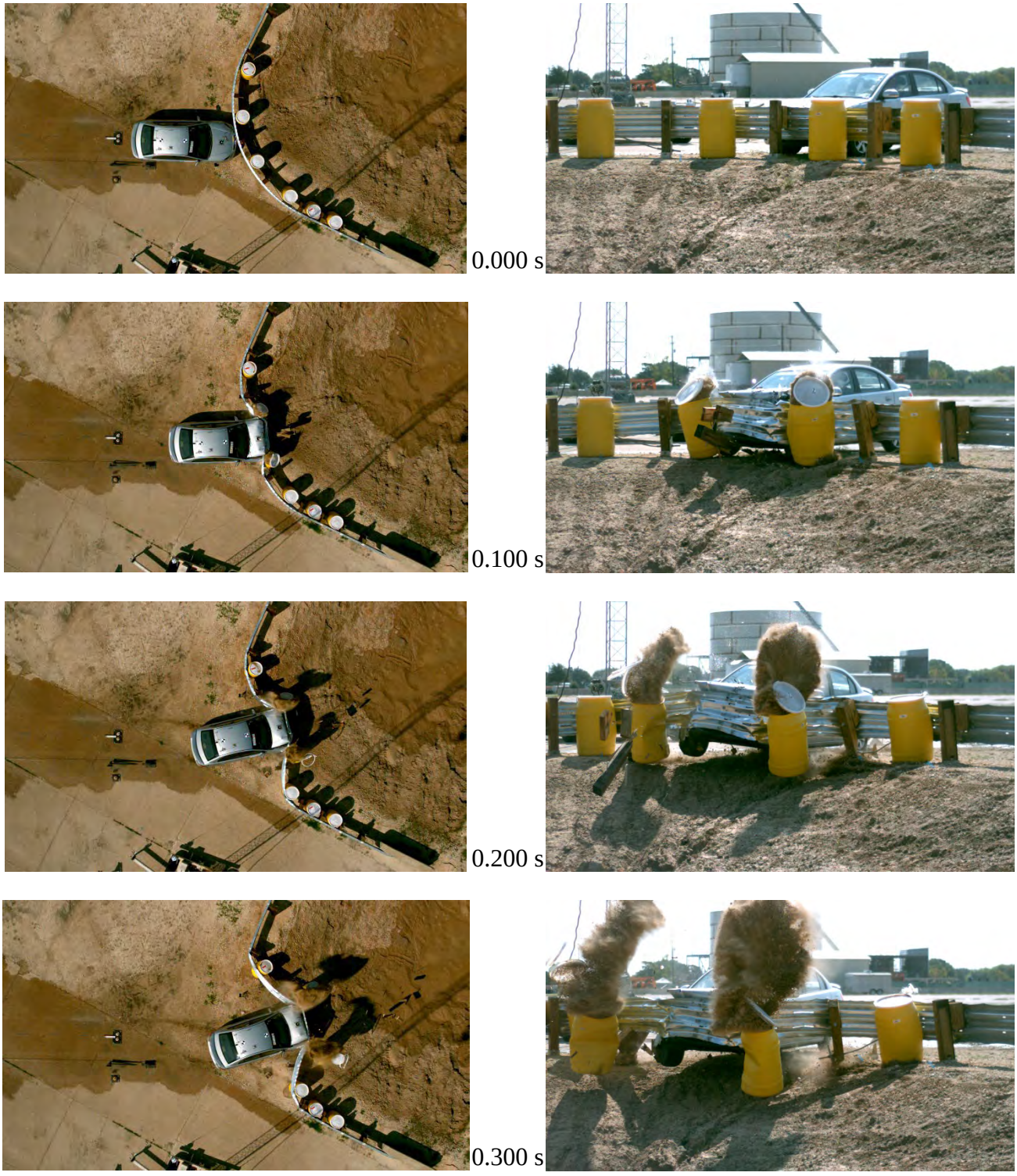


Figure E.1. Sequential Photographs for Test No. 469137-3-2 (Overhead and Frontal Views).

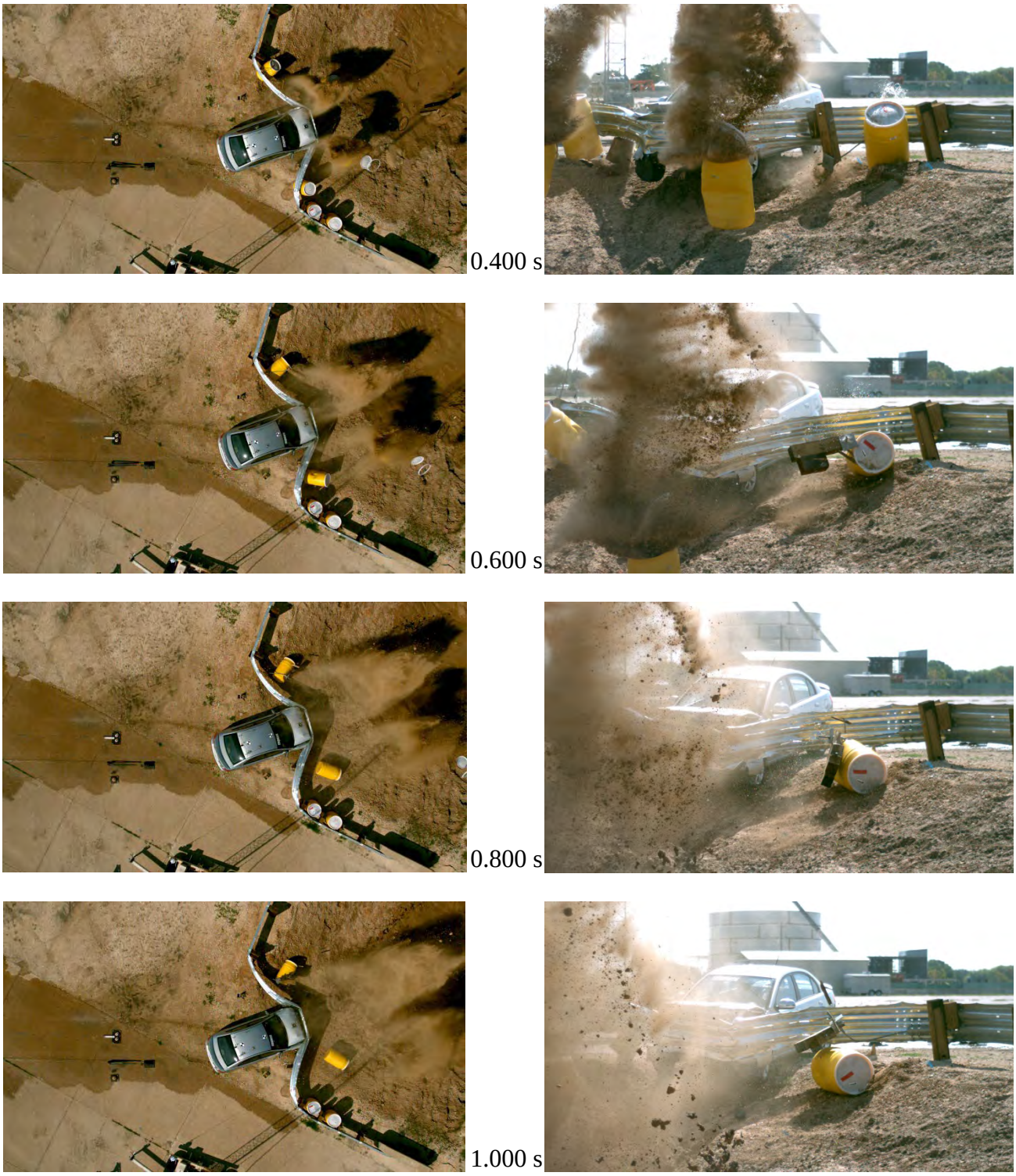


Figure E.1. Sequential Photographs for Test No. 469137-3-2 (Overhead and Frontal Views) (Continued).

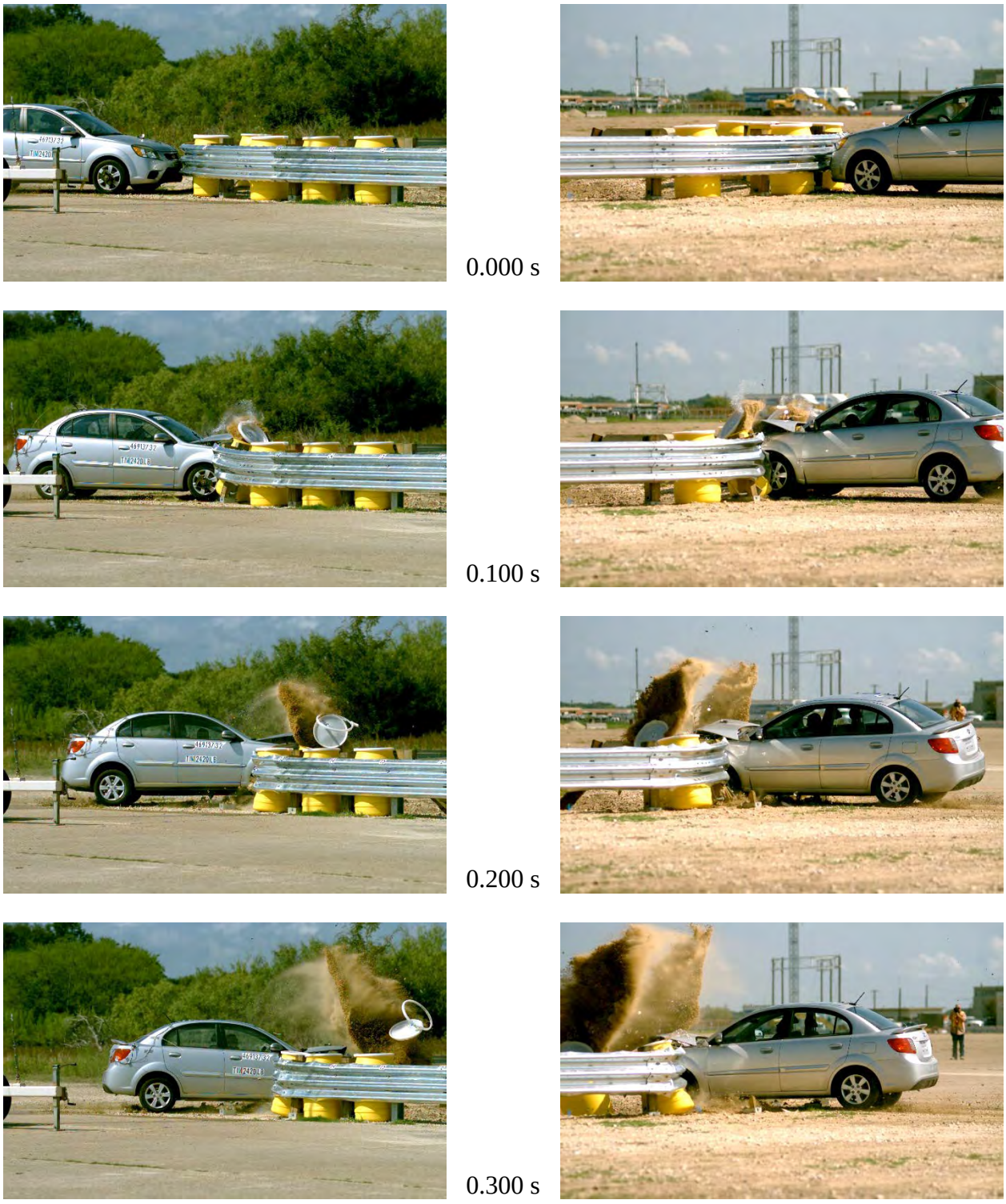
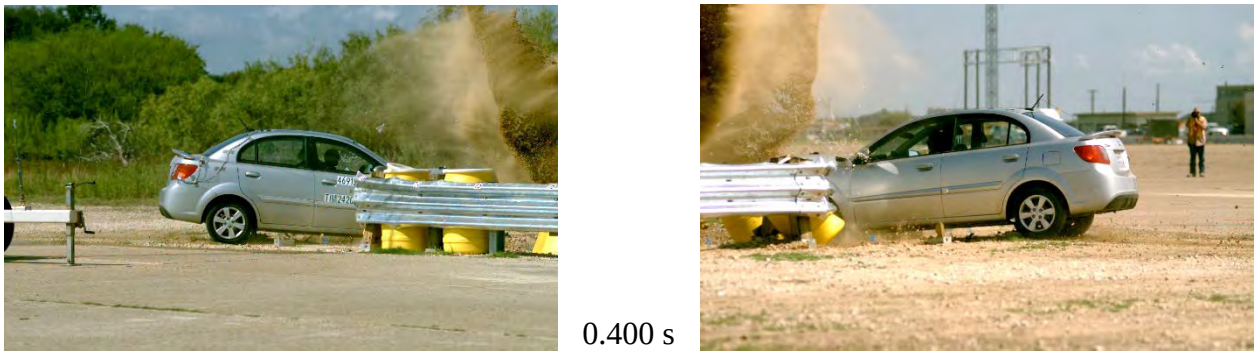


Figure E.2. Sequential Photographs for Test No. 469137-3-2 (Perpendicular Views).


0.400 s


0.600 s


0.800 s

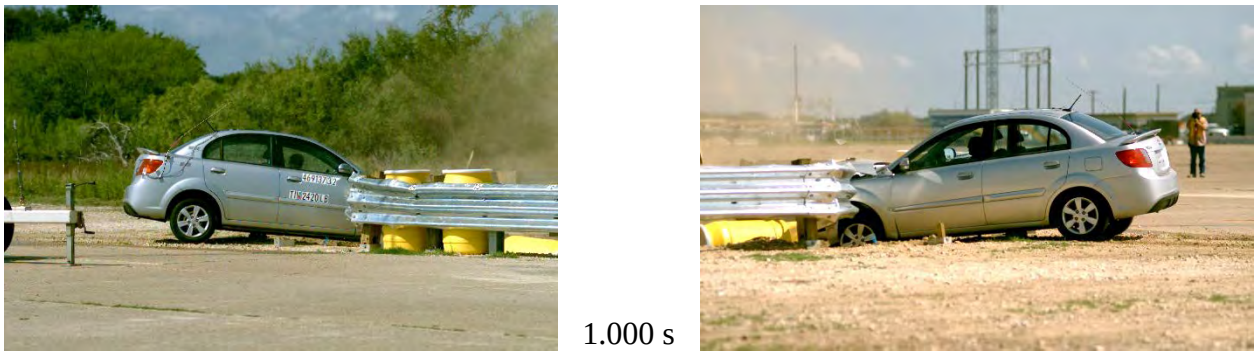

1.000 s

Figure E.2. Sequential Photographs for Test No. 469137-3-2 (Perpendicular Views) (Continued).

E.3 VEHICLE ANGULAR DISPLACEMENTS

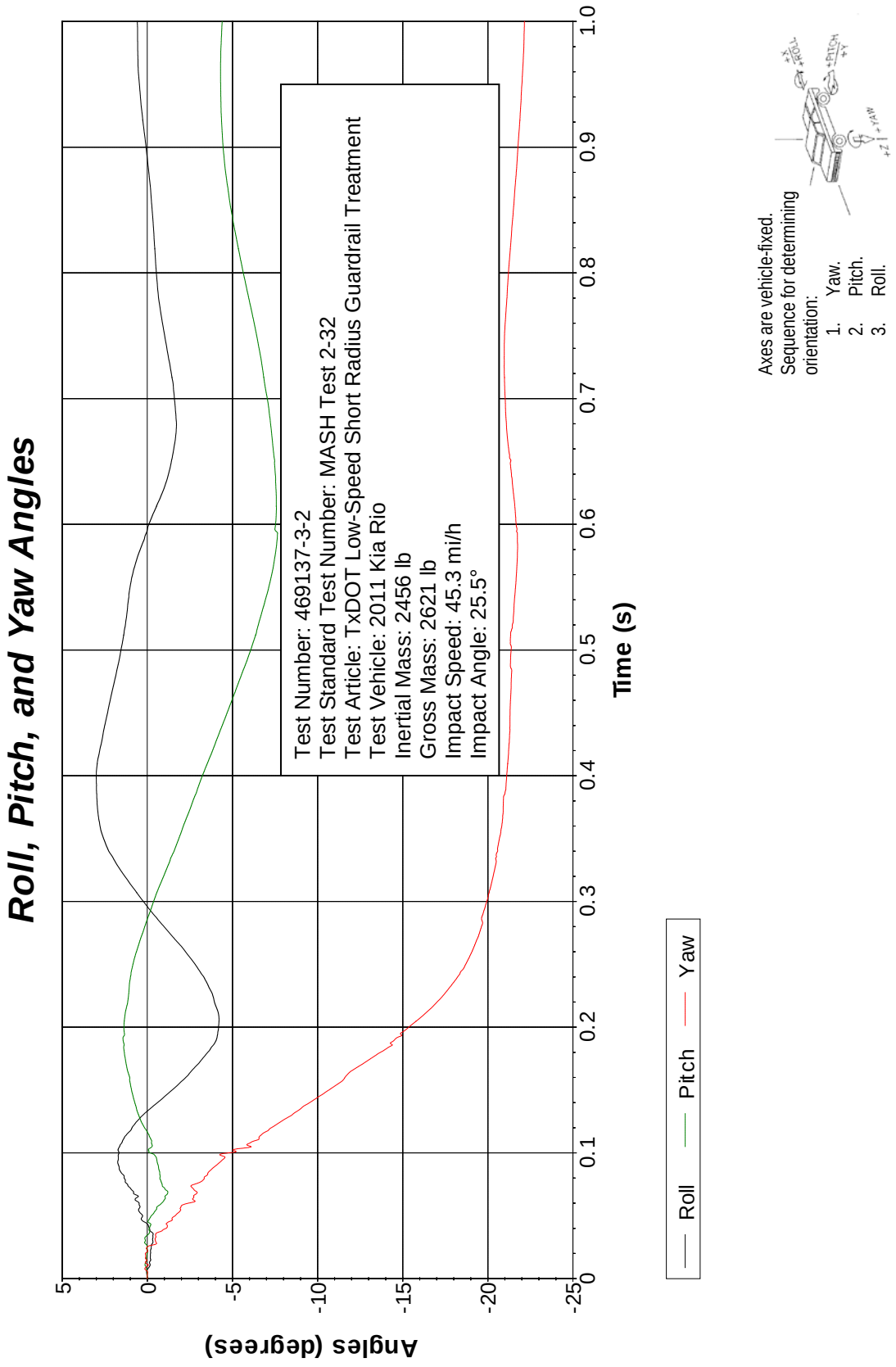


Figure E.3. Vehicle Angular Displacements for Test No. 469137-3-2.

E.4 VEHICLE ACCELERATIONS

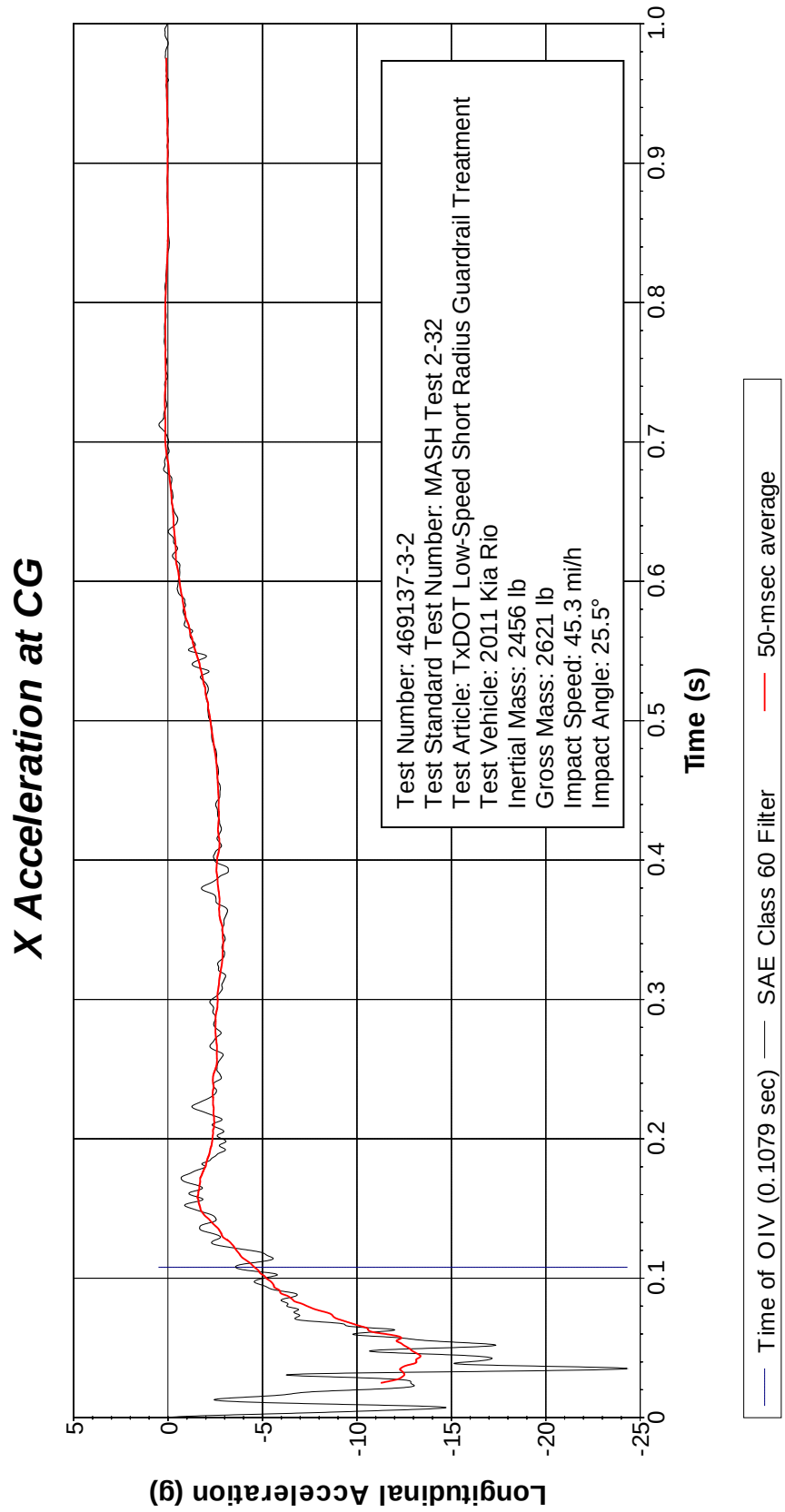


Figure E.4. Vehicle Longitudinal Accelerometer Trace for Test No. 469137-3-2 (Accelerometer Located at Center of Gravity).

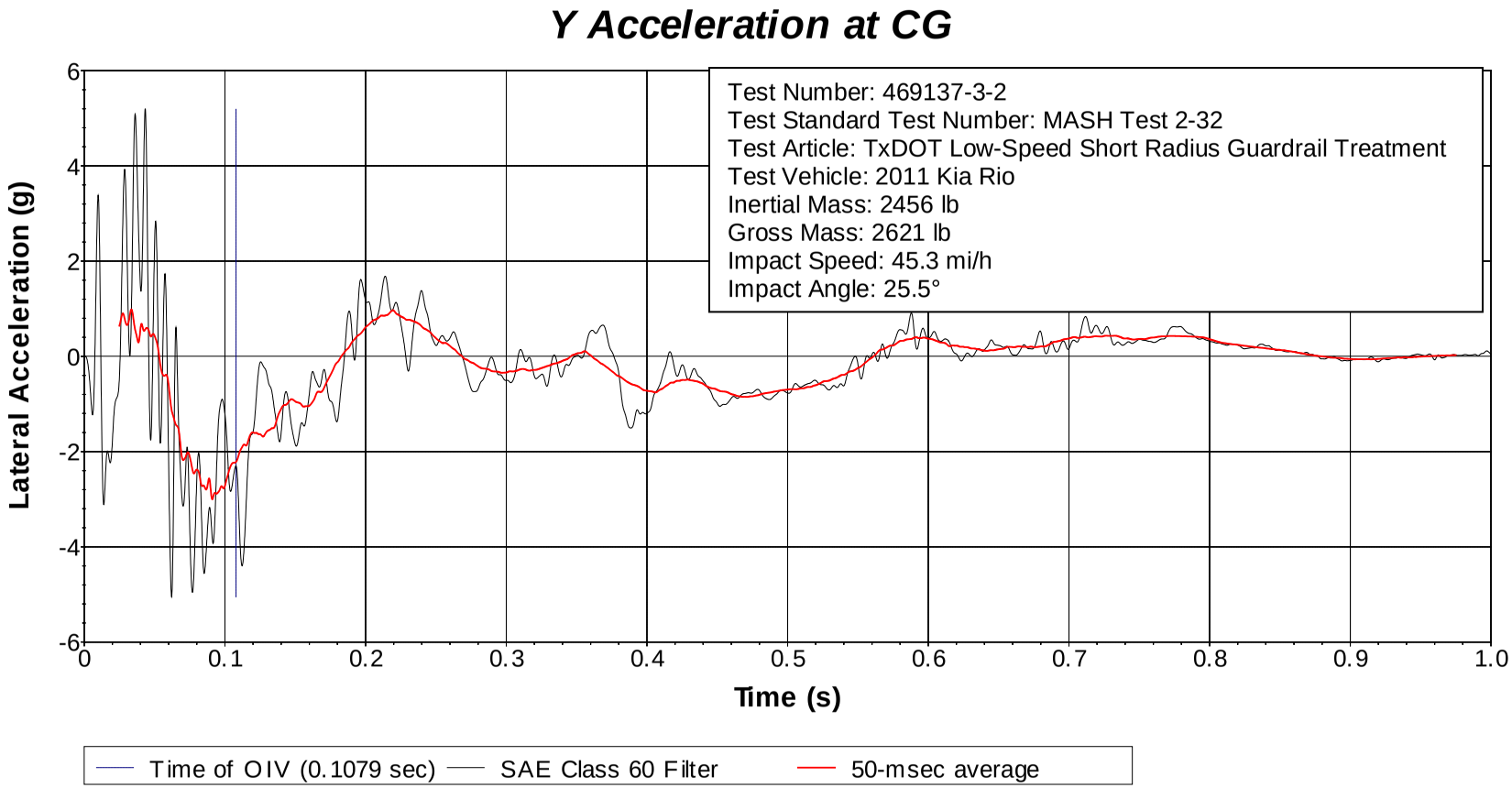


Figure E.5. Vehicle Lateral Accelerometer Trace for Test No. 469137-3-2 (Accelerometer Located at Center of Gravity).

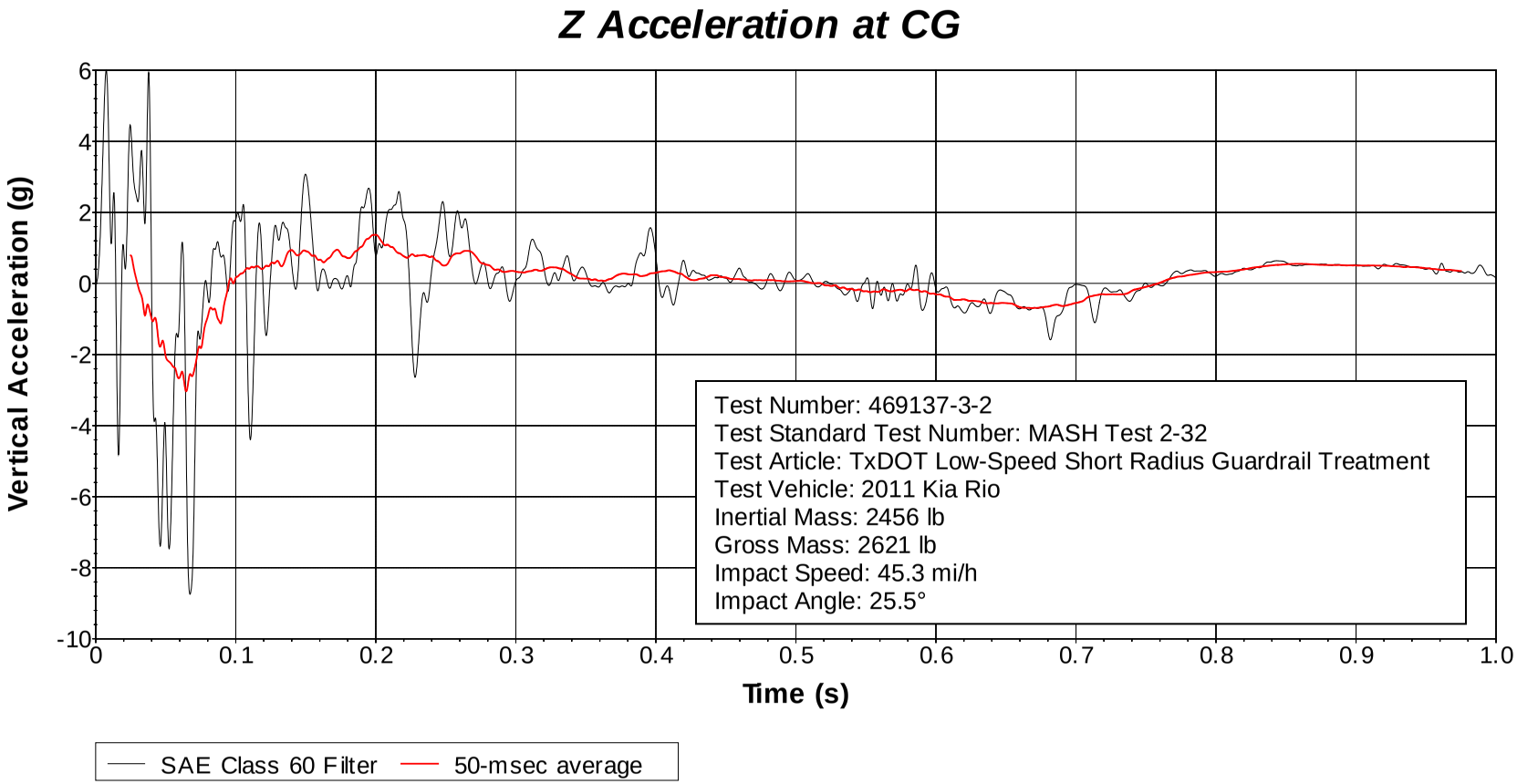


Figure E.6. Vehicle Vertical Accelerometer Trace for Test No. 469137-3-2 (Accelerometer Located at Center of Gravity).

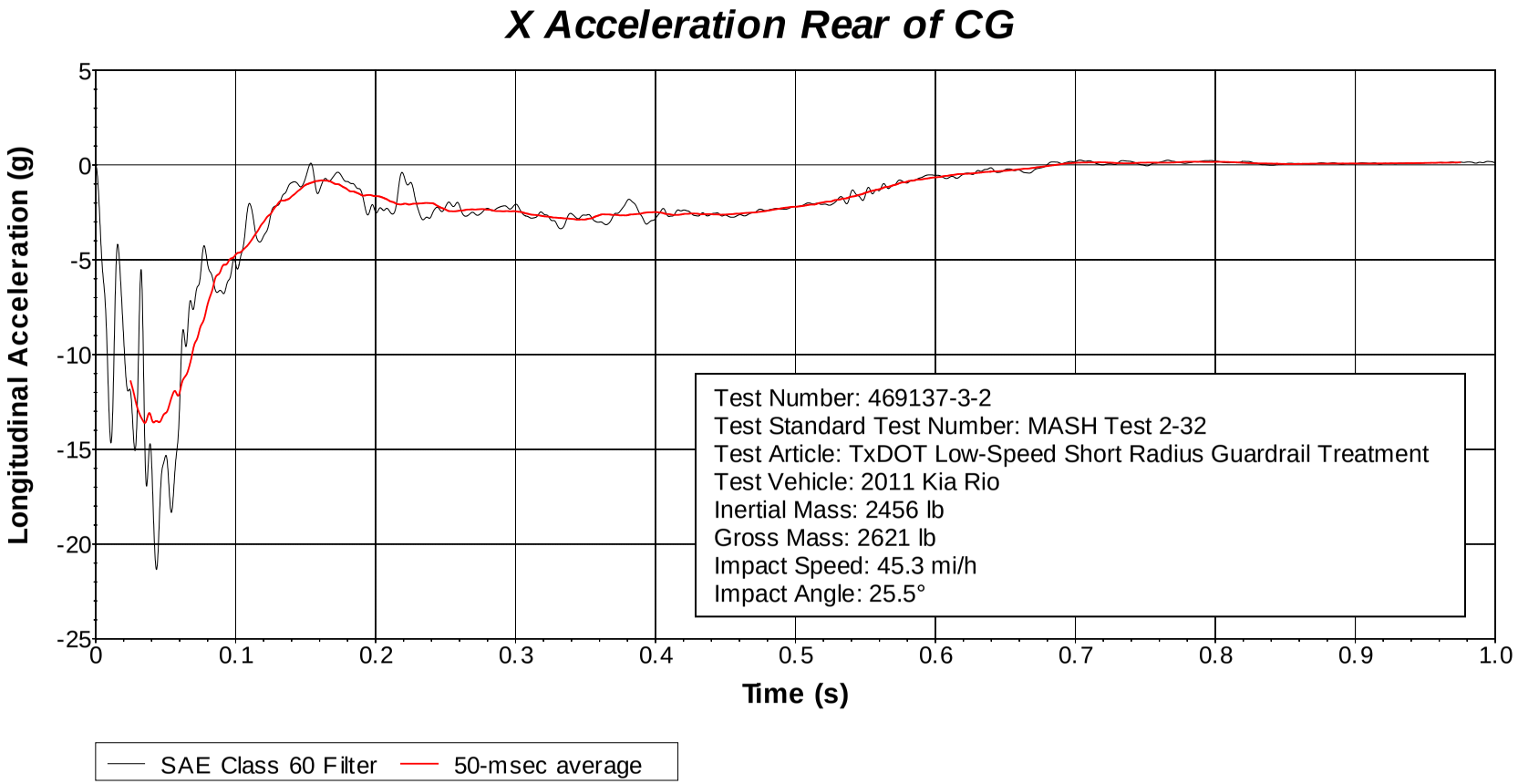


Figure E.7. Vehicle Longitudinal Accelerometer Trace for Test No. 469137-3-2 (Accelerometer Located Rear of Center of Gravity).

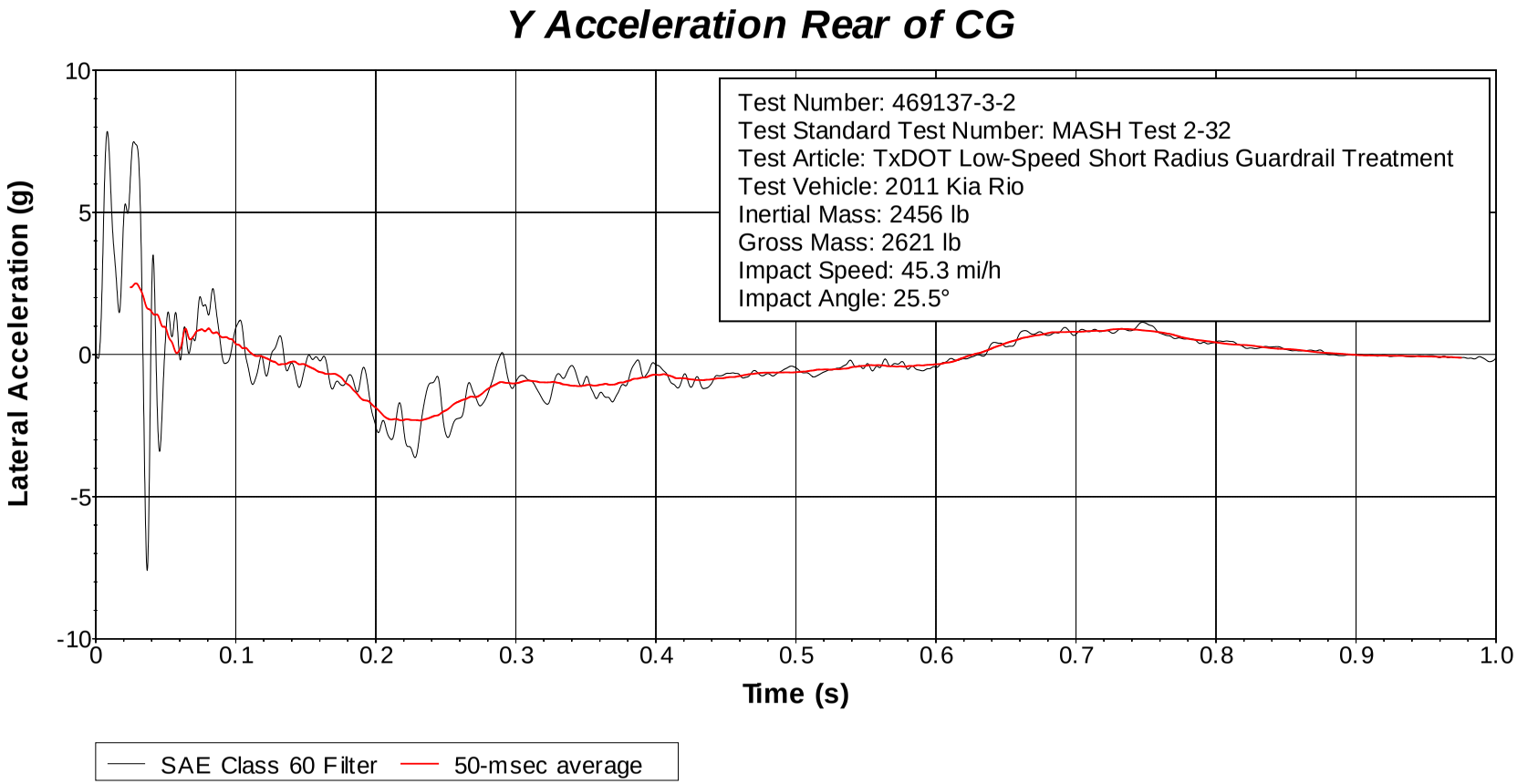


Figure E.8. Vehicle Lateral Accelerometer Trace for Test No. 469137-3-2 (Accelerometer Located Rear of Center of Gravity).

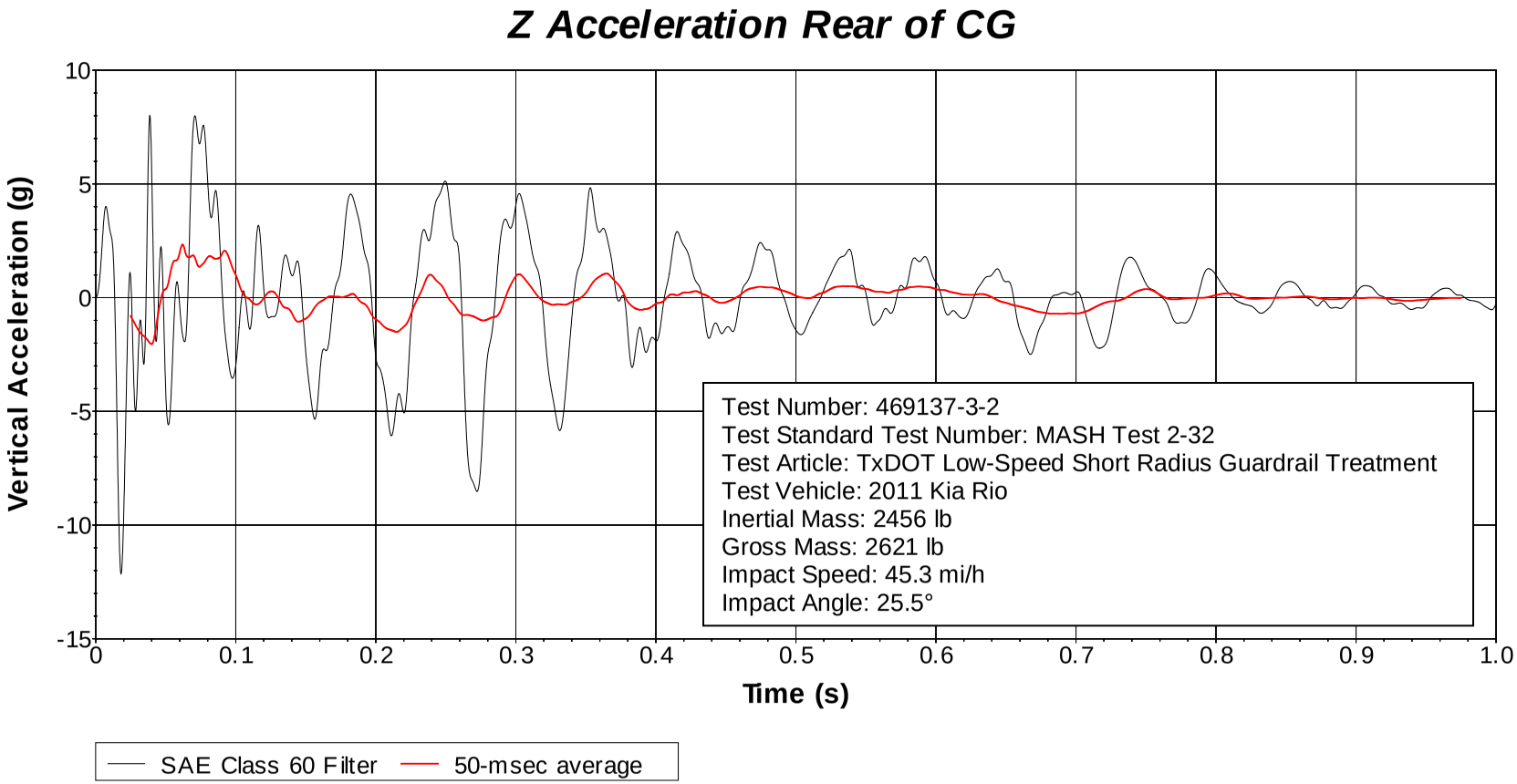


Figure E.9. Vehicle Vertical Accelerometer Trace for Test No. 469137-3-2 (Accelerometer Located Rear of Center of Gravity).

APPENDIX F. *MASH* TEST 2-31 (CRASH TEST NO. 469138-3-3)

F.1 VEHICLE PROPERTIES AND INFORMATION

Table F.1. Vehicle Properties for Test No. 469138-3-3.

Date: 2017-09-15 Test No.: 469138-3-3 VIN No.: 1C6RD6FP6CS180345

Year: 2012 Make: Dodge Model: RAM 1500

Tire Size: 265/70R17 Tire Inflation Pressure: 35 psi

Tread Type: Highway Odometer: 195261

Note any damage to the vehicle prior to test: None

• Denotes accelerometer location.

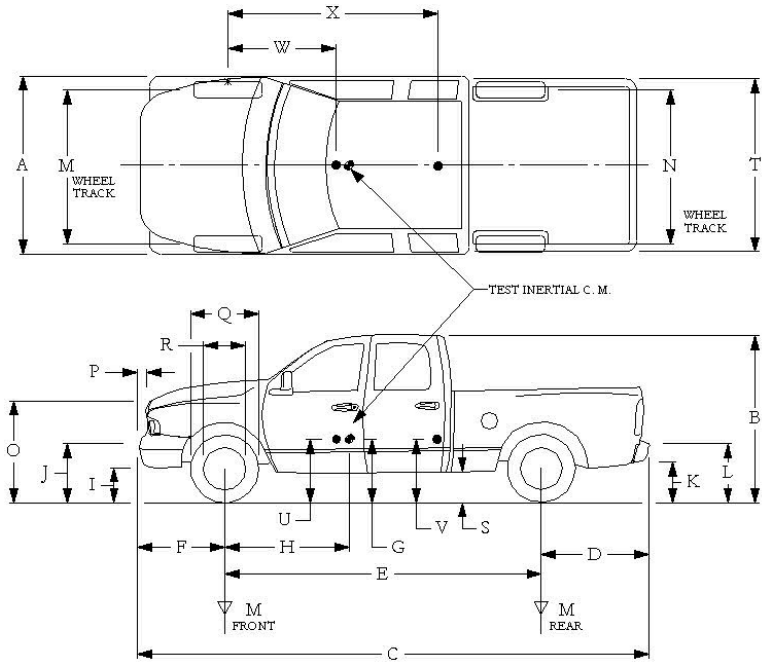
NOTES: None

Engine Type: V-8
Engine CID: 4.7 liter

Transmission Type:
x Auto or ____ Manual
____ FWD x RWD ____ 4WD

Optional Equipment:
None

Dummy Data:
Type: None
Mass: NA
Seat Position: NA



Geometry: inches

A	78.50	F	40.00	K	20.75	P	3.00	U	27.50
B	75.00	G	28.25	L	29.50	Q	30.50	V	30.25
C	227.50	H	62.15	M	68.50	R	18.00	W	62.10
D	47.00	I	11.00	N	68.00	S	13.25	X	78.50
E	140.50	J	26.50	O	46.00	T	77.00		

Wheel Center Height Front	14.75	Wheel Well Clearance (Front)	6.00	Bottom Frame Height - Front	17.00
Wheel Center Height Rear	14.75	Wheel Well Clearance (Rear)	9.25	Bottom Frame Height - Rear	25.50

GVWR Ratings:		**Mass:** lb	Curb	Test Inertial	Gross Static
Front	3700	M_{front}	2944	2807	------
Back	3900	M_{rear}	2170	2227	------
Total	6700	M_{Total}	5114	5034	------

(Allowable Range for TIM and GSM = 5000 lb ±110 lb)

Mass Distribution:

lb	LF:	RF:	LR:	RR:
	1383	1424	1128	1099

Table F.2. Measurements of Vehicle Vertical CG for Test No. 469137-3-1.

Date: 2017-09-15 Test No.: 469138-3-3 VIN: 1C6RD6FP6CS180345

Year: 2012 Make: Dodge Model: RAM 1500

Body Style: Quad Cab Mileage: 195261

Engine: 4.7 liter V-8 Transmission: Automatic

Fuel Level: Empty Ballast: 172 lb (440 lb max)

Tire Pressure: Front: 35 psi Rear: 35 psi Size: 265/70R17

Measured Vehicle Weights: (lb)								
LF:	1383	RF:	1424	Front Axle:	2807			
LR:	1128	RR:	1099	Rear Axle:	2227			
Left:	2511	Right:	2523	Total:	5034			
				5000 ±110 lb allowed				
Wheel Base:	140.5 inches	Track: F:	68.5 inches	R:	68 inches			
148 ±12 inches allowed			Track = (F+R)/2 = 67 ±1.5 inches allowed					
Center of Gravity, SAE J874 Suspension Method								
X:	62.16 inches	Rear of Front Axle	(63 ±4 inches allowed)					
Y:	0.08 inches	Left - Right +	of Vehicle Centerline					
Z:	28.25 inches	Above Ground	(minumum 28.0 inches allowed)					

Hood Height: 46.00 inches
43 ±4 inches allowed

Front Bumper Height: 26.50 inches

Front Overhang: 40.00 inches
39 ±3 inches allowed

Rear Bumper Height: 29.50 inches

Overall Length: 227.50 inches
237 ±13 inches allowed

Table F.3. Exterior Crush Measurements of Vehicle for Test No. 469138-3-3.

Date: 2017-09-15 Test No.: 469137-3-1 VIN No.: 1C6RD6FP6CS180345

Year: 2012 Make: Dodge Model: RAM 1500

VEHICLE CRUSH MEASUREMENT SHEET[1]

Complete When Applicable	
End Damage	Side Damage
Undeformed end width _____ Corner shift: A1 _____ A2 _____ End shift at frame (CDC) (check one) < 4 inches _____ ≥ 4 inches _____	Bowing: B1 _____ X1 _____ B2 _____ X2 _____ Bowing constant $\frac{X1+X2}{2}$ = _____

Note: Measure C_1 to C_6 from Driver to Passenger Side in Front or Rear impacts – Rear to Front in Side Impacts.

Specific Impact Number	Plane* of C-Measurements	Direct Damage		Field L**	C_1	C_2	C_3	C_4	C_5	C_6	±D
		Width** (CDC)	Max*** Crush								
1	Front plane at bumper ht	20	9	36	9	7	2	1	1	0	-18
2	Side plane at bumper ht	20	8	24	--	8	7	7	--	--	+88
	Measurements recorded										
	in inches										

[1]Table taken from National Accident Sampling System (NASS).

*Identify the plane at which the C-measurements are taken (e.g., at bumper, above bumper, at sill, above sill, at beltline, etc.) or label adjustments (e.g., free space).

Free space value is defined as the distance between the baseline and the original body contour taken at the individual C locations. This may include the following: bumper lead, bumper taper, side protrusion, side taper, etc.
Record the value for each C-measurement and maximum crush.

**Measure and document on the vehicle diagram the beginning or end of the direct damage width and field L (e.g., side damage with respect to undamaged axle).

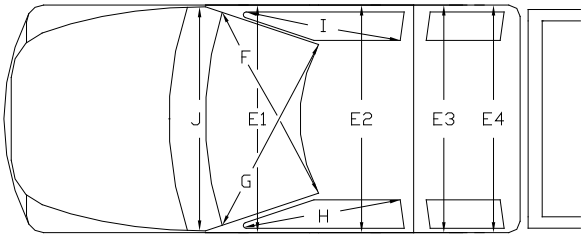
***Measure and document on the vehicle diagram the location of the maximum crush.

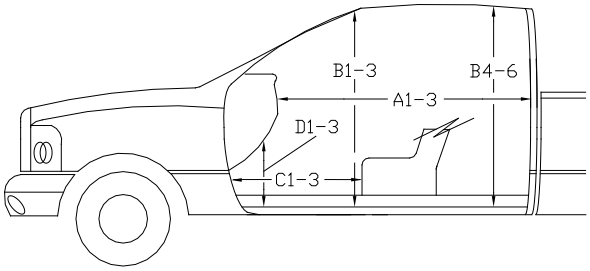
Note: Use as many lines/columns as necessary to describe each damage profile.

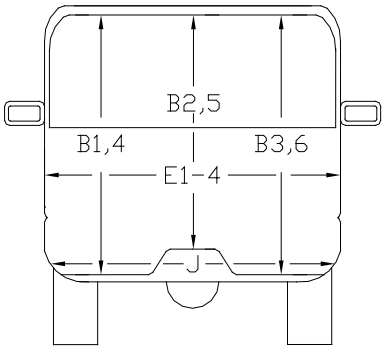
Table F.4. Occupant Compartment Measurements of Vehicle for Test No. 469138-3-3.

Date: 2017-08-18 Test No.: 469137-3-1 VIN No.: 1C6RD6FP6CS180345

Year: 2012 Make: Dodge Model: RAM 1500







*Lateral area across the cab from driver's side kickpanel to passenger's side kickpanel.

OCCUPANT COMPARTMENT DEFORMATION MEASUREMENT

	Before	After (inches)	Differ.
A1	65.00	65.00	0
A2	63.00	63.00	0
A3	65.50	65.50	0
B1	44.50	44.50	0
B2	38.25	38.25	0
B3	44.50	44.50	0
B4	39.50	39.50	0
B5	43.00	43.00	0
B6	39.50	39.50	0
C1	27.00	27.00	0
C2	-----	-----	-
C3	27.00	27.00	0
D1	11.25	11.25	0
D2	-----	-----	-
D3	11.25	11.25	0
E1	58.75	58.75	0
E2	63.50	63.50	0
E3	63.50	63.50	0
E4	63.25	63.25	0
F	59.00	59.00	0
G	59.00	59.00	0
H	37.00	37.00	0
I	37.00	37.00	0
J*	23.00	23.00	0

F.2 SEQUENTIAL PHOTOGRAPHS

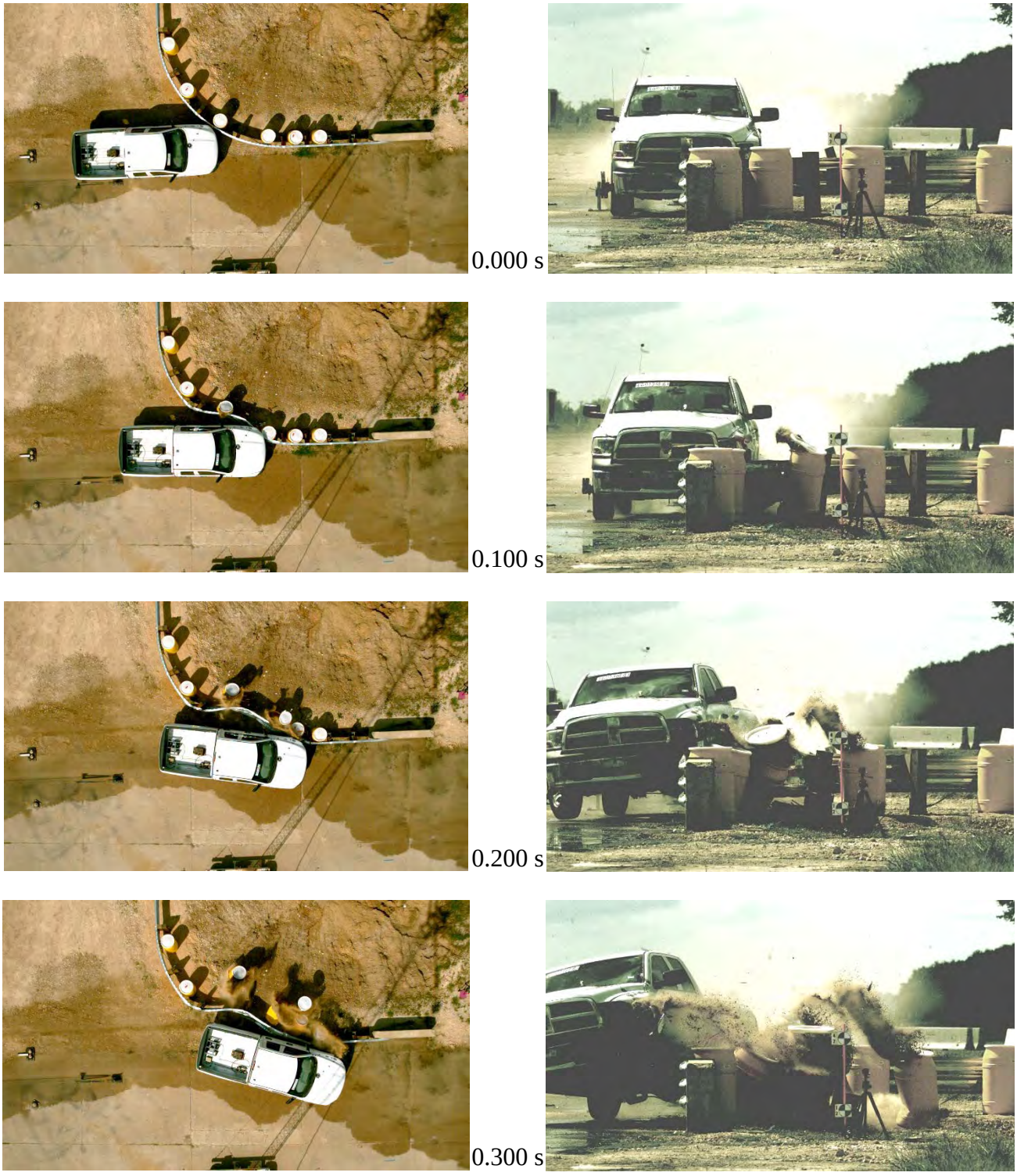
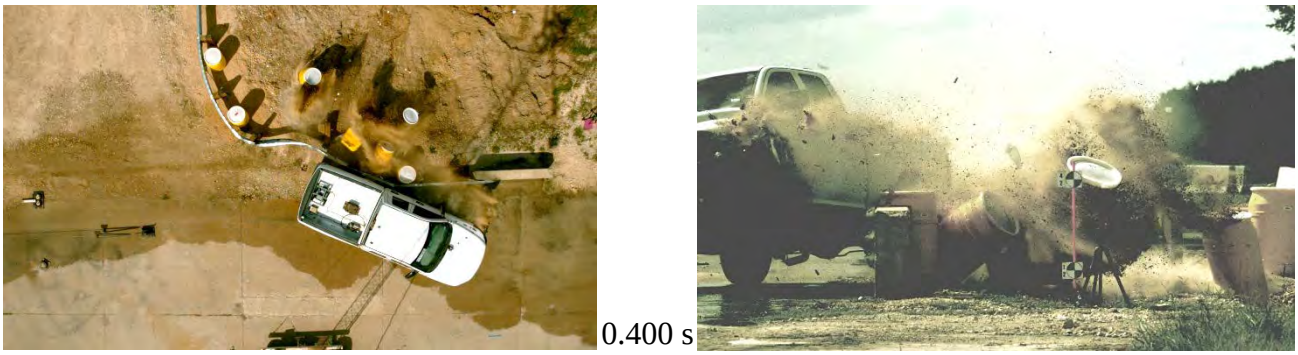
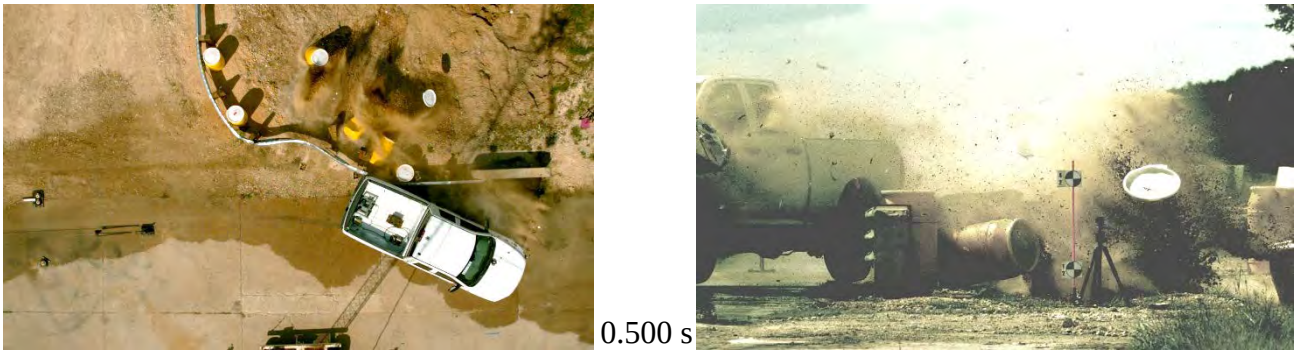
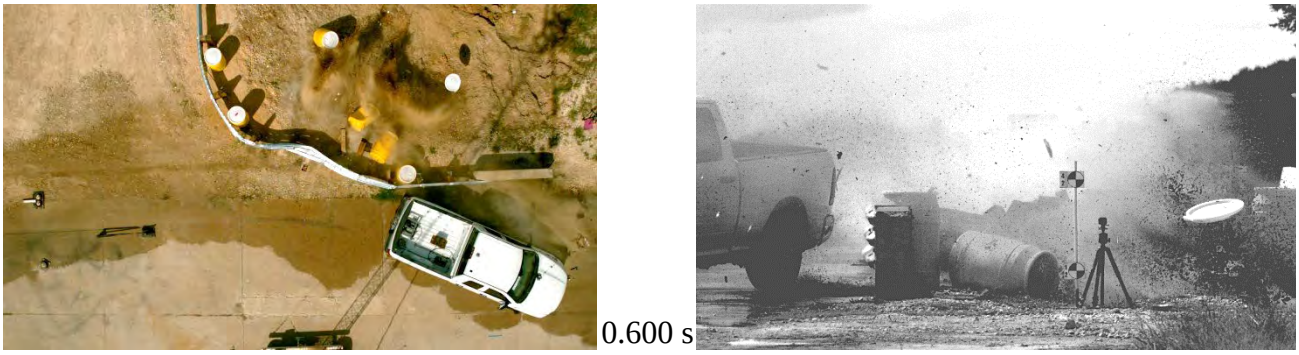


Figure F.1. Sequential Photographs for Test No. 469138-3-3 (Overhead and Frontal Views).


0.400 s


0.500 s


0.600 s

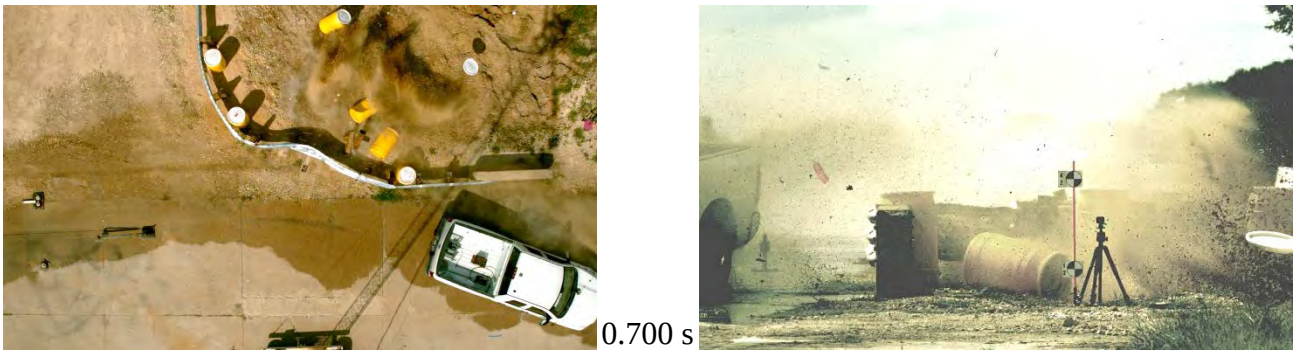

0.700 s

Figure F.1. Sequential Photographs for Test No. 469138-3-3 (Overhead and Frontal Views) (Continued).


0.000 s


0.400 s


0.100 s


0.500 s


0.200 s


0.600 s


0.300 s


0.700 s

Figure F.2. Sequential Photographs for Test No. 469138-3-3 (Perpendicular View).

F.3 VEHICLE ANGULAR DISPLACEMENT

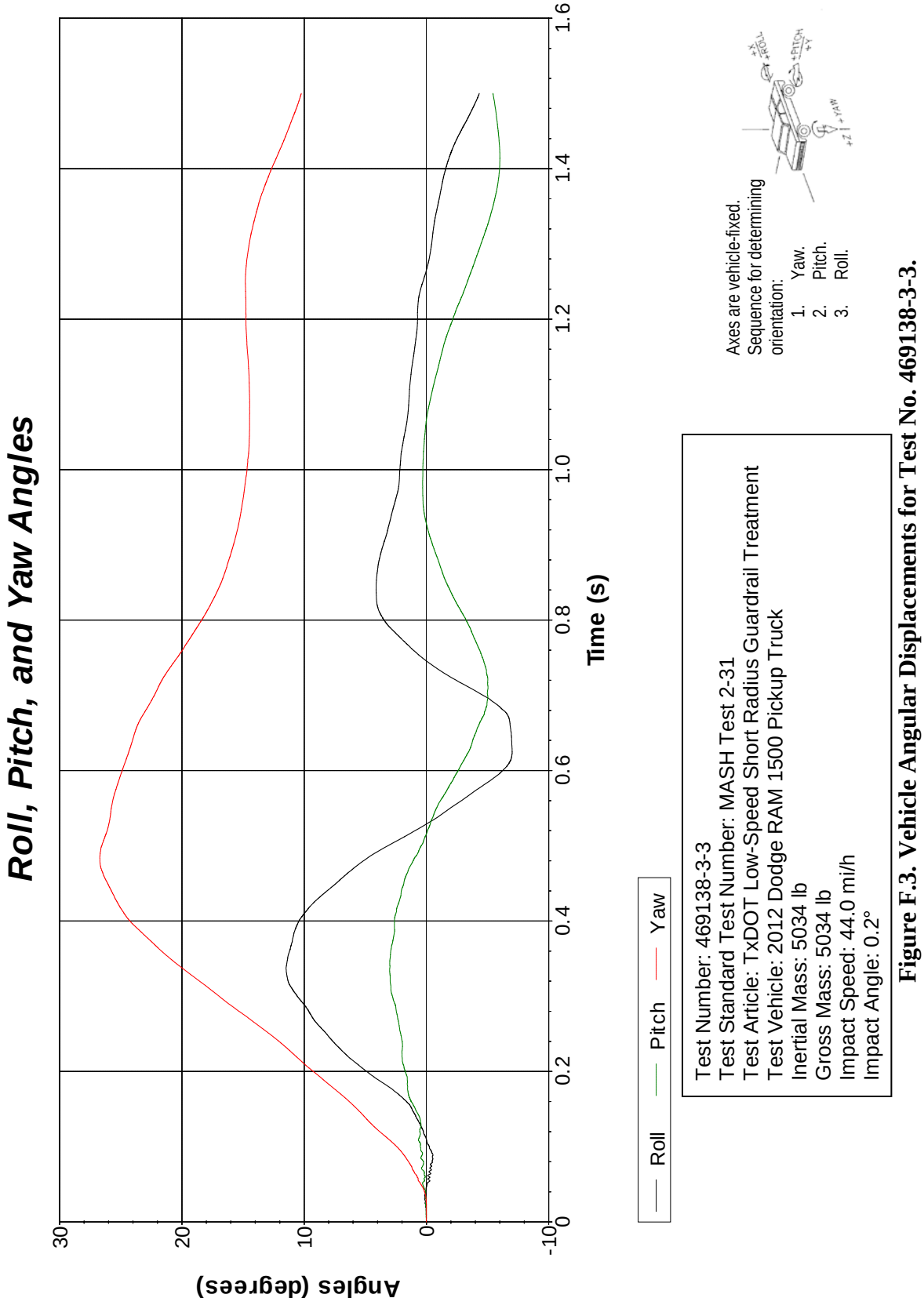


Figure F.3. Vehicle Angular Displacements for Test No. 469138-3-3.

F.4 VEHICLE ACCELERATIONS

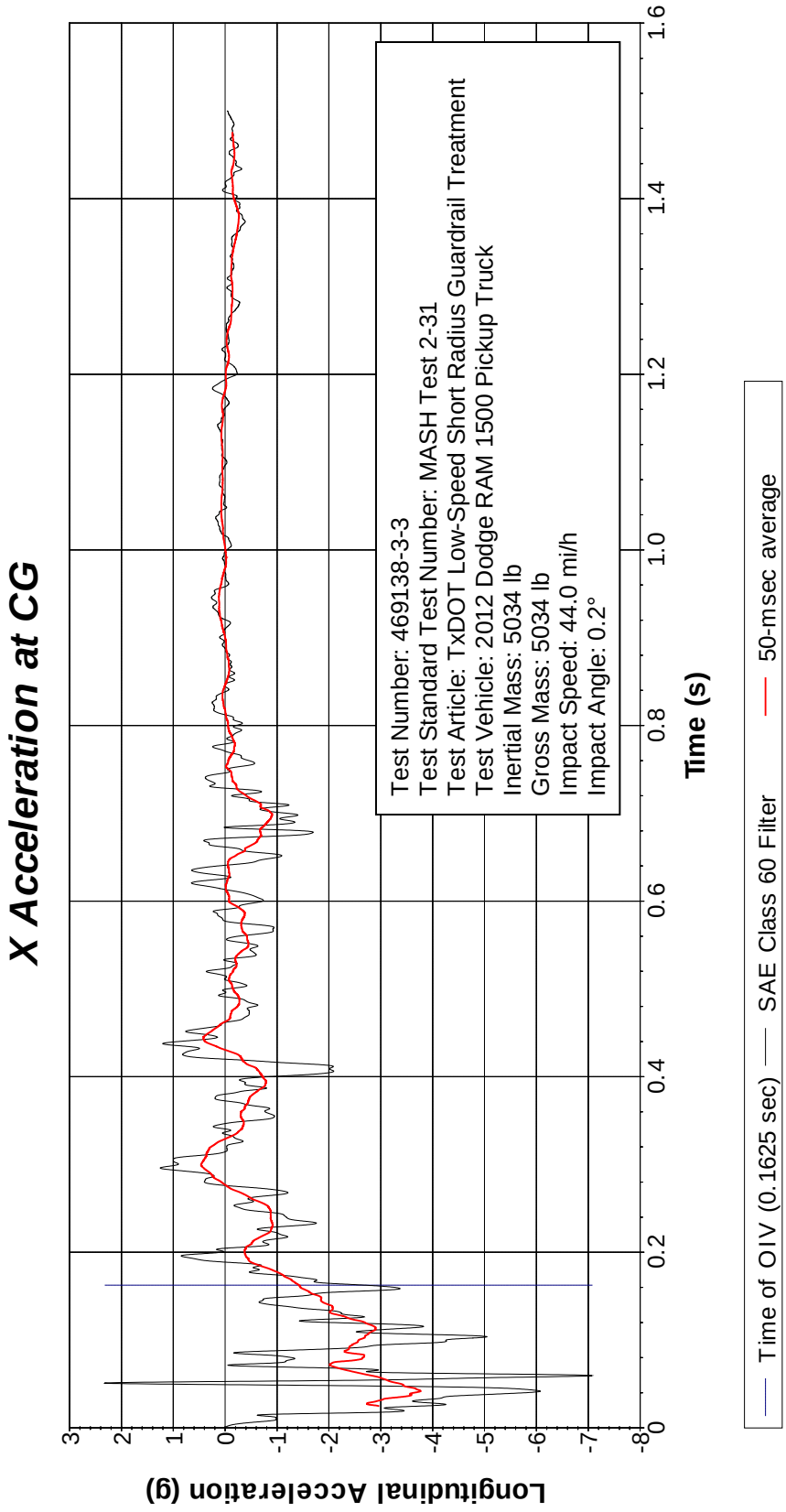


Figure F.4. Vehicle Longitudinal Accelerometer Trace for Test No. 469138-3-3 (Accelerometer Located at Center of Gravity).

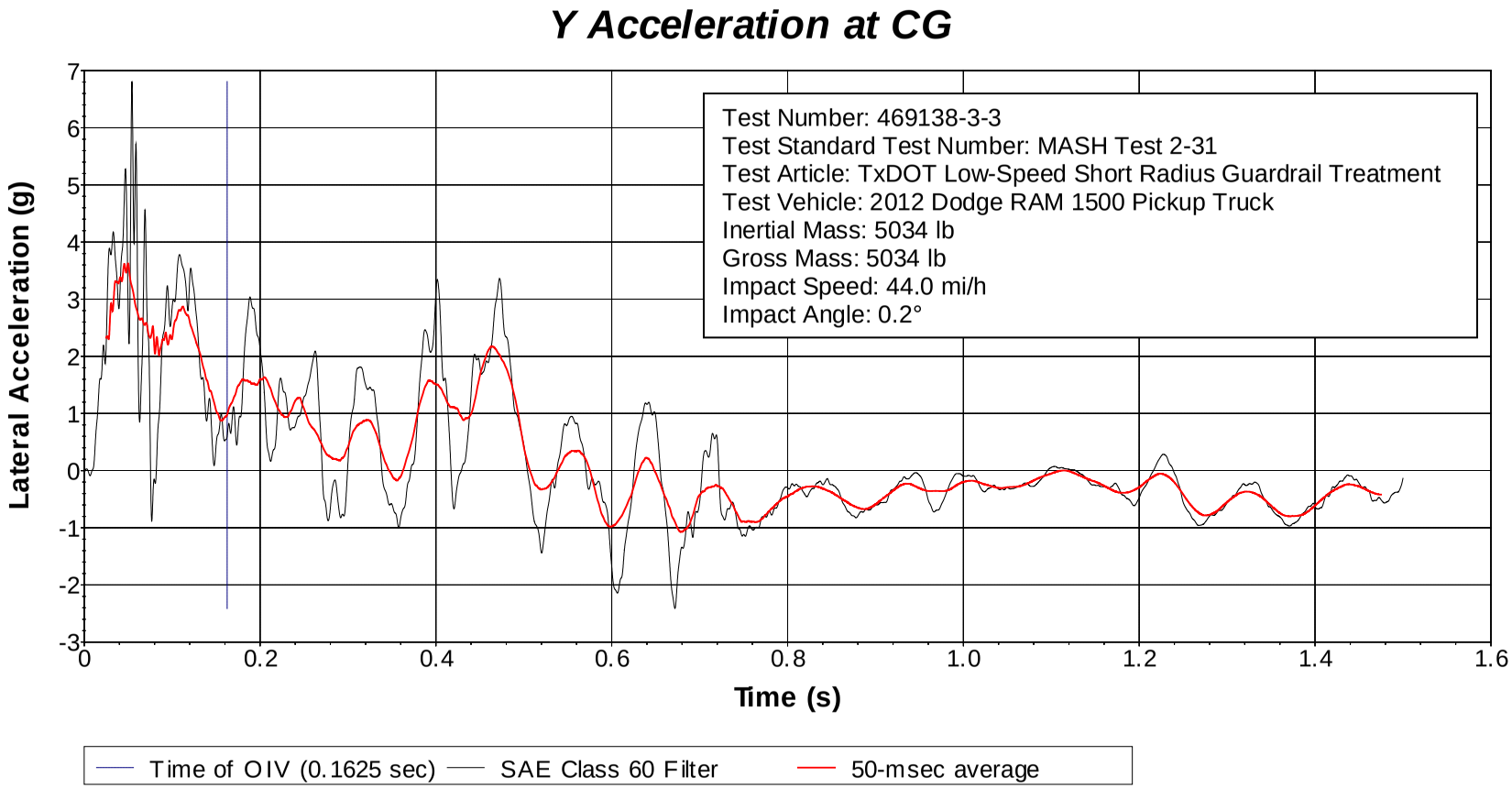


Figure F.5. Vehicle Lateral Accelerometer Trace for Test No. 469138-3-3 (Accelerometer Located at Center of Gravity).

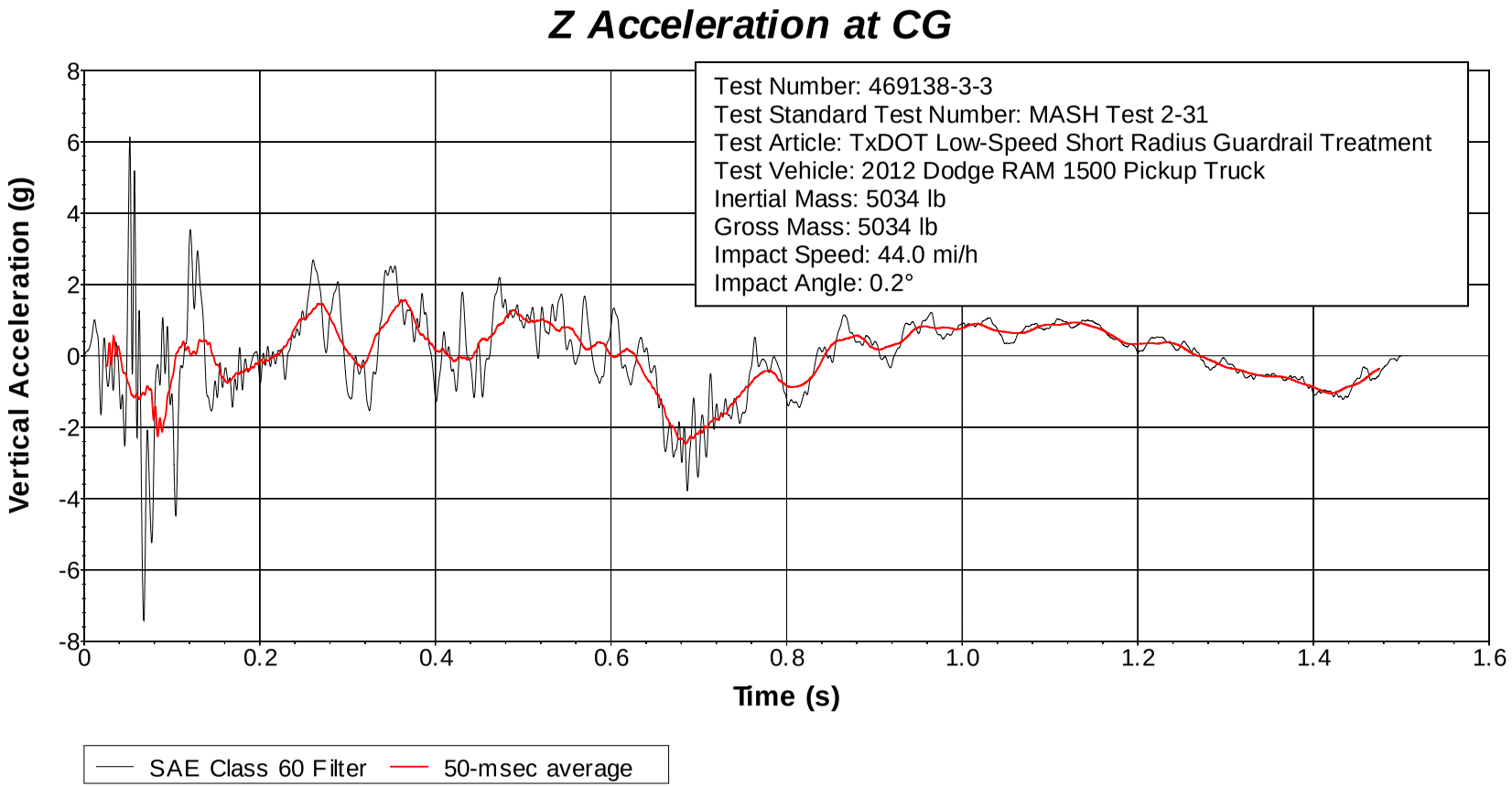


Figure F.6. Vehicle Vertical Accelerometer Trace for Test No. 469138-3-3 (Accelerometer Located at Center of Gravity).

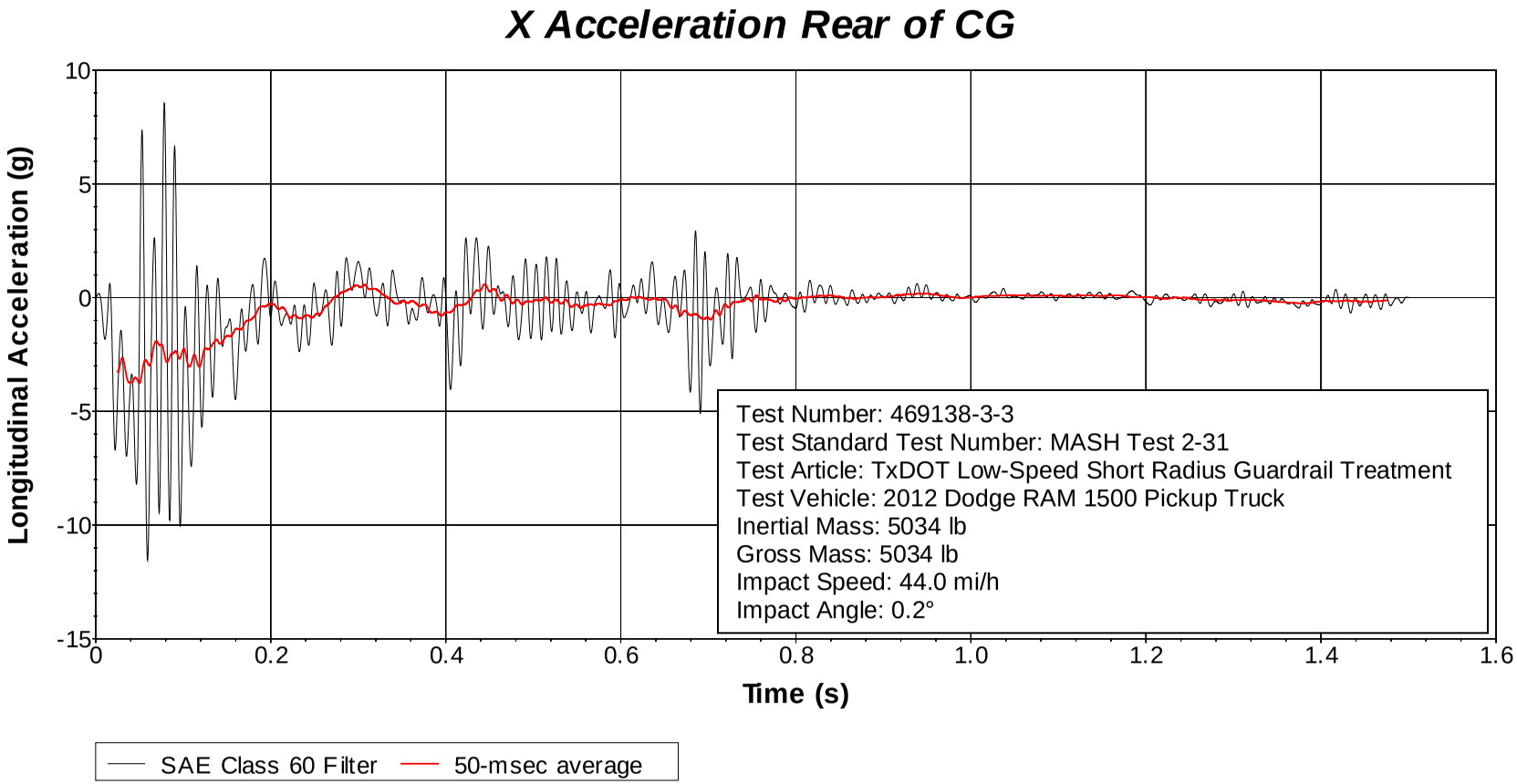


Figure F.7. Vehicle Longitudinal Accelerometer Trace for Test No. 469138-3-3 (Accelerometer Located Rear of Center of Gravity).

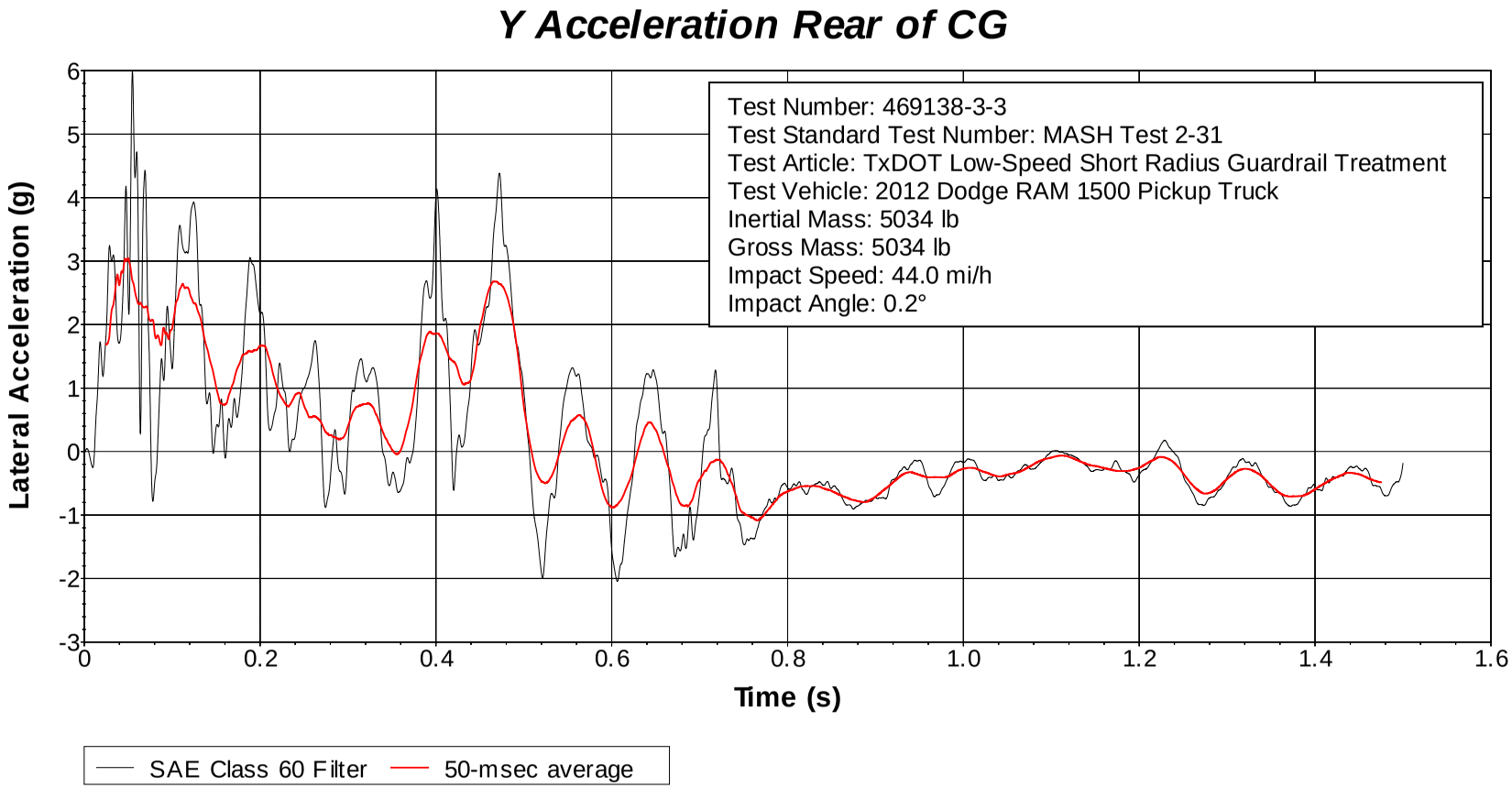


Figure F.8. Vehicle Lateral Accelerometer Trace for Test No. 469138-3-3 (Accelerometer Located Rear of Center of Gravity).

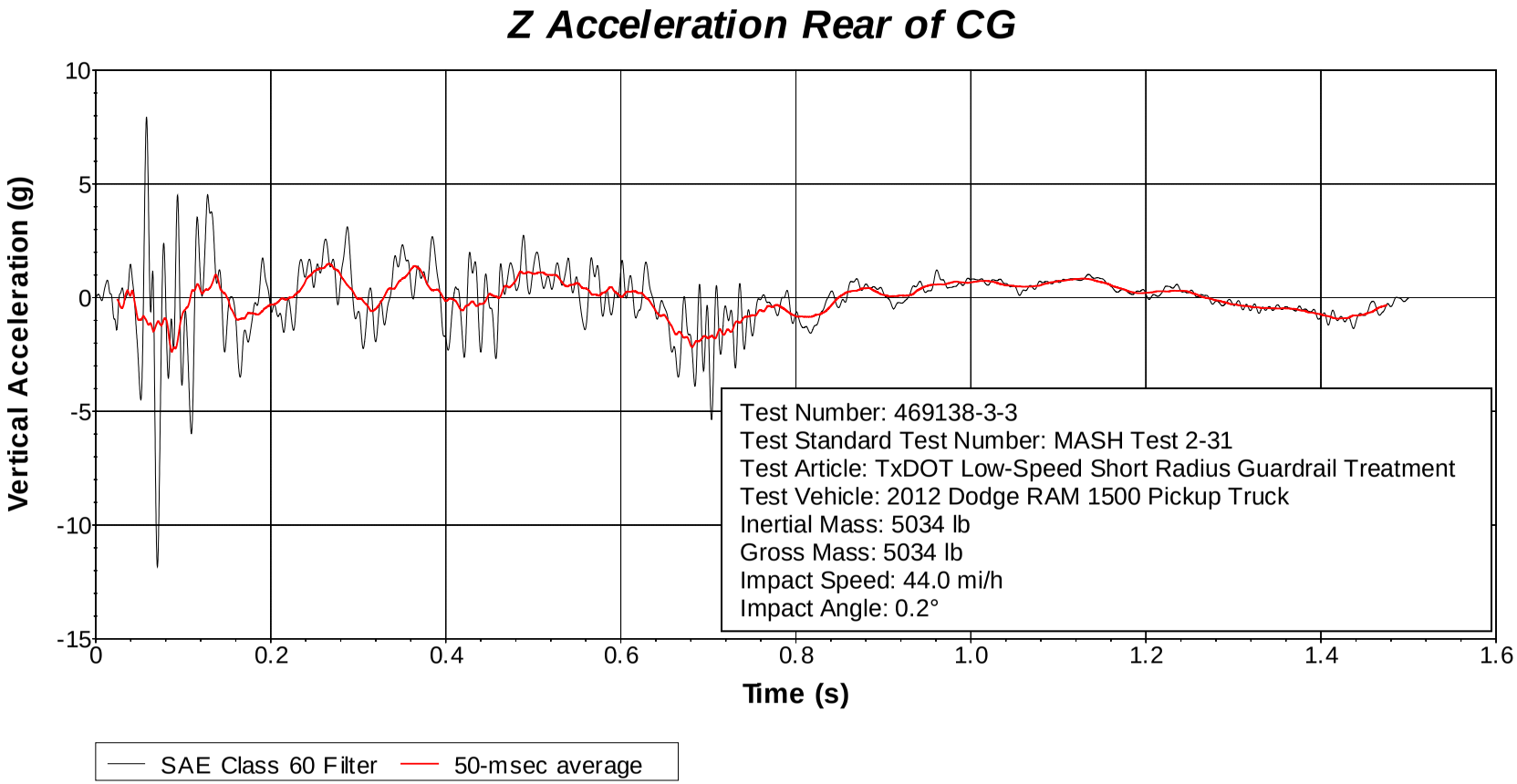


Figure F.9. Vehicle Vertical Accelerometer Trace for Test No. 469138-3-3 (Accelerometer Located Rear of Center of Gravity).

APPENDIX G. *MASH* TEST 2-35 (CRASH TEST NO. 469138-3-4)

G.1 VEHICLE PROPERTIES AND INFORMATION

Table G.1. Vehicle Properties for Test No. 469138-3-4.

Date: 2017-09-28 Test No.: 469138-3-4 VIN No.: 1C6RD6FP6C3242469

Year: Make: Dodge Model: RAM 1500

Tire Size: 265/70R17 Tire Inflation Pressure: 35 psi

Tread Type: Highway Odometer: 180536

Note any damage to the vehicle prior to test: None

• Denotes accelerometer location.

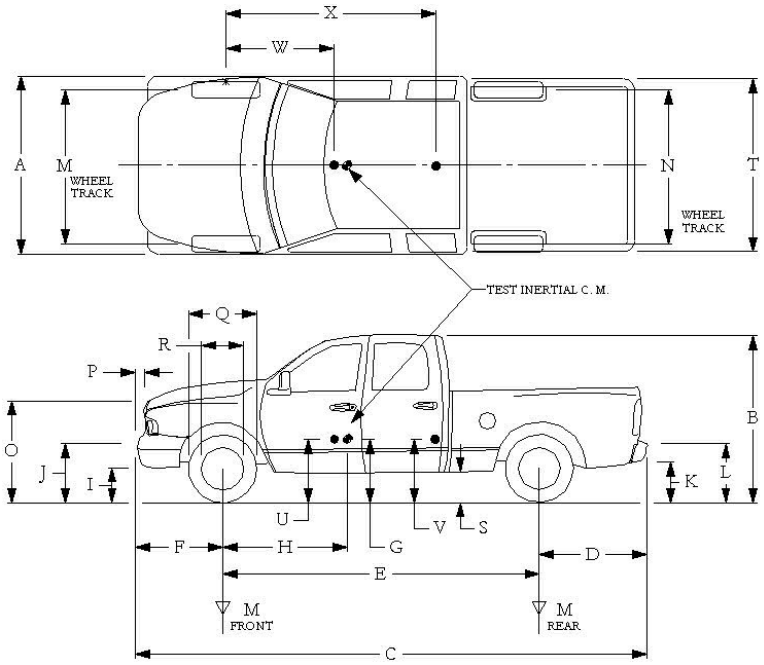
NOTES: None

Engine Type: V-8
Engine CID: 4.7 liter

Transmission Type:
x Auto or ___ Manual
___ FWD x RWD ___ 4WD

Optional Equipment:
None

Dummy Data:
Type: None
Mass: NA
Seat Position: NA



Geometry: inches

A	78.50	F	40.00	K	18.75	P	3.00	U	27.00		
B	75.00	G	28.62	L	28.00	Q	30.50	V	30.00		
C	227.50	H	62.17	M	68.50	R	18.00	W	63.10		
D	47.00	I	11.25	N	68.00	S	12.75	X	78.30		
E	140.50	J	26.50	O	45.50	T	77.00				
Wheel Center Height Front	14.75			Wheel Well Clearance (Front)	6.00			Bottom Frame Height - Front	12.00		
Wheel Center Height Rear	14.75			Wheel Well Clearance (Rear)	9.25			Bottom Frame Height - Rear	25.50		

GVWR Ratings:		**Mass:** lb	Curb	Test Inertial	Gross Static
Front	3700	M_{front}	2890	2764	------
Back	3900	M_{rear}	2009	2258	------
Total	6700	M_{Total}	4899	5022	------

(Allowable Range for TIM and GSM = 5000 lb ±110 lb)

Mass Distribution:
lb LF: 1379 RF: 1385 LR: 1098 RR: 1160

Table G.2. Measurements of Vehicle Vertical CG for Test No. 469138-3-4.

Date: 2017-09-28 Test No.: 469138-3-4 VIN: 1C6RD6FP6C3242469

Year: 2012 Make: Dodge Model: RAM 1500

Body Style: Quad Cab Mileage: 180536

Engine: 4.7 liter V-8 Transmission: Automatic

Fuel Level: Empty Ballast: 270 lb (440 lb max)

Tire Pressure: Front: 35 psi Rear: 35 psi Size: 265/70R17

Measured Vehicle Weights: (lb)								
LF:	1379	RF:	1385	Front Axle:	2764			
LR:	1098	RR:	1160	Rear Axle:	2258			
Left:	2477	Right:	2545	Total:	5022			
				5000 ±110 lb allowed				
Wheel Base:	140.5 inches	Track: F:	68.5 inches	R:	68 inches			
148 ±12 inches allowed			Track = (F+R)/2 = 67 ±1.5 inches allowed					
Center of Gravity, SAE J874 Suspension Method								
X:	63.17 inches	Rear of Front Axle	(63 ±4 inches allowed)					
Y:	0.46 inches	Left -	Right +	of Vehicle Centerline				
Z:	28.625 inches	Above Ground	(minumum 28.0 inches allowed)					

Hood Height: 45.50 inches Front Bumper Height: 26.50 inches

43 ±4 inches allowed

Front Overhang: 40.00 inches Rear Bumper Height: 28.00 inches

39 ±3 inches allowed

Overall Length: 227.50 inches

237 ±13 inches allowed

Table G.3. Exterior Crush Measurements of Vehicle for Test No. 469138-3-4.

Date: 2017-09-28 Test No.: 469138-3-4 VIN No.: 1C6RD6FP6C3242469

Year: 2012 Make: Dodge Model: RAM 1500

VEHICLE CRUSH MEASUREMENT SHEET[1]

Complete When Applicable	
End Damage	Side Damage
Undeformed end width _____ Corner shift: A1 _____ A2 _____ End shift at frame (CDC) (check one) < 4 inches _____ ≥ 4 inches _____	Bowing: B1 _____ X1 _____ B2 _____ X2 _____ Bowing constant $\frac{X1+X2}{2}$ = _____

Note: Measure C_1 to C_6 from Driver to Passenger Side in Front or Rear impacts – Rear to Front in Side Impacts.

Specific Impact Number	Plane* of C-Measurements	Direct Damage		Field L**	C_1	C_2	C_3	C_4	C_5	C_6	±D
		Width** (CDC)	Max*** Crush								
1	Front plane at bumper ht	24	10	36	10	8	6	3.5	1	0	-18
	Measurements recorded										
	in inches										

[1]Table taken from National Accident Sampling System (NASS).

*Identify the plane at which the C-measurements are taken (e.g., at bumper, above bumper, at sill, above sill, at beltline, etc.) or label adjustments (e.g., free space).

Free space value is defined as the distance between the baseline and the original body contour taken at the individual C locations. This may include the following: bumper lead, bumper taper, side protrusion, side taper, etc.
Record the value for each C-measurement and maximum crush.

**Measure and document on the vehicle diagram the beginning or end of the direct damage width and field L (e.g., side damage with respect to undamaged axle).

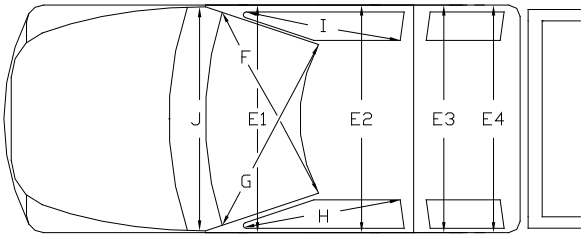
***Measure and document on the vehicle diagram the location of the maximum crush.

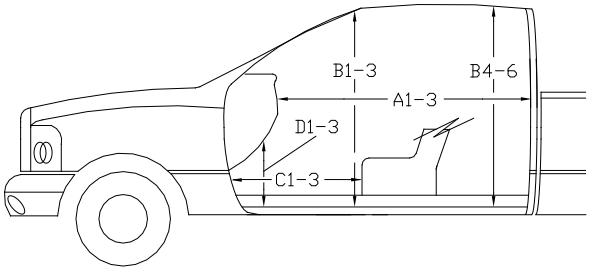
Note: Use as many lines/columns as necessary to describe each damage profile.

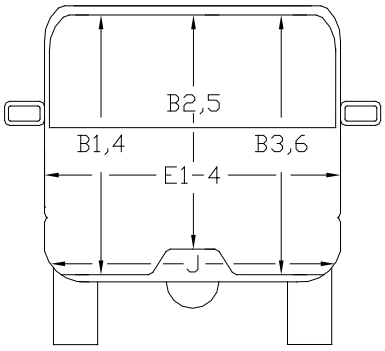
Table G.4. Occupant Compartment Measurements of Vehicle for Test No. 469138-3-4.

Date: 2017-09-28 Test No.: 469138-3-4 VIN No.: 1C6RD6FP6C3242469

Year: 2012 Make: Dodge Model: RAM 1500







*Lateral area across the cab from driver's side kickpanel to passenger's side kickpanel.

OCCUPANT COMPARTMENT DEFORMATION MEASUREMENT

	Before	After (inches)	Differ.
A1	65.00	65.00	0
A2	62.50	62.50	0
A3	65.25	65.25	0
B1	44.75	44.75	0
B2	38.00	38.00	0
B3	44.75	44.75	0
B4	39.50	39.50	0
B5	43.00	43.00	0
B6	39.50	39.50	0
C1	26.50	26.50	0
C2	-----	-----	-
C3	26.50	26.50	0
D1	11.25	11.25	0
D2	-----	-----	-
D3	11.25	11.25	0
E1	58.50	58.50	0
E2	63.50	63.50	0
E3	63.50	63.50	0
E4	63.50	63.50	0
F	59.00	59.00	0
G	59.00	59.00	0
H	37.50	37.50	0
I	37.50	37.50	0
J*	23.50	23.50	0

G.2 SEQUENTIAL PHOTOGRAPHS

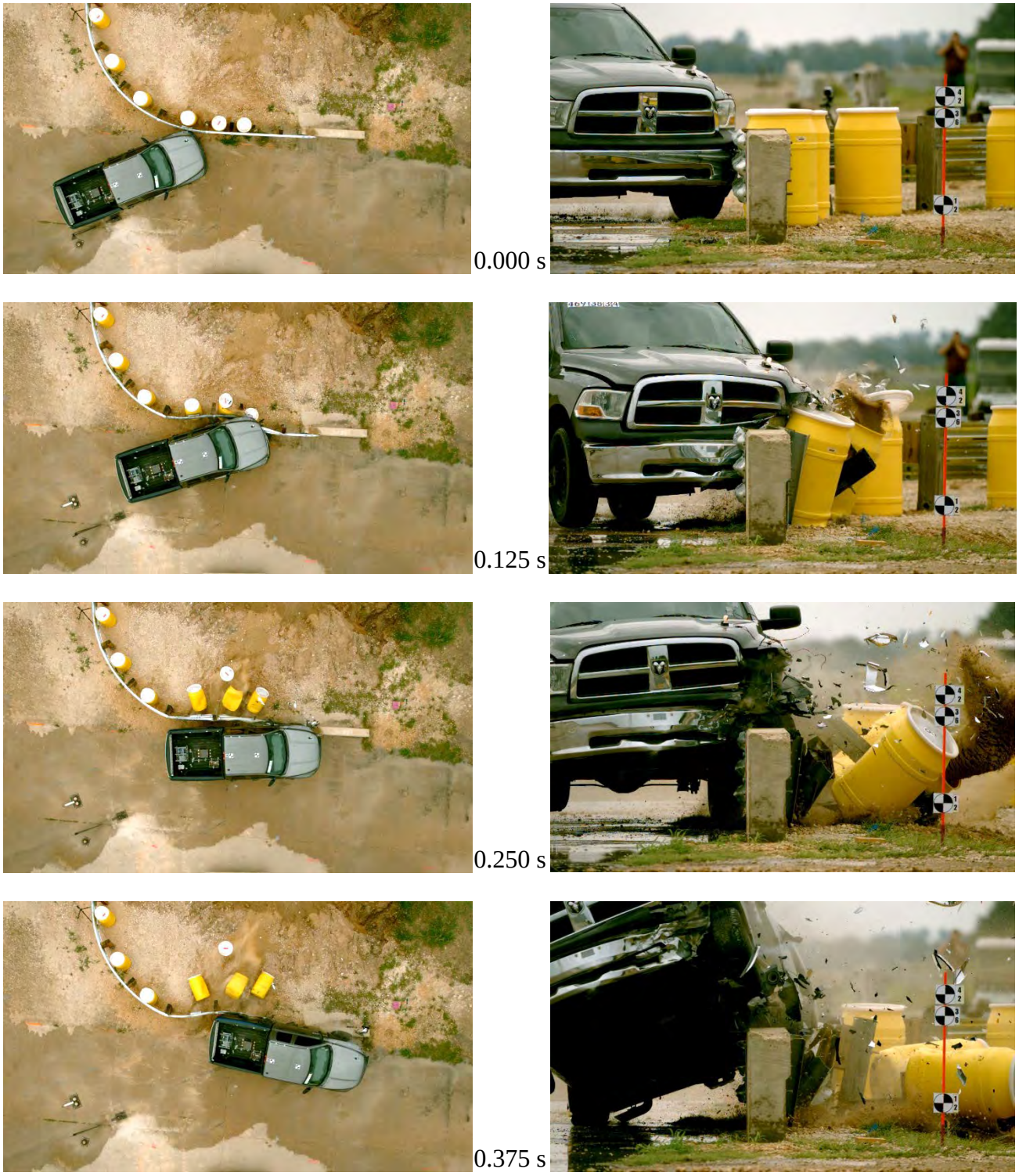


Figure G.1. Sequential Photographs for Test No. 469138-3-4 (Overhead and Frontal Views).



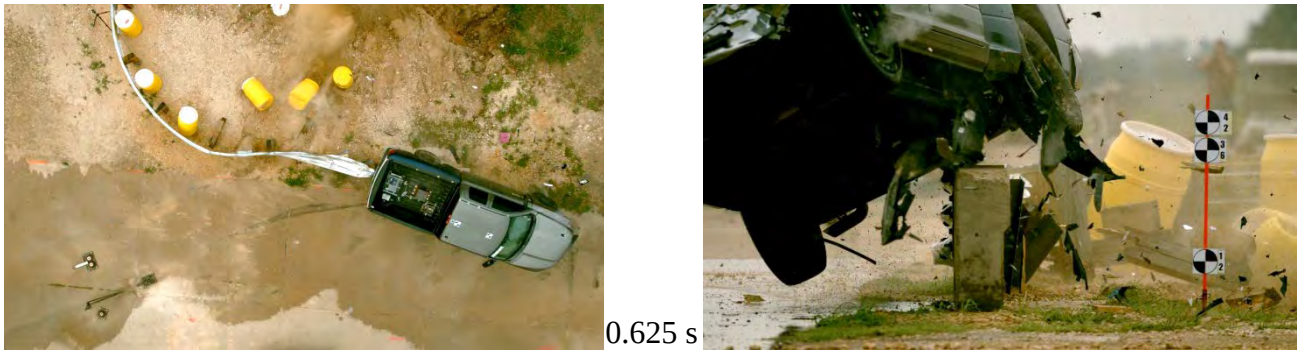






Figure G.1. Sequential Photographs for Test No. 469138-3-4 (Overhead and Frontal Views) (Continued).


0.000 s


0.500 s


0.125 s


0.625 s


0.250 s


0.750 s


0.375 s


0.875 s

Figure G.2. Sequential Photographs for Test No. 469138-3-4 (Rear View).

G.3 VEHICLE ANGULAR DISPLACEMENT

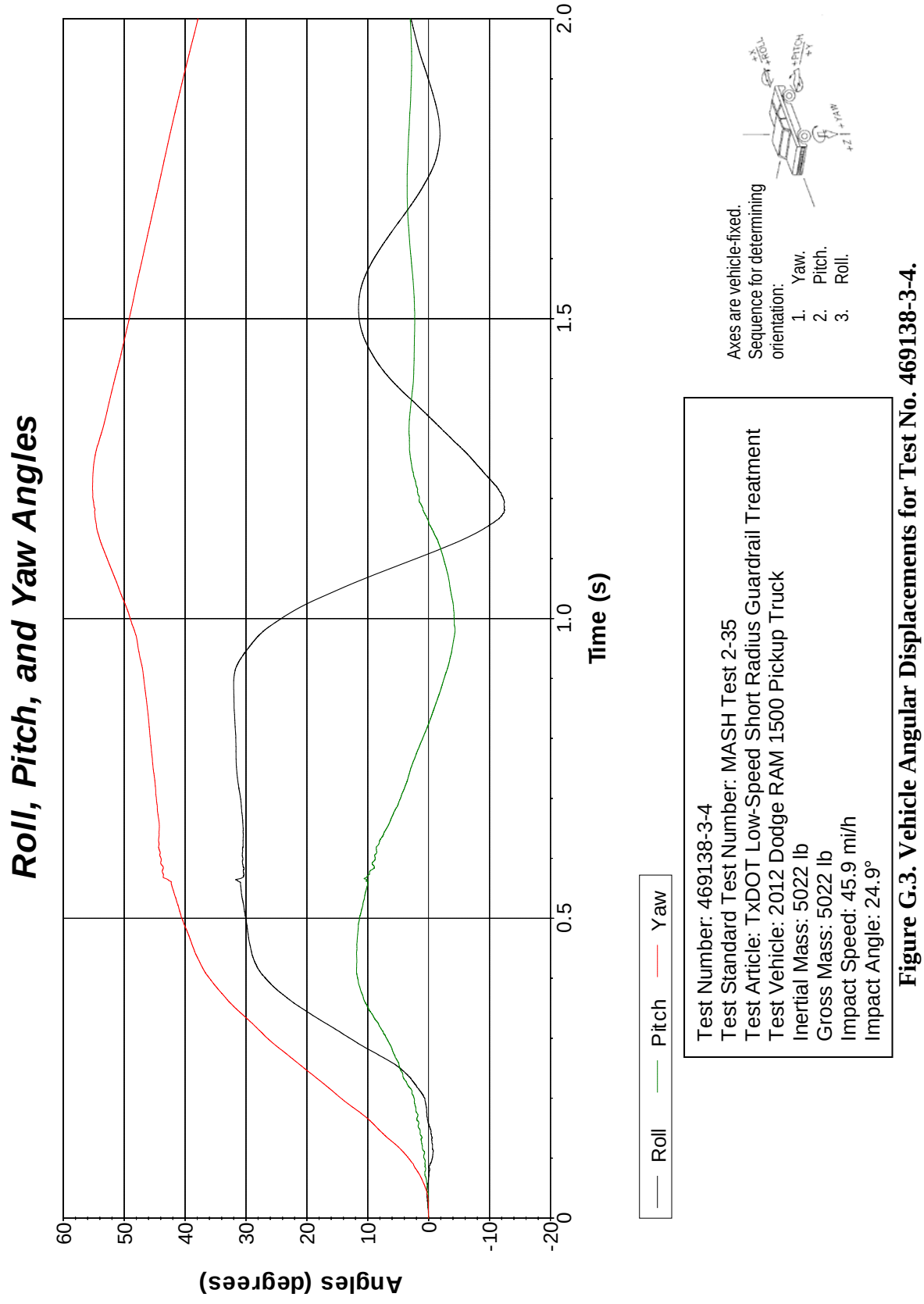


Figure G.3. Vehicle Angular Displacements for Test No. 469138-3-4.

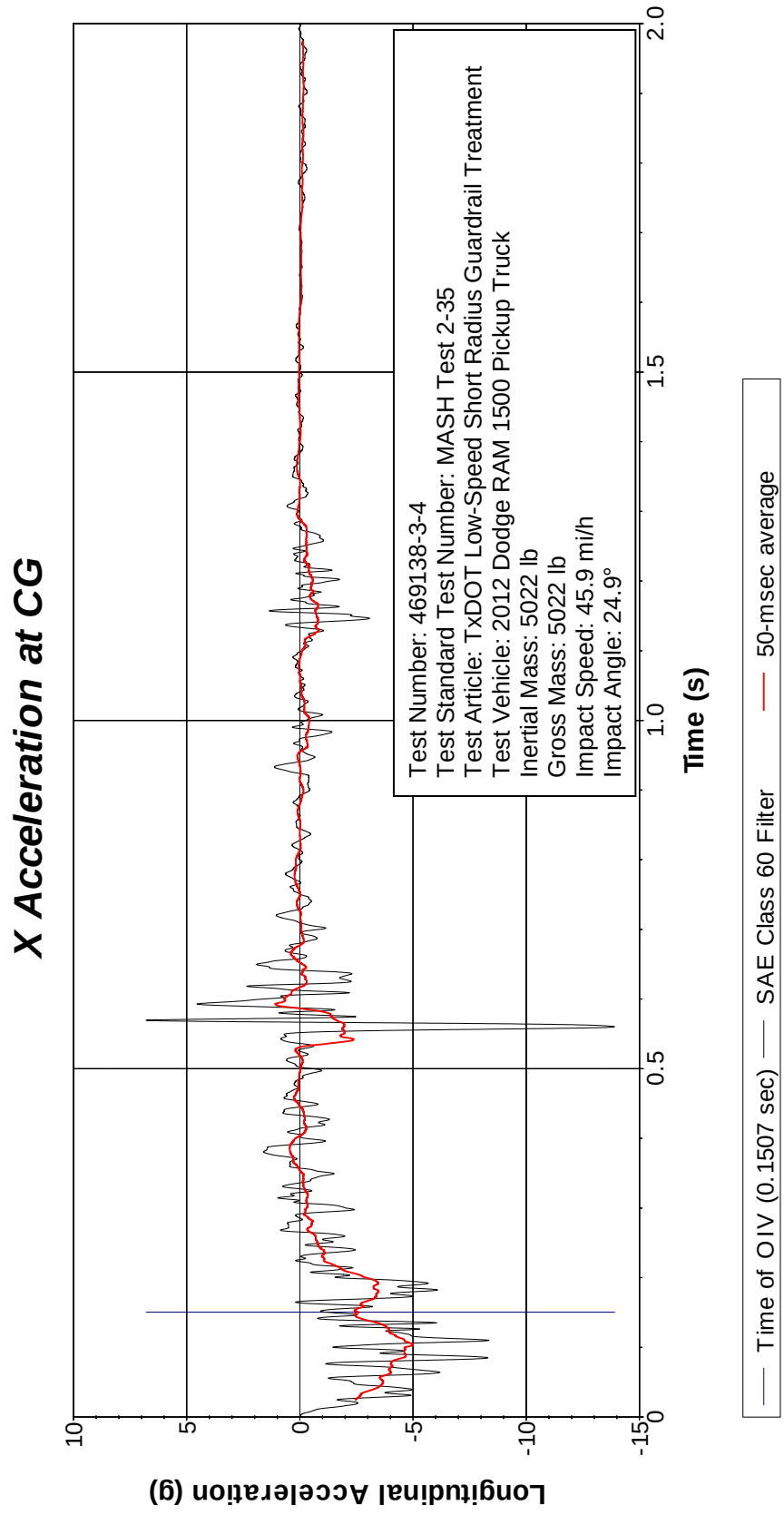


Figure G.4. Vehicle Longitudinal Accelerometer Trace for Test No. 469138-3-4 (Accelerometer Located at Center of Gravity).

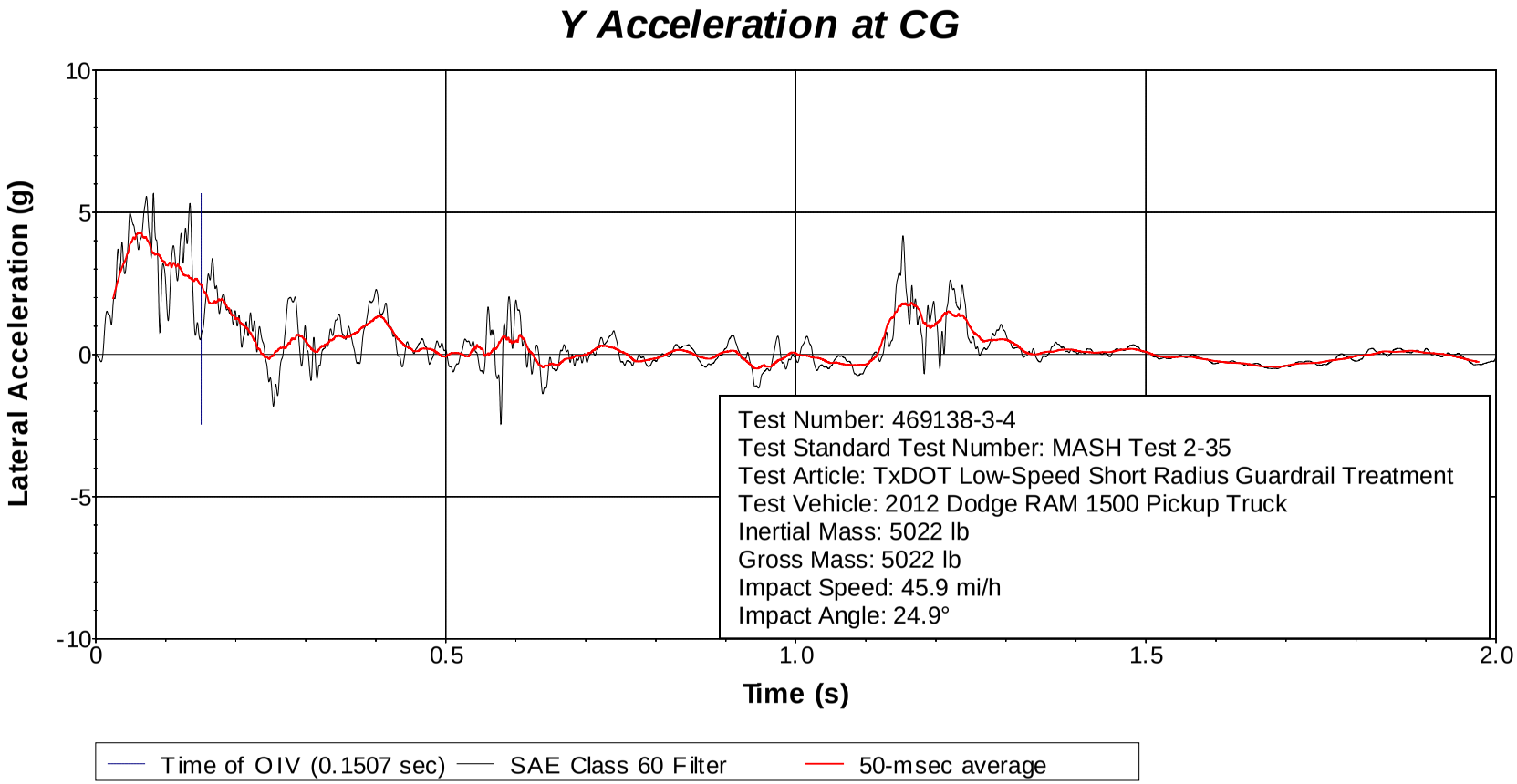


Figure G.5. Vehicle Lateral Accelerometer Trace for Test No. 469138-3-4 (Accelerometer Located at Center of Gravity).

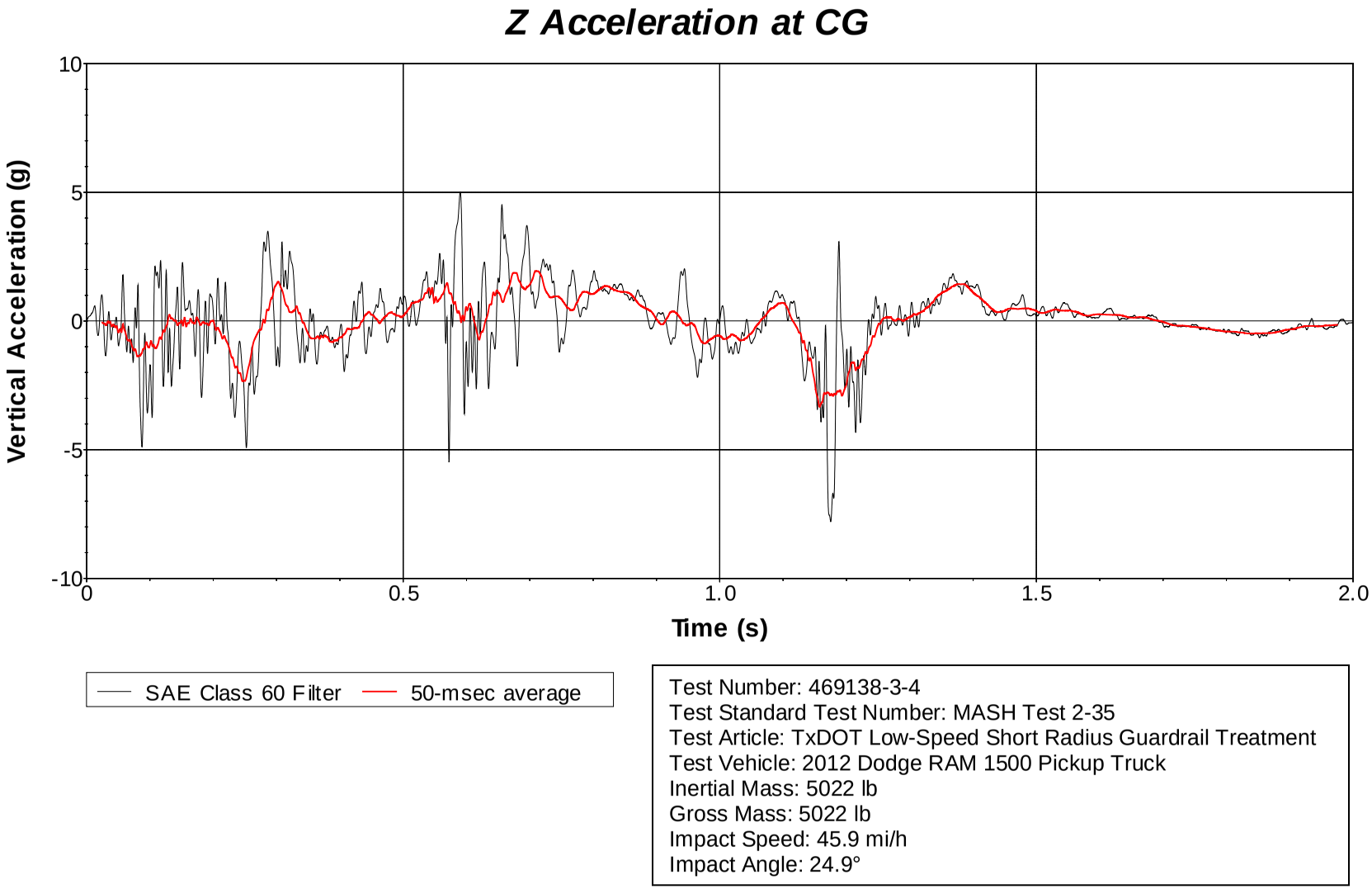


Figure G.6. Vehicle Vertical Accelerometer Trace for Test No. 469138-3-4 (Accelerometer Located at Center of Gravity).

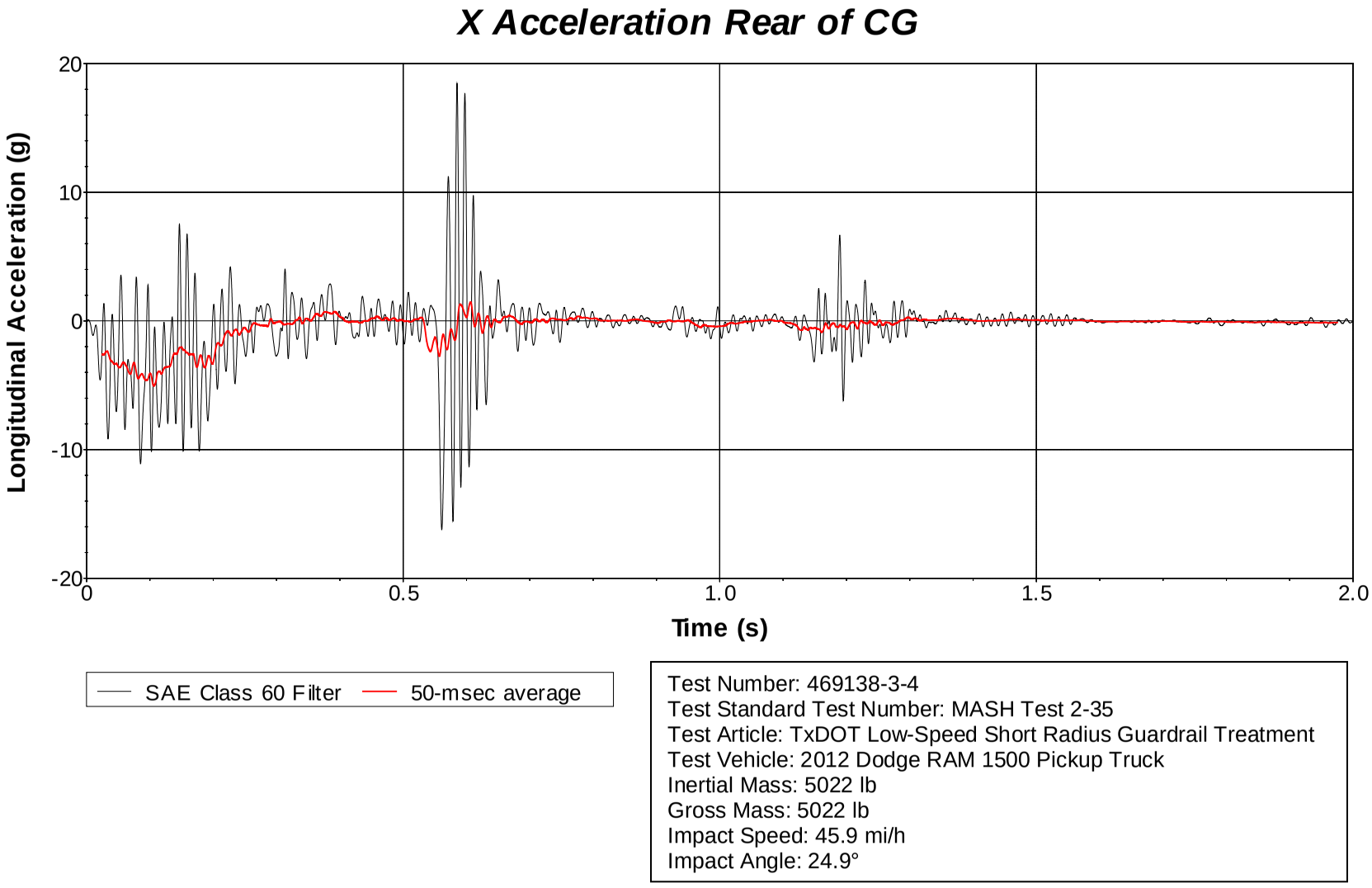


Figure G.7. Vehicle Longitudinal Accelerometer Trace for Test No. 469138-3-4 (Accelerometer Located Rear of Center of Gravity).

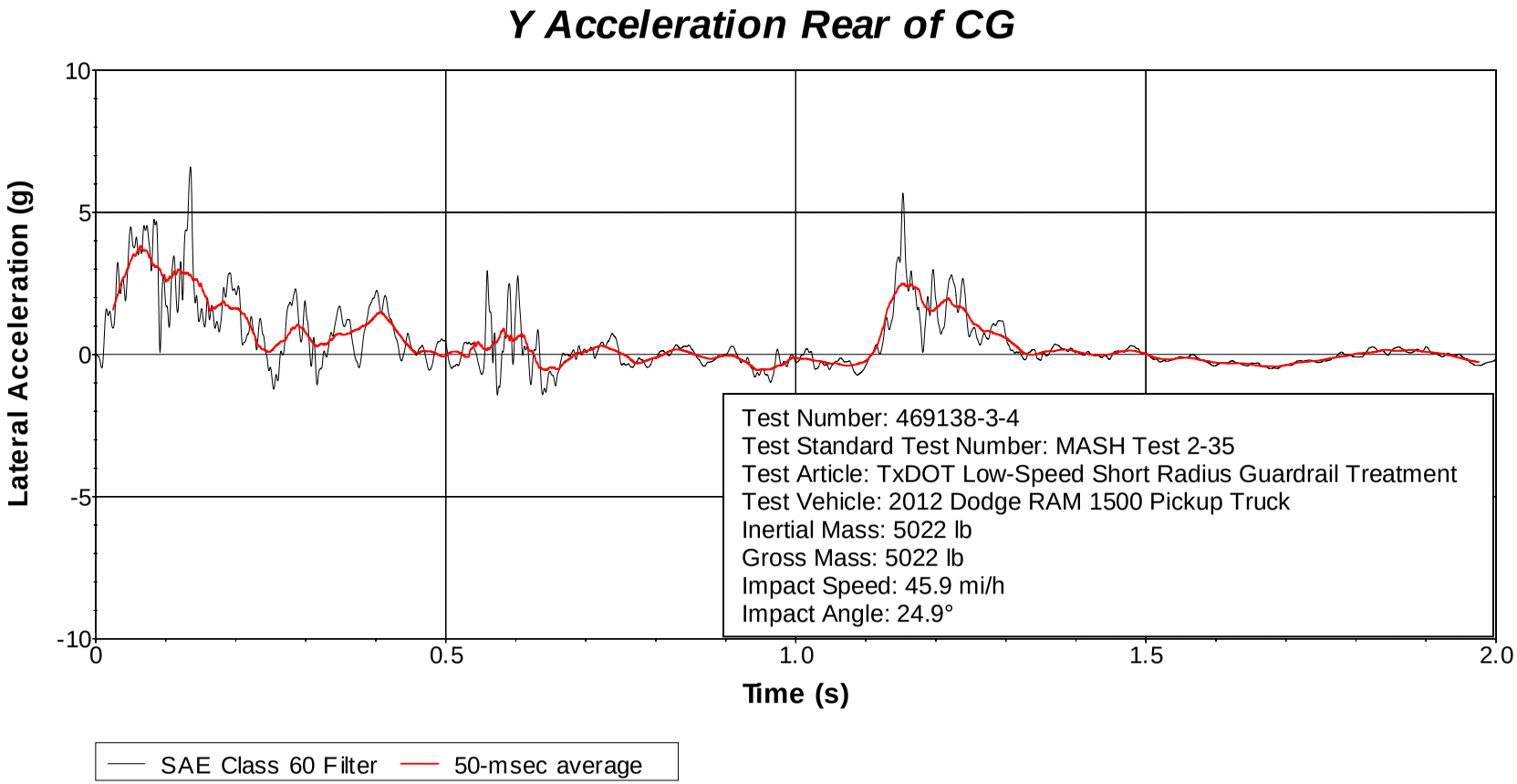


Figure G.8. Vehicle Lateral Accelerometer Trace for Test No. 469138-3-4 (Accelerometer Located Rear of Center of Gravity).

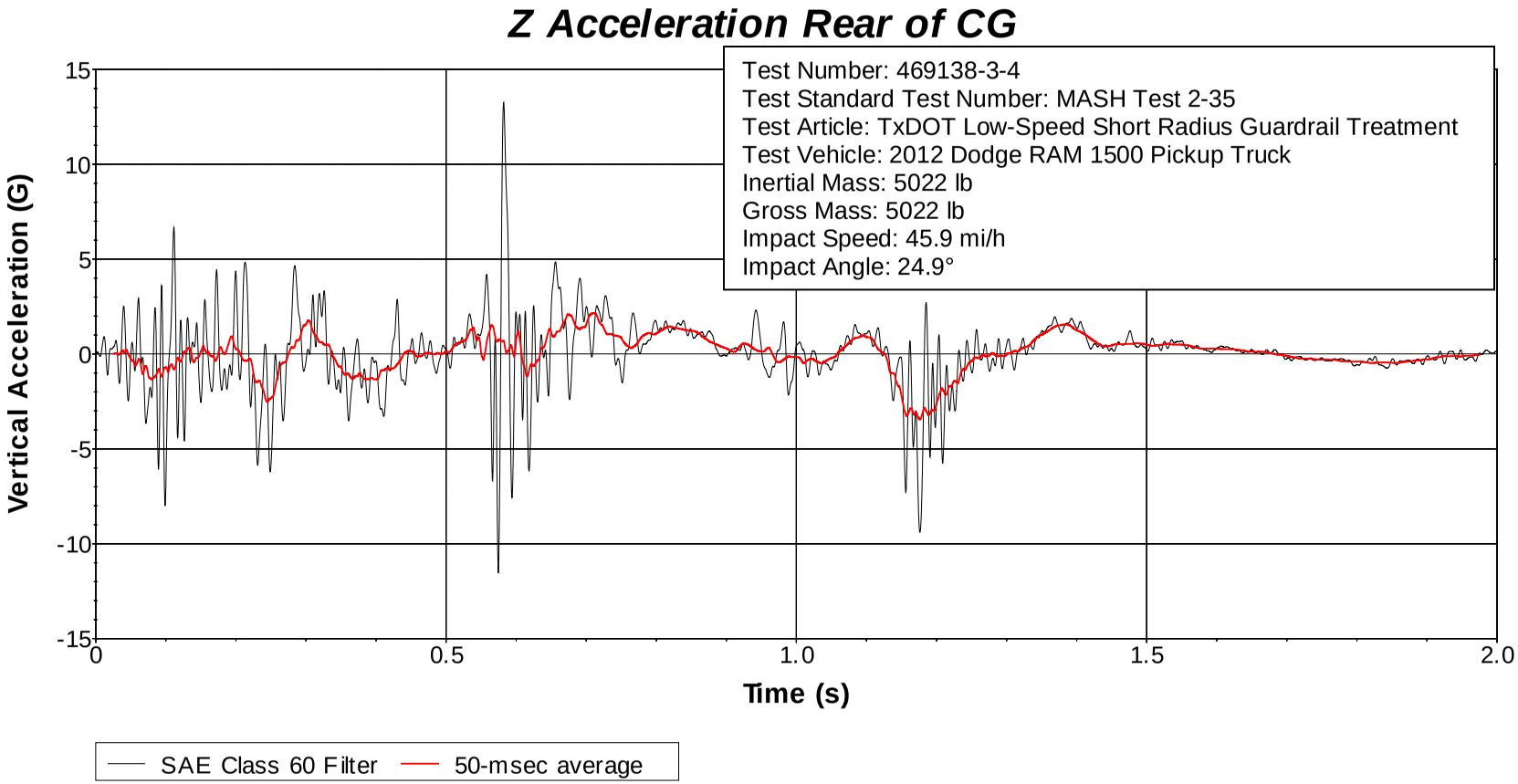


Figure G.9. Vehicle Vertical Accelerometer Trace for Test No. 469138-3-4 (Accelerometer Located Rear of Center of Gravity).

APPENDIX H. MODIFIED *MASH* TEST 2-34 (CRASH TEST NO. 469138-3-5)

H1 VEHICLE PROPERTIES AND INFORMATION

Table H.1. Vehicle Properties for Test No. 469138-3-5.

Date: 2017-12-14 Test No.: 469138-3-5 VIN No.: KNADE223396448357

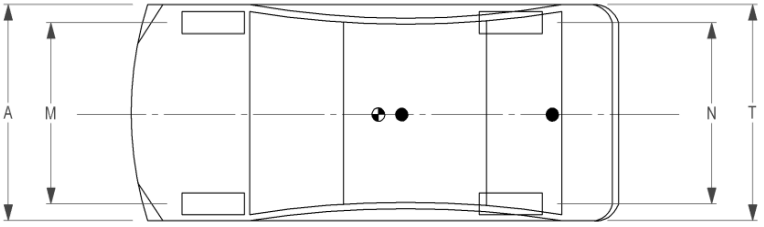
Year: 2009 Make: Kia Model: Rio

Tire Inflation Pressure: 32 psi Odometer: 227215 Tire Size: 185/65R14

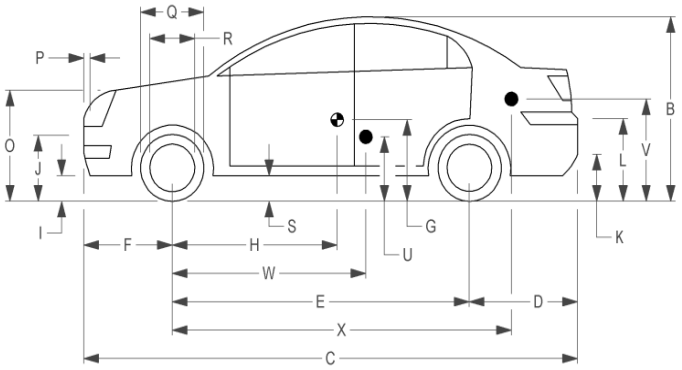
Describe any damage to the vehicle prior to test: the head of the dummy cracked the windshield when loading it into the vehicle; starburst crack near the top just left of center;

● Denotes accelerometer location.

NOTES: None



Engine Type: 4 cylinder
Engine CID: 1.6 liter
Transmission Type:
x Auto or ____ Manual
x FWD ____ RWD ____ 4WD
Optional Equipment:
None
None



Dummy Data:
Type: 50th percentile male
Mass: 165 lb
Seat Position: Driver position

Geometry: inches

A	66.38	F	33.00	K	10.50	P	4.12	U	14.75
B	58.00	G	-----	L	24.50	Q	22.50	V	20.00
C	165.75	H	35.88	M	57.75	R	15.50	W	35.88
D	34.00	I	7.75	N	57.75	S	9.00	X	105.75
E	98.75	J	21.00	O	28.12	T	66.25		
Wheel Center Ht Front		11.00		Wheel Center Ht Rear		11.00	W-H	0	

GVWR Ratings:		**Mass:** lb	Curb	Test Inertial	Gross Static
Front	1718	M_{front}	1585	1556	1641
Back	1874	M_{rear}	898	888	968
Total	3638	M_{Total}	2483	2444	2609

Allowable TIM = 2420 lb ±55 lb | Allowable GSM = 2585 lb ± 55 lb

Mass Distribution:
lb LF: 778 RF: 778 LR: 455 RR: 433

Table H.2. Exterior Crush Measurements for Test No. 469138-3-5.

Date: 2017-12-14 Test No.: 469138-3-5 VIN No.: KNADE223396448357

Year: 2009 Make: Kia Model: Rio

VEHICLE CRUSH MEASUREMENT SHEET[1]

Complete When Applicable	
End Damage	Side Damage
Undeformed end width _____ Corner shift: A1 _____ A2 _____ End shift at frame (CDC) (check one) < 4 inches _____ ≥ 4 inches _____	Bowing: B1 _____ X1 _____ B2 _____ X2 _____ Bowing constant $\frac{X1+X2}{2}$ = _____

Note: Measure C_1 to C_6 from Driver to Passenger Side in Front or Rear impacts – Rear to Front in Side Impacts.

Specific Impact Number	Plane* of C-Measurements	Direct Damage		Field L**	C_1	C_2	C_3	C_4	C_5	C_6	±D
		Width** (CDC)	Max*** Crush								
1	Front plane at bumper ht	17	26	26	17	12	3	1	--	--	0
	Measurements recorded										
	in inches										

[1]Table taken from National Accident Sampling System (NASS).

*Identify the plane at which the C-measurements are taken (e.g., at bumper, above bumper, at sill, above sill, at beltline, etc.) or label adjustments (e.g., free space).

Free space value is defined as the distance between the baseline and the original body contour taken at the individual C locations. This may include the following: bumper lead, bumper taper, side protrusion, side taper, etc. Record the value for each C-measurement and maximum crush.

**Measure and document on the vehicle diagram the beginning or end of the direct damage width and field L (e.g., side damage with respect to undamaged axle).

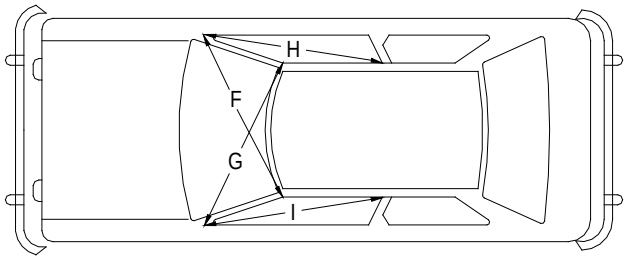
***Measure and document on the vehicle diagram the location of the maximum crush.

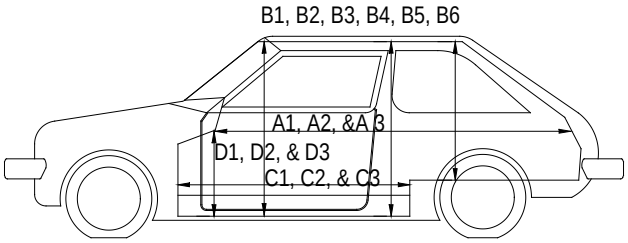
Note: Use as many lines/columns as necessary to describe each damage profile.

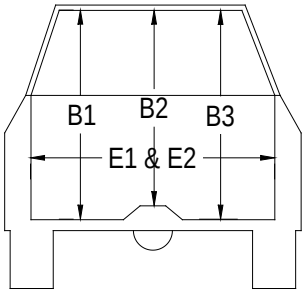
Table H.3. Occupant Compartment Measurements for Test No. 469138-3-5.

Date: 2017-12-14 Test No.: 469138-3-5 VIN No.: KNADE223396448357

Year: 2009 Make: Kia Model: Rio







OCCUPANT COMPARTMENT DEFORMATION MEASUREMENT

	Before	After (inches)	Differ.
A1	67.75	67.75	0
A2	67.00	67.00	0
A3	67.50	67.50	0
B1	40.50	40.50	0
B2	37.00	37.00	0
B3	40.50	40.50	0
B4	36.00	36.00	0
B5	35.50	35.50	0
B6	36.00	36.00	0
C1	26.00	26.00	0
C2	-----	-----	-
C3	26.00	26.00	0
D1	9.50	9.50	0
D2	-----	-----	-
D3	9.50	9.50	0
E1	51.50	51.50	0
E2	51.00	51.00	0
F	51.00	51.00	0
G	51.00	51.00	0
H	37.00	37.00	0
I	37.00	37.00	0
J*	51.00	51.00	0

*Lateral area across the cab from
driver's side kickpanel to passenger's side kickpanel.

H2 SEQUENTIAL PHOTOGRAPHS

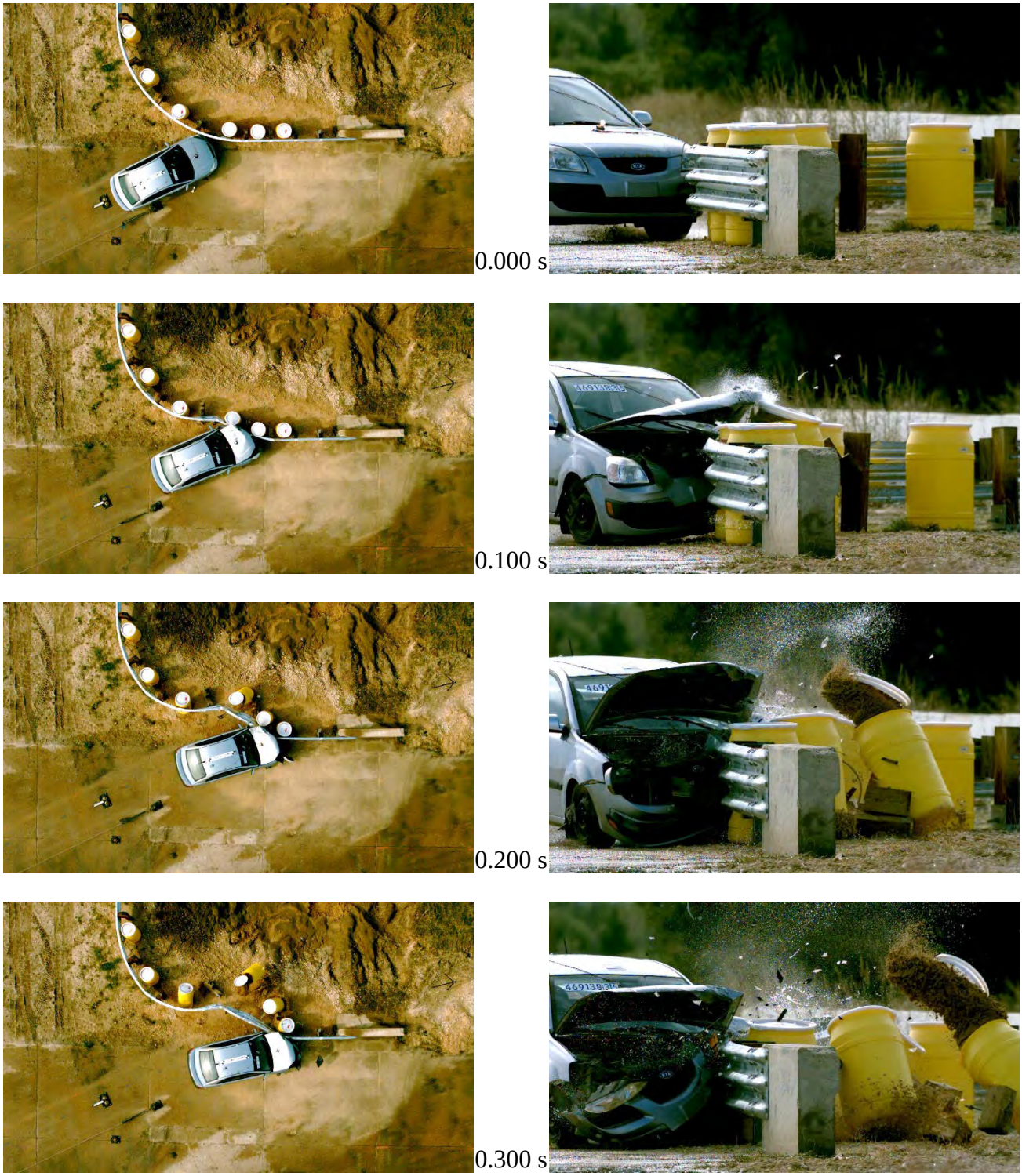
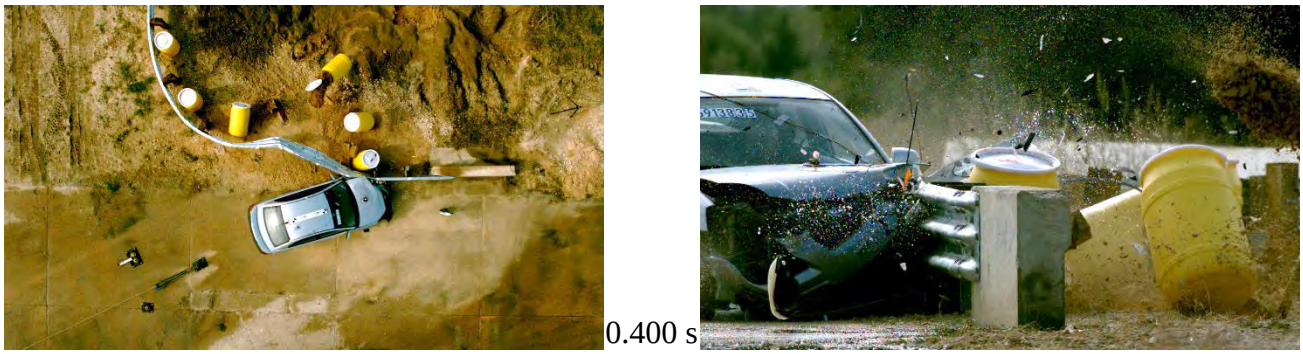
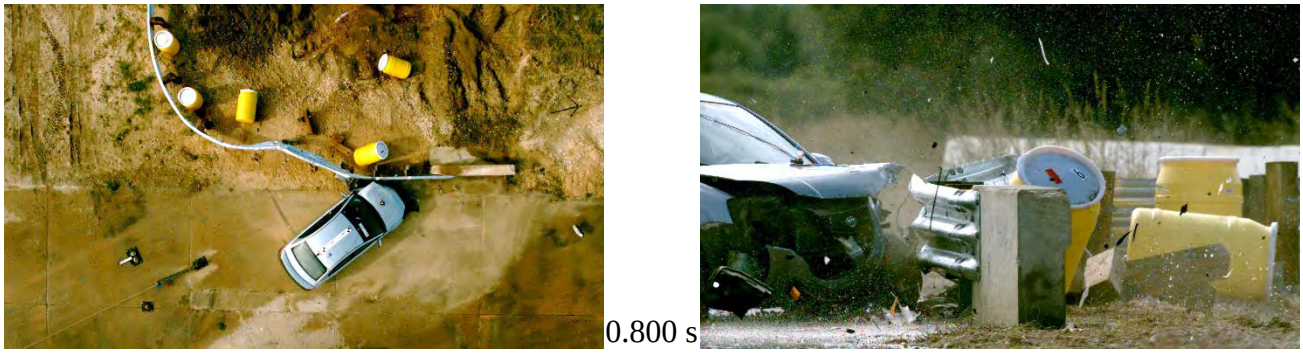


Figure H.1. Sequential Photographs for Test No. 469138-3-5 (Overhead and Frontal Views).


0.400 s


0.600 s


0.800 s

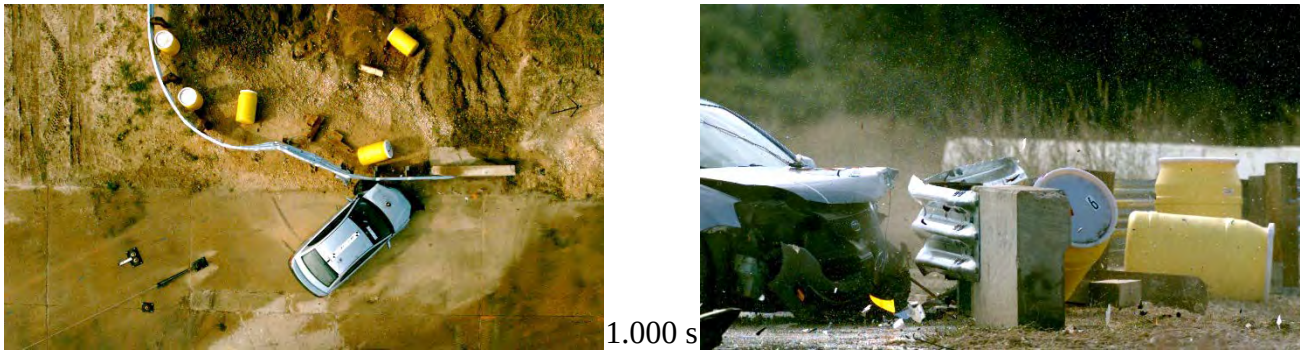

1.000 s

Figure H.1D.1**. Sequential Photographs for Test No. 469138-3-5 (Overhead and Frontal Views) (Continued).**

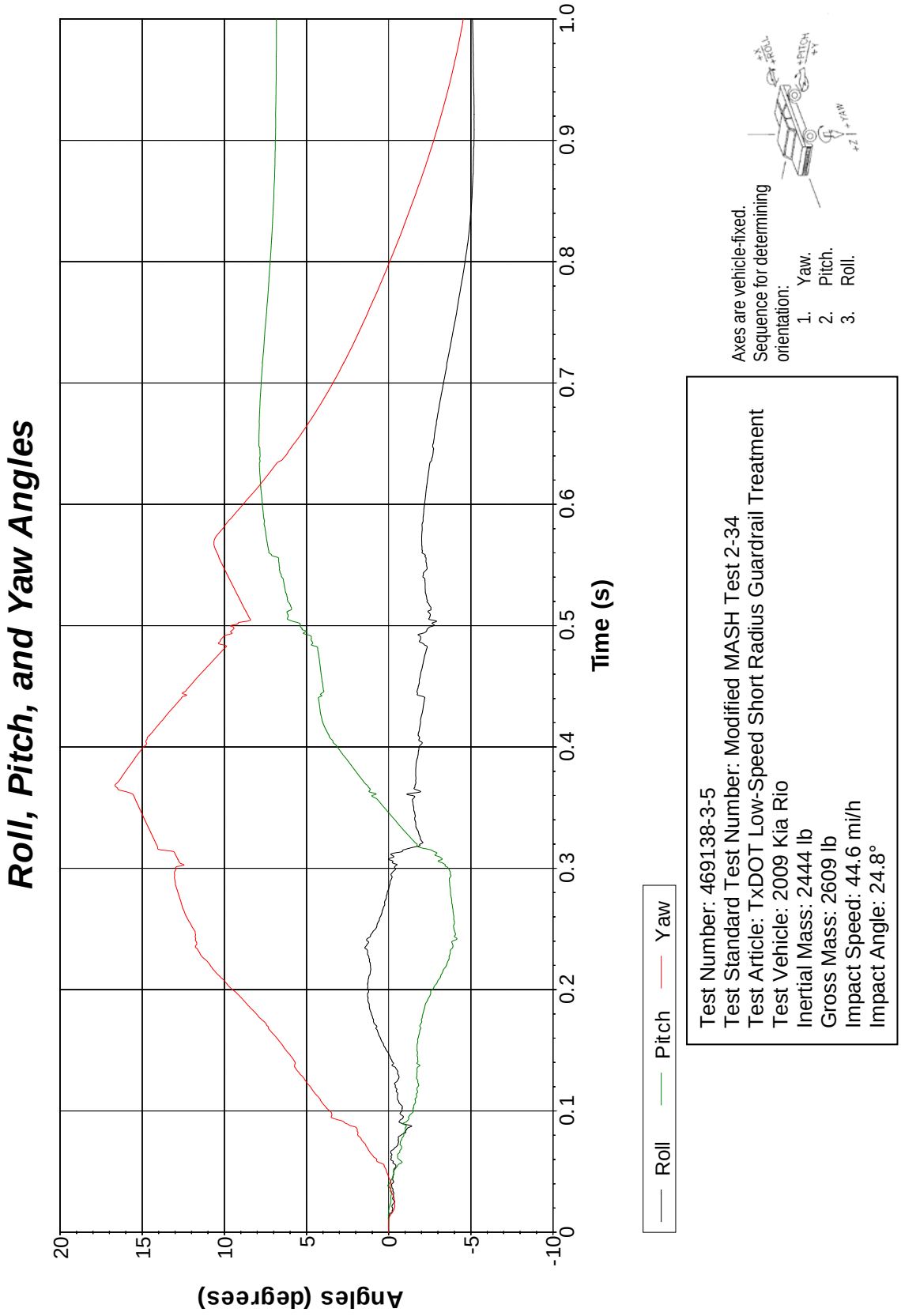


Figure H.2. Vehicle Angular Displacements for Test No. 469138-3-5.

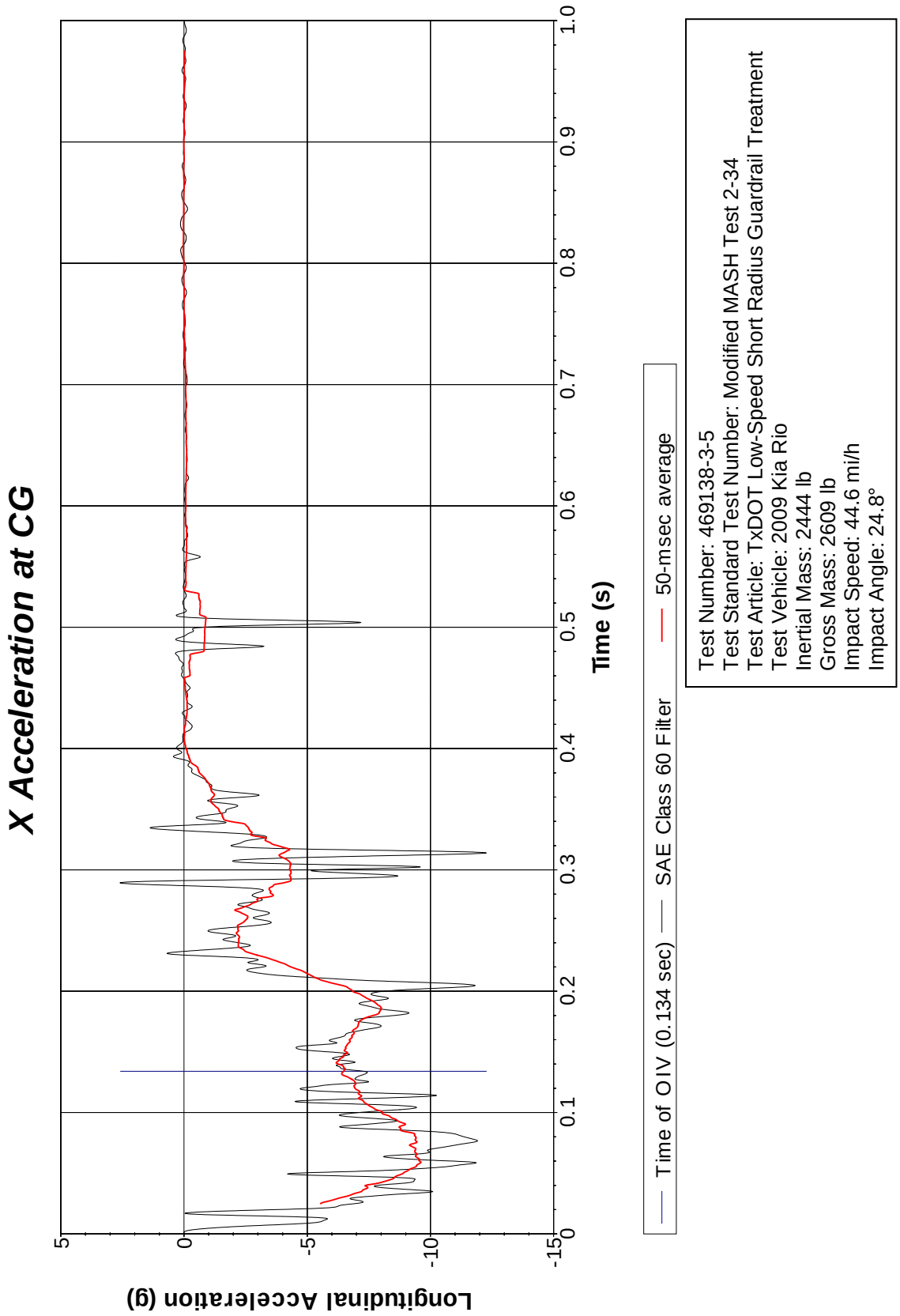


Figure H.3. Vehicle Longitudinal Accelerometer Trace for Test No. 469138-3-5 (Accelerometer Located at Center of Gravity).

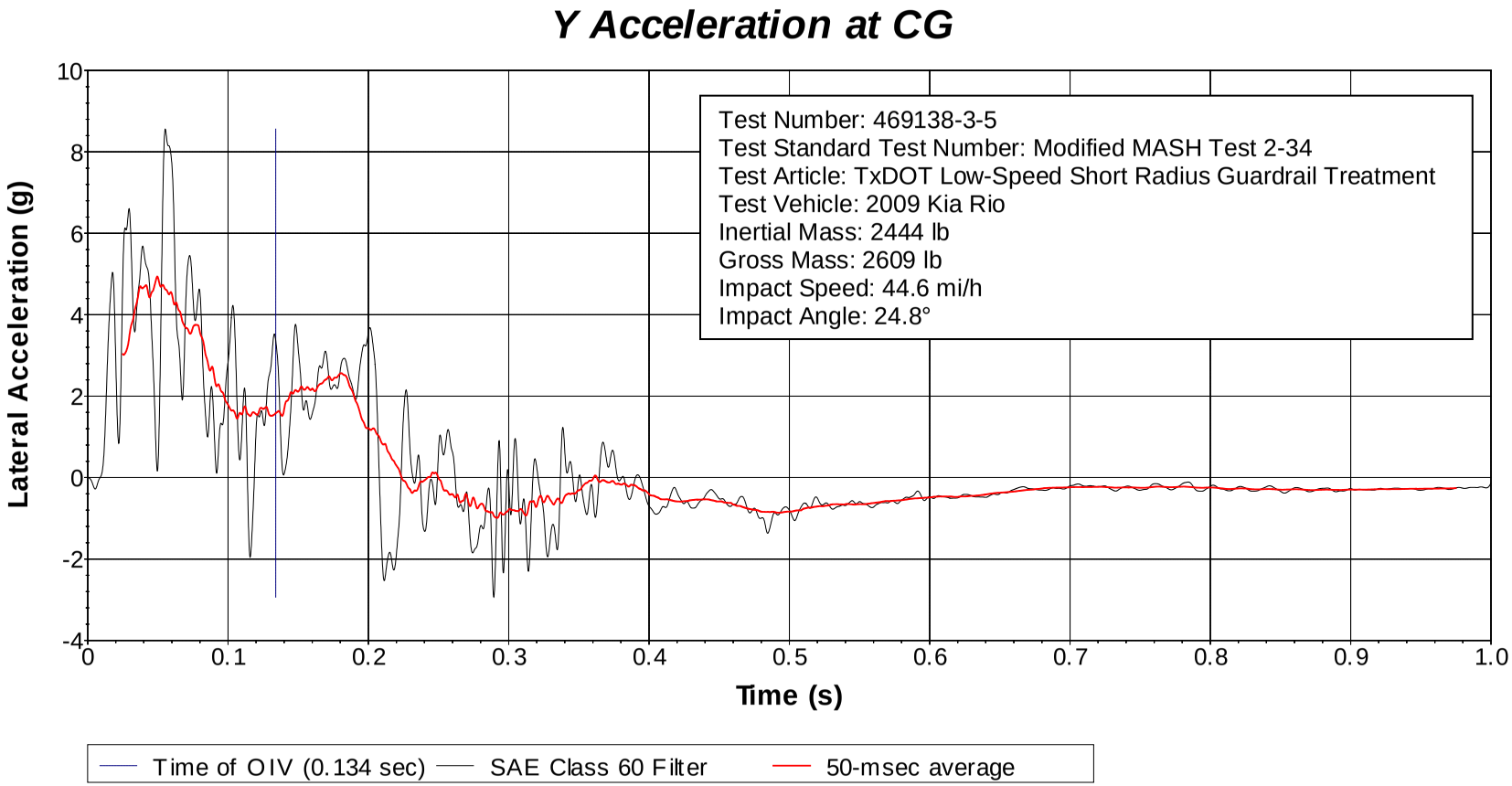


Figure H.4. Vehicle Lateral Accelerometer Trace for Test No. 469138-3-5 (Accelerometer Located at Center of Gravity).

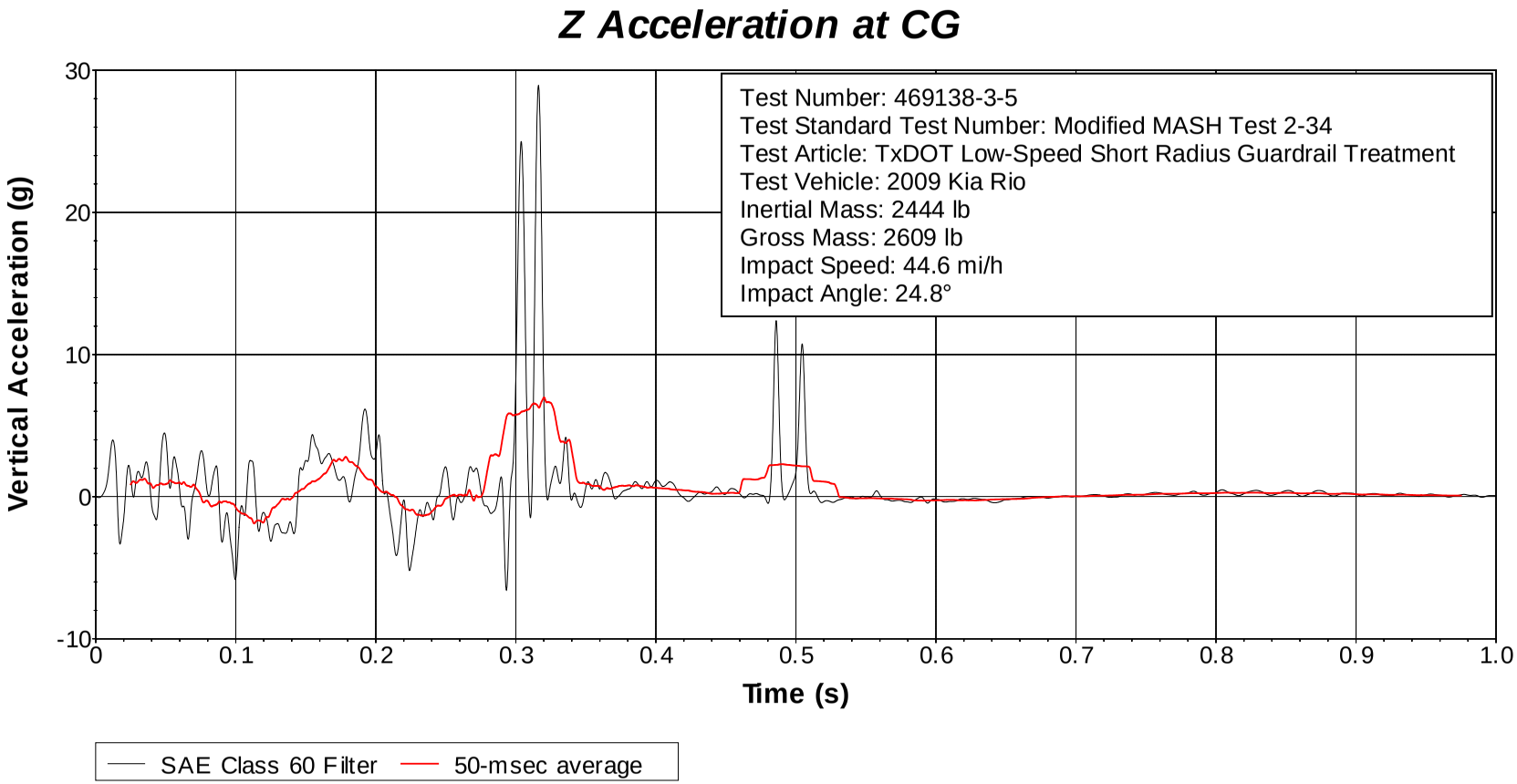


Figure H.5. Vehicle Vertical Accelerometer Trace for Test No. 469138-3-5 (Accelerometer Located at Center of Gravity).

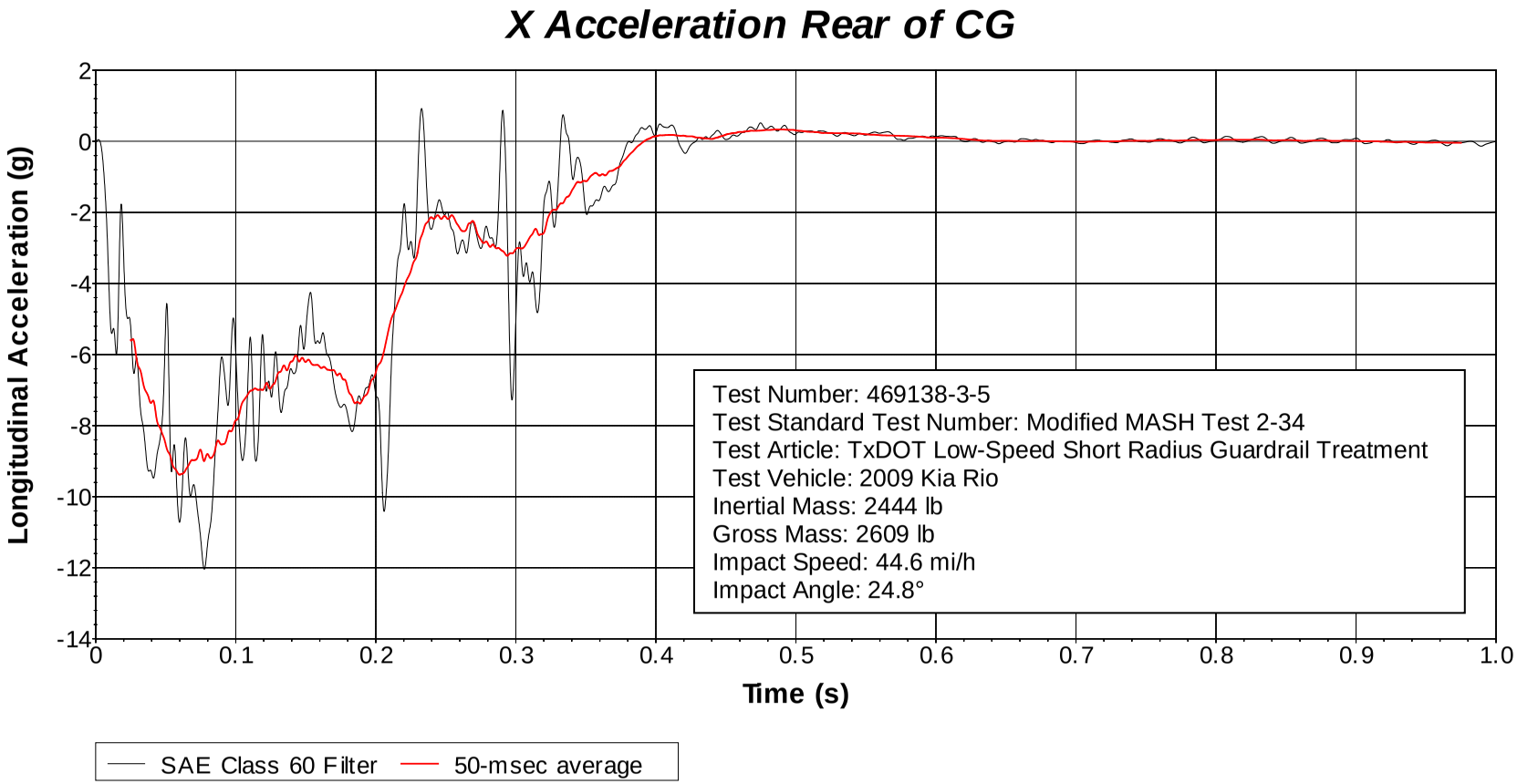


Figure H.6. Vehicle Longitudinal Accelerometer Trace for Test No. 469138-3-5 (Accelerometer Located Rear of Center of Gravity).

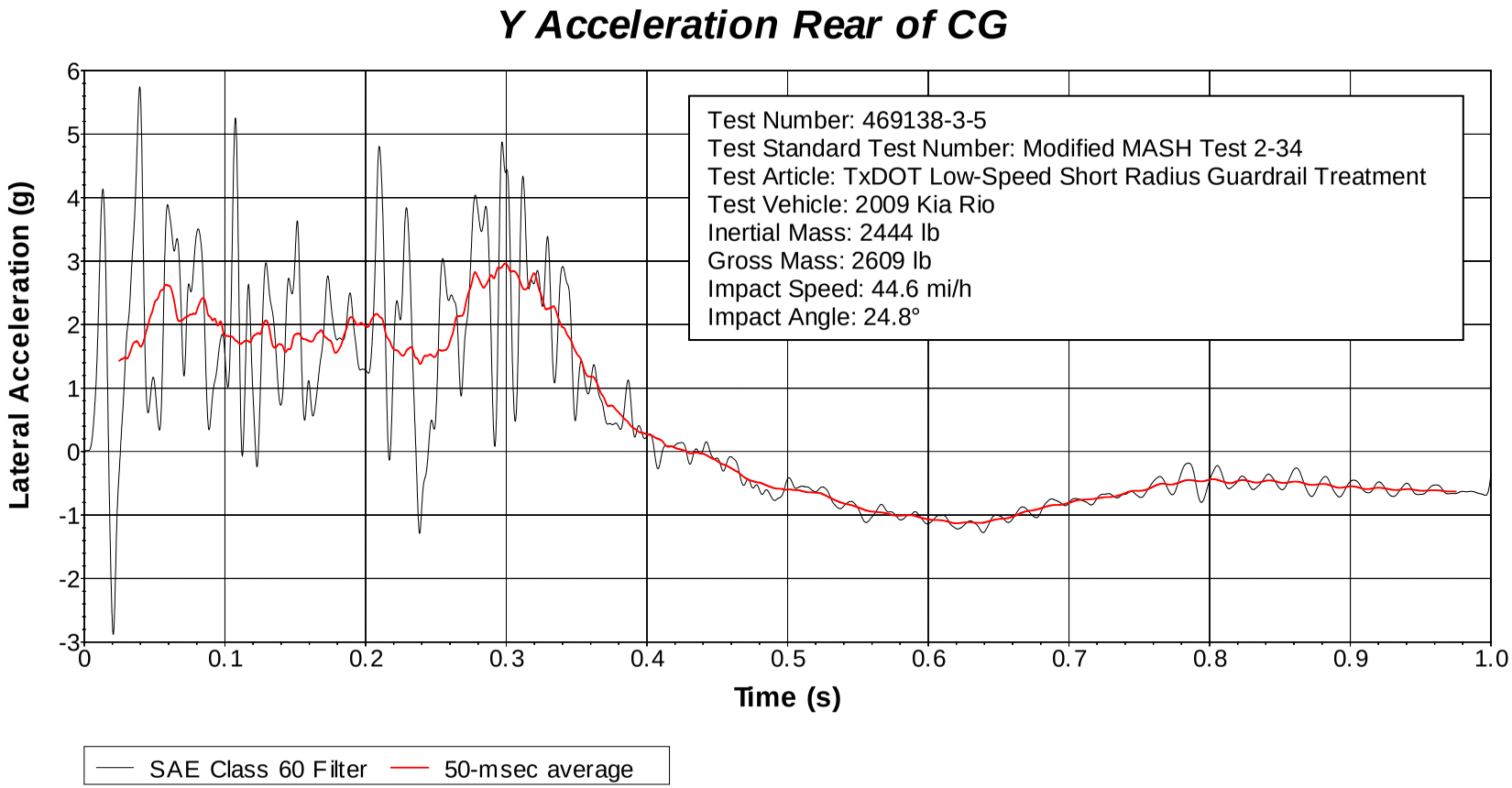


Figure H.7. Vehicle Lateral Accelerometer Trace for Test No. 469138-3-5 (Accelerometer Located Rear of Center of Gravity).

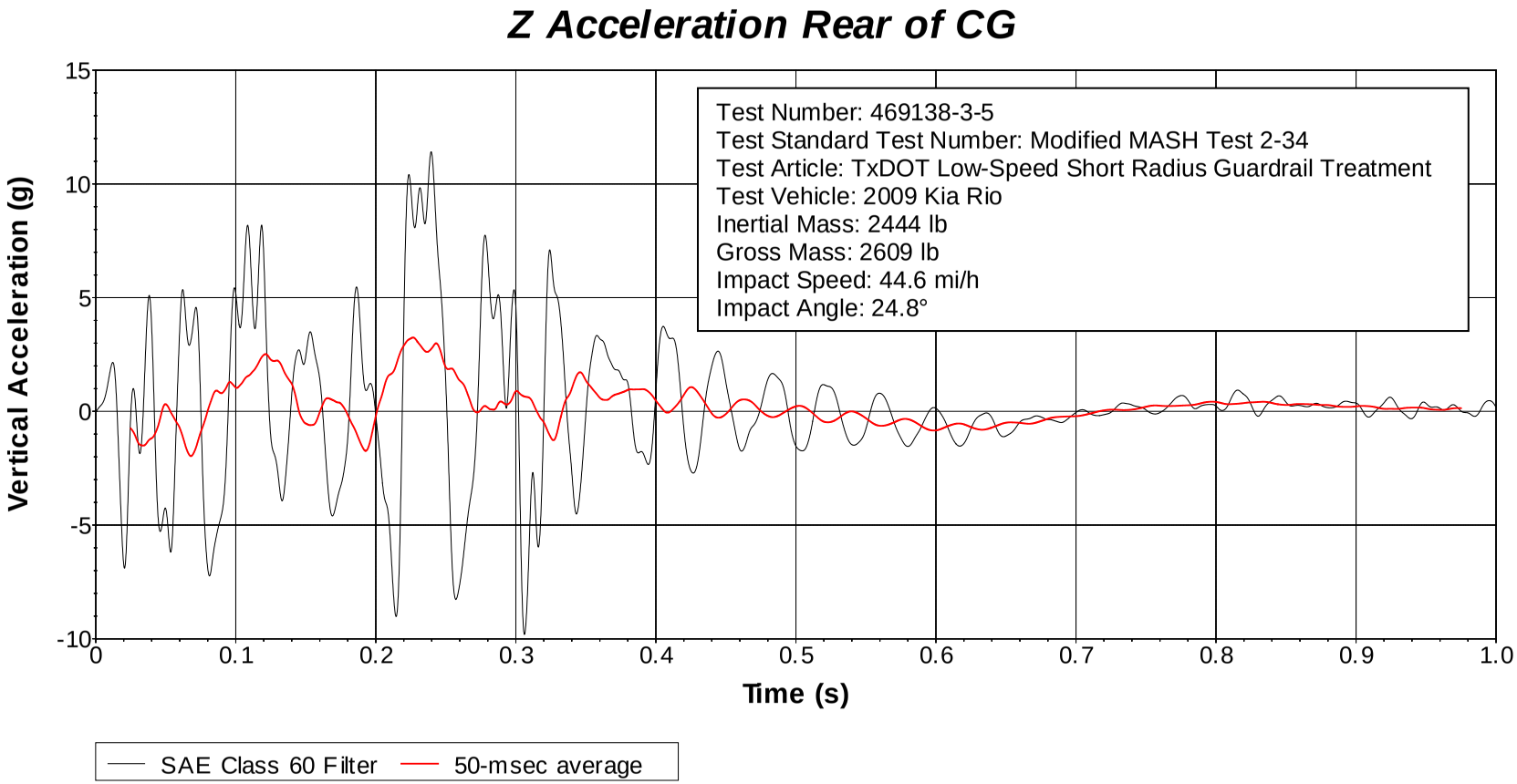


Figure H.8. Vehicle Vertical Accelerometer Trace for Test No. 469138-3-5 (Accelerometer Located Rear of Center of Gravity).